

**CARBON DIOXIDE DESORPTION/ ABSORPTION WITH
AQUEOUS MIXTURES OF METHYLDIETHANOLAMINE
AND DIETHANOLAMINE AT 40 TO 120°C**

by

MSAFIRI MMASA MSHEWA, B.Sc., M.S.

DISSERTATION

Presented to the Faculty of the Graduate School of

The University of Texas at Austin

in Partial Fulfillment

of the Requirements

for the Degree of

DOCTOR OF PHILOSOPHY

THE UNIVERSITY OF TEXAS AT AUSTIN

August, 1995


Acknowledgements

I take this opportunity to express my gratitude to my advisor, Professor Gary T. Rochelle for his patience and supervision in the course of this study. I wish also to thank the members of my committee: Dr. William J. Koros, Dr. James R. Fair, Dr. John C. Gilbert and Dr. Robert S. Schechter for their willingness to serve. The financial support for this work came from the Gas Research Institute and the Gas Processors Association (contract No. 5092-260-2495) and from the Separations Research Program of the University of Texas at Austin.

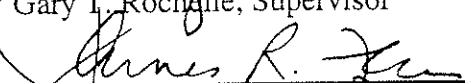
Above all, I give thanks to God Almighty the original source of all things.

CARBON DIOXIDE DESORPTION/ ABSORPTION WITH
AQUEOUS MIXTURES OF METHYLDIETHANOLAMINE
AND DIETHANOLAMINE AT 40 TO 120°C


APPROVED BY
DISSERTATION COMMITTEE:



Gary T. Rochelle, Supervisor



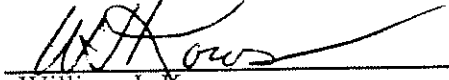
James R. Fair



John C. Gilbert



Robert S. Schechter



William J. Koros

Copyright
by
Msafiri M. Mshewa
1995

**CARBON DIOXIDE DESORPTION/ ABSORPTION WITH
AQUEOUS MIXTURES OF METHYLDIETHANOLAMINE
AND DIETHANOLAMINE AT 40 TO 120°C**

Publication No. _____

Msafiri Mmasa Mshewa, Ph.D.

The University of Texas at Austin, 1995

Supervisor: Gary T. Rochelle

Carbon dioxide absorption and desorption from aqueous solutions of alkanolamines occur by a process of mass transfer enhanced by chemical reactions in the boundary layer. Fundamental understanding of these reactions is important for efficient modeling, design and retrofitting of acid gas treating processes. Satisfactory data are available in the literature for carbon dioxide reactions with single alkanolamines at low temperatures, typical of the absorber. However, no significant data are available at stripper operating temperatures for single alkanolamines or for mixtures of alkanolamines

A laboratory wetted-wall column was designed and fabricated. Its effective mass transfer area was 37.39 cm². The wetted-wall column has mass transfer coefficient characteristics comparable to industrial units. Rates of CO₂

absorption/ desorption by aqueous solutions of methyldiethanolamine (MDEA) and diethanolamine (DEA), and mixtures of MDEA and DEA were measured in this device at 40, 80, and 120°C. The CO₂ loading in the solutions ranged from 0.01 zero to 0.50 mol/ mol amine. Carbon dioxide partial pressure ranged from 0.02 to 6.56 bar.

A mass transfer model based on approximate film theory was developed. The model incorporates chemical kinetics and equilibrium. Solution speciation was calculated by a model using the electrolyte-NRTL equation to estimate activity coefficients in the liquid phase. The mass transfer model was used in conjunction with a parameter estimation package, GREG. Lower apparent rate constants than expected were observed for both 50 wt% MDEA, 25 wt% DEA and the mixtures, especially at high temperatures.

Overall mass transfer coefficients, K_G , were calculated at all experimental conditions. At all conditions the 25 wt% DEA gave the highest values of the overall mass transfer coefficient. It was followed by 25 wt% DEA/ 25 wt% MDEA, 5 wt% DEA /45 wt% MDEA, and the lowest was 50 wt% MDEA. The highest value of K_G measured was 16.5×10^{-6} kmol/ (m²s bar) and was obtained with 25 wt% DEA at 40°C. Both the increases in temperature and CO₂ loading lowered the overall mass transfer coefficient.

Table of Contents

List of Figures	xii
List of Tables	xvi
CHAPTER ONE	1
Introduction to Gas Treating with Aqueous Alkanolamine Solutions.....	1
1.1 Acid Gases and Gas Treating	1
1.2 Gas Treating by absorption/ stripping	2
1.2.1 Chemical Solvents	2
1.2.1.1 Equilibrium Effects.....	3
1.2.1.2 Non Equilibrium Effects	4
1.2.2 Process Flow Sheet	6
1.2.3 Commercially Important Alkanolamines	8
1.3 Previous Reaction Rate Measurements	8
1.3.1 Rate Data for Methyldiethanolamine (MDEA)	8
1.3.2 Rate Data for Diethanolamine (DEA)	9
1.3.3 Rate Data for Mixed Amine (MDEA/ DEA).....	12
1.4 Objectives and Scope of this Work	13
CHAPTER TWO	15
Chemistry of CO ₂ -Alkanolamine Systems	15
2.1 Reactions of CO ₂ in Aqueous Solutions	16
2.2 CO ₂ Reactions with Tertiary Alkanolamines.....	18
2.2.1 Mechanisms	18
2.3 CO ₂ Reactions with Primary and Secondary Alkanolamines	20
2.3.1 Mechanisms	20
2.4 CO ₂ Reactions with Mixed Alkanolamines	22

CHAPTER THREE	24
Modeling	24
3.1 Physical Mass Transfer Models	24
3.1.1 Film Model	24
3.1.2 The Penetration Model	25
3.2 Bulk Phase Equilibrium	27
3.2.1 Vapor Liquid Equilibrium Model	27
3.2.2 Derivation of Equilibrium Constants	28
3.3 Interfacial Speciation	30
3.5 Parameter Estimation	33
CHAPTER FOUR	36
Experimental	36
4.1 Experimental Apparatus and Methods	36
4.1.1 Wetted-wall Column	36
4.1.2 Experimental Set Up	36
4.1.3 Mass Flow Controllers	41
4.1.3.1 Calibration of Mass Flow Controllers	41
4.1.4 Carbon Dioxide Analyzers	43
4.1.4.1 Calibration of Carbon Dioxide Analyzers	43
4.1.5 Liquid Phase Carbon Analyzer	46
4.2 Physical Calibration of Apparatus	47
4.2.1 Theory	47
4.2.2 Procedure	48
4.2.3 Dimensionless Mass Transfer Correlation	48
4.3 Reactive Absorption/ Desorption	52
4.3.1 Rate Measurements	52
4.4 Rate Kinetics from Mass Transfer Measurements	54
4.5 Chemicals	57
4.6 Gas Phase Resistance	57

CHAPTER FIVE	59
Results and Discussions	59
5.1 Rate Measurements	59
5.1.1 MDEA	59
5.1.2 DEA	63
5.1.3 DEA/ MDEA	67
5.1.3.1 5 wt% DEA/ 45 wt% MDEA	67
5.1.3.2 25 wt % DEA/ 25 wt% MDEA	71
5.2 Equilibrium Measurements	75
5.3 Temperature Effects	81
5.4 Sensitivity Analysis	84
5.5 Overall Gas Phase Mass Transfer Coefficient	86
5.5.1 Temperature Effect	87
5.5.1.1 50 wt% MDEA	87
5.5.1.2 25 wt% DEA	88
5.5.1.3 5 wt% DEA/ 45 wt% MDEA	89
5.5.1.4 25 wt% DEA/ 25 wt% MDEA	90
5.5.2 Solution Type Effect	91
5.5.2.1 Solution Type Effect at 40°C	91
5.5.2.2 Solution Type Effect at 80°C	92
5.5.2.3 Solution Type Effect at 120°C	93
CHAPTER SIX	95
Conclusions and Recommendations	95
6.1 Conclusions on Experiment	95
6.2 Conclusions on Modeling	96
6.3 Recommendations	96
APPENDIX A	97
Modeling	97
A.1 Bulk Phase Speciation	97
A.2 Interfacial Calculations	99

APPENDIX B	103
Derivation of the Liquid Film Mass Transfer Coefficient Correlation.....	103
APPENDIX C	106
Physical Properties Correlations	106
C.1 Viscosity	106
C.1.1 Viscosity of the Unloaded Solution	106
C.1.2 Viscosity of Loaded Solution	107
C.2 Density of the Solution	107
C.3 Diffusion Coefficients	108
C.4 Solubility.....	112
APPENDIX D	119
Experimental Data	119
D.1 MDEA Raw Data.....	119
D.2 DEA Raw Rate Measurements	121
D.3 DEA/MDEA Raw Rate Measurements	123
APPENDIX E	127
Main Program	127
APPENDIX F	130
Model Code and Input	130
APPENDIX G	144
Program Output	144
G.1 GREG Result for 50 wt% MDEA	145
G.1.1 Results at 40°C	145
G.1.2 Results at 80°C	147
G.1.3 Results at 120°C	149
G.2 GREG Result for 25 wt% DEA	152
G.2.1 Results at 40°C	152
G.2.2 Results at 80°C	154

G.2.3	Results at 120°C	156
G.3	GREG Result for 5 wt% DEA/ 45 wt% MDEA	159
G.3.1	Results at 40°C	159
G.3.2	Results at 80°C	162
G.3.3	Results at 120°C	163
G.4	GREG Result for 25 wt% DEA/ 25 wt% MDEA	165
G.4.1	Results at 40°C	165
G.4.2	Results at 80°C	167
G.4.3	Results at 120°C	169
APPENDIX H		173
	Detailed Program Output	173
APPENDIX I		180
	Limitations on Experimental Conditions	180
I.1	Case 1	181
I.2	Case 2	182
APPENDIX J		184
	Overall Gas Phase Mass Transfer Coefficient	184
APPENDIX K		190
	SRP Annual Report	190
	Carbon dioxide Desorption/ Absorption with Aqueous Mixtures of Methyldiethanolamine and Diethanolamine at 40 to 120°C	190
K.1	Introduction	190
K.2	Overall Gas Phase Mass Transfer Coefficient	191
K.2.1	Temperature Effect	192
K.2.2	Solution Type Effect	194
K.2.2.1	Solution Type Effect at 40°C	194
K.3	Conclusions	195

NOTATION	201
Greek Letters	204
Subscripts	205
Superscripts	205
BIBLIOGRAPHY	206
VITA	

List of Figures

Figure 1.1	Equilibrium of CO ₂ with a Physical System and Chemical System.....	5
Figure 1.2	Typical Absorber/ Stripper System for Acid Gas Removal	7
Figure 2.1	Molecular Structure of Typical Amines Used in Acid Gas Treating Processes	17
Figure 3.1	Outline of the Computer Program.	35
Figure 4.1	High Temperature Wetted-wall Column	37
Figure 4.2	Experimental Apparatus for Absorption/ Desorption of CO ₂ with Amine Solution	38
Figure 4.3	Mass Flow Meter Calibration Using a Soap Flow Meter	42
Figure 4.4	Mass Flow Meter Calibration Curve for S/N 9203HCO37102	42
Figure 4.5	Strip Chart Calibration for a Typical Experimental Set Up	45
Figure 4.6	Strip Chart Calibration Curve for the 0-1% Range CO ₂ Analyzer	45
Figure 4.7	Correlation Curve for the Liquid Film Mass Transfer Coefficient...	51
Figure 4.8	Instantaneous Enhancement Factors for 50 wt% MDEA and 25 wt% DEA	57
Figure 5.1	Comparison of Model Calculated CO ₂ Flux with Experimental Measurements for 50 wt% MDEA at 40°C	62
Figure 5.2	Comparison of Model Calculated CO ₂ Flux with Experimental Measurements for 50 wt% MDEA at 80°C	62

Figure 5.3	Comparison of Model Calculated CO ₂ Flux with Experimental Measurements for 50 wt% MDEA at 120°C	63
Figure 5.4	Comparison of Model Calculated CO ₂ Flux with Experimental Measurements for 25 wt% DEA at 40°C	66
Figure 5.5	Comparison of Model Calculated CO ₂ Flux with Experimental Measurements for 25 wt% DEA at 80°C	66
Figure 5.6	Comparison of Model Calculated CO ₂ Flux with Experimental Measurements for 25 wt% DEA at 120°C	67
Figure 5.7	Comparison of Model Calculated CO ₂ Flux with Experimental Measurements for 5 wt% DEA/ 45 wt% MDEA at 40°C	70
Figure 5.8	Comparison of Model Calculated CO ₂ Flux with Experimental Measurements for 5 wt% DEA/ 45 wt% MDEA at 80°C	70
Figure 5.9	Comparison of Model Calculated CO ₂ Flux with Experimental Measurements for 5 wt% DEA/ 45 wt% MDEA at 120°C	71
Figure 5.10	Comparison of Model Calculated CO ₂ Flux with Experimental Measurements for 25 wt% DEA/ 25 wt% MDEA at 40°C	74
Figure 5.11	Comparison of Model Calculated CO ₂ Flux with Experimental Measurements for 25 wt% DEA/ 25 wt% MDEA at 80°C	74
Figure 5.12	Comparison of Model Calculated CO ₂ Flux with Experimental Measurements for 25 wt% DEA/ 25 wt% MDEA at 120°C	75
Figure 5.13	Equilibrium Pressure for 50 wt% MDEA as a Function of CO ₂ Loading at Different Temperatures	77
Figure 5.14	Equilibrium Pressure for 25 wt% DEA as a Function of CO ₂ Loading at Different Temperatures	78

Figure 5.15	Equilibrium Pressure for 5 wt% DEA/ 45 wt% MDEA as a Function of CO ₂ Loading at Different Temperatures	78
Figure 5.16	Equilibrium Pressure for 25 wt% DEA/ 25 wt% MDEA as a Function of CO ₂ Loading at Different Temperatures	79
Figure 5.17	α as a Function of Solution Type at 80°C	80
Figure 5.18	α as a Function of Solution Type at 120°C	80
Figure 5.19	α as a Function of Loading and Solution Type at Different Temperatures	81
Figure 5.20	Temperature Dependence of Effective Rate Constants	82
Figure 5.21	Temperature Dependence of MDEA Kinetics	83
Figure 5.22	Temperature Dependence of DEA Kinetics	83
Figure 5.23	Sensitivity Analysis for 50 wt % MDEA at 120°C	85
Figure 5.24	K_G for MDEA at Different Temperatures	88
Figure 5.25	K_G for DEA at Different Temperatures	89
Figure 5.26	K_G for 5 wt% DEA/ 45 wt% MDEA at Different Temperatures.	90
Figure 5.27	K_G for 25 wt% DEA/ 25 wt% MDEA at Different Temperatures ..	91
Figure 5.28	K_G at 40°C for the Four Solutions	92
Figure 5.29	K_G at 80°C for the Four Solutions	93
Figure 5.30	K_G at 120°C for the Four Solutions	94
Figure B.1	Cross Section of the Wetted-wall Column Showing the Liquid Velocity Profile and Important Dimensions	103
Figure C.1	Diffusivity of CO ₂ in Water as a Function of Temperature, Versteeg and van Swaaij (1988c), and Tamimi et al. (1994)	110

Figure C.2. Diffusivity of N_2O in Water as a Function of Temperature, Versteeg and van Swaaij (1988c), and Tamimi et al. 1994).....	111
Figure C.3. Solubility of N_2O in Water as a Function of Temperature	114
Figure C.4 Solubility of CO_2 in Water as a Function of Temperature.....	115
Figure C.5 Solubility of N_2O in 50 wt% MDEA as a Function of Temperature, Sandall et al., (1993).	116
Figure C.6 Solubility of N_2O in 30 wt% DEA as a Function of Temperature, Sandall et al. (1993).	116
Figure K.1 K_G for 50 wt% MDEA at Different Temperatures	197
Figure K.2 K_G for 25 wt% DEA at Different Temperatures.....	197
Figure K.3 K_G for 5 wt% DEA/ 45 wt% MDEA at Different Temperatures .	198
Figure K.4 K_G for 25 wt% DEA/25 wt% MDEA at Different Temperatures .	198
Figure K.5 K_G at 40 °C for the Four Solutions	199
Figure K.6 K_G at 80 °C for the Four Solutions	199
Figure K.7 K_G at 120°C for the Four Solutions	200

List of Tables

Table 1.1	Heats of Reaction of CO ₂ with Common Alkanolamines. (Kohl and Riesenfeld, 1985)	8
Table 1.2	Summary of Methyldiethanolamine (MDEA) Kinetic Data	10
Table 1.3	Literature Data on the Reaction Between CO ₂ and Aqueous DEA.	11
Table 1.4	Literature Data on the Reaction Between CO ₂ and Aqueous Blended Amine, MDEA/ DEA.	13
Table 3.1	Correlation for Equilibrium Constant Expression	29
Table 4.1	Ranges of Brooks Mass Flow Controllers	43
Table 4.2	Mass Transfer Coefficient Calibration Data	50
Table 4.3	Regression results for the mass transfer coefficient correlation	51
Table 4.4	Conditions for Absorption/ Desorption of CO ₂ into Concentrated Alkanolamine Solutions.....	52
Table 4.5	Instantaneous Enhancement Factors for Some Specific Conditions	56
Table 4.6	Gas Phase Mass Transfer Coefficient Estimation	58
Table 5.1.	Rate Data for MDEA. Initial Unloaded MDEA Solution is 50 wt%.	60
Table 5.2.	Rate Data for DEA. Initial Unloaded DEA Solution is 25 wt% DEA	64

Table 5.3.	Rate Data for DEA/MDEA . Initial Unloaded Solution is 5 wt%	
	DEA/ 45 wt% MDEA	68
Table 5.4.	Rate data for DEA/MDEA. Initial Unloaded Solution is 25 wt%	
	DEA/ 25 wt% MDEA	72
Table 5.5	Equilibrium Pressure Over Amine Solutions	76
Table 5.6	Sensitivity Analysis at 120°C	85
Table C.1	Some Properties of the Solution Components	108
Table C.2	Diffusivity of CO ₂ in Water Used for Correlation Development ..	109
Table C.3	Diffusivity of N ₂ O in Water Used for Correlation Development .	110
Table C.4	Solubility of N ₂ O in Water.....	113
Table C.5	Solubility of CO ₂ in Water.....	114
Table C.6	Effect of CO ₂ Loading on Solubility.....	118
Table D.1	Rate Data for MDEA. Initial Unloaded Solution is 50 wt%	
	MDEA at 40°C.	119
Table D.2	Rate Data for MDEA. Initial Unloaded Solution is 50 wt%	
	MDEA at 80°C.	120
Table D.3	Rate Data for MDEA. Initial Unloaded Solution is 50 wt%	
	MDEA at 120°C.	120
Table D.4	Rate Data for DEA. Initial Unloaded DEA Solution is 25 wt%	
	DEA at 40°C.	121
Table D.5	Rate Data for DEA. Initial Unloaded DEA Solution is 25 wt%	
	DEA at 80°C.	122
Table D.6	Rate Data for DEA. Initial Unloaded DEA Solution is 25 wt%	
	DEA at 120°C.	122

Table D.7	Rate Data for DEA/ MDEA. Initial Unloaded Solution is 5 wt% DEA/ 45 wt% MDEA at 40°C.....	123
Table D.8	Rate Data for DEA/ MDEA. Initial Unloaded Solution is 5 wt% DEA/ 45 wt% MDEA at 80°C.....	124
Table D.9	Rate Data for DEA/ MDEA. Initial Unloaded Solution is 5 wt% DEA/ 45 wt% MDEA at 120°C.....	124
Table D.10	Rate Data for DEA/ MDEA. Initial Unloaded Solution is 25 wt% DEA/ 25 wt% MDEA at 40°C.	125
Table D.11	Rate Data for DEA/ MDEA. Initial Unloaded Solution is 25 wt% DEA/ 25 wt% MDEA at 80°C.	125
Table D.12	Rate Data for DEA/ MDEA. Initial Unloaded Solution is 25 wt% DEA/ 25 wt% MDEA at 120°C.	126
Table J.1	Overall Mass Transfer Coefficient	184
Table K.1	Apparent Rate Constant	196
Table K.2	Equilibrium Pressure Over Amine Solution	196

CHAPTER ONE

Introduction to Gas Treating with Aqueous Alkanolamine Solutions

1.1 ACID GASES AND GAS TREATING

The removal of acid gases from gas streams, commonly referred to as acid gas treating, and also as gas sweetening, is an important industrial process. Acid gases, primarily hydrogen sulfide (H_2S) and carbon dioxide CO_2 , are constituents of a variety of sour gas mixtures including natural gas, synthesis gas, flue gas, and various refinery streams. In addition, CO_2 is a by-product of ammonia and hydrogen manufacture. Normally, H_2S must be nearly completely removed from a gas stream due to its toxicity and corrosiveness, and to avoid catalyst poisoning in refinery operations. Carbon dioxide is removed from natural gas because it acts as a diluent, increasing transportation costs and reducing the energy value per unit volume of gas. Carbon dioxide is separated from reformer product gas in the production of ammonia because it poisons synthesis catalyst in the ammonia converter.

Hydrogen sulfide or CO_2 concentrations in the mentioned gas streams vary widely, from several parts per million to 50 percent by volume of the gas stream. Cleanup specifications also vary widely depending on the process and nature of the impurity. Astarita et al. (1983) provide a more comprehensive summary of major industrial processes that require gas treating as well as common cleanup specifications.

The primary operation of acid gas treating processes generally falls into one of the three categories (Kohl and Riesenfeld, 1985): absorption into liquid; adsorption on a solid; and chemical conversion to another compound. This work falls under the category of absorption into liquid.

1.2 GAS TREATING BY ABSORPTION/ STRIPPING

1.2.1 Chemical Solvents

Aqueous solutions of alkanolamines are widely used in absorption/ stripping operations to separate H_2S and CO_2 from source gas streams. Absorption/ stripping of acid gases with aqueous alkanolamine solvents is characterized as mass transfer enhanced by chemical reaction; following absorption into aqueous solution the acid gases react either directly or through an acid-base buffer mechanism with the alkanolamines to form nonvolatile ionic species. Mass transfer of acidic gases from the bulk gas to a bulk liquid phase in which chemical reaction occurs, such as an aqueous alkanolamine solution, can be described as follows (Astarita, 1967):

(1) Diffusion of one or more acidic components from the bulk gas phase to the gas-liquid interface followed by absorption into the liquid. Physical equilibria are normally assumed for molecular species at the gas-liquid interface.

(2) Diffusion and convection of the reactants from the gas-liquid interface to the bulk liquid phase.

(3) Reaction between the dissolved gas and the liquid reactant in the liquid phase occurs simultaneously with mass transfer,.

(4) Diffusion of the reaction products into the bulk liquid phase due to concentration gradients created by the chemical reactions.

The use of aqueous alkanolamine solutions for gas treating results in two important effects that make these solutions preferable to physical solvents for gas absorption. These are equilibrium effects and non equilibrium effects. We will review each of these effects separately.

1.2.1.1 Equilibrium Effects

The presence of an alkanolamine drastically affects the solubility of an acid gas in water. Acid gases in the vapor phase come to equilibrium (phase) with the unreacted molecular form of the same acid gas in water. That is, at equilibrium, the solubility of an unreacted acid in an aqueous solution containing a reactive solvent is a function of the partial pressure of that gas above the liquid. If the gas reacts in the aqueous phase to form nonvolatile products, then additional gas can be solubilized at a given acid gas partial pressure. As a result, alkanolamines significantly enhance the solubility of acid gases in the aqueous phase.

Consider the expression for the mass transfer rate in terms of the overall gas-phase mass transfer coefficient:

$$R = \frac{P - P^*}{\frac{1}{k_G} + \frac{H}{E k_L^o}} = K_G (P - P^*) \quad (1.1)$$

For the moment, let us concentrate on the driving force $(P - P^*)$. Where, P^* is the equilibrium partial pressure corresponding to the concentration of acid gas in solution. For a given concentration of acid gas, we obtain the equilibrium

partial pressure from the solution of an equilibrium model. The effect of a chemical reaction is to lower this equilibrium partial pressure for a particular concentration of acid gas in solution, thus increasing the driving force for absorption.

We take, for example, the CO_2 -DEA-MDEA system and compare it to CO_2 in water. The CO_2 -water case is represented by the first case in Figure 1.1 (Astarita et al., 1983), whereby the molecular CO_2 in the liquid phase is in equilibrium with the vapor-phase and other ionic species in the liquid phase. In this case of CO_2 in water, the ionic equilibria may be neglected under most conditions. For the CO_2 -DEA-MDEA system, the behavior is that of the second case. In this case, the concentration of CO_2 in chemically combined forms is significant, and dominates at all but extremely high loading, well beyond the validity of the equilibrium models used here.

The ramifications of this behavior on the equilibrium partial pressure of CO_2 as a function of the CO_2 concentration in the liquid phase is such that the reactions between CO_2 and basic species greatly decrease this equilibrium partial pressure, and would therefore increase the driving force for the absorption rate of the acid gases relative to the non-acid gases such as methane, which do not react with the amines.

1.2.1.2 *Non Equilibrium Effects*

We saw in the last section that chemical reaction can have a profound influence on the solubility of reactive gases in solution. This will in turn affect the absorption rate by increasing the driving force for absorption. However, the

primary objective of this work is to understand the non equilibrium, or rate, phenomena associated with the alkanolamine-based acid gas treating processes.

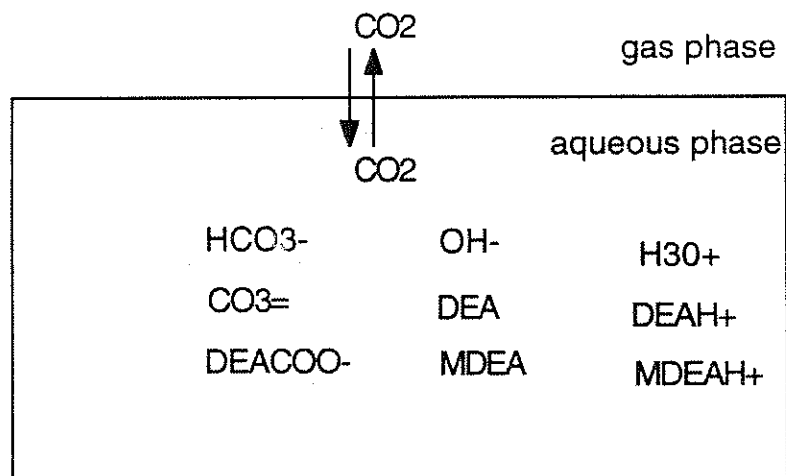
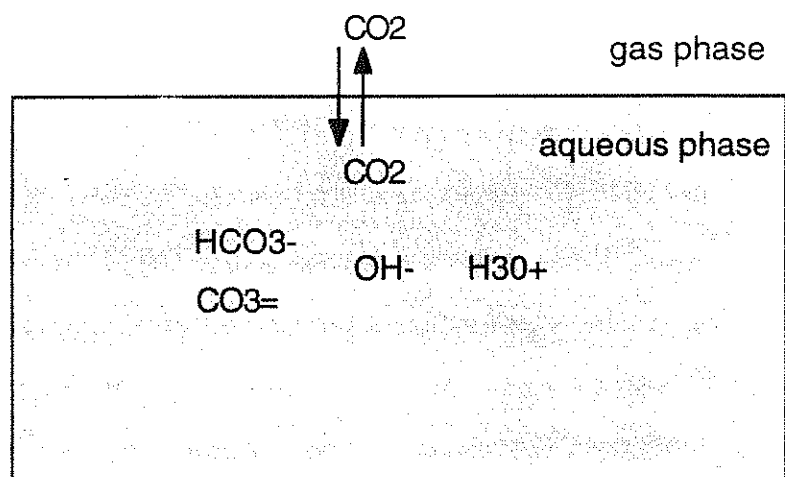


Figure 1.1 Equilibrium of CO_2 with a Physical System and Chemical System

This type of information is necessary for the rate-based approach to acid gas treating (Astarita et al., 1983; Seader, 1989). Consider the transport Equation (1.1). This expression is equivalent to the standard expression for physical absorption except for the presence of the parameter E , the enhancement factor, which is defined as the ratio of the rate of absorption with reaction to that without reaction. For a given concentration of acid gas species in solution, the equilibrium model will provide the equilibrium partial pressure, P^* . However, it is the rate model which must provide the enhancement factor. Chemical reactions can create very steep gradients in the concentration profiles of absorbing species in the liquid at the gas-liquid interface. This further enhances the rate of absorption of the acid gases into the aqueous solution.

1.2.2 Process Flow Sheet

A general process schematic for removing acid gases is depicted in Figure 1.2. A feed gas consisting typically of hydrocarbons along with the acidic components is contacted countercurrently in a packed or plate column with the aqueous solution. The "sweet gas" comes out from the top of the absorption column. The loaded solution may be carried through a flash tank in order to recover any of the hydrocarbons. The solution is then fed to the stripper where it is heated at slightly above ambient pressure. Energy is provided to the reboiler for two reasons:

(1) to produce enough water vapor so that the vapor phase partial pressure of CO_2 is low enough to provide a driving force for desorption, and

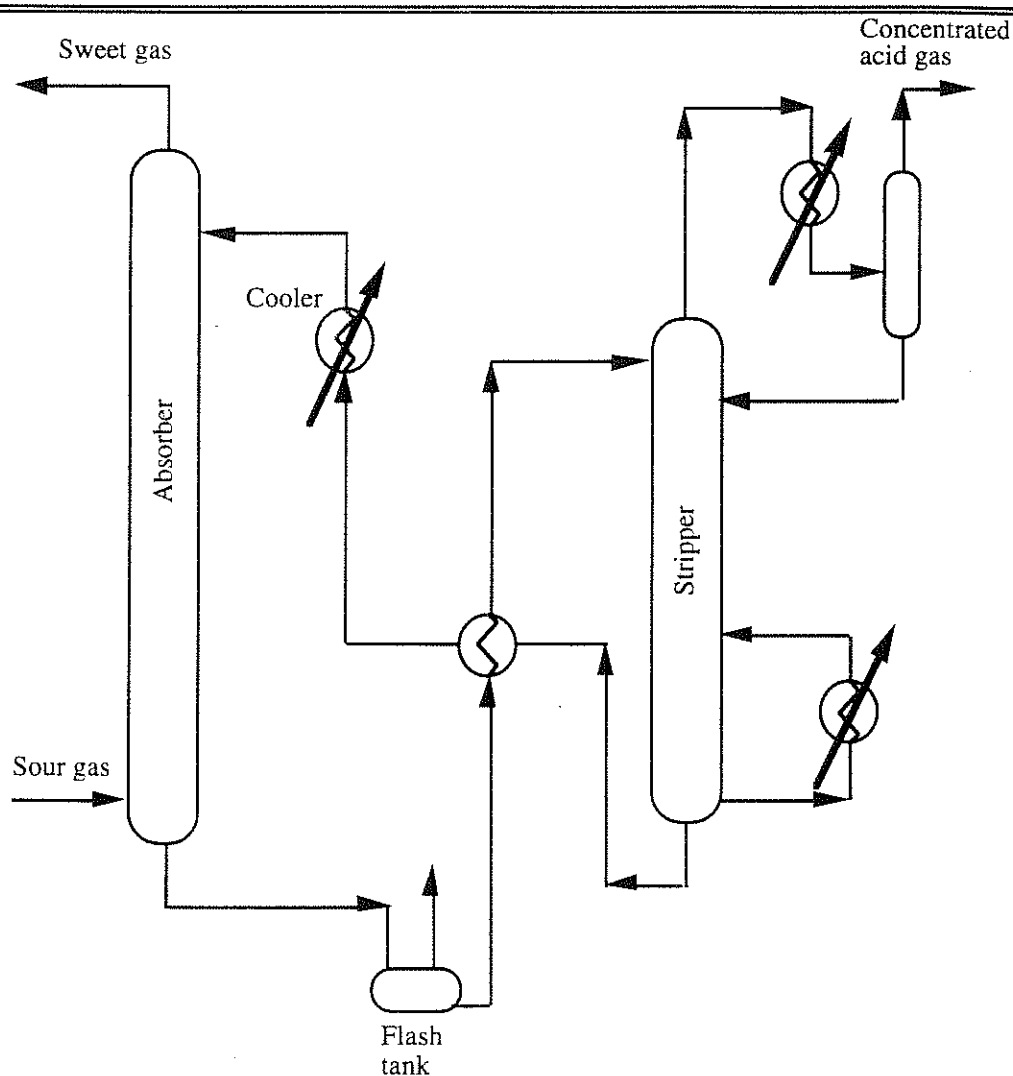


Figure 1.2 Typical Absorber/ Stripper System for Acid Gas Removal

(2) to provide enough energy to reverse the reactions which occurred in the absorber. In fact, the reactions of CO_2 with aqueous alkanolamine solutions are highly exothermic (see Table 1.1), releasing energy in the absorber and requiring energy in the stripper. Reboiler heat duty is the most significant

operating cost of this type of system (Blauwhoff et al., 1985). It is desirable, therefore, to find solvents and/ or operating modes which reduce this reboiler heat duty.

1.2.3 Commercially Important Alkanolamines

Alkanolamines are characterized as containing both hydroxyl groups and amino groups. The hydroxyl groups serve to reduce vapor pressure and increase water solubility while the amino group provides the necessary alkalinity in aqueous solution to react with acid gases (Kohl and Riesenfeld, 1985).

Monoethanolamine (MEA), a primary amine, and diethanolamine (DEA), a secondary amine, have been the most widely employed gas treating alkanolamine agents during the last several decades (Kohl and Riesenfeld, 1985). Other commercially important alkanolamines include diglycolamine, DGA[®], and methyldiethanolamine, MDEA. Monoethanolamine (MEA), DEA, and DGA[®] react directly with CO₂ primarily to form carbamates of the respective amines. These are rapid, but finite rate, reactions.

Table 1.1 Heats of Reaction of CO₂ with Common Alkanolamines. (Kohl and Riesenfeld, 1985)

Amine	ΔH_{RXN} (kcal/gmol CO ₂)
DEA	16.0
DGA	20.8
MDEA	11.6

1.3 PREVIOUS REACTION RATE MEASUREMENTS

1.3.1 Rate Data for Methyldiethanolamine (MDEA)

The rate data for MDEA, the most significant commercial tertiary amine, are summarized in Table 1.2. The apparent second order rate constants vary by a

factor of 2 depending on the authors. This range of discrepancy does not seem large, and is to some extent a function of experimental conditions. A discussion of the chemistry of this system is presented in the next chapter.

1.3.2 Rate Data for Diethanolamine (DEA)

Because DEA is widely used, the literature data is extensive. The review of Blauwhoff et al. (1984) has been extended to include more recent data (Table 1.3). However, there is general disagreement as to the order and rate of reaction with respect to DEA. The zwitterion mechanism (to be discussed in the next chapter), with its ability to allow the order of reaction to vary with changing conditions, does help to reconcile the existing data.

Table 1.2 Summary of Methyldiethanolamine (MDEA) Kinetic Data

Reference	T (K)	[MDEA] ($\frac{\text{kmol}}{\text{m}^3}$)	[PCO ₂] (atm)	k _{Tref} ($\frac{\text{m}^3}{\text{kmol} \cdot \text{s}}$)	T _{ref}	E _a ($\frac{\text{kcal}}{\text{gmole}}$)	method
Barth et al. (1981)	293-313	0.02-0.2	0.003-0.03	2.85	298		stopped-flow
Barth et al. (1984)	293	0.02-0.2	0.003-0.03	3.2	298		stopped-flow
Blauwhoff et al. (1984)	298	0.45-1.6	<1	4.8	298		stirred tank
Yu et al. (1985)	313-333	0.25-2.5	1	12.1	313	9.2	stirred tank
Tomcej et al. (1986)	298-348	1.7-3.4				9.7	single sphere
Critchfield and Rochelle (1987)	282-350	1.7	1	2.53	298	13.7	stirred tank
Haimour et al. (1987)	288-308	0.85-1.7	<1	2.35	298	17.1	stirred tank
Versteeg and van Swaaij(1988b)	293-333	0.2-3	<1	4.4 5.1*	298	10.1	stirred tank
Toman and Rochelle (1989)	298-308	4.3	0.02-0.12	5.5	298		stirred tank
Tomcej and Otto (1989)	298-348	1.6 -3.4	0.95	5.37	298	10.2	single sphere
Glasscock(1990)	298	1.7	0.1-1	3 - 10	298	6.5 -10	stirred tank and data regression
Littel et al. (1990)	298	0.2-2.7	< 1	5.2	298	11.5	stirred tank
Cordi and Bullin (1992)		1.7-3.4	1	2.1		15.7	stirred tank

* The second order reaction rate constant as reinterpreted by Littel et al. (1990)

Table 1.3 Literature Data on the Reaction Between CO₂ and Aqueous DEA.

Reference	T (K)	[DEA] ($\frac{\text{kmoles}}{\text{m}^3}$)	$k_1 = \frac{r}{\text{CO}_2}$ [s ⁻¹]	Ea ($\frac{\text{kJ}}{\text{mole}}$)	method
Van Krevelen and Hofijzer (1948)	292- 329	0.05 -3.0	260 [DEA] ²		Packed column
Jensen et al. (1954)	291	0.1,0.2	5080 [DEA]		competitive reaction with 0.1,0.2M NaOH
Nunge and Gill (1963)	302.4- 313.6	0.17-4.63	$k^*[\text{DEA}]^2$	54.4	stirred reactor
Leder (1971)	353		$1.78 \times 10^5 [\text{DEA}]$	43.9	stirred cell
Coldrey and Harris (1976)	292	0.1-1.0	$\frac{430[\text{DEA}] + 1000[\text{OH}^-]^{1/2} \cdot 60([\text{DEAH}] + [\text{Product}])}{[\text{DEA}][\text{CO}_2]}$ 1340[DEA]		Rapid mixing techniques
Sada et al. (1976)	25	0.249- 1.922			Laminar jet
Hikita et al. (1977)	278.8 - 313	0.174- 0.719	$10^{(12.41 - \frac{2775}{T})} * [\text{DEA}]^2$		rapid mixing technique with 0.002-0.005 M NaOH
Alvarez-Fuster et al. (1980)	293	0.25-0.82	840[DEA] ²		wetted wall column
Laddha and Danckwerts (1981)	298	0.46-2.88	$\frac{[\text{DEA}]}{\frac{1}{1410} + \frac{1}{1200[\text{DEA}]}}$		stirred cell
Laddha and Danckwerts (1982)	284	0.5-2.0	$\frac{[\text{DEA}]}{\frac{1}{890} + \frac{1}{1560[\text{DEA}]}}$		stirred cell
Barth et al. (1983)	298	0.00111- 0.084	$110 \pm 15 \text{ M}^{-1} \text{s}^{-1}$ at 298K		stopped Flow
Blauwhoff et al. (1984)	298	0.509- 2.308	$\frac{[\text{DEA}]}{\frac{1}{k_2} + \frac{1}{5.34 \times 10^{-6}[\text{H}_2\text{O}] + 7.05 \times 10^{-2}[\text{OH}^-] + 0.228 \times 10^{-3}[\text{DEA}]}}$		stirred cell
Blanc and Demarais (1984)	293- 333	.005-4.0	$10^{(10.4493 - \frac{2274.5}{T})} * [\text{DEA}]$	10.5	wetted wall column

Table 1.3 Continued

Reference	T (K)	[DEA] ($\frac{\text{kmol}}{\text{m}^3}$)	$k_1 = \frac{r}{\text{CO}_2}$ [s ⁻¹]	Ea ($\frac{\text{kJ}}{\text{mole}}$)	method
Savage and Kim (1985)	45	2-3	$k[\text{DEA}]^{1.13}$		single sphere absorber
Barth et al. (1986)	298	0.0192- 0.0212	$110(\pm 15)[\text{DEA}]$	23.2	stopped flow
Versteeg and van Swaaij -1988a	298		$\frac{[\text{DEA}]}{k_2 + 3.7 \times 10^{-6}[\text{H}_2\text{O}] + 8.52 \times 10^{-2}[\text{OH}^-] + 0.479 \times 10^{-3}[\text{DEA}]}$ $k_2 > 7.3 \text{ m}^3/\text{mol-s}$		stirred vessel
Versteeg and Oyeveaar (1989)	298	0.086- 4.358	$\frac{[\text{DEA}]}{(0.309 + \frac{1}{1.71 \times 10^{-6}[\text{H}_2\text{O}] + 7.07 \times 10^{-4}[\text{DEA}]})}$		
Glasscock et al. (1991)	298 - 313	0.5 - 3.0	$0.03(\pm 19\%)[\text{DEA}][\text{H}_2\text{O}] + 18.5(\pm 10\%)[\text{DEA}]^2$		Regression

1.3.3 Rate Data for Mixed Amine (MDEA/ DEA)

Glasscock (1990) and Critchfield (1988) have measured absorption rates of CO₂ into mixtures of MDEA and DEA up to DEA concentrations of 30 mol% in 2 M amine solution. Littel et al. (1992) reported kinetic data in a mixture of 0.5 M DEA and 2 M MDEA. Rangwala et al. (1992) measured rates of absorption in blends of TEA/ MEA and MDEA/ MEA. Their highest concentration for MDEA/MEA was 24.7 wt%/ 15.6 wt%. A summary of the available previous work for MDEA/DEA mixtures is presented in Table 1.4.

Table 1.4 Literature Data on the Reaction Between CO₂ and Aqueous Blended Amine, MDEA/ DEA.

Reference	T (K)	[DEA]/[MDEA] (M)	$k_1 = \frac{r}{CO_2}$ [s ⁻¹]	method
Critchfield (1988)	298	5-30% DEA in 2M total	$r = \frac{[DEA]([CO_2] - [CO_2]_e)}{\left(\frac{1}{1410} + \frac{1}{1200[DEA] + 2326[DEA]}\right)}$	stirred cell
Glasscock (1990)	313	0.1 / 0.9; 0.3/0.7	$[DEA](4.75[H_2O] + 464[DEA] + 468[MDEA])$	stirred cell
Littel et al. (1992)		0.2-0.5M DEA/ 1-3M MDEA	$\frac{1}{3.13 + 1.68 \times 10^{-6}[H_2O] + 7.23 \times 10^{-4}[DEA] + 3.54 \times 10^{-4}[MDEA]}$	stirred cell
Chakravarti (1992)	298, 313	50 wt% total amine of molar ratios 10% DEA/90% MDEA; 50 wt% MDEA/50 wt% MDEA	$[DEA](15.8 \pm 23\%)[H_2O] + 32.7 \pm 155\%[MDEA]$	wetted wall column

1.4 OBJECTIVES AND SCOPE OF THIS WORK

Most of the previous work has covered the range of temperatures that is typical of the absorber, that is between 40°C and 60°C. No experimental investigation of CO₂ absorption and desorption in alkanolamines or mixtures thereof at stripper operating temperature (110°C to 120°C) has been done.

Most of the previous work has been on low MDEA and DEA concentrations. Very few rate measurements have been made at higher amine concentrations. High concentrations like 50 wt% alkanolamine becomes significant in operations that will utilize MDEA only or mixtures of DEA and MDEA. Industrial concentration for DEA is limited to about 25 wt% due to corrosion effects.

There were three main objectives of this work. The first was to design and construct a mass transfer apparatus for measurements of carbon dioxide

absorption and desorption in the alkanolamine solutions. The second, to perform the experiments with concentrated solutions at higher temperatures typical of the stripper. The Third, model the absorption/desorption process and use the model in estimation of kinetic parameters.

A laboratory wetted wall column was used as a mass transfer apparatus to collect high temperature data on CO₂ absorption/ desorption into concentrated MDEA, DEA and mixtures of MDEA and DEA solutions. These data can be used as is for industrial calculations because the mass transfer characteristics of the laboratory wetted wall column falls in the range of the industrial equipment. Thus, this work will report the overall mass transfer coefficients under widely varying conditions.

CHAPTER TWO

Chemistry of CO₂-Alkanolamine Systems

The fundamental mechanism for the reaction of CO₂ with alkanolamines is still not fully understood; however, much progress has been made in accumulating rate data and developing kinetic expressions which can represent the experimental data reasonably well. Within the context of alkanolamines, the most distinguishing characteristic separating the reactants is the number of carbon-containing groups attached to the nitrogen atom. The amine is referred to as a primary, secondary or tertiary amine if one, two or three carbon-containing groups are attached to the nitrogen atom, respectively.

Figure 2.1 shows the molecular structure of amines one often finds discussed in the literature. The primary amines MEA and DGA are noted for their fast reaction rates with CO₂. The secondary amines DEA and diisopropanolamine (DIPA) have intermediate reaction rates, and finally triethanolamine (TEA) and MDEA, being tertiary amines, have much slower reaction rates with CO₂. Historically, TEA was the first alkanolamine used in the gas processing industry (Kohl and Reisenfeld, 1985). It has, however, been largely replaced by the primary and secondary amines for bulk CO₂ removal, and MDEA for selective H₂S removal. Mixed amine systems can also be used for bulk CO₂ removal. While TEA has properties similar to MDEA, it has a larger molecular weight, hence, a larger weight fraction of TEA is required to accomplish the same task as MDEA. It must also be mentioned that the traditional aqueous alkanolamine

systems must now compete with combined physical solvent/amine systems and the so-called hindered amines for many applications. A hindered amine, an example of which is 2-amino 2-methylpropanol (AMP) shown in Figure 2.1, is defined as "a primary amine in which the amino group is attached to a tertiary carbon atom, or a secondary amine in which the amino group is attached to a secondary or a tertiary carbon atom" (Sartori and Savage, 1983).

The purpose of this chapter is to review the existing literature on reaction rates of CO₂ with amines and discuss the possible mechanisms from which kinetic expressions can be derived. The development of a kinetic mechanism is, of course, a prerequisite to the mass transfer/ reaction modeling of CO₂ with amine systems.

2.1 REACTIONS OF CO₂ IN AQUEOUS SOLUTIONS

In aqueous solution CO₂ reacts with hydroxide and water to form bicarbonate and carbonic acid, respectively:



The water reaction is usually negligible compared to the hydroxide reaction for alkaline solutions. However, it has been shown conclusively to be catalyzed by "anions of weak acids or by molecules having a high affinity for protons" (Sherwood et al., 1975).

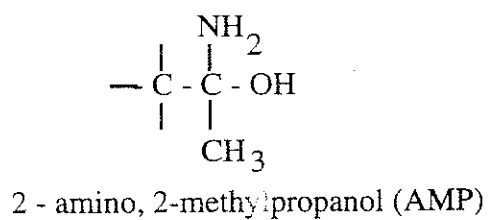
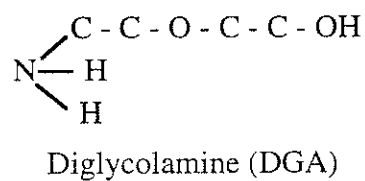
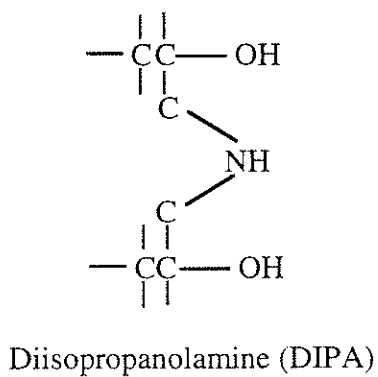
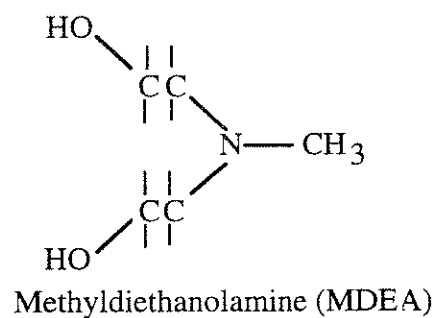
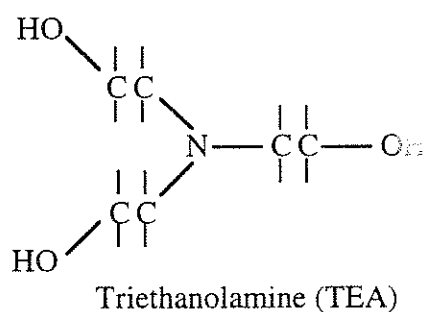
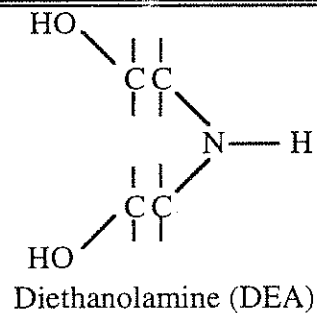
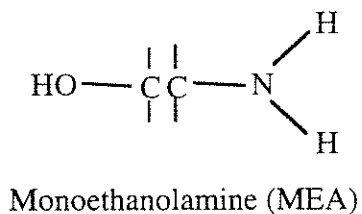


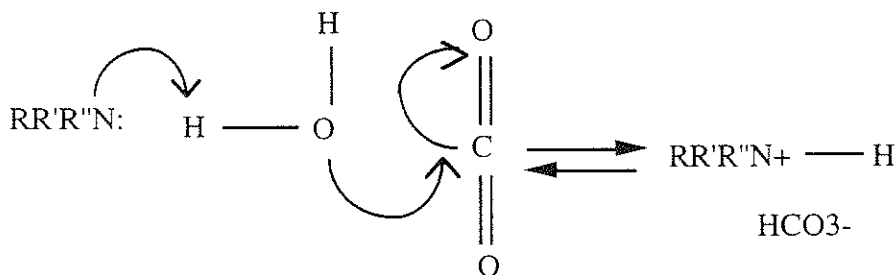
Figure 2.1 Molecular Structure of Typical Amines Used in Acid Gas Treating Processes

2.2 CO₂ REACTIONS WITH TERTIARY ALKANOLAMINES

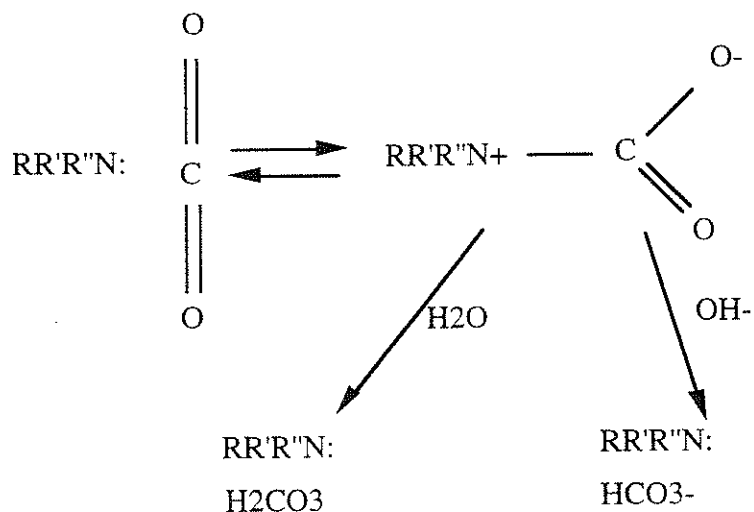
2.2.1 Mechanisms

Some of the early research into tertiary amines was concerned with whether or not the enhanced CO_2 absorption rate could be explained by the hydroxide reaction (Barth et al., 1981; Jorgensen and Faurholt, 1954; Jorgensen, 1956). It has been demonstrated by numerous authors that this reaction alone does not account for the enhanced absorption rates. It has been proposed, however, that the amine serves to catalyze the CO_2 hydrolysis reaction rate. This is not the only possibility, however. Barth et al. (1981) provide an enlightening discussion of the possible mechanisms for the reaction of CO_2 with alkanolamines, and the following mechanistic discussion follows their work.

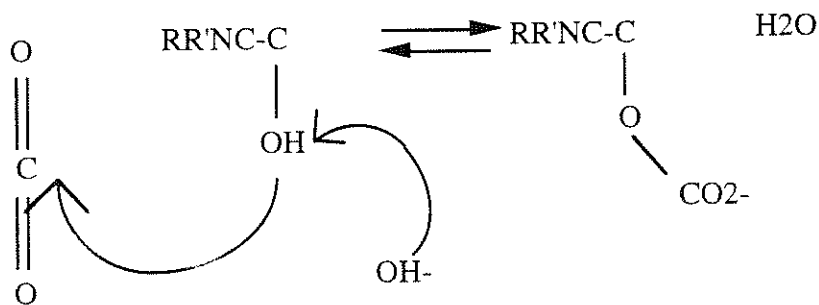
The most common theory is that the amine enhances the reaction rate of CO_2 by a homogeneous catalytic effect:



However, two other possibilities exist which should not be ignored. The first is the possibility of forming an intermediary such as in the zwitterion mechanism.



The other possibility is the formation of alkylcarbonates, which is generally considered unlikely except in solutions of very high pH (Blauwhoff et al., 1984):



Methyldiethanolamine (MDEA) is currently being studied with fervor due to its industrial significance (Barth et al., 1981; Critchfield, 1988; Haimour et al., 1987; Haimour and Sandall, 1984; Hikita et al., 1977; Tomcej et al., 1986; Tomcej and Otto, 1989; Versteeg and van Swaaij, 1988b; Yu et al., 1985). Its widespread use is due to the fact that it has a relatively low heat of reaction with

CO₂, as compared with DEA and MEA, and it can be used for selective H₂S removal since its reaction rate with CO₂ is relatively slow. There is much discrepancy in the literature for the reaction rate of CO₂ with MDEA, most likely due to the fact that the reaction mechanism is more complex than that which most authors assume. The generally accepted mechanism for the reaction of CO₂ with MDEA is a base catalysis of the direct reaction of CO₂ with water ending with formation of bicarbonate:



In order to explain both absorption and desorption, reversibility of the reactions should be considered. The appropriate rate expression is

$$\text{Rate} = ([\text{CO}_2] - [\text{CO}_2]_e)[\text{MDEA}]_i k_{\text{MDEA}} \quad (2.4)$$

The variable $[\text{CO}_2]_e$ refers to the CO₂ concentration in chemical equilibrium with HCO₃⁻. The effective second order rate constant k_{MDEA} was regressed from the absorption and desorption data for 50 wt% MDEA.

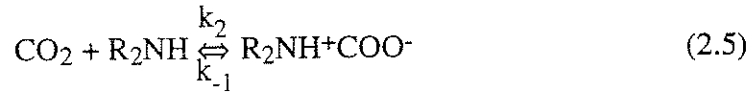
2.3 CO₂ REACTIONS WITH PRIMARY AND SECONDARY ALKANOLAMINES

2.3.1 Mechanisms

Before covering the specific amine systems, it would be advantageous to discuss the mechanism for the reaction of CO₂ with alkanolamines in general. There has been much disagreement as to the mechanism and the order of reaction. Caplow (1968) presented a hypothesized mechanism for the carbamate formation involving the formation of an intermediate zwitterion (a locally ionic, net neutral, molecule). Danckwerts (1979) introduced this mechanism into the chemical

engineering literature, and Blauwhoff et al. (1984) showed that this mechanism reconciled much of the data in the literature, especially for DEA. Critchfield and Rochelle (1987) introduced reversibility into this mechanism, which must necessarily be included for one to describe both absorption and desorption conditions. Presented below is a derivation of the mechanism, leading to a rate law describing the rate of reaction of CO₂ with primary or secondary amines.

Consider the two-step zwitterion mechanism:



The b_i term designates any species in solution that can act as a base to abstract the proton from the zwitterion in the second reaction step. The first step in describing the rate for this reaction is to assume a pseudo-steady state concentration for the zwitterion (consistent with the evidence that the zwitterion intermediate has a very short lifetime (Johnson and Morrison, 1972)):

$$\frac{\partial[Z]}{\partial t} = k_2[\text{CO}_2][\text{R}_2\text{NH}] + \sum k_{-b_i}[\text{R}_2\text{NCOO}^-][b_i\text{H}^+] - k_{-1}[Z] - \sum k_{b_i}[Z][b_i] = 0 \quad (2.7)$$

The summation is over all of the bases in solution. We can solve for the zwitterion concentration:

$$[Z] = \frac{k_2[\text{CO}_2][\text{R}_2\text{NH}] + \sum k_{-b_i}[\text{R}_2\text{NCOO}^-][b_i\text{H}^+]}{k_{-1} + \sum k_{b_i}[b_i]} \quad (2.8)$$

The rate of reaction of CO₂ via the zwitterion mechanism is given by Equation 2.9:

$$r_{\text{CO}_2, \text{zwit}} = k_2[\text{CO}_2][\text{R}_2\text{NH}] - k_{-1}[\text{Z}]$$

$$r_{\text{CO}_2, \text{zwit}} = \frac{[\text{CO}_2][\text{R}_2\text{NH}] - \frac{k_{-1}}{k_2}[\text{R}_2\text{NCOO}^-] \frac{\sum k_{b_i}[\text{b}_i\text{H}^+]}{\sum k_{b_i}[\text{b}_i]}}{\frac{1}{k_2} + \frac{k_{-1}}{k_2 \sum k_{b_i}[\text{b}_i]}} \quad (2.9)$$

It is also possible to write Equation 2.9 in terms of the equilibrium concentration of CO₂, [CO₂]_e, as opposed to using the reverse rate constants (Critchfield, 1988):

$$r_{\text{CO}_2, \text{zwit}} = \frac{[\text{R}_2\text{NH}] \{ [\text{CO}_2] - [\text{CO}_2]_e \}}{\frac{1}{k_2} + \frac{k_{-1}}{k_2 \sum k_{b_i}[\text{b}_i]}} \quad (2.10)$$

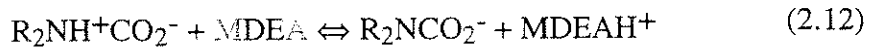
In analyzing the pure DEA data all the constants are combined into an effective rate constant, k_{DEA} , with the rate represented as:

$$\text{rate} = \{ [\text{CO}_2] - [\text{CO}_2]_e \} [\text{DEA}] k_{\text{DEA}} \quad (2.11)$$

where [CO₂]_e is the concentration of CO₂ that would be in chemical equilibrium with carbamate, protonated amine and free amine.

2.4 CO₂ REACTIONS WITH MIXED ALKANOLAMINES

CO₂ reactions with mixed amines involves all the above reactions specific to MDEA and DEA systems. In addition, MDEA will be an extra basic species in solution capable of abstracting a proton off the zwitterion ion. Thus, the following additional reaction has to be considered.



The rate expression for mixed amines becomes:

$$\begin{aligned} \text{rate} = & ([CO_2] - [CO_2]_e)[MDEA]_i k_{MDEA} + \\ & ([CO_2] - [CO_2]_e)[DEA]_i \{k_{DEA} + k_{DEA MDEA}[MDEA]_i\} \end{aligned} \quad (2.13)$$

A discussion will follow in Chapter 3 to describe how these rate equations are implemented into the mass transfer model.

CHAPTER THREE

Modeling

3.1 PHYSICAL MASS TRANSFER MODELS

3.1.1 Film Model

The simplest theory for the transport of mass from the gas-liquid interface into a bulk liquid is the widely used film theory. In this model, the resistance to mass transfer is assumed to lie in a stagnant film adjacent to the interface. The film is postulated to be of constant thickness, Z , and sufficiently thin such that steady-state molecular diffusion occurs within it. At distances from the interface greater than that corresponding to the film thickness, the liquid is assumed to be well mixed and of uniform composition. Integration of the diffusion equation, subject to the boundary condition of a fixed driving force (ΔC_A) and steady-state conditions yields the following expression for the flux, N_A :

$$N_A = \frac{D_A}{Z} \Delta C_A = k_{LA}^o \Delta C_A \quad (3.1)$$

Note that if this model actually reflected physical reality, k_{LA}^o would be proportional to the first power of the diffusion coefficient, D_A of the species, whereas in reality it is usually found to be proportional to a power of D_A much closer to one-half than to one (Danckwerts, 1970). The usefulness of the concept, however, was that it provided a basis for the definition of the liquid-side film coefficient which could be used in gas absorption tower design (Vivian and

Peaceman, 1956). Furthermore, the model can and does provide very accurate results in many situations (Sherwood, 1975) and because of its simplicity, is useful for analyzing the effects of other complicating factors such as that of simultaneous chemical reaction occurring near the interface. Additionally, the film model serves as a limiting case for hybrid theories which combine this and other models .

3.1.2 THE PENETRATION MODEL

A more realistic model describing the nature of resistance of the liquid phase to mass transfer was developed by Higbie (1935). The model is one that describes the unsteady diffusion of a species into a liquid element of effectively infinite depth, after it is suddenly exposed to a step change in concentration at the interface. As opposed to the film theory, in which molecular diffusion is assumed to occur in series spacially with turbulent transfer, over the time frame for which the mathematical model describing the penetration theory is defined, unsteady molecular diffusion is considered to be the only operative mass transfer mechanism. The process is completed at the end of the exposure period when the fluid element is remixed with the remaining bulk liquid. Assuming the time of exposure to a fixed surface concentration is equal to t , the diffusion equation can be integrated to give the following expression for the flux:

$$N_A = \sqrt{\frac{4D_A}{\pi t}} \Delta C_A \quad (3.2)$$

where the proportionality constant between flux and driving force is the time average mass transfer coefficient over the period. It is clear that the mass transfer

coefficient is proportional to the square root of the diffusion coefficient, according to this model.

The assumptions on which the penetration model are based apply well to the situation in which a volatile solute interacts with a liquid which flows as a film over a short solid surface. A short wetted-wall column, described in Chapter 4, was utilized as a contacting device in this study.

In other situations, the assumption that liquid elements are exposed for a fixed period of time would appear not to apply. In a stirred-cell, for example, eddies approaching the surface from the bulk liquid would be expected to remain at the surface for periods of time that would be variable. To accommodate this, Danckwerts (1951) developed a model based on random surface renewal that leads to the following expression for the flux:

$$N_A = \sqrt{D_A s} \Delta C_A \quad (3.3)$$

where s is the surface renewal rate. Although there does not appear to be a good way of correlating s with fluid properties or hydrodynamic conditions, the model does predict a square root dependence of the mass transfer coefficient on the diffusivity to the one-half power, typical of the values found in this type of apparatus.

The mass transfer model must be integrated with kinetic information in order to predict the combined effects of reaction and mass transfer. The transport problem is complicated by the necessity of including chemical equilibria in the analysis.

3.2 BULK PHASE EQUILIBRIUM

The distribution of an electrolyte in the liquid phase between its free molecular and chemically combined or ionic forms depends on the ionic equilibria. It is the molecular form of the weak electrolyte that comes to equilibrium with the same component in the vapor phase, chemical equilibria significantly affects phase equilibria and vice-versa.

3.2.1 Vapor Liquid Equilibrium Model

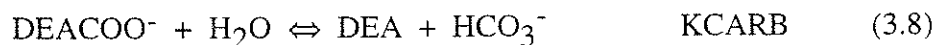
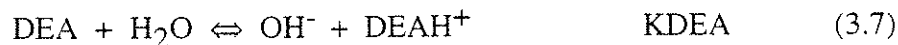
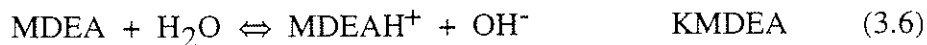
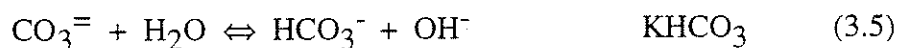
Austgen (1989) developed a physico-chemical model for representing liquid phase chemical equilibria and vapor-liquid (phase) equilibria of H_2S - CO_2 -alkanolamine-water systems. The equilibrium composition of the liquid phase is determined by minimization of the Gibbs free energy. Activity coefficients are represented with the Electrolyte-NRTL equation treating both long-range electrostatic interactions and short-range binary interactions between liquid phase species. Vapor phase fugacity coefficients are calculated using the Redlich-Kwong-Soave equation of state.

Adjustable parameters of the model, binary interaction parameters and carbamate stability constants, were fitted on published binary system (alkanolamine-water) and ternary system (H_2S -alkanolamine-water, CO_2 -alkanolamine-water) VLE data. The Data Regression System of ASPEN PLUSTM, based upon the Maximum Likelihood Principle, was used to estimate adjustable parameters. Ternary system measurements used in parameter estimation ranged in temperature from 25 to 120°C, in alkanolamine concentration from 1 to 5 M, in acid gas loading from 0 to 1.5 moles per mole alkanolamine,

and in acid gas partial pressure from 0.1 to 1000 kPa. Austgen also extended his model to represent CO₂ solubility in aqueous mixtures of MDEA with MEA or DEA. For details of the model and actual values of different parameters one is referred to the Austgen dissertation (1989).

3.2.2 Derivation of Equilibrium Constants

In this work a pseudo equilibrium model for speciation was developed based on Austgen (1989). CO₂ reacts through an acid-base buffer mechanism in an aqueous alkanolamine solution. The various equilibrium considered in this work are:



The equilibrium constants based on concentrations (in kmol/m³) for reactions 3.4 to 3.8 as a function of loading and temperature for mixed alkanolamine solutions, were derived by solving the problem with Austgen's model in Aspen Plus, and using the resulting concentrations to calculate the equilibrium constants. This allowed for a stand alone simplified method for solving the bulk equilibrium speciation in conjunction with rate modeling. Six temperatures were used: 25, 40, 60, 80, 100, and 120°C. Eleven values of loading

ranging from 0.001 to 0.70 mol CO₂/ mol amine were used. The functionality and coefficients for the equilibrium constant expressions are given on Table 3.1.

Table 3.1. Correlation for Equilibrium Constant Expression:

$$K_i = \exp (a_0 + a_1/T + a_2 \ln(T) + a_3 \text{ LCO}_2 + a_4 (\text{LCO}_2)^2)$$

DEA /MDEA	Constant	a ₀	a ₁	a ₂	a ₃	a ₄
wt Fraction	i					
0.00/0.50	CO ₂	13.74	8497.83	- 0.68	0.08	0.07
	HCO ₃	-118.80	1202.72	18.63	8.05	7.45
	MDEA	78.13	-5356.06	- 12.89	7.94	- 8.75
0.25/0.00	CO ₂	-53.23	-4468.44	8.81	-0.43	0.44
	HCO ₃	-96.59	87.93	15.37	-4.78	4.32
	DEA	170.61	-8775.92	-26.63	3.7804	-4.33
	CARB	-58.44	815.27	9.69	-2.05	1.42
0.05/0.45	CO ₂	7.12	-8199.09	0.31	-0.105	0.24
	HCO ₃	-119.71	1297.45	18.73	-8.02	7.41
	MDEA	83.08	-5653.88	-13.58	7.86	-8.76
	DEA	107.29	-6096.32	-17.42	7.21	-8.01
	CARB	-76.11	1947.24	12.06	-0.95	0.39
0.25/0.25	CO ₂	-2.73	-7856.90	1.84	-0.87	1.00
	HCO ₃	-118.02	1283.33	18.42	-7.69	7.05
	MDEA	81.19	-5436.03	-13.27	5.84	-7.18
	DEA	89.22	-4947.64	-14.77	4.99	-6.39
	CARB	-76.19	1924.30	12.12	-3.09	2.73

In solving the bulk equilibrium problem the following three material balance equations are utilized. Total specified carbon dioxide in solution, TCO₂ is equal to free molecular CO₂ and chemically combined CO₂ in the form of bicarbonate, carbonate, and carbamate:

$$\text{TCO}_2 = \text{CO}_2 + \text{HCO}_3^- + \text{CO}_3^{2-} + \text{DEACOO}^- \quad (3.9)$$

Total MDEA, TMDEA, in solution is equal to molecular MDEA and its protonated form :

$$\text{TMDEA} = \text{MDEA} + \text{MDEAH}^+ \quad (3.10)$$

Material balance for DEA is given as below:

$$\text{TDEA} = \text{DEA} + \text{DEAH}^+ + \text{DEACOO}^- \quad (3.11)$$

The last equation needed is the charge balance. The solution should stay electrically neutral:

$$\text{DEAH}^+ + \text{MDEAH}^+ - \text{HCO}_3^- - 2 \text{CO}_3^{2-} - \text{DEACOO}^- - \text{OH}^- = 0 \quad (3.12)$$

The electrical charge balance, Equation 3.12, has been written neglecting the concentration of hydrogen ions, this simplification is reasonable in even slightly alkaline solutions. Concentrations of all nine species (CO_2 , CO_3^{2-} , HCO_3^- , DEACOO^- , DEAH^+ , DEA , MDEAH^+ , MDEA , and OH^-) are calculated using the nine equations above (3.4 to 3.12) simultaneously in the model.

MINPACK routine developed by Garbow et al. (1983), which utilizes the Powell Hybrid method, is used in solving the system of the nonlinear algebraic equations.

For the case of pure MDEA solution, that is with no DEA in solution, three fewer species (DEA , DEAH^+ , and DEACOO^-) are in solution and Equations 3.7, 3.8, and 3.11 do not apply. A similar situation applies for pure DEA solutions, the two missing species are MDEA and MDEAH^+ and the unoperative Equations are 3.6 and 3.10.

3.3 INTERFACIAL SPECIATION

Film theory with modification to approximate surface renewal theory is used to solve for the interfacial speciation and estimation of CO_2 flux. First we

assume that the interface is not at equilibrium which is necessary if we are to have any absorption or desorption. The following equations hold true and should be satisfied:

Charge flux between the bulk phase and the interface is zero for electroneutrality purposes. ∴

$$k_{\text{LCO}_2}^o \sqrt{\frac{1.0}{D_{\text{CO}_2}}} \{ \sqrt{D_{\text{MDEAH}^+}} \Delta[\text{MDEAH}^+] + \sqrt{D_{\text{DEAH}^+}} \Delta[\text{DEAH}^+] \} =$$

$$k_{\text{LCO}_2}^o \sqrt{\frac{1.0}{D_{\text{CO}_2}}} \{ \sqrt{D_{\text{OH}^-}} \Delta[\text{OH}^-] + 2 \sqrt{D_{\text{CO}_3^{2-}}} \Delta[\text{CO}_3^{2-}] + \sqrt{D_{\text{HCO}_3^-}} \Delta[\text{HCO}_3^-]$$

$$+ \sqrt{D_{\text{DEACOO}^-}} \Delta[\text{DEACOO}^-] \} \quad (3.13)$$

The amine flux across the interface is zero, that is, there is no net flux of nonvolatile components. This is expressed mathematically by the next two equations for DEA and MDEA respectively:

$$\sqrt{D_{\text{DEA}}} \Delta[\text{DEA}] + \sqrt{D_{\text{DEAH}^+}} \Delta[\text{DEAH}^+] + \sqrt{D_{\text{DEACOO}^-}} \Delta[\text{DEACOO}^-] = 0 \quad (3.14)$$

$$\sqrt{D_{\text{MDEA}}} \Delta[\text{MDEA}] + \sqrt{D_{\text{MDEAH}^+}} \Delta[\text{MDEAH}^+] = 0 \quad (3.15)$$

where Δ implies the difference between interface and bulk concentration.

Equilibrium Equation 3.4 is used at the interface to calculate the concentration of $[\text{CO}_2]$ that would be in equilibrium with the local (interfacial) concentrations of bicarbonate and hydroxide. The combination of 3.4 and 3.8 allows for the equation to calculate the concentration of CO_2 that would be in equilibrium with local concentrations of DEA, hydroxide, and carbamate ions. At the interface equilibrium Equations 3.5 - 3.7 also apply.

The flux of total CO₂ , that is free CO₂, bicarbonate, carbonate, and carbamate can be calculated in two different ways:

$$\text{Diffusional flux} = k_{\text{LCO}_2}^0 \Delta[\text{CO}_2] + k_{\text{LHCO}_3^-}^0 \Delta[\text{HCO}_3^-] + k_{\text{LCO}_3^{=}}^0 \Delta[\text{CO}_3^{=}] + k_{\text{LDEACOO}^-}^0 \Delta[\text{DEACOO}^-] \quad (3.16)$$

$$\text{Enhancement flux} = k_{\text{LCO}_2}^0 E_{\text{CO}_2} \Delta[\text{CO}_2] \quad (3.17)$$

The next equation is derived by taking into account the kinetic preference of CO₂ towards its dissolved states. The approximation states that the ratio of carbamate flux (FLUXCARB) to bicarbonate flux (FLUXBIC) is equal to the ratio of the rates through the respective mechanisms.

$$\text{Bicarbonate Flux} \cdot \text{Carbamate rate} = \text{Carbamate Flux} \cdot \text{Bicarbonate rate} \quad (3.18)$$

Carbamate Flux is calculated by the next equation whereby the mass transfer coefficient for carbamate ions is evaluated based on the mass transfer coefficient of CO₂ corrected by square root of the ratio of the diffusion coefficients of carbamate and CO₂.

$$\text{FLUXCAR} = k_{\text{LCO}_2}^0 \sqrt{\frac{D_{\text{DEACOO}^-}}{D_{\text{CO}_2}}} \Delta[\text{DEACOO}^-] \quad (3.19)$$

Bicarbonate Flux is calculated by the summation of CO₂, CO₃⁼ and HCO₃⁻ fluxes:

$$\text{FLUXBIC} = k_{\text{LCO}_2}^0 \left[\Delta[\text{CO}_2] + \sqrt{\frac{D_{\text{HCO}_3^-}}{D_{\text{CO}_2}}} \Delta[\text{HCO}_3^-] + \sqrt{\frac{D_{\text{CO}_3^{=}}}{D_{\text{CO}_2}}} \Delta[\text{CO}_3^{=}] \right] \quad (3.20)$$

Rate of formation of carbamate is given as

$$\text{RATCARB} = k_{\text{DEA}} \cdot [\text{DEA}] \cdot (\text{CO}_2\text{I} - \text{CO}_2^*) \quad (3.21)$$

where, CO_2^* is the CO_2 concentration that would be in equilibrium with the local concentrations of carbamate, protonated DEA and other species in solution.

Rate of formation of bicarbonate, RATBICA:

$$RATBICA = k_{MDEA} [MDEA] \cdot (CO_2I - CO_2^{**}) \quad (3.22)$$

where, CO_2^{**} is the CO_2 concentration that would be in equilibrium with the local concentrations of bicarbonate, protonated MDEA and other species in solution.

Concentration of CO_2 at the interface is calculated from gas phase partial pressure and CO_2 solubility, m_{CO_2} . Solubility estimation is discussed in detail in Appendix C.

$$CO_2I = m_{CO_2} P_{CO_2} \quad (3.23)$$

The MINIPAC routine is also used to solve this system of equations. The complete listing of equations and unknowns as applied in the model is provided in Appendix A.

3.5 PARAMETER ESTIMATION

The problem of parameter estimation using non-linear models for single and multi-response experiments has been studied by many investigators. Objective functions and methods of obtaining estimates of parameters and their confidence intervals have been studied by Box and Draper (1965, 1972), Stewart (1987, 1992), Caracotsios (1986) and others. Generalized REGression (GREG), a FORTRAN program written by Caracotsios (1986) is used to calculate

parameter estimates and confidence intervals. GREG is used with the Level 10, generalized nonlinear square minimization, and at 95% confidence level.

The model described in this chapter is used along with GREG and experimental data to estimate the kinetic parameters for MDEA, DEA and their blends at three temperatures: 40, 80, and 120°C. Also, to account for uncertainties in equilibrium, a factor α , correcting the value of K_{CO_2} is estimated for each series of experimental data. Thus, in addition to the rate parameter, an improved value of the CO_2 equilibrium constant, αK_{CO_2} is obtained.

An outline to the organization of the computer program is shown on Figure 3.1. The main program, which includes the experimental fluxes as the observed variable, calls GREG, the parameter estimation package. GREG in turn calls the MODEL which calculates the fluxes.

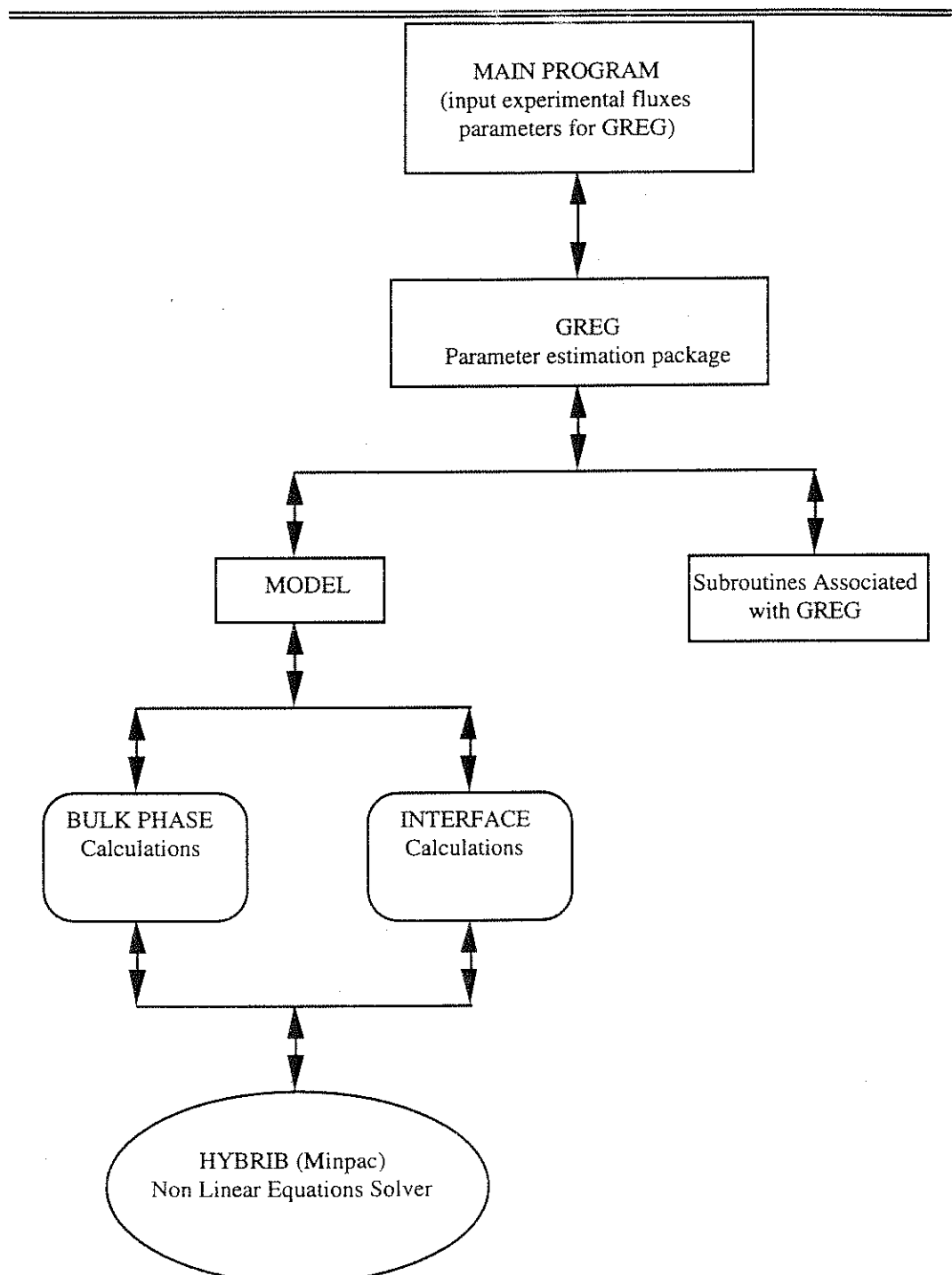


Figure 3.1 Outline of the Computer Program.

CHAPTER FOUR

Experimental

4.1 EXPERIMENTAL APPARATUS AND METHODS

4.1.1 Wetted Wall Column

CO₂ mass transfer was studied in a laboratory wetted wall column contactor. Figure 4.1 depicts the important features of the wetted wall column apparatus. The column was constructed from a stainless steel tube of 1.26 cm outside diameter and had an exposed length of 9.1 cm. The column was enclosed in a thick walled glass tube of 2.54 cm outside diameter which formed an absorption/ desorption chamber. The seal was provided by top and bottom O-ring seals compressed by stainless steel flanges. Three nuts on each side provided the compressive force on tightening. This assembly was enclosed in a heat bath constructed from a 10.16 cm OD thick walled glass tube. The seals on both ends were provided by two flanges and O-rings between flanges and glass. Compression was provided from the top flange by the three equally spaced nuts on the threaded rods. This enclosure formed a heating bath for the absorption/ desorption chamber.

4.1.2 Experimental Set Up

Figure 4.2 depicts a flow diagram of the experimental apparatus. Amine solution was contained in a 400 cm³ stainless steel reservoir. A bleed line was

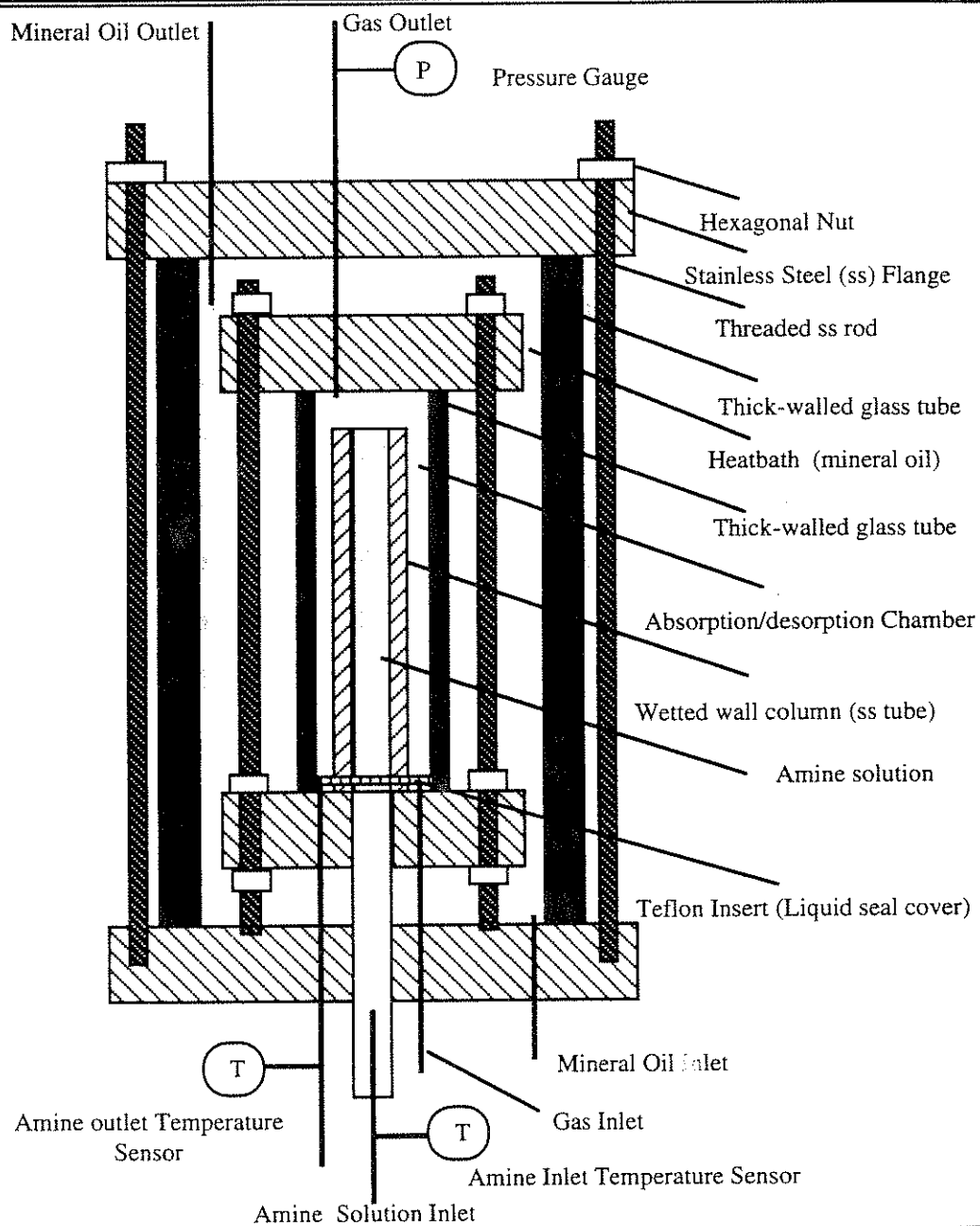


Figure 4.1 High Temperature Wetted Wall Column

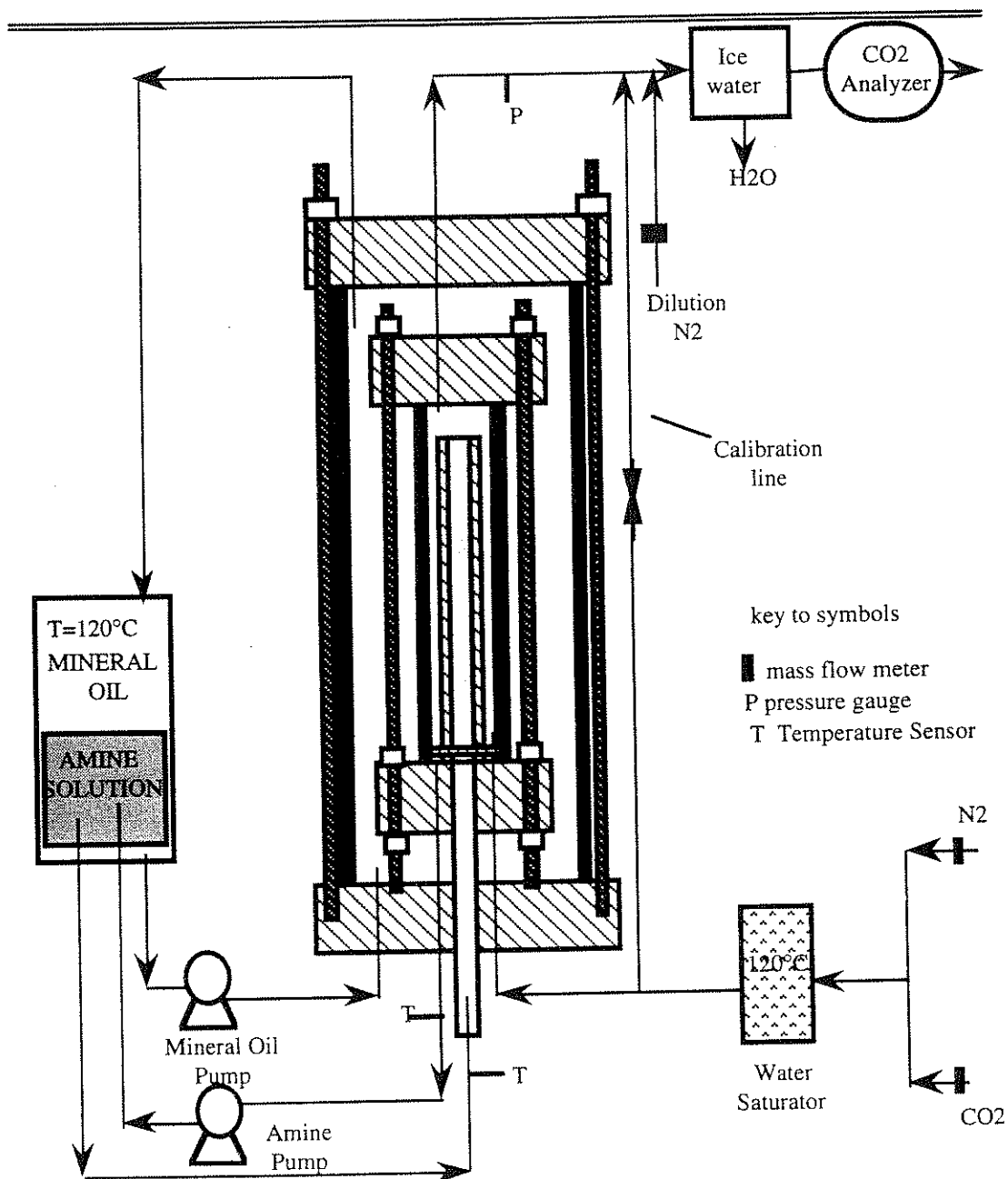


Figure 4.2 Experimental Apparatus for Absorption/ Desorption of CO₂ with Amine Solution

installed on the top of reservoir. The reservoir was placed in a heating bath of mineral oil to keep the amine solution at the temperature of the experiment.

The gas stream to the wetted wall column was saturated with water at the experiment temperature to avoid heat imbalances in the absorption/desorption chamber. A stainless steel container similar to the amine reservoir was half filled with water and placed in a heat bath of paraffin oil (CAS 8012-95-1 from EM Science). Gas feed to the wetted wall column bubbled through a water depth of about 5 cm in the saturator before entering the absorption/desorption chamber.

Nitrogen gas was supplied from a liquid N₂ cylinder and CO₂ was supplied from cylinders with discharge pressure maintained at 125 - 130 psig. The flow rate of gases was regulated using Brooks Model 5850E mass flow controllers. The mixture of CO₂ and N₂ was either sent through the wetted wall column or through the bypass. The practice in this work was to first send the gas through the bypass to the CO₂ analyzer to perform calibration. Before the gas reached the analyzer it was diluted to the required level using N₂ (whose flowrate was regulated by a flow controller). The typical flow rate of dilution N₂ was 1200 cm³/min. In an experimental mode the gas was then sent through the wetted wall column where it countercurrently contacted the downward flowing amine solution.

The gas that left the column was diluted with nitrogen, the same as during calibration, then sent through an ice bath, which consisted of a 125 cm³ erlenmeyer flask placed in a 2000 cm³ beaker filled with ice water to condense water in the gas phase. Placing the condenser after the dilution point rather than before it minimizes the concern on the amount of CO₂ that may be removed with

the water, because the partial pressure of CO_2 is drastically reduced. It also acted as an additional mixing chamber for the dilution gas and the gas coming out of the wetted wall column. Significant amounts of water in the gas phase could affect the working of the infrared CO_2 analyzer. The output of the analyzer was monitored by a strip chart recorder.

The amine reservoir was filled with the solution and then sealed. In order to fill the lines and purge the system of entrapped air, about 60 cm^3 of additional amine was introduced through the feed port (gas outlet line from the column) on top of the absorption/desorption chamber by a syringe. At all times a liquid seal was maintained to avoid any gas leak into the liquid line. Amine solution was pumped from the reservoir up through the inside of the wetted wall column and flowed down the outside as a thin liquid film. The amine solution was recycled back to the reservoir. The effective mass transfer contact area provided by the column was 37.39 cm^2 . The longitudinal area was 36.13 cm^2 and the top of the wetted wall column provided 1.25 cm^2 . The liquid was circulated by a Cole-Parmer micro pump (Masterflex® Drive model number L-07520-25 with ten turn speed controls; head and adapter model numbers L-07002-23 and L-07002-15 respectively). The manufacturer's gear assembly was replaced with one constructed of polyethyl ethyl ketone (PEEK) to handle temperatures above 100°C . J- type thermocouples were installed in the solution inlet and outlet lines to the wetted wall column for temperature measurement.

4.1.3 Mass Flow Controllers

Brooks mass flow controllers 5850 series were used to regulate the flow rates of N_2 and CO_2 . The thermal mass flow sensing technique used in 5850 series works as follows. A precision power supply provides a constant power heat input at the heater, which is located at the midpoint of the sensor tube. Temperature sensors are positioned at the inlet (T_i) and outlet (T_o) of the sensor tube. At zero, or no flow conditions the heat reaching each temperature sensor is equal. Therefore the temperatures T_i and T_o are equal. When gas flows through the tube the upstream sensor is cooled and the downstream sensor is heated, producing a temperature difference. The temperature difference ($T_o - T_i$) is directly proportional to the gas mass flow.

4.1.3.1 *Calibration of Mass Flow Controllers*

The flow controllers were calibrated for N_2 and CO_2 by means of a soap film meter. At a known room temperature and pressure a soap flow meter assembly, as shown in Figure 4.3, is set up. The time taken for a soap bubble to travel between two marks is noted by use of a stop watch. Three measurements are collected for each flow meter controller setting and the average is used in generation of the calibration curve. For the example depicted on Figure 4.3, the calibration curve, Figure 4.4, was obtained. The same procedure was adopted for all mass flow controllers. Table 4.1 lists all the gas mass flow controllers used.

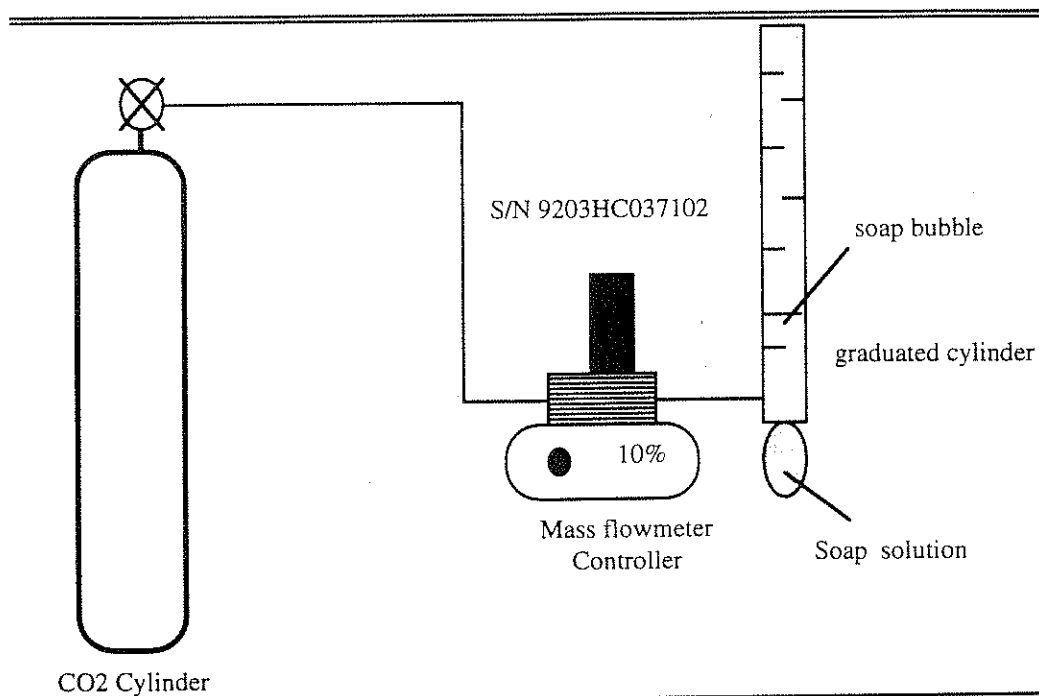


Figure 4.3 Mass Flow meter Calibration Using a Soap Flow Meter

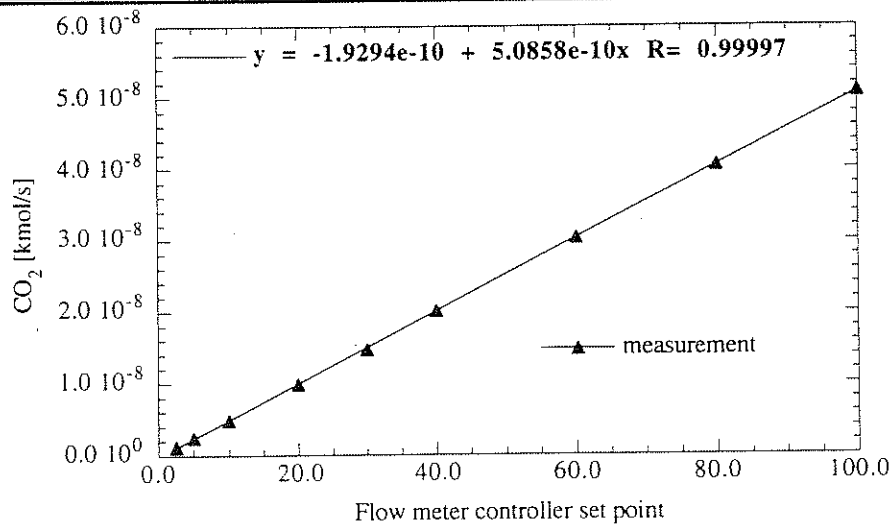


Figure 4.4 Mass Flow Meter Calibration Curve for S/N 9203HC037102

Table 4.1 Ranges of Brooks Mass Flow Controllers

Flow controllers Serial Number	Model Number	Range ^a cm ³ /min	Calibration gas
9310HC038403	5850E	2000	N2
9203HCO37102	5850E	100	CO2
8507HC02754/010/-1	5850C	500	N2
9310HC038404/1	5850C	250	N2
9103HC037044/2	5850E	20	CO2

^a range refers to the upper limit on the flow rate. The lower limit is always 0.0 cm³/min.

4.1.4 Carbon Dioxide Analyzers

HORIBA Model PIR-2000 Infrared gas phase analyzers were used to determine the flux of CO₂ from the gas to the flowing amine solution in the wetted wall column. These analyzers use infrared absorption spectroscopy to measure the CO₂ concentration in the gas phase. The principle of measurement is based on the fact that carbon dioxide absorbs infrared radiation of a specific wavelength and the degree of absorption is proportional to the concentration at constant pressure. The infrared radiation emitted by the light source passes through the sample and reference cells to the rotating chopper where it is modulated. If a portion of the infrared radiation passing through the sample is absorbed by the sample gas, a decrease in the amount of radiation reaching the sample side of the detector cell will result. This difference causes a membrane between the sample and reference cells in the detector to produce an electrical output which is amplified and directed to a meter and/or recording device. In our case a strip chart recorder was used.

4.1.4.1 Calibration of Carbon Dioxide Analyzers

The CO₂ flux into the liquid phase from the gas phase was determined by the difference of the CO₂ flow rate in the gas stream into and out of the wetted

wall column. The flow rate of CO₂ into the column corresponded to the setting on the CO₂ mass flow controller as described in the previous section. To obtain the flowrate out of the column a calibration was necessary. The analyzer was calibrated in the configuration that was to be used during the actual experiment. A typical set up is given in Figure 4.5. This figure sketches the set up actually used for experimental runs 39 to 55. Mass flow controllers S/N 9310HC038404/1 and S/N 9203HC038403 are set at 38% and 64.9% respectively which corresponded to constant flows of N₂ of 6.322×10^{-8} kmol/s and 4.3954×10^{-7} . With the two flow rates constant, the flow rate of CO₂ through the mass flow controller S/N 9310HC037102 was varied step wise from 0% to 100% and at each setting the steady state strip chart reading was recorded. The calibration curve obtained is plotted in Figure 4.6. Dilution N₂ was used so that the total flow of gas into the analyzer was between 500 and 1500 cm³/min. This was prescribed by the manufacturers. The analyzers used in this work had ranges of 0-0.25%, 0-1%, and 0-25% (volume basis).

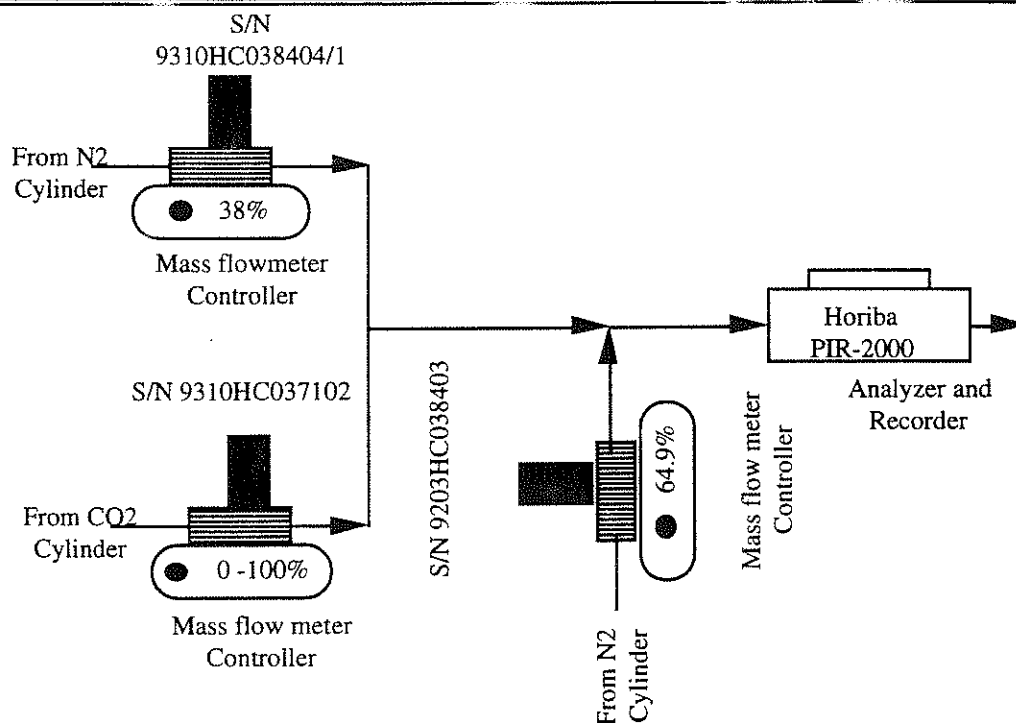


Figure 4.5 Strip Chart Calibration for a Typical Experimental Set Up

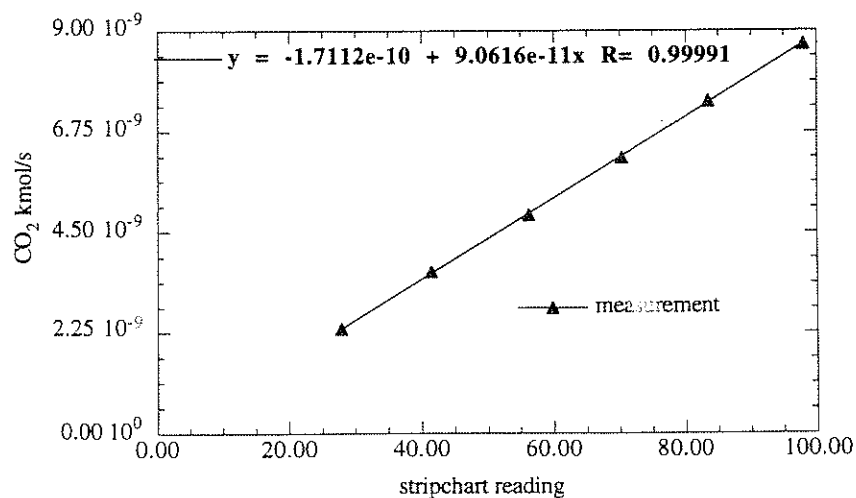


Figure 4.6 Strip Chart Calibration Curve for the 0-1% Range CO₂ Analyzer

4.1.5 Liquid Phase Carbon Analyzer

Liquid phase CO₂ concentration, or the CO₂ loading, was determined by an Oceanography International Model 525 Carbon Analyzer. It uses nitrogen gas as the carrier gas. A small amount of liquid sample (100 µl) is injected into a solution of 30 wt% phosphoric acid which instantly frees the CO₂ chemically combined with the amine. The total CO₂ is carried by the nitrogen stream to the Horiba analyzer with a range of 0 - 0.25 volume %. The total signal is integrated and this value is a direct measure of the carbon dioxide concentration in the liquid phase.

When steady state was reached during an experimental run a sample (100 µl) of amine solution was withdrawn through a sampling port located on the line coming from the wetted wall column. The sample was quickly transferred into 10 ml of distilled water contained in a 16 ml vial (short form black molded screw cap, catalogue number 66011-121).

Prior to analyzing the liquid sample a calibration curve was generated. To facilitate this, calibration with a liquid of known CO₂ content becomes necessary. A 7 mM Na₂CO₃ solution (prepared by mixing the requisite amounts of solid anhydrous Na₂CO₃ with distilled water) was used for this purpose. A calibration was performed every time the carbon analyzer was used. This was essential as the calibration had a tendency to drift.

4.2 PHYSICAL CALIBRATION OF APPARATUS

4.2.1 Theory

The flux of CO₂ (that is being absorbed or desorbed) is given by the following equation:

$$N = E k_{\text{LCO}_2}^0 \Delta C \quad (4.1)$$

where ΔC is the driving force, E is the enhancement factor and $k_{\text{LCO}_2}^0$ is the physical mass transfer coefficient in the liquid phase. It is difficult to estimate $k_{\text{LCO}_2}^0$ while absorbing CO₂ into a solution of alkanolamine since the mass transfer is accompanied by chemical reaction. Hence, it is necessary to run experiments involving purely physical absorption or desorption of CO₂. For this purpose aqueous solutions of ethylene glycol (which do not react chemically with CO₂) and water were used. The enhancement factor is unity for this case.

In the desorption mode, the governing material balance equation for the liquid phase is:

$$V_L \frac{dc}{dt} = -k_{\text{LCO}_2}^0 a (C - C_i) \quad (4.2)$$

and for the gas phase material balance:

$$k_{\text{LCO}_2}^0 (C - C_i) = G (C_{\text{gout}} - C_{\text{gin}}) = G C_g \quad (4.3)$$

where G is the gas flow rate through the wetted wall column and the CO₂ analyzer, C_g is the concentration of CO₂ in the gas stream. Concentration of CO₂ in the inlet gas, C_{gin} , was always zero. The change in liquid concentration across the absorber was neglected in estimating the driving force. Substituting for C_i in terms of gas phase partial pressure using Henry's law and then solving for C from

Equation 4.3. On integration of Equation 4.2 under the assumption that partial pressure of CO₂ in the gas phase is zero (pure N₂ was used for desorption), the result is

$$\ln C_{gout} = \ln \left(-\frac{k_{LCO_2}^0}{G} C_0 \right) - \frac{k_{LCO_2}^0}{V_L} t \quad (4.4)$$

By measuring the concentration of CO₂ out from the wetted wall column, C_g, the slope of a plot of ln C_g versus time provides the mass transfer coefficient, k_{LCO₂}⁰.

4.2.2 Procedure

A number of experiments were conducted to measure the mass transfer coefficient of CO₂ in aqueous solutions. The solutions used are given in Table 4.2 and consist of pure water at various temperatures and ethylene glycol-water solutions of various concentrations at 25°C. All the experiments were performed in desorption mode. The experiment involved:

1. Filling the solution reservoir with the ethylene glycol solution of known concentration.
2. Absorbing CO₂ into the solution by running CO₂ for 2 to 4 hours.
3. Stripping the CO₂ from the solution in the wetted wall column using CO₂-free N₂.

4.2.3 Dimensionless Mass Transfer Correlation

For a falling film as in a wetted wall column, Vivian and Peaceman (1956) suggested that the liquid film mass transfer coefficient for a wetted wall column could be correlated in terms of the four dimensionless groups: Reynolds number,

Re; Sherwood number, Sh; Schmidt number, Sc; and Galileo number, Ga. Theoretical prediction based on penetration theory is given as:

$$Sh = 0.724 Re^{1/3} Sc^{1/2} Ga^{1/6} \quad (4.5)$$

The theoretical Equation 4.5 is derived in appendix B.

These dimensionless groups are defined as follows

$$Sh = \frac{k_{LCO_2}^o l}{D_{CO_2}} \quad (4.6)$$

$$Re = \frac{4q}{\nu} \quad (4.7)$$

$$Sc = \frac{\nu}{D_{CO_2}} \quad (4.8)$$

$$Ga = \frac{g l^3}{\nu^2} \quad (4.9)$$

where D_{CO_2} is the diffusivity of CO_2 in the solution, ν is the kinematic viscosity of the solution, l is the effective contact length of the wetted wall column (9.1 cm) and q is the volumetric flow rate per unit length which in this case is the perimeter of the wetted wall column.

Deviations from theory are mainly due to end effects and ripple formation. The short wetted wall column used here was calibrated by measurement of physical mass transfer coefficient, $k_{LCO_2}^o$, by CO_2 desorption from aqueous solutions of ethylene glycol. The CO_2 diffusion coefficient, density, and viscosity for ethylene glycol solutions were obtained from Hayduk and Malik (1971). The diffusion coefficient of CO_2 in water was calculated using the correlation presented in Appendix C.

Table 4.2 Mass Transfer Coefficient Calibration Data

Solution	T °C	$D_{CO_2} \times 10^9$ [m ² /s]	Density x 10 ⁻³ [kg/m ³]	Viscosity [cP]	Flowrate x 10 ⁶ [m ³ /s]	$k_{LCO_2}^o \times 10^5$ [m/s]
50 wt%EG	25	0.90	1.058	4.490	1.58	5.97
80 wt% EG	25	0.61	1.088	8.549	0.85	3.32
95 wt% EG	25	0.38	1.105	13.365	0.72	2.82
water	25	1.92	0.997	0.890	1.62	9.47
water	50	3.33	0.988	0.547	2.18	12.67
water	75	5.33	0.975	0.378	2.54	15.35
water	80	6.07	0.973	0.352	0.67	10.80
water	120	11.40	0.943	0.231	0.67	16.00

Experimental conditions, physical properties, and physical mass transfer coefficient results are presented in Table 4.2. Equation 4.5 is used as the basis in correlating the experimental mass transfer coefficient measurements. Firstly, Equation 4.5 is rewritten with an arbitrary constant coefficient, γ , and a Reynolds number exponent m :

$$Sh = \gamma Re^m Sc^{1/2} Ga^{1/6} \quad (4.10)$$

Equation 4.10 is then rearranged and written in a form that is amenable to linear regression as follows:

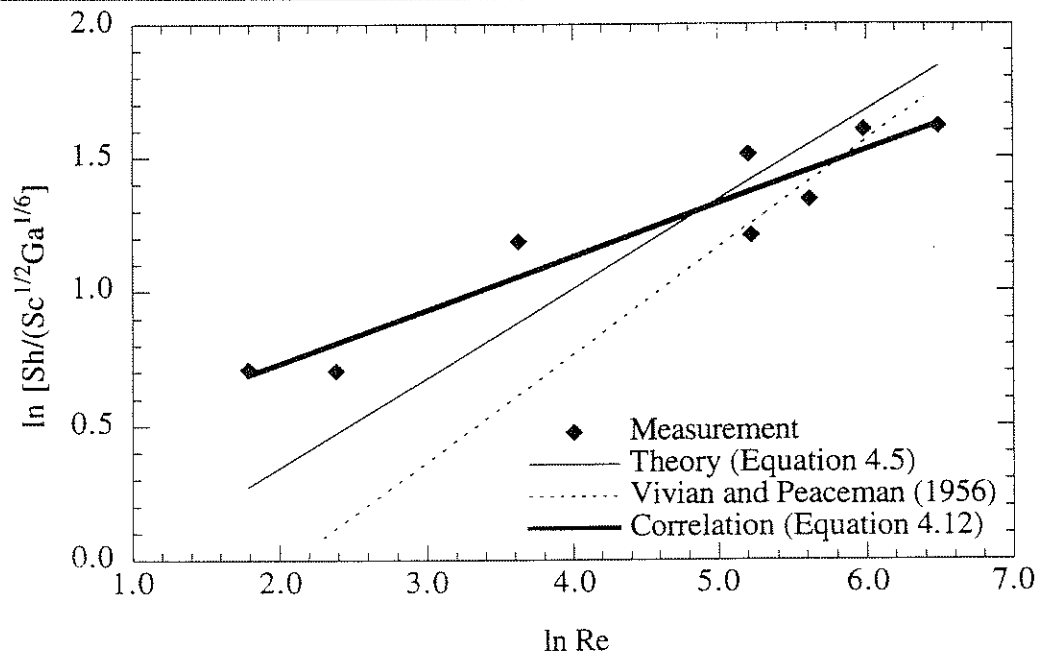
$$\ln(\text{Group}) = \ln \frac{Sh}{Sc^{1/2} Ga^{1/6}} = \ln \gamma + m \ln Re \quad (4.11)$$

The linear regression result gave $\ln \gamma = 0.331 \pm 0.131$ and $m = 0.199 \pm 0.027$

Table 4.3 presents the detailed results of the regression. The results are also presented as a plot in Figure 4.7.

Table 4.3 Regression results for the mass transfer coefficient correlation

T °C	Sh x 10 ⁻³	Sc x 10 ⁻³	Ga x 10 ⁻⁹	Re x 10 ⁻²	lnRe	ln(Group)	
						Experimental	Predicted
25	6.02	4.71	0.37	0.38	3.62	1.19	1.05
25	4.99	12.99	0.10	0.11	2.39	0.71	0.81
25	6.73	31.70	0.04	0.06	1.79	0.71	0.69
25	4.49	0.47	9.32	1.83	5.21	1.51	1.37
50	3.46	0.17	24.72	3.97	5.98	1.60	1.52
75	2.62	0.07	51.71	6.60	6.49	1.62	1.62
80	1.62	0.06	59.66	1.86	5.23	1.21	1.37
120	1.28	0.02	138.54	2.75	5.62	1.34	1.45

**Figure 4.7 Correlation Curve for the Liquid Film Mass Transfer Coefficient**

The mass transfer coefficient $k_{\text{LCO}_2}^0$ of the wetted wall column was correlated by the following expression:

$$\text{Sh} = 1.39 \text{Re}^{0.199} \text{Sc}^{1/2} \text{Ga}^{-1/6} \quad (4.12)$$

Equation 4.12 is used throughout in this work for estimating the liquid film mass transfer coefficient. The physical properties for various solutions used in this work were estimated using the correlations presented in appendix C.

A similar Equation by Vivian and Peaceman (1956) for their short wetted wall columns is given below:

$$Sh = 0.433 Re^{0.40} Sc^{1/2} Ga^{1/6} \quad (4.13)$$

The deviations from theory for both the Vivian and Peaceman (1956) and the correlation developed here (Equation 4.12) are of the same order of magnitude. It is also interesting to note that Vivian and Peaceman (1956) used several wetted wall columns ranging in height from 1.9 to 4.3 cm. The one used here was 9.1 cm in height.

4.3 REACTIVE ABSORPTION/ DESORPTION

4.3.1 Rate Measurements

Absorption rates of CO₂ into concentrated alkanolamine solutions of MDEA and DEA were studied for a range of conditions as shown in Table 4.4. The blend composition is expressed on a mass basis. All compositions are on a CO₂ free basis.

Table 4.4 Conditions for Absorption/ Desorption of CO₂ into Concentrated Alkanolamine Solutions

Amine	Temperature °C	Loading $\frac{\text{mol CO}_2}{\text{mol amine}}$	CO ₂ partial pressure (atm)
50% MDEA	40, 80, 120	0 - 0.5	0.02 - 6.6
5% DEA - 45% MDEA	40, 80, 120	0 - 0.5	0.02 - 2.6
25% DEA - 25% MDEA	40, 80, 120	0 - 0.5	0.02 - 5.9
25% DEA	40, 80, 120	0 - 0.5	0.02 - 2.8

The percentages are on a mass basis.

The apparatus was set up as shown earlier in Figure 4.1. The flow controller for N₂ was kept at a constant value of about 6.3×10^{-8} kmol/s while the CO₂ mass flow controller was set stepwise to attain a series of desired partial pressures of CO₂ in the wetted wall column. A series of runs were made for a particular amine at a constant temperature for a range of partial pressures. At steady state, a sample (100 μ l) of alkanolamine is withdrawn for purposes of CO₂ loading measurement.

While making these measurements, the gas mixture was sent through wetted wall column with no liquid flowing until a constant signal output corresponding to the concentration of CO₂ in the gas mixture was obtained. Then the liquid flow was started. Absorption or desorption then took place indicated by a deflection on the strip chart recorder. The process was continued till the deflection on the analyzer had become constant. This would be indicated by a flat curve on the strip chart recorder. This deflection was noted. The difference corresponded to the absorption/desorption rate of CO₂. The partial pressure was then changed and the whole process was repeated for a different partial pressure. Normally the dilution rate and rate of N₂ used for mixing were kept fixed for all experiments.

The raw data obtained in this work are presented in Appendix . The inlet and outlet CO₂ partial pressures are measured based on the N₂ and CO₂ flow rates. The log mean partial pressure is calculated from Equation 4.14:

$$P_{\log \text{ mean}} = \frac{P_{\text{in}} - P_{\text{out}}}{\ln \frac{P_{\text{in}}}{P_{\text{out}}}} \quad (4.14)$$

The absorption rate is essentially the difference of the CO₂ flow rates in and out of the wetted wall column. The flow rates are measured by the CO₂ analyzer and converted to flux by dividing with the contact area of the wetted wall column.

4.4 RATE KINETICS FROM MASS TRANSFER MEASUREMENTS

Mass transfer measurement experiments should be designed such that statistically sound kinetics information can be obtained from them. To do this two important considerations should be taken into account. The first consideration is that a significant absorption/ desorption rate greater than the physical rate should be obtained. This condition can be expressed in terms of Hatta number, Ha, which gives the relative indication of the speeds of chemical reaction and mass transfer. Mathematically we can write:

$$Ha = \sqrt{\frac{k_2 [\text{amine}] D_{CO_2}}{k_{LCO_2}^o{}^2}} > 1 \quad (4.15)$$

or

$$\sqrt{k_2 [\text{amine}] D_{CO_2}} > k_{LCO_2}^o \quad (4.16)$$

This implies that the chemical kinetics will have enhanced the CO₂ mass transfer rate. This consideration gives the lower bound. The second establishes the upper bound. When the rates of reactions are infinitely fast, chemical equilibrium is established instantaneously. Carbon dioxide can then diffuse in both its physically dissolved and its chemically combined form, with no kinetic resistance to the transformation from one form to the other. The mass transfer rate is

governed by a driving force measured in terms of the total concentration of $\Delta[\text{CO}_2]_T$, instead of the concentration of its physical dissolved form, $\Delta[\text{CO}_2]$. Mathematically this is stated as limiting mass transfer rate:

$$k_{Lp}^0 \Delta[\text{CO}_2]_T > \sqrt{k_{L\text{CO}_2}^0{}^2 + k_2[\text{am}] D_{\text{CO}_2}} \Delta[\text{CO}_2] \quad (4.17)$$

where k_{Lp}^0 is the mass transfer coefficient for the ionic products which is estimated from that of CO_2 by the square root of the ratio of diffusivities of ionic product and CO_2 . Equation 4.17 can then be written as:

$$k_{L\text{CO}_2}^0 \sqrt{\frac{D_i}{D_{\text{CO}_2}}} \Delta[\text{CO}_2]_T > \sqrt{k_{L\text{CO}_2}^0{}^2 + k_2[\text{am}] D_{\text{CO}_2}} \Delta[\text{CO}_2] \quad (4.18)$$

The two considerations (Equations 4.16 and 4.18) may be combined to end up with Equation 4.19:

$$1 < \frac{\sqrt{k_2[\text{am}] D_{\text{CO}_2}}}{k_{L\text{CO}_2}^0} < \sqrt{\frac{D_i}{D_{\text{CO}_2}} \cdot \frac{\Delta[\text{CO}_2]_T^2}{\Delta[\text{CO}_2]^2} - 1} = \sqrt{E_{\text{ins}}^2 - 1} \quad (4.19)$$

The complete derivation of the condition expressed in 4.19 is presented in Appendix I. Equation 4.19 states that there is a window of conditions whereby absorption and desorption measurements can be made that would result in statistically sound kinetics values. These conditions are functions of amine concentration, rate constant and mass transfer coefficients. Indirectly, temperature, amine solution type, amine concentrations, and CO_2 loading affect the window.

In Equation 4.19 E_{ins} refers to the instantaneous enhancement, the limiting value of enhancement achieved when reactions are at chemical

equilibrium. This value is calculated for specific conditions corresponding to lowest, medium and highest CO₂ loading for 50 wt% MDEA and 25 wt% DEA at 40°C and 120°C. The sample calculations are given in Appendix I. The values obtained are presented in Table 4.5 and plotted on Figure 4.8. It is clear from the result that E_{ins} is a strong function of solution type, temperature, CO₂ loading, and also the CO₂ partial pressure.

Table 4.5 Instantaneous Enhancement Factors for Some Specific Conditions

Solution	T °C	P _{CO2} [bar]	CO ₂ Loading [mol/ mol amine]	E_{ins}	E_{actual}
50 wt% MDEA	40	0.29	0.019	150	4.4
	40	1.90	0.271	33	3.2
	40	4.72	0.403	15	3.0
	120	0.96	0.0354	7.9	3.7
	120	2.18	0.064	3.6	1.9
	120	5.28	0.156	1.5	2.1
25 wt% DEA	40	0.029	0.037	865	13.0
	40	0.583	0.161	67	10.5
	40	0.750	0.342	44	8.3
	120	1.612	0.149	19	4.7
	120	0.972	0.219	17	5.4
	120	2.43	0.291	10	4.7

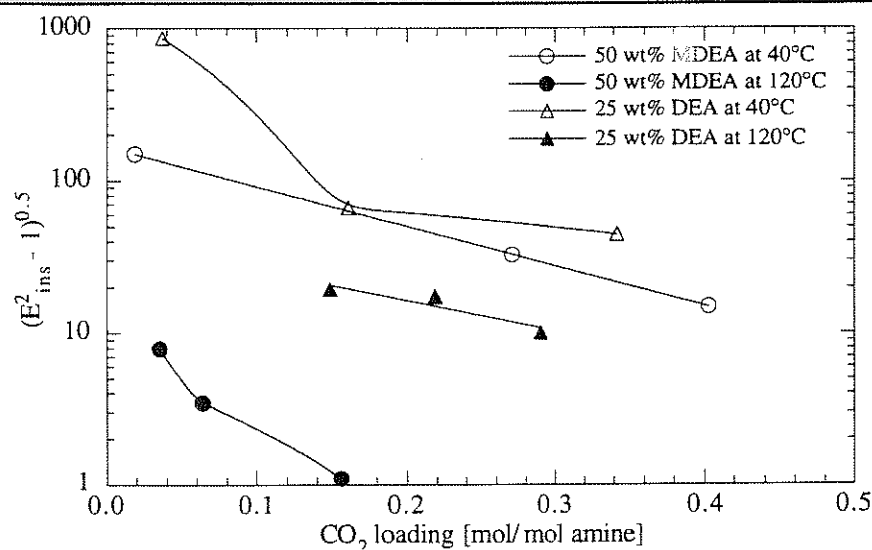


Figure 4.8 Instantaneous Enhancement Factors for 50 wt% MDEA and 25 wt% DEA

4.5 CHEMICALS

The DEA was from Texaco Chemical, lot # 7H-1184/ODS-92-0232, and listed as 100% pure. The MDEA was Texaco "Textreat® M", lot number ODS92-0179, and listed as 95-99.99% pure. Distilled water was used in preparing all solutions. Certified A.C.S sodium carbonate Lot number 860576 was obtained from Fisher Scientific. N₂ was supplied from a liquid N₂ cylinder. CO₂ was a K- grade (purity better than 99.5%) supplied by Wilson Oxygen.

4.6 GAS PHASE RESISTANCE

This section is included for the purpose of validating the assumption that liquid film resistance controlled the mass transfer process in this work. To

achieve this, Film theory is used to estimate the gas phase mass transfer coefficient:

$$k_G = \frac{D_{CO_2}}{\delta R T} \quad (4.20)$$

The values of gas phase mass transfer coefficient calculated at three temperatures are given in Table 4.6. The highest measured value of overall mass transfer coefficient based on the gas phase, K_G , was $16.5 \times 10^{-6} \text{ kmol/ (m}^2\text{bar s)}$. The lowest estimate of gas phase mass transfer coefficient was $2.5 \times 10^{-4} \text{ kmol/ (m}^2\text{bar s)}$. From these two values, it is found that gas resistance contributes less than 7.0% of the total resistance. This being the limiting condition it is fair to assume that for all the conditions encountered in this work liquid phase controlled the mass transfer process.

Table 4.6 Gas Phase Mass Transfer Coefficient Estimation

T	CO ₂ Diffusion coefficient in N ₂	Gas film thickness, δ	k_G
[K]	$\left[\frac{\text{m}^2}{\text{s}}\right]$	[m]	$\left[\frac{\text{kmol}}{\text{bar m}^2\text{s}}\right]$
313	1.80E-05	2.75E-03	2.51E-04
353	2.15E-05	2.75E-03	2.67E-04
393	2.53E-05	2.75E-03	2.81E-04

CHAPTER FIVE

Results and Discussions

5.1 RATE MEASUREMENTS

5.1.1 MDEA

Results on CO₂ absorption/ desorption into 50 wt% MDEA are summarized in Table 5.1. Measured fluxes and model calculated fluxes are tabulated. The results of rate constant estimation using GREG package are given. The apparent second order rate constant, k_{MDEA} , was estimated to be 7.96 ± 1.42 m³/kmol-s at 40°C. The sensitivity on α for all series of experiments at 40°C could not be determined, probably because equilibrium is not important at these conditions. These rate data are plotted in a parity plot on Figure 5.1. The model fits the data well.

The apparent second order rate constant of 6.02 ± 5.98 m³/kmol-s was estimated at 80°C. For the three experimental series at 80°C the values of α were determined to be 1.38 ± 0.31 , 1.35 ± 0.22 , and 1.09 ± 0.89 . These rate data are also shown in the parity plot on Figure 5.2.

At 120°C a smaller value of the effective rate constant, k_{MDEA} of $2.4 \pm \infty$ m³/kmol-s is obtained, the insensitivity of the data on this rate constant may be because equilibrium effects are controlling the process. The high temperature favoring the reverse reactions causes the reactions to be at equilibrium and the diffusion of the products from, and of reactants to the boundary layer control the

mass transfer phenomena. The values of α deviate significantly from 1.0 indicating the influence of equilibrium in the data. The five series of experiments at 120°C are presented in Table 5.1 and plotted on Figure 5.3.

Table 5.1. Rate Data for MDEA. Initial Unloaded Solution is 50 MDEA wt%

Bulk Loading mol CO ₂ mol amine	log mean PCO ₂ [bar]	Outlet PCO ₂ [bar]	mCO ₂ kmol m ³ -bar	k _L x 10 ⁵ [m/s]	Flux x 10 ⁶ [$\frac{\text{kmol}}{\text{m}^2\text{s}}$]	
					Meas.	Model
T = 40°C, k _{MDEA} = 7.96 ± 1.42 m ³ /kmol-s, D _{CO₂} = 7.5 x 10 ⁻¹⁰ , D _i = 2.3 x 10 ⁻¹⁰ m ² /s						
$\alpha = 1.0 \pm \infty$, PCO ₂ * (at loading = 0.019) = 0.001 bar						
0.019	0.293	0.173	0.0202	4.21	0.67	1.30
0.033	0.588	0.383	0.0200	4.19	1.21	1.85
0.048	0.973	0.691	0.0197	4.18	1.81	2.97
0.103	1.621	1.120	0.0188	4.11	4.04	4.48
0.147	2.235	1.644	0.0180	4.07	5.78	5.67
0.329	2.781	2.171	0.0153	3.87	7.20	4.92
$\alpha = 1.0 \pm \infty$, PCO ₂ * (at loading = 0.253) = 0.074 bar						
0.253	0.478	0.377	0.0164	3.95	0.54	0.89
0.262	1.048	0.816	0.0163	3.94	1.47	2.08
0.271	1.899	1.585	0.0161	3.93	2.55	3.79
0.286	2.568	2.221	0.0159	3.92	3.55	4.99
0.395	3.127	2.788	0.0144	3.81	4.30	4.76
$\alpha = 1.0 \pm \infty$, PCO ₂ * (at loading = 0.136) = 0.027 bar						
0.136	0.415	0.275	0.0182	4.08	0.78	1.10
0.164	0.950	0.655	0.0178	4.05	1.90	2.33
0.184	1.660	1.181	0.0174	4.03	3.86	3.94
0.240	2.329	1.801	0.0166	3.97	5.22	4.97
0.271	2.923	2.416	0.0161	3.93	6.13	5.86
0.403	4.723	4.723	0.0143	3.80	7.70	7.10
T = 80°C, k _{MDEA} = 6.02 ± 5.98 m ³ /kmol-s, D _{CO₂} = 6.6 x 10 ⁻¹⁰ m ² /s, D _i = 2.2 x 10 ⁻¹⁰ m ² /s						
$\alpha = 1.38 \pm 0.31$, PCO ₂ * (at loading = 0.243) = 1.78 bar						
0.242	1.243	1.473	0.0116	7.19	-1.44	-1.14
0.243	1.809	1.803	0.0116	7.19	0.05	0.12
0.245	2.291	2.163	0.0116	7.18	1.25	1.15
0.245	2.703	2.505	0.0116	7.18	2.32	2.07

Table 5.1. Continued

Bulk Loading mol CO ₂ mol amine	log mean P _{CO2} [bar]	Outlet P _{CO2} [bar]	m _{CO2} kmol m ³ -bar	k _L × 10 ⁵ [m/s]	Flux × 10 ⁶ [$\frac{\text{kmol}}{\text{m}^2\text{s}}$]	
					Meas.	Model
$\alpha = 1.35 \pm 0.22$, P _{CO2} * (at loading = 0.288) = 2.36 bar						
0.309	1.009	1.64	0.0109	7.06	-3.44	-3.35
0.309	1.502	1.78	0.0109	7.06	-1.93	-2.33
0.288	2.226	2.32	0.0111	7.10	-0.87	-0.21
0.295	2.742	2.69	0.0111	7.09	0.62	0.65
0.301	3.190	3.07	0.0110	7.08	1.68	1.35
$\alpha = 1.09 \pm 0.89$, P _{CO2} * (at loading = 0.308) = 2.17 bar						
0.308	2.474	2.525	0.0109	7.06	-0.52	0.66
0.306	2.864	2.814	0.0110	7.07	0.60	1.52
0.316	3.232	3.151	0.0109	7.05	1.18	1.95
0.445	6.562	6.562	0.0097	6.81	3.56	1.98
T = 120°C, k _{MDEA} = $2.4 \pm \infty$ m ³ /kmol-s, D _{CO2} = 5.4×10^{-9} m ² /s, D _i = 1.64×10^{-9} m ² /s						
$\alpha = 1.263 \pm 0.647$, P _{CO2} * (at loading = 0.016) = 0.18 bar						
0.016	0.074	0.149	0.0106	11.61	-0.43	-0.27
0.026	0.749	0.696	0.0105	11.58	0.41	0.73
0.033	1.234	1.064	0.0105	11.56	1.62	1.35
$\alpha = 0.864 \pm 0.347$, P _{CO2} * (at loading = 0.021) = 0.20 bar						
0.021	0.152	0.300	0.0106	11.59	-0.91	-0.15
0.021	0.401	0.370	0.0106	11.59	0.19	0.50
0.033	1.215	1.030	0.0105	11.55	1.76	1.80
0.047	1.698	1.510	0.0104	11.51	2.21	1.92
$\alpha = 2.277 \pm 0.637$, P _{CO2} * (at loading = 0.023) = 0.67 bar						
0.021	0.266	0.530	0.0106	11.59	-1.66	-0.61
0.023	0.496	0.570	0.0106	11.59	-0.46	-0.29
0.021	0.718	0.640	0.0106	11.59	0.62	0.48
0.041	2.010	1.920	0.0104	11.53	1.25	0.87
$\alpha = 1.248 \pm 0.209$, P _{CO2} * (at loading = 0.035) = 0.77 bar						
0.036	0.527	0.612	0.0105	11.55	-0.56	-0.61
0.035	0.958	0.919	0.0105	11.55	0.32	0.47
0.064	2.179	2.130	0.0102	11.46	0.71	0.30
0.064	2.592	2.547	0.0102	11.46	0.84	1.20
$\alpha = 0.481 \pm 0.055$, P _{CO2} * (at loading = 0.08) = 1.14 bar						
0.156	5.280	5.280	0.0094	11.18	3.65	3.75
0.100	0.984	1.160	0.0099	11.35	-1.39	-1.75
0.080	1.466	1.489	0.0101	11.41	-0.23	0.54
0.100	2.374	2.268	0.0099	11.35	1.74	1.34

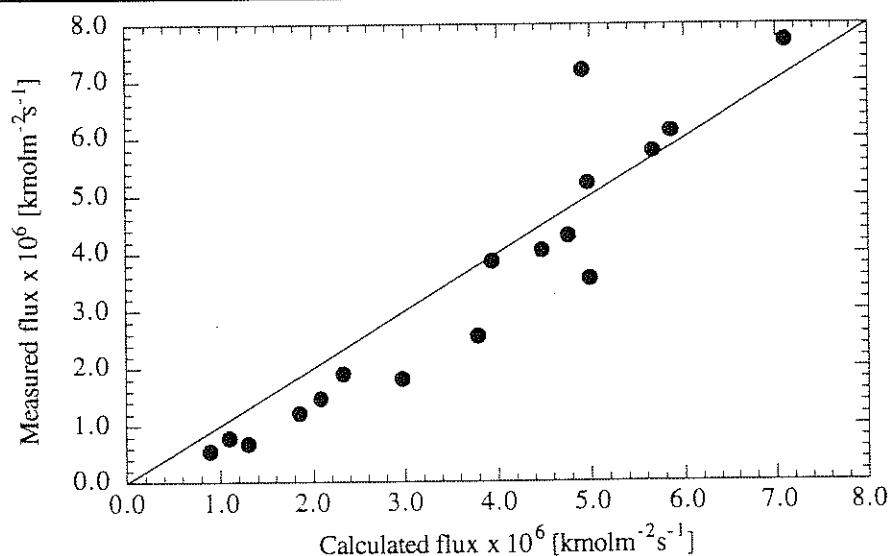


Figure 5.1 Comparison of Model Calculated CO₂ Flux with Experimental Measurements for 50 wt% MDEA at 40°C

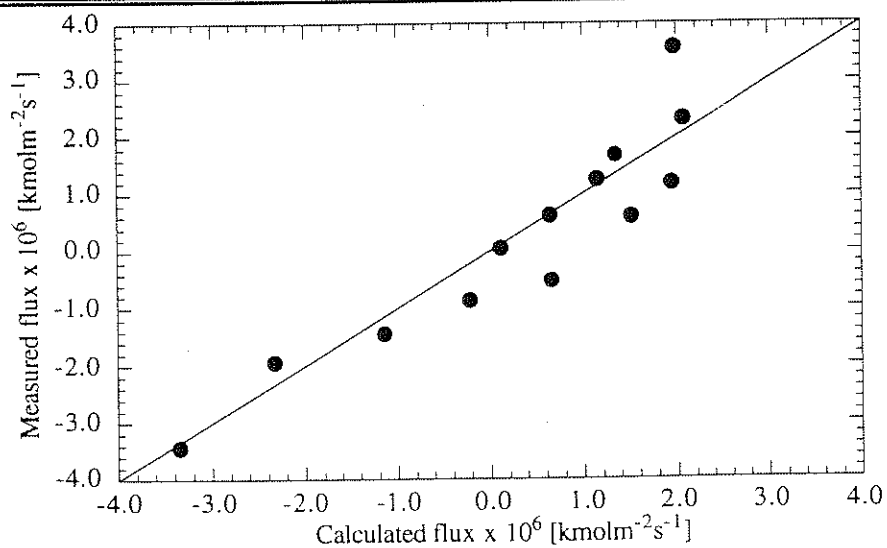


Figure 5.2 Comparison of Model Calculated CO₂ Flux with Experimental Measurements for 50 wt% MDEA at 80°C

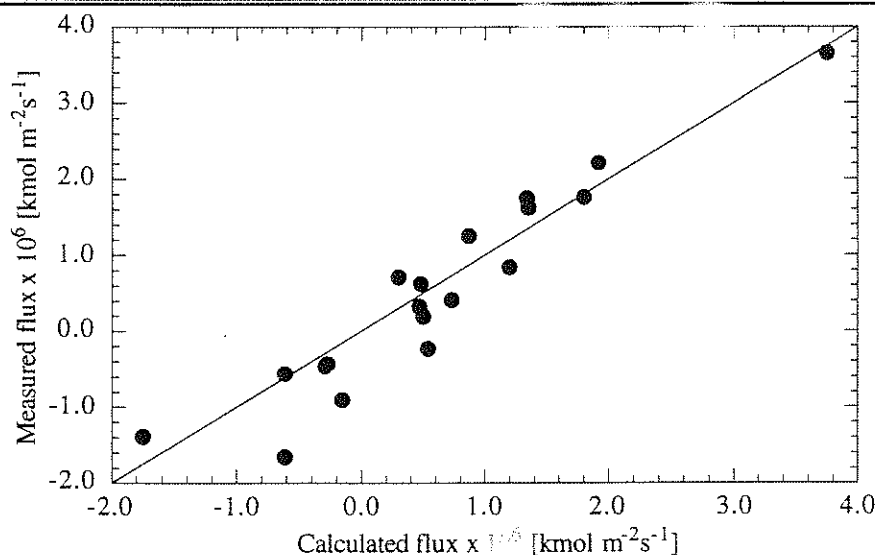


Figure 5.3 Comparison of Model Calculated CO₂ Flux with Experimental Measurements for 50 wt% MDEA at 120°C.

5.1.2 DEA

Absorption and desorption data for CO₂ into 25 wt% DEA is presented in Table 5.2 for all three temperatures: 40, 80, and 120°C. The effective second order rate constant was estimated to be 186 ± 30 , 66 ± 68 , and 68 ± 33 m³/kmol s at 40, 80, and 120°C respectively. The respective plots are given in Figures 5.4, 5.5, and 5.6. The model calculations agree with the measurements.

Table 5.2. Rate Data for DEA. Initial Unloaded Solution is 25 wt% DEA

Bulk Loading mol CO ₂ mol amine	log mean PCO ₂ [bar]	Outlet PCO ₂ [bar]	mCO ₂ kmol m ³ -bar	k _L x 10 ⁵ [m/s]	Flux x 10 ⁶ [$\frac{\text{kmol}}{\text{m}^2\text{s}}$]	
					Meas	Model
T= 40°C, k _{DEA} = 186. ± 30 m ³ /kmol-s, D _{CO₂} = 1.5 x 10 ⁻⁹ m ² /s, D _i = 5.0 x 10 ⁻¹⁰ m ² /s						
$\alpha = 1.0 \pm \infty$, PCO ₂ * (at loading = 0.037) = 0.00006 bar						
0.040	0.024	0.015	0.0206	6.15	0.4	0.39
0.037	0.029	0.014	0.0206	6.15	0.76	0.47
0.046	0.037	0.017	0.0205	6.14	1.03	0.60
0.075	0.047	0.023	0.0199	6.12	1.27	0.71
$\alpha = 1.0 \pm \infty$, PCO ₂ * (at loading = 0.075) = 0.00024 bar						
0.075	0.139	0.023	0.0199	6.12	1.29	2.06
0.095	0.313	0.053	0.0195	6.10	3.24	4.34
0.161	0.583	0.120	0.0182	6.04	6.42	6.71
0.242	0.954	0.312	0.0168	5.97	9.2	8.58
0.305	1.516	0.804	0.0158	5.92	10.81	10.80
$\alpha = 1.0 \pm \infty$, PCO ₂ * (at loading = 0.232) = 0.0029 bar						
0.232	0.003	0.006	0.0170	5.98	-0.01	0.003
0.262	0.194	0.053	0.0165	5.96	1.22	1.83
0.307	0.403	0.094	0.0158	5.92	3.14	3.30
0.342	0.750	0.209	0.0152	5.88	6.21	5.31
T= 80°C, k _{DEA} = 65.59 ± 67.94 m ³ /kmol-s, D _{CO₂} = 3.66 x 10 ⁻⁹ m ² /s, D _i = 1.1 x 10 ⁻⁹ m ² /s						
$\alpha = 2.126 \pm 0.636$, PCO ₂ * (at loading = 0.294) = 0.47 bar						
0.294	0.463	0.384	0.0090	9.62	0.43	0.002
0.297	0.907	0.640	0.0089	9.61	1.80	1.89
0.296	1.484	0.988	0.0089	9.61	4.18	4.32
0.316	2.070	1.488	0.0088	9.59	5.92	5.95
0.340	2.646	2.083	0.0086	9.55	6.95	7.02
$\alpha = 0.552 \pm 0.511$, PCO ₂ * (at loading = 0.395) = 0.32 bar						
0.395	0.601	0.655	0.0081	9.47	-0.28	1.06
0.400	1.047	0.877	0.0081	9.46	1.12	2.57
0.426	1.565	1.116	0.0079	9.43	3.78	3.77
0.470	2.203	1.709	0.0075	9.36	5.10	4.44
0.496	2.774	2.308	0.0074	9.33	5.91	5.05

Table 5.2. Continued

Bulk Loading mol CO ₂ mol amine	log mean P _{CO2} [bar]	Outlet P _{CO2} [bar]	m _{CO2} kmol m ³ -bar	k _L x 10 ⁵ [m/s]	Flux x 10 ⁶ [$\frac{\text{kmol}}{\text{m}^2\text{s}}$]	
					Meas	Model
T = 120°C, k _{DEA} = 68 ± 33 m ³ /kmol-s, D _{CO2} = 7.5 x 10 ⁻⁹ m ² /s, D _i = 2.25 x 10 ⁻⁹ m ² /s						
$\alpha = 1.07 \pm 0.11$, P _{CO2} * (at loading = 0.149) = 1.27 bar						
0.156	0.734	1.140	0.0065	14.00	-2.70	-2.84
0.149	1.095	1.214	0.0065	14.00	-0.99	-0.71
0.149	1.612	1.539	0.0065	14.00	0.81	1.55
0.165	2.022	1.841	0.0064	14.00	2.49	2.37
0.168	2.377	2.147	0.0064	14.00	3.88	3.17
$\alpha_2 = 0.34 \pm 0.03$, P _{CO2} * (at loading = 0.219) = 0.87 bar						
0.226	0.627	0.863	0.0061	13.90	-1.54	-1.57
0.219	0.972	0.959	0.0061	13.90	0.11	0.31
0.233	1.530	1.382	0.0060	13.80	1.60	2.17
0.292	2.106	2.100	0.0057	13.70	1.48	1.28
0.303	2.489	2.359	0.0056	13.70	2.29	1.98
$\alpha = 0.35 \pm 0.04$, P _{CO2} * (at loading = 0.215) = 0.87 bar						
0.251	0.704	1.059	0.0059	13.80	-2.34	-2.42
0.215	1.022	1.059	0.0061	13.87	-0.31	0.57
0.229	1.527	1.375	0.0060	13.85	1.64	2.20
0.249	1.980	1.762	0.0059	13.80	2.97	3.04
0.291	2.427	2.239	0.0057	13.72	3.22	2.31

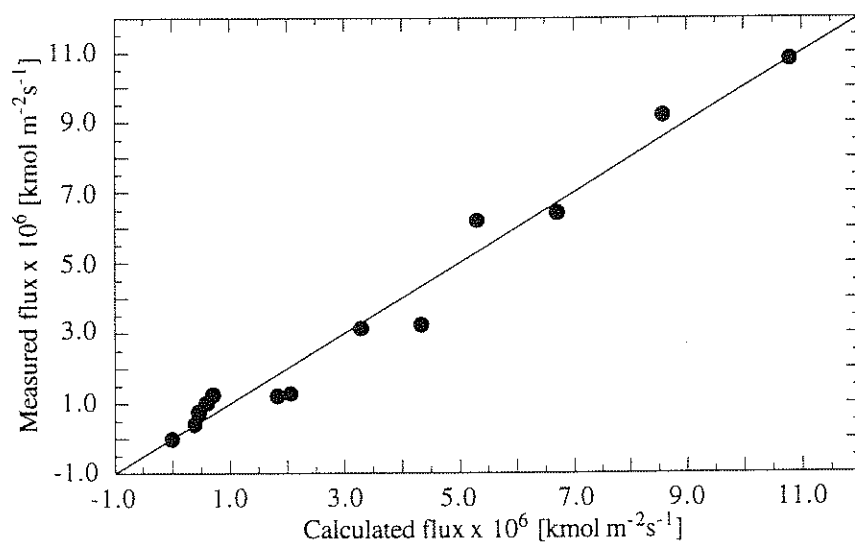


Figure 5.4 Comparison of Model Calculated CO₂ Flux with Experimental Measurements for 25 wt% DEA at 40°C

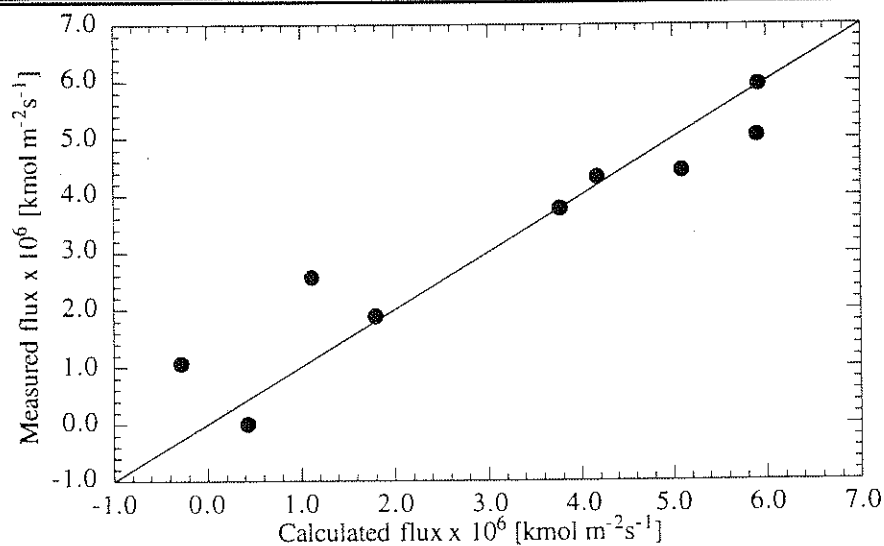


Figure 5.5 Comparison of Model Calculated CO₂ Flux with Experimental Measurements for 25 wt% DEA at 80°C

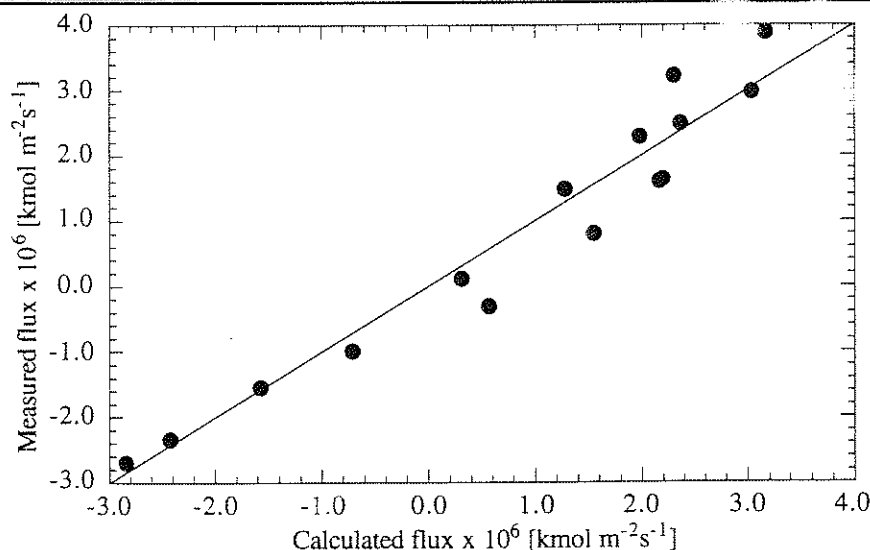


Figure 5.6 Comparison of Model Calculated CO₂ Flux with Experimental Measurements for 25 wt% DEA at 120°C

5.1.3 DEA/ MDEA

An interaction rate constant, k_{DEAMDEA} , is determined from the analysis of mixed amine data. The rate constants determined from pure cases, that is, k_{DEA} and k_{MDEA} , are used.

5.1.3.1 5 wt% DEA/ 45 wt% MDEA

The results for CO₂ absorption/ desorption into 5 wt% DEA/ 45 wt% MDEA solutions are presented in Table 5.3. At 40°C the value of the interaction rate constant, k_{DEAMDEA} was $60.08 \pm 0.13 \text{ m}^6/\text{kmol}^2\text{s}$. The parity plot in Figure 5.7 shows a very good agreement between measured and calculated values. This constant was found to be 49 ± 5 and $14.5 \pm 0.6 \text{ m}^6/\text{kmol}^2\text{s}$ at 80 and 120°C

respectively. Plots of measured flux against model calculated flux are plotted in Figure 5.8 and Figure 5.9.

Table 5.3. Rate Data for DEA/MDEA . Initial Unloaded Solution is 5 wt% DEA/ 45 wt% MDEA

Bulk Loading mol CO ₂ mol amine	log mean P _{CO2} [bar]	Outlet P _{CO2} [bar]	mCO ₂ kmol m ³ -bar	k _L x 10 ⁵ [m/s]	Flux x 10 ⁶ [$\frac{\text{kmol}}{\text{m}^2\text{s}}$]	
					Meas	Model
T= 40°C, k _{MDEA} = 7.96 m ³ /kmol-s, k _{DEA} = 186.08 m ³ /kmol-s, k _{DEAMDEA} = 60.08 ± 0.13 m ⁶ /kmol ² -s; D _{CO2} = 7.1 x 10 ⁻¹⁰ m ² /s, D _i = 2.2 x 10 ⁻¹⁰ m ² /s.						
$\alpha = 0.997 \pm \infty$, P _{CO2} * (at loading = 0.201) = 0.036 bar						
0.201	0.011	0.02	0.0172	4.01	-0.11	-0.11
0.198	0.117	0.05	0.0173	4.02	0.50	0.34
0.200	0.347	0.20	0.0172	4.02	1.04	1.22
0.225	0.659	0.37	0.0168	3.99	2.31	2.12
0.271	1.132	0.79	0.0161	3.94	3.01	3.08
0.306	2.026	1.60	0.0156	3.90	5.22	4.75
$\alpha = 1.00 \pm \infty$, P _{CO2} * (at loading = 0.298) = 0.082 bar						
0.298	0.029	0.057	0.0158	3.91	-0.15	-0.17
0.294	0.173	0.125	0.0158	3.92	0.29	0.29
0.290	0.330	0.225	0.0159	3.92	0.70	0.78
0.301	0.882	0.601	0.0157	3.91	2.29	2.21
0.338	1.665	1.304	0.0152	3.87	3.82	3.64
0.374	2.339	2.013	0.0147	3.83	4.50	4.51
$\alpha = 0.998 \pm \infty$, P _{CO2} * (at loading = 0.385) = 0.16 bar						
0.385	0.058	0.004	0.0146	3.82	-0.31	-0.06
0.377	0.207	0.060	0.0147	3.83	0.13	0.14
0.384	0.391	0.173	0.0146	3.82	0.40	0.55
0.384	0.850	0.473	0.0146	3.82	1.40	1.56
0.431	1.491	1.192	0.0140	3.78	2.91	2.40
0.497	2.095	1.805	0.0132	3.71	3.56	2.64
0.532	2.606	2.364	0.0128	3.68	3.74	2.86
$\alpha = 1.00 \pm \infty$, P _{CO2} * (at loading = 0.086) = 0.0079 bar						
0.086	0.319	0.117	0.0191	4.14	1.68	1.72
0.118	0.688	0.330	0.0186	4.10	3.12	3.09
0.172	1.479	1.002	0.0177	4.05	4.99	5.08
0.196	2.149	1.679	0.0173	4.02	6.23	6.51

Table 5.3. Continued

Bulk Loading $\frac{\text{mol CO}_2}{\text{mol amine}}$	log mean PCO ₂ [bar]	Outlet PCO ₂ [bar]	mCO ₂ $\frac{\text{kmol}}{\text{m}^3 \cdot \text{bar}}$	k _L x 10 ⁵ [m/s]	Flux x 10 ⁶ $\frac{\text{kmol}}{\text{m}^2 \cdot \text{s}}$	
					Meas	Model
T= 80°C, k _{MDEA} = 6.02 ± 5.98 m ³ /kmol-s, k _{DEA} = 65.59 ± 5.9 m ³ /kmol-s; k _{DEAMDEA} = 48.77 ± 5.17 m ⁶ /kmol ² -s, D _{CO₂} = 2.35 x 10 ⁻⁹ m ² /s, D _i = 7.3 x 10 ⁻¹⁰ m ² /s						
$\alpha_1 = 0.998 \pm 0.215$, PCO ₂ [*] (at loading = 0.038) = 0.044 bar						
0.039	0.020	0.040	0.0136	7.60	-0.18	-0.03
0.038	0.070	0.051	0.0136	7.60	0.13	0.16
0.036	0.126	0.073	0.0136	7.61	0.40	0.54
0.045	0.244	0.134	0.0135	7.59	0.88	1.07
0.062	0.489	0.292	0.0133	7.55	1.71	2.00
$\alpha_2 = 0.972 \pm 0.023$, PCO ₂ [*] (at loading = 0.171) = 0.57 bar						
0.102	0.925	0.601	0.0129	7.47	3.29	2.90
0.129	1.692	1.282	0.0125	7.42	5.62	9.26
0.178	0.331	0.667	0.0120	7.32	-1.66	-1.04
0.171	0.408	0.598	0.0121	7.33	-0.84	-0.13
0.170	0.768	0.763	0.0121	7.34	0.07	0.70
0.176	1.190	0.996	0.0120	7.33	1.43	2.00
0.183	1.660	1.292	0.0120	7.31	3.22	3.28
0.199	2.190	1.705	0.0118	7.28	5.15	4.37
T= 120°C, k _{MDEA} = 6.02 m ³ /kmol-s, k _{DEA} = 67.98 m ³ /kmol-s; k _{DEAMDEA} = 14.47 ± 0.57 m ⁶ /kmol ² -s, D _{CO₂} = 5.5 x 10 ⁻⁹ m ² /s, D _i = 1.69 x 10 ⁻⁹ m ² /s						
$\alpha = 1.899 \pm 0.245$, PCO ₂ [*] (at loading = 0.027) = 0.64 bar						
0.018	0.183	0.366	0.0102	11.61	-1.08	-0.09
0.027	0.454	0.466	0.0101	11.58	-0.07	-0.42
0.019	0.882	0.768	0.0102	11.61	0.91	1.44
0.028	1.500	1.291	0.0101	11.58	2.19	1.99
$\alpha = 1.858 \pm 0.9775$, PCO ₂ [*] (at loading = 0.010) = 0.11 bar						
0.010	0.127	0.254	0.0102	11.63	-0.10	0.02
0.011	0.366	0.301	0.0102	11.63	0.43	0.74
0.010	0.818	0.655	0.0102	11.64	1.32	0.71
0.018	1.504	1.000	0.0102	11.61	2.14	1.63
0.032	2.082	1.408	0.0101	11.57	2.37	2.84
$\alpha = 2.31 \pm 0.986$, PCO ₂ [*] (at loading = 0.010) = 0.11 bar						
0.009	0.270	0.540	0.0103	11.60	-0.33	0.16
0.012	0.893	0.788	0.0102	11.60	0.84	1.96
0.023	1.575	1.130	0.0101	11.60	1.54	0.76
0.028	2.103	1.948	0.0101	11.60	2.12	2.87
0.035	2.531	2.387	0.0100	11.60	2.49	2.92

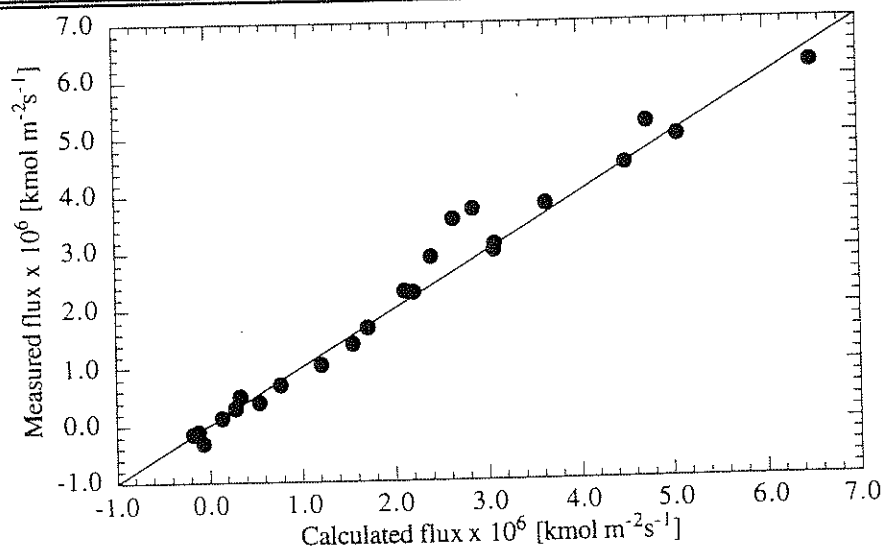


Figure 5.7 Comparison of Model Calculated CO₂ Flux with Experimental Measurements for 5 wt% DEA/ 45 wt% MDEA at 40°C

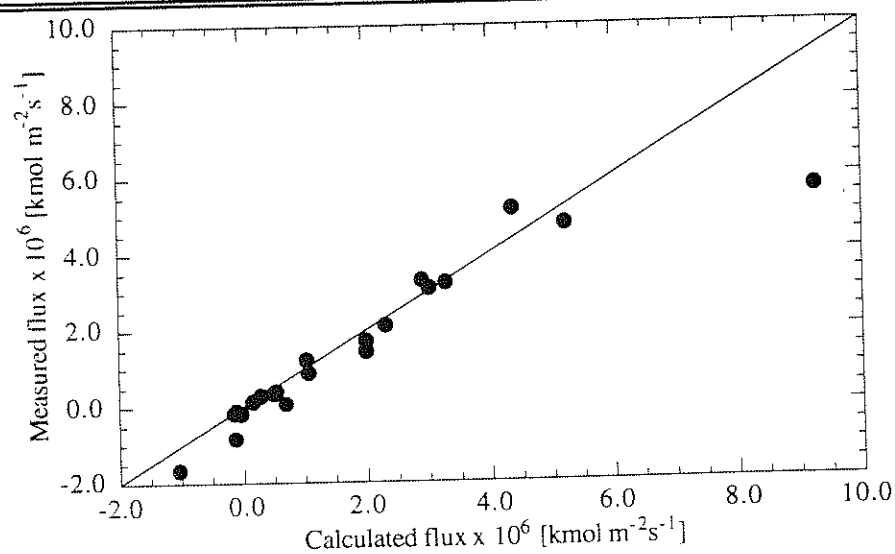


Figure 5.8 Comparison of Model Calculated CO₂ Flux with Experimental Measurements for 5 wt% DEA/ 45 wt% MDEA at 80°C

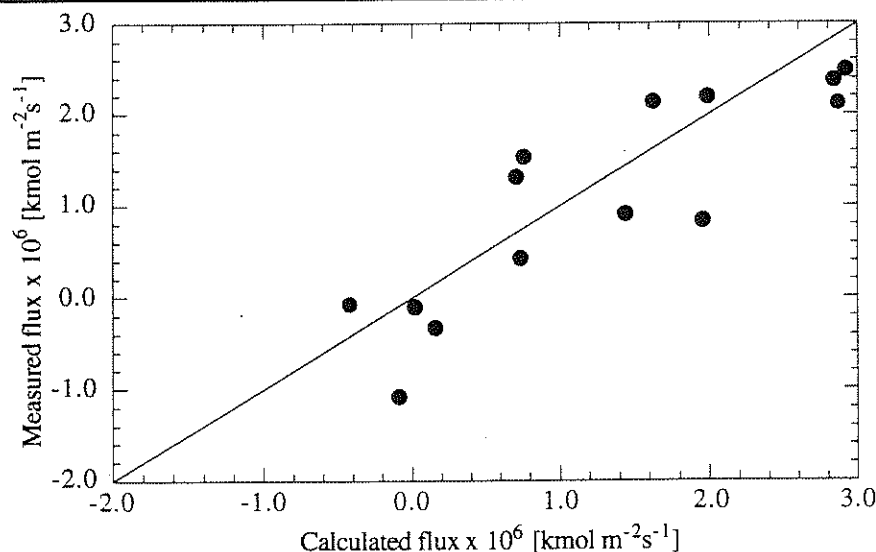


Figure 5.9 Comparison of Model Calculated CO₂ Flux with Experimental Measurements for 5 wt% DEA/ 45 wt% MDEA at 120°C

5.1.3.2 25 WT% DEA/ 25 WT% MDEA

Table 5.4 presents the results pertaining to the 25 wt% DEA/ 25 wt% MDEA solution. The same pure solution rate constants from DEA and MDEA data are used in the analysis for the interaction rate constant k_{DEAMDEA} . At 40°C the value of k_{DEAMDEA} was obtained to be 43 ± 159 . The corresponding values at 80 and 120°C were found to be $22.4 \pm 0.6 \text{ m}^6/\text{kmol}^2\text{s}$ and 21.1 ± 0.1 . These results are also presented in Figure 5.11 and Figure 5.12.

The complete set of data for 25 wt% DEA/ 25 wt% MDEA at 80°C is used as an illustrative example for the modeling and parameter estimation. The main program including the measured fluxes as the observed variable is presented in Appendix E. In appendix F, the model code and input data for this particular case

is presented. Parameter estimation results from GREG for 25 wt% DEA/25 wt% MDEA at 80°C along with the rest of results are presented in appendix G. A detailed set of results showing concentrations of all chemical species at both the interface and the bulk, and enhancement factors is given in appendix H for the specific case of the 25 wt% DEA/ 25 wt% MDEA at 80°C only.

Table 5.4. Rate data for DEA/MDEA. Initial Unloaded Solution is 25 wt% DEA/ 25 wt% MDEA

Bulk Loading mol CO ₂ mol amine	log mean PCO ₂ [bar]	Outlet PCO ₂ [bar]	mCO ₂ kmol m ³ -bar	k _L x 10 ⁵ [m/s]	Flux x 10 ⁶ [$\frac{\text{kmol}}{\text{m}^2\text{s}}$]	
					Meas.	Model
T= 40°C, k _{MDEA} = 7.96 m ³ /kmol-s, k _{DEA} = 186.08 m ³ /kmol-s, k _{DEAMDEA} = 42.68 ± 159.12 m ⁶ /kmol ² -s ; DCO ₂ = 7.5 x 10 ⁻¹⁰ m ² /s, D _i = 2.25 x 10 ⁻¹⁰ m ² /s						
$\alpha = 1.0 \pm \infty$, PCO ₂ * (at loading = 0.08) = 0.0010 bar						
0.080	0.193	0.032	0.0206	4.17	1.33	2.34
0.040	0.491	0.113	0.0200	4.22	3.21	5.87
0.083	0.811	0.174	0.0206	4.17	6.49	8.57
0.136	1.111	0.263	0.0203	4.11	9.71	9.80
0.190	1.374	0.356	0.0201	4.05	12.91	10.10
$\alpha = 1.107 \pm 0.314$, PCO ₂ * (at loading = 0.378) = 0.054 bar						
0.345	1.610	0.564	0.0193	3.89	12.40	7.33
0.389	1.530	0.655	0.0191	3.84	8.75	6.06
0.415	1.230	0.580	0.0190	3.82	5.52	4.58
0.423	0.976	0.697	0.0200	3.81	1.79	3.78
0.378	0.387	0.234	0.0192	3.85	0.88	1.76
T= 80°C, k _{MDEA} = 6.02 m ³ /kmol-s, k _{DEA} = 65.59 m ³ /kmol-s, k _{DEAMDEA} = 22.41 ± 0.57 m ⁶ /kmol ² -s ; DCO ₂ = 2.2 x 10 ⁻⁹ m ² /s, D _i = 6.6 x 10 ⁻⁹ m ² /s						
$\alpha = 0.920 \pm 0.783$, PCO ₂ * (at loading = 0.456) = 2.88 bar						
0.487	2.923	1.042	0.0116	6.77	-3.79	-5.12
0.464	2.474	1.608	0.0125	6.81	-2.95	-2.12
0.456	1.831	2.253	0.0117	6.83	-1.15	-0.35
0.456	1.262	3.210	0.0117	6.83	1.42	1.92
0.485	0.749	5.902	0.0117	6.78	5.40	4.99

Table 5.4. Continued

Bulk Loading mol CO ₂ mol amine	log mean P _{CO2} [bar]	Outlet P _{CO2} [bar]	mCO ₂ kmol m ³ -bar	k _L x 10 ⁵ [m/s]	Flux x 10 ⁶ [$\frac{\text{kmol}}{\text{m}^2\text{s}}$]	
					Meas.	Model
$\alpha = 0.753 \pm 0.171$, P _{CO₂} * (at loading = 0.101) = 0.057 bar						
0.101	0.105	0.052	0.0128	7.51	-0.25	-0.14
0.103	0.129	0.279	0.0127	7.50	1.00	1.62
0.107	0.159	0.506	0.0125	7.49	2.92	3.16
0.122	0.264	0.772	0.0127	7.46	4.65	4.80
0.143	0.330	0.929	0.0126	7.42	5.81	5.34
0.164	0.492	1.206	0.0126	7.38	7.36	6.43
T= 120°C, k _{MDEA} = 2.4 m ³ /kmol-s, k _{DEA} = 67.98 m ³ /kmol-s ; k _{DEAMDEA} = 21.13 ± 0.13 m ⁶ /kmol ² -s; D _{CO₂} = 5.38 x 10 ⁻⁹ m ² /s, D _i = 1.61 x 10 ⁻⁹ m ² /s						
$\alpha = 0.391 \pm 0.001$, P _{CO₂} * (at loading = 0.053) = 0.24 bar						
0.068	0.181	0.362	0.0087	11.49	-1.17	-1.22
0.053	0.363	0.323	0.0085	11.54	0.28	0.11
0.071	0.668	0.468	0.0087	11.48	1.77	-0.31
0.086	1.184	0.864	0.0087	11.44	3.54	3.40
0.106	1.578	1.303	0.0087	11.38	3.49	3.85
$\alpha = 0.394 \pm \infty$, P _{CO₂} * (at loading = 0.085) = 0.52 bar						
0.096	0.342	0.683	0.0087	11.41	-2.34	-0.32
0.097	0.565	0.762	0.0087	11.4	-1.34	-0.12
0.085	0.875	0.835	0.0087	11.44	0.35	0.32
0.087	1.169	1.016	0.0085	11.4	1.56	3.04
0.096	1.349	1.145	0.0087	11.4	2.28	3.42
0.106	1.648	1.428	0.0087	11.37	2.83	4.07

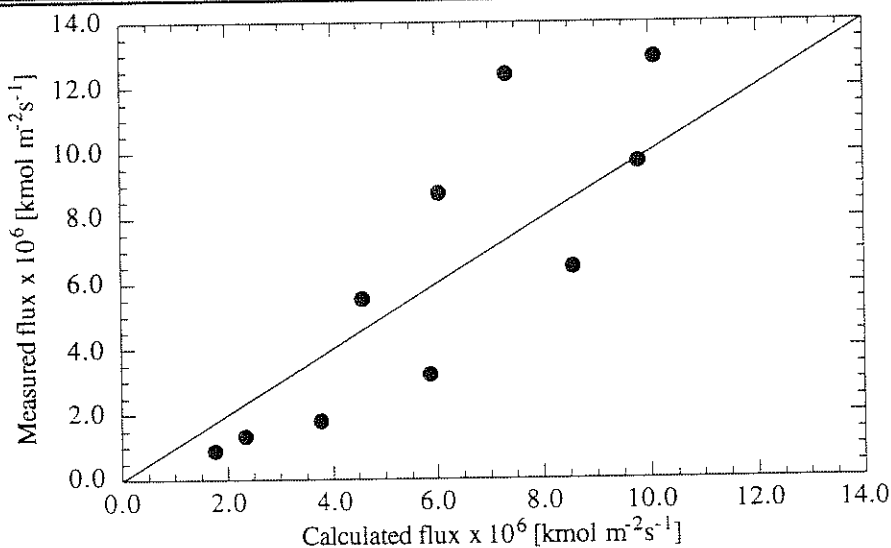


Figure 5.10 Comparison of Model Calculated CO_2 Flux with Experimental Measurements for 25 wt% DEA/ 25 wt% MDEA at 40°C

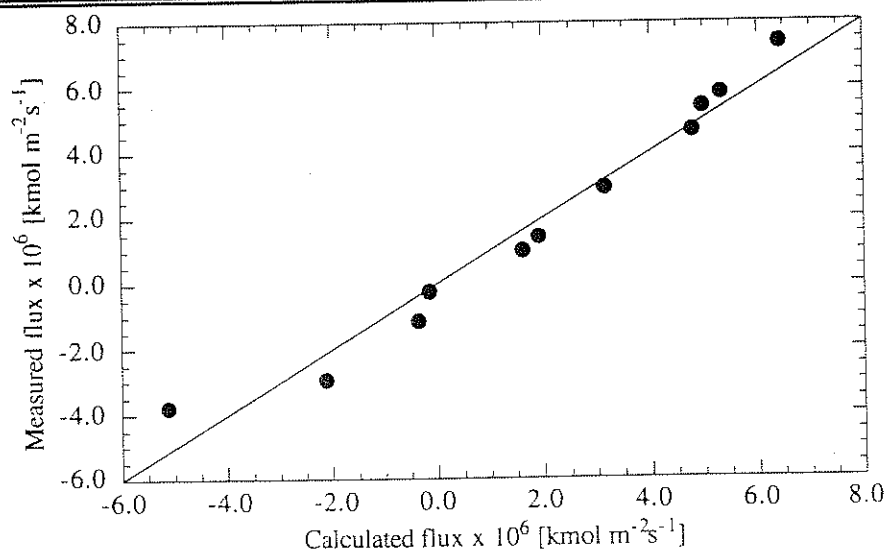


Figure 5.11 Comparison of Model Calculated CO_2 Flux with Experimental Measurements for 25 wt% DEA/ 25 wt% MDEA at 80°C

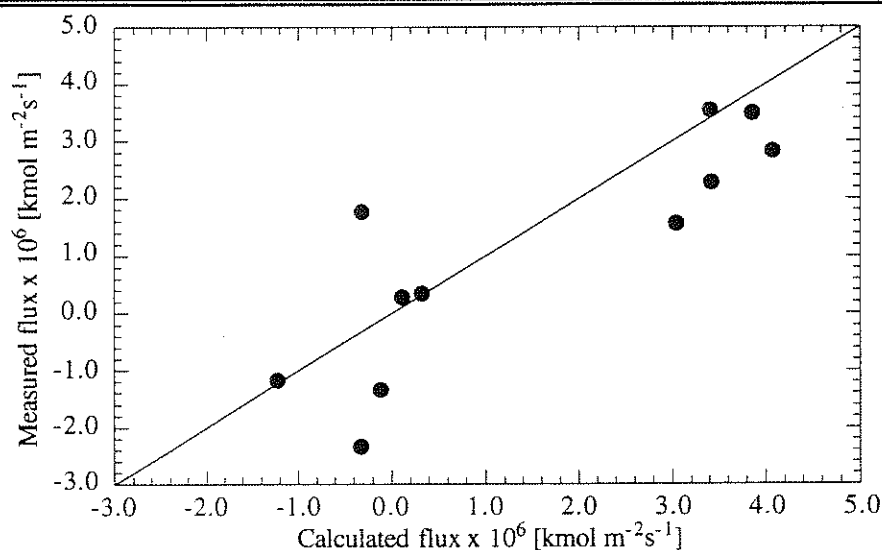
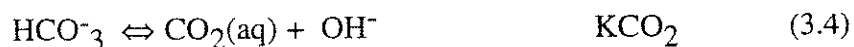


Figure 5.12 Comparison of Model Calculated CO₂ Flux with Experimental Measurements for 25 wt% DEA/ 25 wt% MDEA at 120°C

5.2 EQUILIBRIUM MEASUREMENTS

During the rate measurements, experiments were carried out in a stepwise manner by increasing CO₂ partial pressure, such that absorption and desorption rates were measured in each series of experiments. This allowed for the equilibrium point to be encompassed at a point of zero flux. This was the case for most of the experiments at 80 and 120°C. In order to determine the equilibrium CO₂ partial pressure, a measured loading corresponding to the data point with the least absolute flux was used in conjunction with equilibrium Equation (3.4) repeated here:



and the relationship between solubility and gas phase CO₂ partial pressure is given as:

$$P^*_{CO_2} = \frac{[CO_2]}{m_{CO_2}} \quad (5.1)$$

combining the two equations above and using the regressed estimate of α for a particular series we obtain the equilibrium pressure as:

$$P^*_{CO_2} = \alpha \frac{K_{CO_2}}{m_{CO_2}} \frac{[HCO_3]}{[OH]} \quad (5.2)$$

The experimental values of $P^*_{CO_2}$ at the particular values of loading are presented in Tables 5.1 through 5.4 alongside the rate data. A more concise presentation is given in Table 5.5. In this table only the values calculated using determinable values of α are given. These values are also presented in Figure 5.13 for 50 wt% MDEA, Figure 5.14 for 25 wt% DEA and Figures 5.15 and 5.16 for 5 wt% DEA/ 45 wt% DEA and 25 wt% DEA/ 25 wt% MDEA respectively.

Table 5.5 Equilibrium Pressure Over Amine Solutions

Solution	Temperature °C	loading	α	$P_{CO_2}^*$, bar
50 wt% MDEA	80	0.243	1.38 ± 0.31	1.78
		0.288	1.35 ± 0.22	2.36
		0.308	1.09 ± 0.89	2.17
		Average	1.27	
	120	0.016	1.26 ± 0.65	0.18
		0.021	0.86 ± 0.35	0.204
		0.023	2.28 ± 0.64	0.67
		0.035	1.29 ± 0.21	0.77
		0.08	0.48 ± 0.06	1.14
25 wt% DEA	Average		1.23	
	Average for 50 wt% MDEA		1.24	
	80	0.294	2.13 ± 0.64	0.47
	80	0.395	0.55 ± 0.51	0.32
	Average		1.34	
	120	0.149	1.07 ± 0.11	1.27
	120	0.219	0.34 ± 0.03	0.87
	120	0.215	0.35 ± 0.04	0.87
	Average		0.59	
	Average: 25 wt% DEA		0.89	

Table 5.5 Continued

Solution	Temperature °C	loading	α	$P_{CO_2}^*$ bar
5 wt% DEA/ 45 wt% MDEA	80	0.038	1.00 ± 0.22	0.044
	80	0.171	0.97 ± 0.023	0.57
		Average	0.99	
	120	0.027	1.90 ± 0.25	0.64
	120	0.010	1.86 ± 0.98	0.11
	120	0.010	2.31 ± 0.99	0.11
		Average	2.02	
Average: 5 wt%/45 wt% MDEA			1.61	
25 wt% DEA/ 25 wt% MDEA	40	0.378	1.11 ± 0.31	0.054
	80	0.456	0.92 ± 0.78	2.88
	80	0.101	0.75 ± 0.17	0.057
		Average	0.84	
	120	0.053	0.391 ± 0.001	0.24
Average: 25 wt% DEA/25 wt% MDEA			0.79	
Overall Average			1.16	

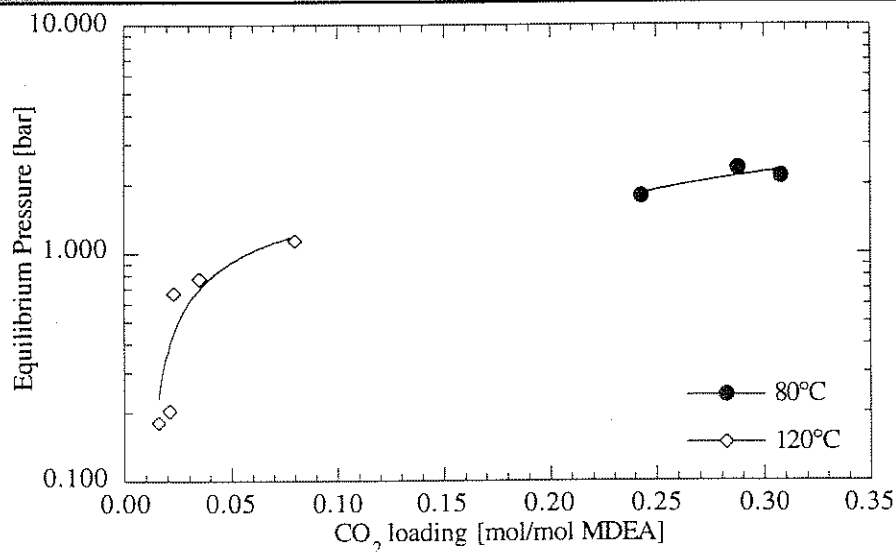


Figure 5.13 Equilibrium Pressure for 50 wt% MDEA as a Function of CO₂ Loading at Different Temperatures

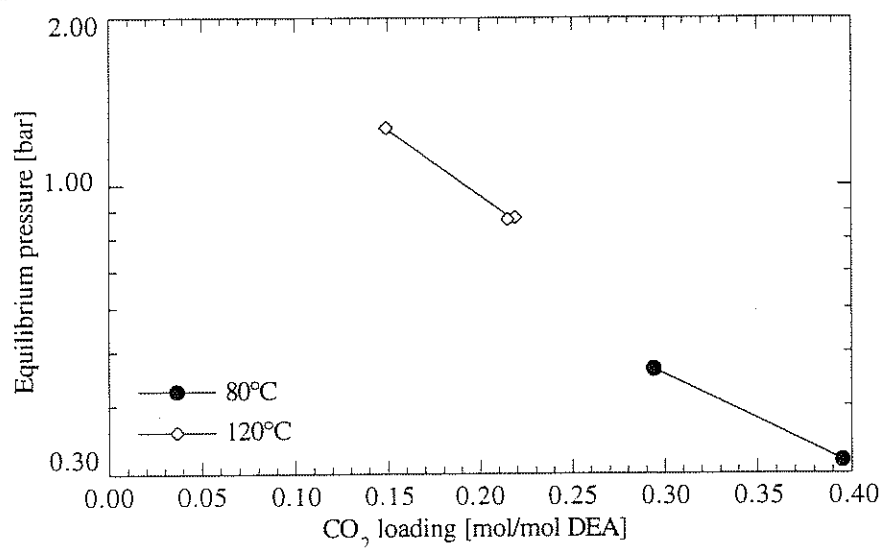


Figure 5.14 Equilibrium Pressure for 25 wt% DEA as a Function of CO₂ Loading at Different Temperatures

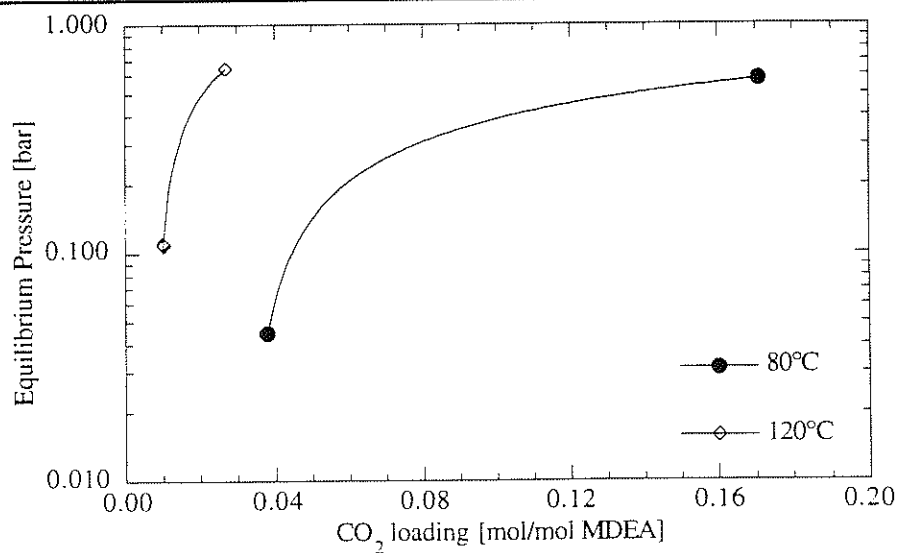


Figure 5.15 Equilibrium Pressure for 5 wt% DEA/ 45 wt% MDEA as a Function of CO₂ Loading at Different Temperatures

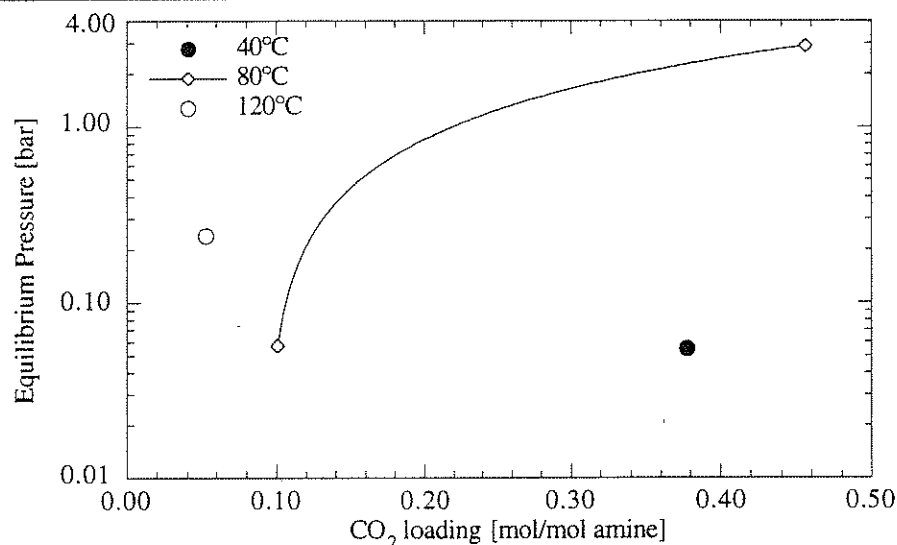


Figure 5.16 Equilibrium Pressure for 25 wt% DEA/ 25 wt% MDEA as a Function of CO₂ Loading at Different Temperatures

Values of α gives a direct indication of how good the equilibrium model is. A value of one would indicate an ideal situation. A plot of α as a function of loading and solution type at 80°C given on Figure 5.17 reveal that all points except one lie between 0.5 and 1.5. This indicates that the equilibrium model is consistent with the data. At 120°C there is significant scatter and α lies well between 0.3 and about 3.0. This indicates uncertainties on the equilibrium constants at higher temperature. On Figure 5.19 all the α values for all conditions are plotted together. The scatter is random and the average value of 1.16 is obtained.

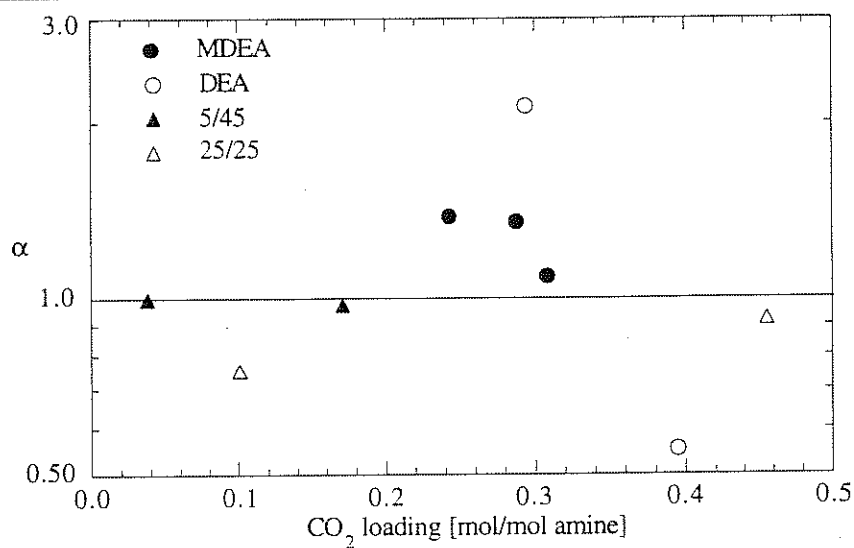


Figure 5.17 α as a Function of Solution Type at 80°C

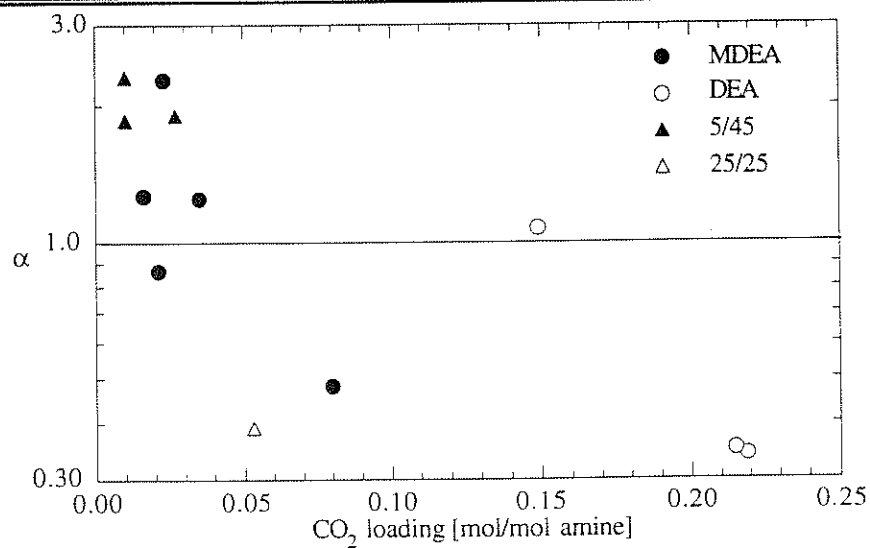


Figure 5.18 α as a Function of Solution Type at 120°C

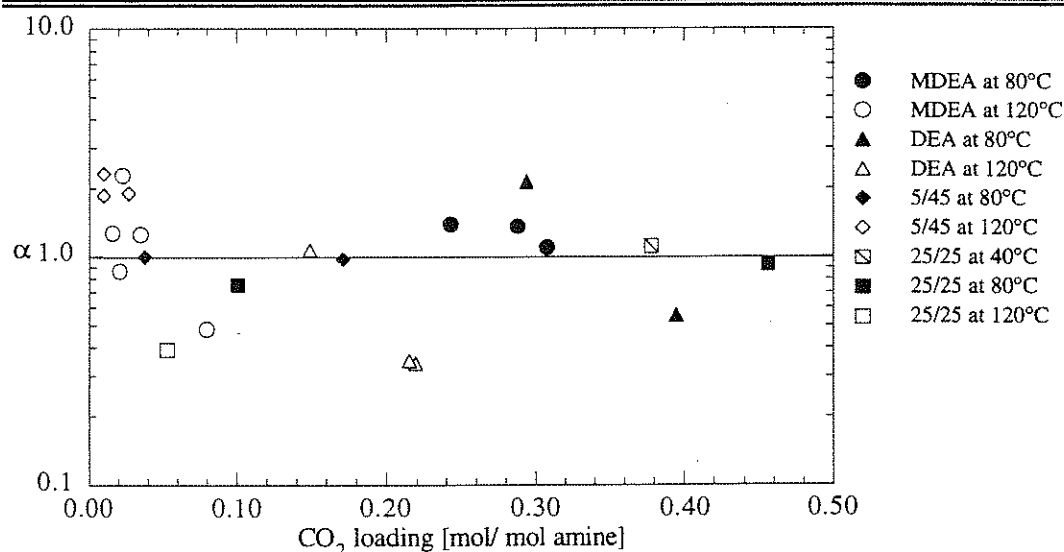


Figure 5.19 α as a Function of Loading and Solution Type at Different Temperatures

5.3 TEMPERATURE EFFECTS

The measured apparent rate constants for both MDEA and DEA decreased with temperature. The trends are shown on Figure 5.20. Apparent rate constants may be compared with other literature values. Comparisons are made on Figure 5.21 for the MDEA case. The value at 40°C coincides well with results from previous researchers, however, the extrapolation of other works are significantly higher than the measured values in this work. There are differences in methods, concentrations, loading and the range of CO₂ partial pressure used. All other works were at zero loading, low amine concentration and CO₂ partial pressure less than or equal to 1 atm.

On Figure 5.22 a similar situation of disagreement is demonstrated for the pure DEA case. The trend, as in the case with MDEA, is completely reversed. It may be argued that along with uncertainties in physical properties at higher temperatures, it is obvious that the apparent rate constants measured are a complex function of the actual rate constant, equilibrium and the physical properties.

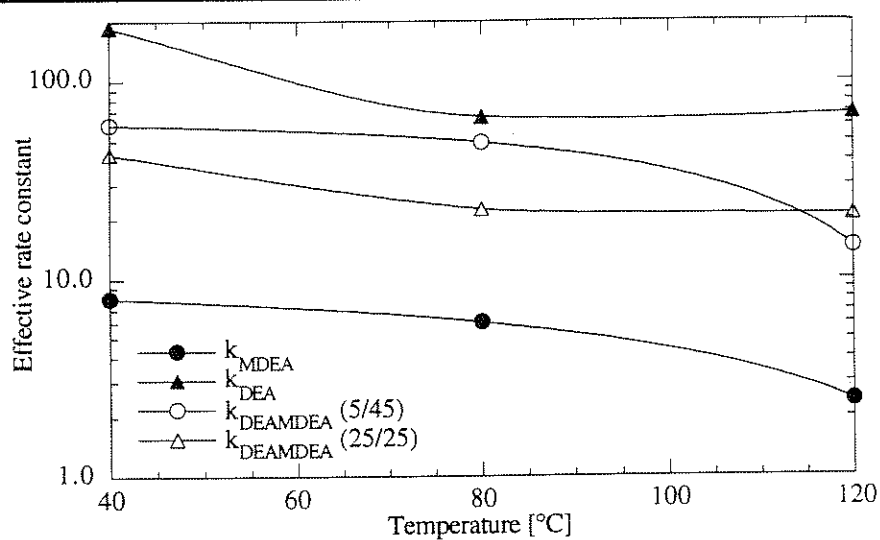


Figure 5.20 Temperature Dependence of Effective Rate Constants.

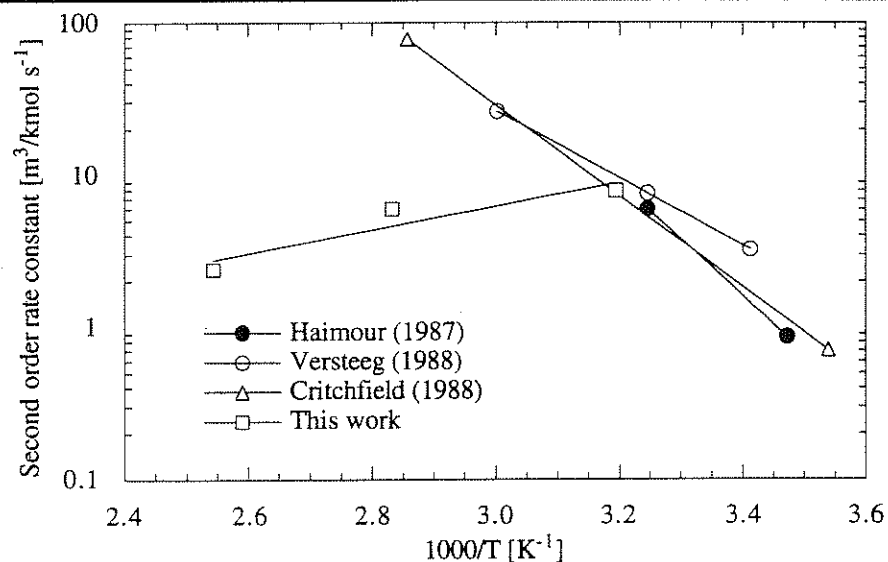


Figure 5.21 Temperature Dependence of MDEA Kinetics

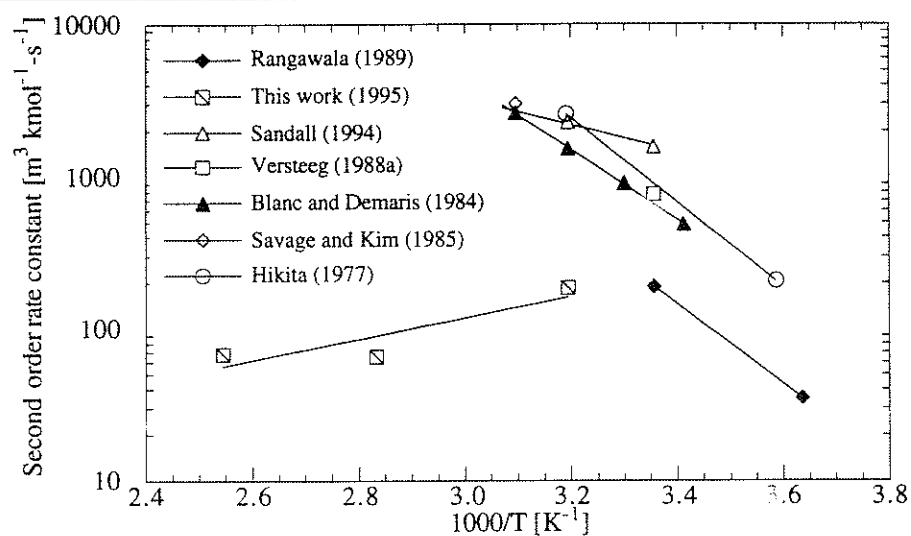


Figure 5.22 Temperature Dependence of DEA Kinetics

5.4 SENSITIVITY ANALYSIS

There is a strong interaction among the value of the effective rate constant, the mass transfer coefficient, and the diffusion coefficient of the ionic products. To demonstrate this an analysis was carried out for 50 wt% MDEA. The base case estimate of diffusion coefficient of ionic products, D_i , for MDEA at 120°C is $1.64 \times 10^{-9} \text{ m}^2/\text{s}$. Calculations were made with this base value, while using different values of apparent rate constant and regressing the CO₂ mass transfer coefficient from experimental data. Three other values of D_i were used. These corresponded to 1/9 ($D_i = 0.18 \times 10^{-9} \text{ m}^2/\text{s}$), 1/4 ($D_i = 0.41 \times 10^{-9} \text{ m}^2/\text{s}$), and 1/2 ($D_i = 0.82 \times 10^{-9} \text{ m}^2/\text{s}$) of the base value. Standard error for each case was also calculated.

A summary of the results for the MDEA case is presented on Figure 5.23. At very low values of the rate constant (less than 1.0), a large value of mass coefficient transfer is necessary to describe the result and this value is insensitive to the rate constant in this range. As the rate constant is increased a lower value of mass transfer coefficient is needed to fit the data, however the standard error increases also. At even higher rate constant (more than 400) the mass transfer coefficient reaches an asymptote as does the standard error.

Standard error is calculated as follows:

$$\text{standard error} = \sqrt{\sum_{i=1}^n \frac{(\text{Residual})^2}{\text{Degrees of Freedom}}} \quad (5.3)$$

Where:

$$\text{Residual} = \text{observed value} - \text{predicted value} \quad (5.4)$$

$$\text{Degrees of Freedom} = \text{no. data points} - \text{no. of parameters} \quad (5.5)$$

Selected detailed numbers for the sensitivity analysis for MDEA and DEA at 120°C are presented in Table 5.6. The first entry for both MDEA and DEA corresponds with the base case calculations. The base case for MDEA with a rate constant of 2.4 m³/kmol.s gave the best fit to the data with a regressed value of CO₂ mass transfer coefficient of $(12.3 \pm 7.5) \times 10^{-5}$ m/s.

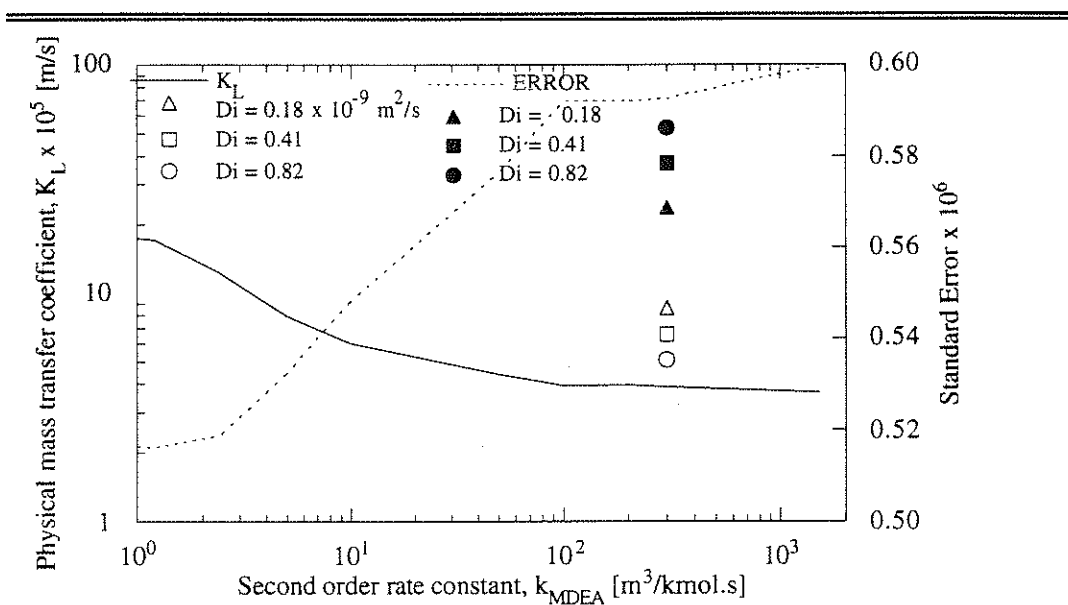


Figure 5.23 Sensitivity Analysis for 50 wt % MDEA at 120°C

Table 5.6 Sensitivity Analysis at 120°C

	Rate Constant m ³ /kmol.s	$k_L \times 10^5$ m/s	$D_i \times 10^9$ m ² /s	Standard Error kmol/m ² .s
MDEA	2.4	12.32 ± 7.50	1.64	0.518
	300.0	3.86 ± 1.33	1.64	0.592
	0.000001	22.29 ± 6.09	1.64	0.519
	300.0	8.59 ± 2.71	0.18	0.569
	300.0	6.57 ± 2.15	0.41	0.579
	300.0	5.09 ± 1.71	0.82	0.586
DEA	68	14.90 ± 6.03	2.25	0.563
	20000	4.84 ± 1.30	2.25	0.883

The lack of confidence in the values of diffusion coefficients especially at high temperature and in the concentrated amines makes the sensitivity analysis an important tool. The results above indicates that if the D_i was to be reduced by a factor of 9 a rate constant , k_{MDEA} , of about $300 \text{ m}^3/\text{kmol}\cdot\text{s}$ would be obtained. The factor of 9 may not be too large for consideration because of the extrapolation and estimations involved in estimating D_i .

With such a low value of D_i the ratio of D_i to D_{CO_2} that enters in determination of the Instantaneous enhancement factor, E_{ins} (as discussed in section 4.4 and Appendix I) would predict a lower values of E_{ins} by as much as a factor of 3 making the window for good data even narrower.

5.5 OVERALL GAS PHASE MASS TRANSFER COEFFICIENT

The two film theory of gas/ liquid mass transfer coefficient usually represents flux by using mass transfer coefficients and driving forces defined in one of several ways. The overall gas film mass transfer coefficient, K_G , uses the bulk gas partial pressure, P_{CO_2} , and the equilibrium partial pressure over the bulk solution, $P^*_{CO_2}$:

$$K_G = \frac{\text{Flux}}{P_{CO_2} - P^*_{CO_2}} \quad (5.6)$$

Equation 5.6 can be used to calculate overall gas phase mass transfer coefficients directly from data obtained in this work for the specific systems. These values will then be available for absorption/ desorption equipment design. Equations 5.2 and 5.6 were used with the mass transfer model to calculate the overall mass transfer coefficient for each experimental data point. The results are tabulated in Table J.1 in Appendix J.

The plots that follow include only the data points with absolute flux greater than $0.45 \times 10^{-6} \text{ kmol/m}^2\text{s}$. This minimizes the uncertainties in the accuracy of the measured fluxes which the model matches in estimating parameters, and thus gives good values of overall mass transfer coefficients. The curves included in the plots are for the purposes of making the reading easier only. The overall gas phase mass transfer coefficient is found to be directly affected by temperature, solution type, and CO_2 loading.

5.5.1 Temperature Effect

For the four solution types: 50 wt% MDEA, 25 wt% DEA, 5 wt% DEA/45 wt% MDEA and 25 wt% DEA/25 wt% MDEA, plots are presented for each system at the three temperatures 40, 80, and 120°C . These plots show the effect of temperature and loading for each solution type.

5.5.1.1 50 wt% MDEA

On Figure 5.24, K_G values for 50 wt% MDEA solution are plotted as a function of CO_2 loading. The general trend is for the K_G to decrease with an increase in CO_2 loading. The values at 40°C varied from $4.46 \text{ kmol}/(\text{m}^2 \text{ s bar})$ at a CO_2 loading of $0.019 \text{ mol/mol MDEA}$ to a lowest value of about $1.6 \text{ kmol}/(\text{m}^2\text{s bar})$ at a loading of $0.4 \text{ mol CO}_2/\text{mol MDEA}$. The values of K_G at 80°C ranged from 2.3 to $1.6 \text{ kmol}/(\text{m}^2\text{s bar})$ for the respective CO_2 loading range of 0.24 to $0.45 \text{ mol CO}_2/\text{mol MDEA}$. In the range of CO_2 loading covered by 80°C data, the K_G values at 40°C are indistinguishable from those at 80°C . Data at 120°C covers a range of CO_2 loading from 0.016 to 0.156 mol for which the

range of K_G values was 2.6 to 2.0. In this range K_G at 120°C are significantly lower than those at 40°C.

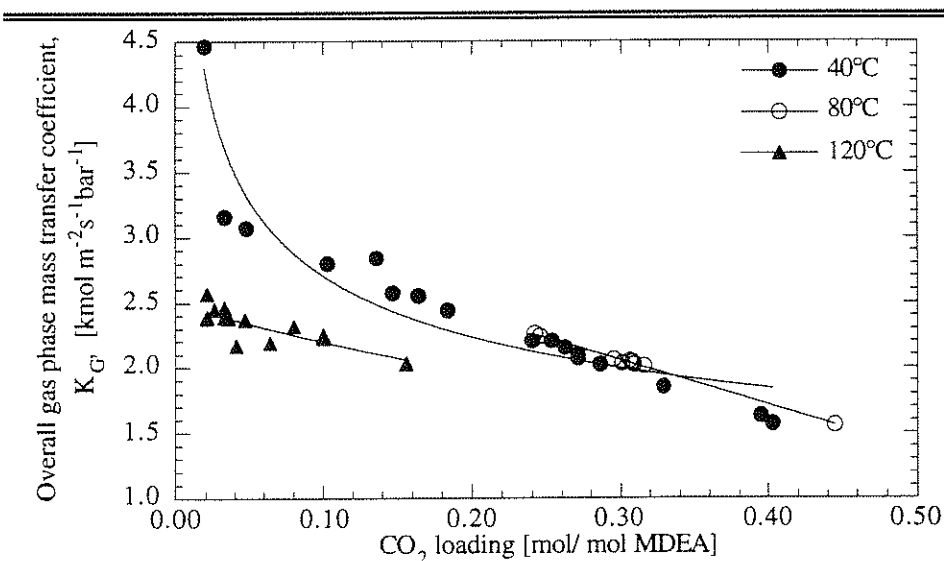


Figure 5.24 K_G in 50 wt% MDEA at Different Temperatures

5.5.1.2 25 wt% DEA

The K_G results for 25 wt% DEA solution are presented in Figure 5.25. At 40°C the K_G decreased from 16.5 to 7.1 kmol/(m²s bar) for corresponding CO₂ loading increase from 0.04 to 0.34 mol/mol DEA. While, at 80°C the range of K_G was from 4.5 to 2.6 kmol/(m²s bars) for an increase in CO₂ loading from 0.39 to 0.5 mol/mol DEA. There was only a slight decrease of K_G value at 120°C. Its value decreased from 4.4 to 3.7 kmol/(m²s bar) for a CO₂ loading increase from 0.15 to 0.29 mol/mol DEA. Generally the K_G value at high temperatures 80 and 120°C were significantly lower than at 40°C for the same loading conditions.

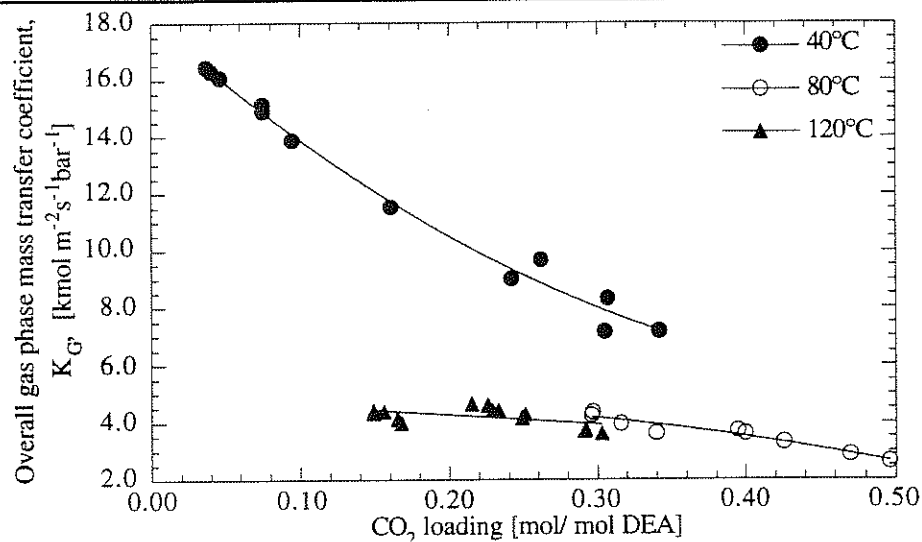


Figure 5.25 K_G in 25 wt% DEA at Different Temperatures

5.5.1.3 5 wt% DEA/45 wt% MDEA

The 40°C data with a CO₂ loading range from 0.09 to 0.53 mol/ mol amine, had the K_G value spanning from 5.5 down to 1.4 kmol/ (m²s bar). The range of loading for 80°C is small but goes to lower end than data at 40°C. It ranged from 0.04 to 0.2 mol/ mol amine, while the K_G values ranged from 6.3 down to 3.0 kmol/ (m²s bar). In the range of data where CO₂ loading overlap for 40°C and 80°C, the K_G for 40°C is just slightly higher than at 80°C. The K_G values at 120°C were the lowest and they fell from about 3.2 kmol/ (m²s bar) at a CO₂ loading of 0.01 mol/ mol amine down to 2.0 kmol/ (m²s bar) at a loading of 0.03 mol/ mol amine. These results are presented on Figure 5.2.

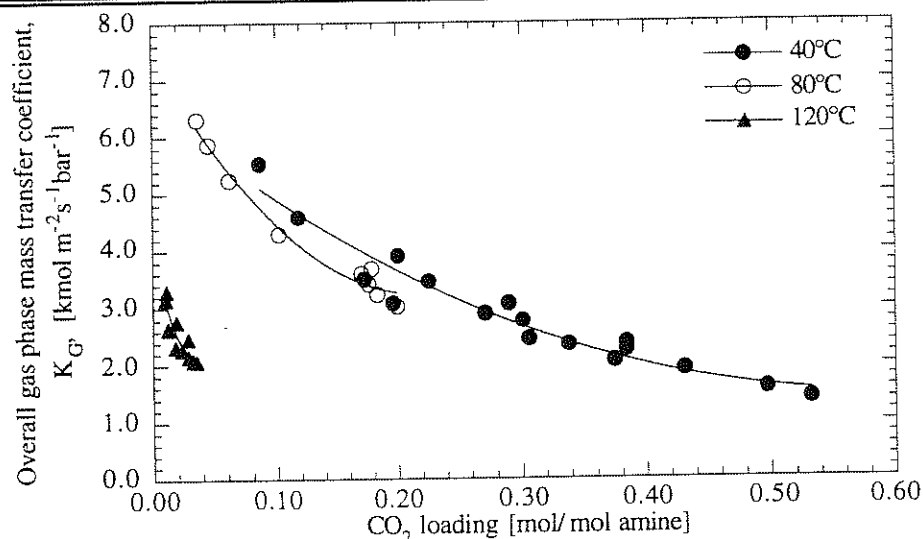


Figure 5.26 K_G in 5 wt% DEA/ 45 wt% MDEA at Different Temperatures.

5.5.1.4 25 wt% DEA/25 wt% MDEA

The results on K_G for 25 wt% DEA/ 25 wt% MDEA are plotted in Figure 5.27. For this system at all loading levels the K_G values decrease with temperature increase. The values at 40°C decreased from 12.2 kmol/ (m²s bar) at a CO₂ loading of 0.08 mol/ mol CO₂ down to 4.0 kmol/ (m²s bar) at a CO₂ loading of 0.42 mol/ mol amine. The range at 80°C was from 8.0 to 1.8 kmol/ (m²s bar) corresponding to CO₂ loading of 0.10 to 0.49 mol/ mol amine. The K_G values at 120°C ranged from 6.4 to 4.8 kmol/ (m²s bar) for a CO₂ loading range of 0.07 to 0.11 mol/ mol CO₂.

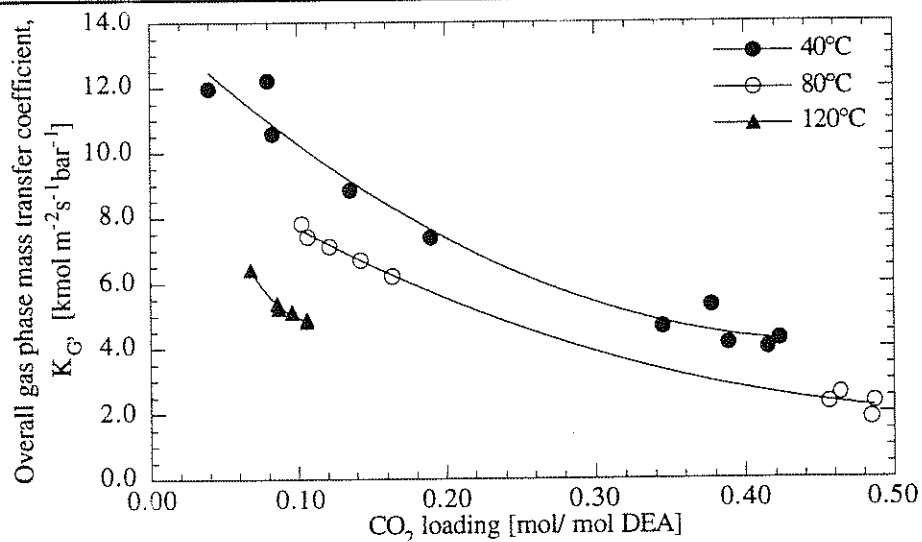


Figure 5.27 K_G for 25 wt% DEA/ 25 wt% MDEA at Different Temperatures

5.5.2 Solution Type Effect

The effect of adding DEA to a solution of MDEA is to increase the overall gas phase mass transfer coefficient at all levels of CO₂ loading and at all three temperatures. The effect of addition of DEA is remarkable at 40°C and decreases with increase in temperature.

5.5.2.1 Solution Type Effect at 40°C

Figure 5.28 shows the results at 40°C for all four solution types. For all solutions K_G value decreased with increasing loading. 25 wt% DEA had the highest K_G followed by 25 wt% DEA/ 25 wt% MDEA, and then 5 wt% MDEA/45 wt% DEA, with MDEA having the lowest value. At CO₂ loadings higher than 0.3 mol/mol amine 50 wt% MDEA and 5 wt% DEA/45 wt% DEA

have almost the same values of K_G . This may be because all the DEA has been depleted by the reaction and only MDEA remains in the mixture.

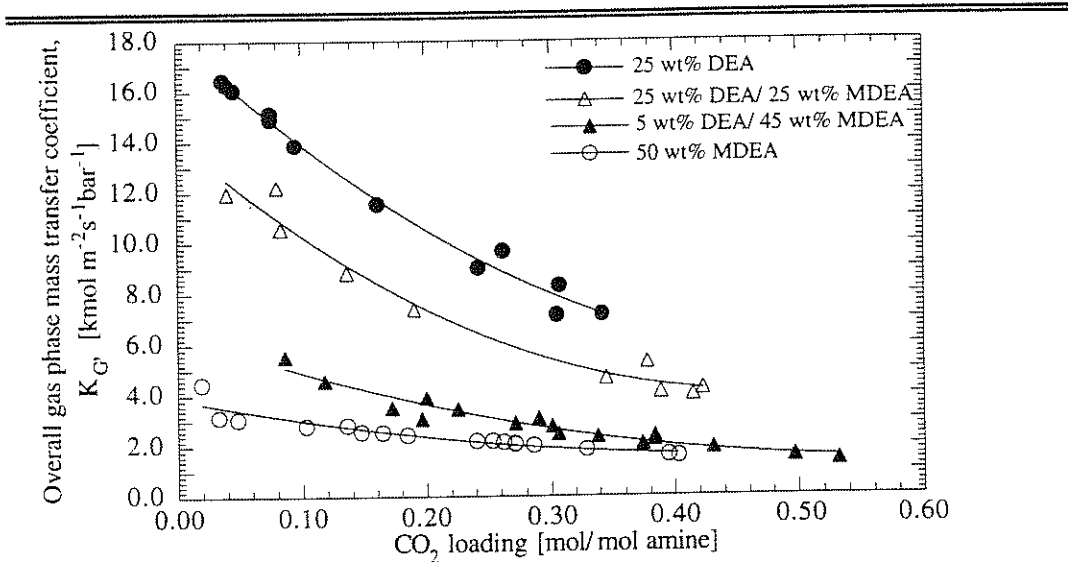


Figure 5.28 K_G at 40°C for the Four Solutions

5.5.2.2 Solution Type Effect at 80°C

Overall mass transfer coefficient, K_G , values for all four solution types at 80°C are plotted on Figure 5.29. Same trends as those described in the previous section for 40°C are observed. 25 wt% DEA providing the highest value and 50 wt% MDEA giving the lowest.

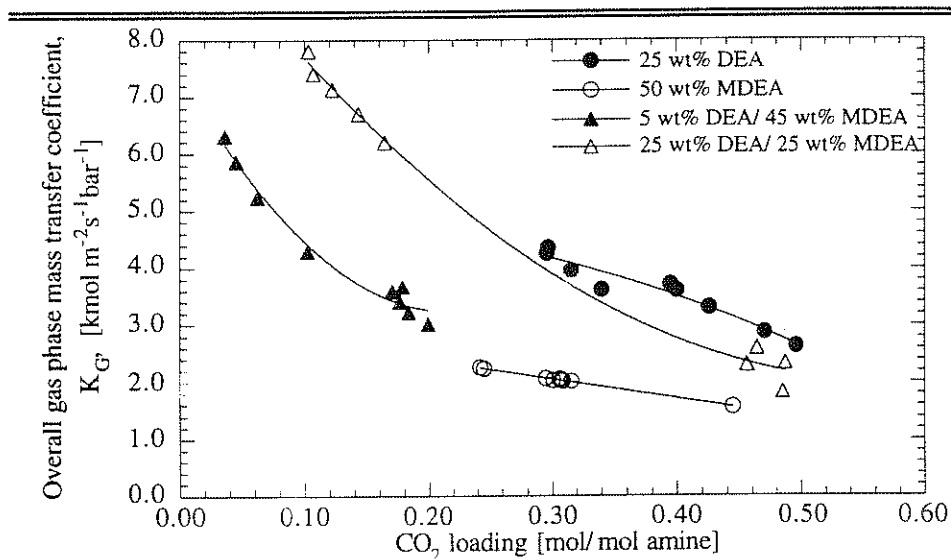


Figure 5.29 K_G at 80°C for the Four Solutions

5.5.2.3 Solution Type Effect at 120°C

Figure 5.30 presents results for all four solutions at 120°C for the range of CO_2 loading where data overlap for 50 wt% MDEA and 5 wt% DEA/45 wt% MDEA the value of K_G are the same. 25 wt% DEA/25 wt% MDEA and 25 wt% DEA seem to have the same values, although data available here do not overlap.

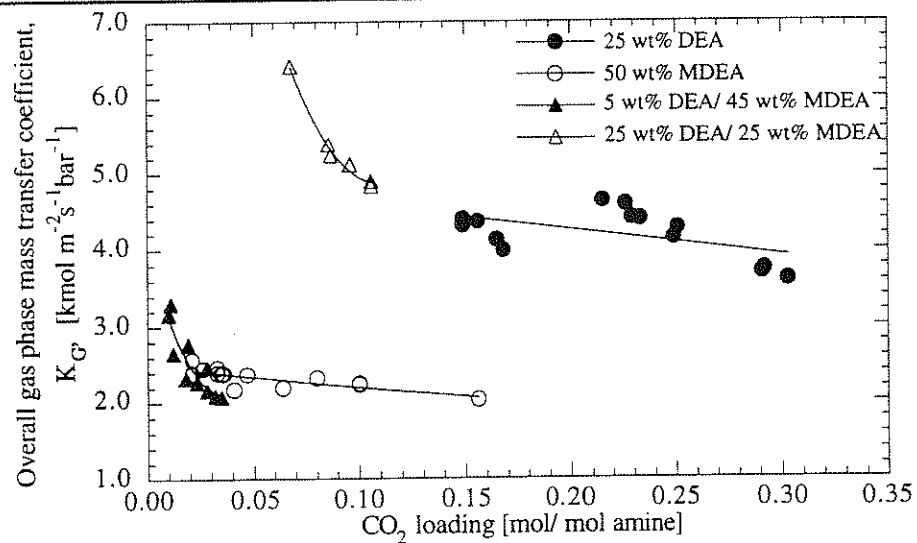


Figure 5.30 K_G at 120°C for the Four Solutions

CHAPTER SIX

Conclusions and Recommendations

6.1 CONCLUSIONS ON EXPERIMENT

A wetted wall column as a laboratory mass transfer device was designed and fabricated. It was then used for collecting data for both absorption and desorption of CO₂ with mixtures of methyldiethanolamine and diethanolamine. A wide range of conditions in terms of CO₂ partial pressure, CO₂ loading and temperature were studied. The data collected are unique as no other work has attempted these measurements at stripper conditions. The data made available here have been used to calculate overall mass transfer coefficients which may then be used in equipment design. These coefficients are given as a function of solution type, CO₂ loading, and temperature.

The overall mass transfer coefficient, K_G , decreased with an increase in temperature. This effect was more significant for the change in temperature from 40° to 80°C than between 80°C and 120°C. At a constant temperature and for a specific amine solution, K_G decreased with increase in CO₂ loading. Addition of DEA in a basic solution of MDEA increased the K_G values at all conditions. Thus K_G values decreased in the following order at all conditions: 25 wt% DEA, 25 wt% DEA/ 25 wt% MDEA, 5 wt% DEA/ 45 wt% MDEA, and 50 wt% MDEA.

6.2 CONCLUSIONS ON MODELING

A mass transfer model based on the film theory that coupled the chemical reaction and equilibrium has been developed. The model was used with a parameter estimation package (GREG). Apparent reaction rate constants and equilibrium correction factors were estimated. CO₂ equilibrium correction factor α was evaluated simultaneously with the apparent rate constants. This parameter allowed for extraction of equilibrium CO₂ partial pressure from the rate measurement data.

Equilibrium data were determined on average within a confidence interval of 16%. CO₂ flux predictions were good. At 80°C and to a larger extent at 120°C, the statistical determination of the apparent rate constants were not good.

6.3 RECOMMENDATIONS

The physical properties at high temperature are not known with good accuracy. Correlations had to be extrapolated beyond their limits. Thus, it would be appropriate for the physical properties required for analysis of data at high temperature to be measured independently.

More care should be given in choosing experimental conditions. The limits outlined in Chapter 4 and in Appendix I should be considered. As a rule an experiment should be designed such that enhancement factor expected is approximately the square root of the instantaneous enhancement factor.

Use of homogeneous kinetic experiments, such as a stopped flow technique, are recommended. Such methods do not need the knowledge of diffusion coefficients and solubility data to interpret the result.

APPENDIX A

Modeling

This appendix will complement in the reading of chapter 3 and the Fortran code.

A.1 BULK PHASE SPECIATION

Species identifiers

CO ₂	=	X(1)
OH ⁻	=	X(2)
HCO ₃ ⁻	=	X(3)
MDEA	=	X(4)
MDEAH ⁺	=	X(5)
DEA	=	X(6)
DEAH ⁺	=	X(7)
DEACOO ⁻	=	X(8)
CO ₃ ⁼	=	X(9)

Equilibrium constants KCO₂, KHCO₃, KMDEA, KDEA, and KCARB referred to in Chapter 3 are represented here and in the model as K1, K2, K3, K4, and K5 respectively.

Bicarbonate equilibrium corresponding to Equation 3.4 becomes:

$$F(1) = \alpha K1 X(3) - X(1) X(2) = 0 \quad (A.1)$$

Carbonate equilibrium represented by chemical equation 3.5 is represented in the model as

$$F(2) = X(3) \cdot X(2) - K_2 \cdot X(9) = 0 \quad (A.2)$$

MDEA equilibrium with MDEAH⁺ in Equation 3.6, is represented as:

$$F(3) = K_3 \cdot X(4) - X(2) \cdot X(5) = 0 \quad (A.3)$$

DEA equilibrium with DEAH⁺, Equation 3.7, is represented as:

$$F(4) = K_4 \cdot X(6) - X(2) \cdot X(7) = 0 \quad (A.4)$$

Carbamate equilibrium with DEA, Equation 3.8 is given by:

$$F(5) = K_5 \cdot X(8) - X(6) \cdot X(3) = 0 \quad (A.5)$$

Material Balance for CO₂, Equation 3.9 is given as:

$$F(6) = TCO_2 - X(1) - X(3) - X(9) - X(8) = 0 \quad (A.6)$$

MDEA material balance, Equation 3.10 is represented by:

$$F(7) = TMDEA - X(4) - X(5) = 0 \quad (A.7)$$

Material balance for DEA, Equation 3.11:

$$F(8) = TDEA - X(6) - X(7) - X(8) = 0 \quad (A.8)$$

Electroneutrality, Equation 3.12:

$$F(9) = X(7) + X(5) - X(3) - 2X(9) - X(8) - X(2) = 0 \quad (A.9)$$

After the solution of the problem is found, the values of X(i) for i =1 to 9 are stored as CO₂B, OHB, HCO₃B, MDEAB, MDEAHB, DEAB, DEAHB, DEACOOB, and CO₃B respectively; and are used in the interfacial calculations that follow next.

A.2 INTERFACIAL CALCULATIONS

To solve for interfacial speciation, CO₂ flux, and Enhancement Factor twelve unknowns and equations are defined:

$$\begin{aligned}
 \text{OH}^- &= X(1) \\
 \text{HCO}_3^- &= X(2) \\
 \text{MDEA} &= X(3) \\
 \text{MDEAH}^+ &= X(4) \\
 \text{DEA} &= X(5) \\
 \text{DEAH}^+ &= X(6) \\
 \text{DEACOO}^- &= X(7) \\
 \text{CO}_3^{=} &= X(8) \\
 \text{DIFFLUX} &= X(9) \\
 \text{CO}_{2e, \text{carb}} &= X(10) \\
 \text{CO}_{2e, \text{HCO}_3} &= X(11) \\
 \text{CO}_{2, \text{com}} &= X(12)
 \end{aligned}$$

Definition of some Intermediate values calculated:

Interfacial CO₂ concentration is calculated via the following equation.

$$\text{CO}_{2I} = m_{\text{CO}_2} P_{\text{CO}_2} \quad (\text{A.10})$$

Effective rate constant for bicarbonate formation, K_{1BICAR}:

$$K_{1BICAR} = k_{\text{MDEA}} X(3) + k_{\text{MDEAOH}} X(3) X(1) \quad (\text{A.11})$$

Effective rate constant for carbamate formation

$$K_{1CARB} = k_{\text{DEA}} X(5) + k_{\text{DEAMDE}} X(3) X(5) \quad (\text{A.12})$$

Rate of formation of carbamate, RATCARB:

$$\text{RATCARB} = K1\text{CARB} (\text{CO2I} - \text{X}(10)) \quad (\text{A.13})$$

Rate of formation of bicarbonate, RATBICA:

$$\text{RATBICA} = K1\text{B1CAR} (\text{CO2I} - \text{X}(11)) \quad (\text{A.14})$$

Flux due to carbamate, FLUXCAR:

$$\text{FLUXCAR} = K_L \sqrt{\frac{D_{\text{DEACOO}^-}}{D_{\text{CO}_2}}} (\text{X}(7) - \text{DEACOOB}) \quad (\text{A.15})$$

Flux due to bicarbonate, FLUXBIC:

$$\begin{aligned} \text{FLUXBIC} = K_L [& (\text{CO2I} - \text{CO2B}) + \sqrt{\frac{D_{\text{HCO}_3^-}}{D_{\text{CO}_3^{=}}}} (\text{X}(2) - \text{HCO3B}) \\ & + \sqrt{\frac{D_{\text{CO}_3^{=}}}{D_{\text{CO}_2}}} (\text{X}(8) - \text{CO3B})] \end{aligned} \quad (\text{A.16})$$

Dimensionless driving force, Φ

$$\Phi = \frac{(\text{X}(12) - \text{CO2B})}{(\text{CO2I} - \text{CO2B})} \quad (\text{A.17})$$

Overall effective rate constant, K1B:

$$K1B = K1\text{BCAR} + K1\text{CARB} \quad (\text{A.18})$$

Enhancement Factor based on pseudo first order approximations

$$\text{EI} = \sqrt{1.0 + \frac{K1B D_{\text{CO}_2}}{k_L^2}} \quad (\text{A.19})$$

The overall Enhancement Factor

$$\text{ECO}_2 = 1.0 + (\text{EI} - 1.0) (1 - \Phi) \quad (\text{A.20})$$

The weighing factor for reaction rates, FCARB is calculated via the following equation:

$$FCARB = \frac{K1CARB}{K1CARB + K1B1CAR} \quad (A.21)$$

The set of twelve functions that are solved simultaneously for the twelve unknowns are given in equations (A.21) through (A.33).

DEA Flux across the interface is zero:

$$F(1) = \sqrt{D_{DEA}} (X(5) - DEAB) + \sqrt{D_{DEAH^+}} \cdot (X(6) - DEAHB) + \sqrt{D_{DEACOO^-}} \cdot (X(7) - DEACOOB) = 0 \quad (A.22)$$

MDEA flux across the interface is zero:

$$F(2) = \sqrt{D_{MDEA}} (X(3) - MDEAB) + \sqrt{D_{MDEAH^+}} \cdot (X(4) - MDEAHB) = 0 \quad (A.23)$$

Electroneutrality:

$$F(3) = \sqrt{D_{MDEAH^+}} (X(4) - MDEAHB) + \sqrt{D_{DEAH^+}} \cdot (X(6) - DEAHB) - \sqrt{D_{HCO_3^-}} (X(2) - HCO_3B) - \sqrt{D_{DEACOO^-}} (X(7) - DEACOOB) - \sqrt{D_{OH^-}} (X(1) - OHB) - 2X\sqrt{D_{CO_3^{2-}}} (X(8) - CO_3B) = 0 \quad (A.24)$$

MDEA Equilibrium with MDEAH⁺:

$$F(4) = K3 \cdot X(3) - X(1) \cdot X(4) = 0 \quad (A.25)$$

DEA equilibrium with DEAH⁺:

$$F(5) = K4 \cdot X(5) - X(1) \cdot X(6) = 0 \quad (A.26)$$

Carbonate equilibrium:

$$F(6) = K2 \cdot X(8) - X(2) \cdot X(1) = 0 \quad (A.27)$$

Diffusional flux:

$$\begin{aligned}
F(7) = & X(9) - K_L [(CO2I - CO2B) + \sqrt{\frac{D_{HCO_3^-}}{D_{CO_2}}} (X(2) - HCO3B) \\
& + \sqrt{\frac{D_{CO_3^{2-}}}{D_{CO_2}}} (X(8) - CO3B) + \sqrt{\frac{D_{DEACOO^-}}{D_{CO_2}}} \\
& (X(7) - DEACOOB)] = 0
\end{aligned} \tag{A.28}$$

Enhancement Flux equals to Diffusional flux:

$$F(8) = K_L E_{CO_2} (CO2I - CO2B) - X(9) = 0 \tag{A.29}$$

Combined concentration of CO₂:

$$F(9) = X(12) - FCARB \cdot X(10) - (1.0DO - FCARB) X(11) = 0 \tag{A.30}$$

For calculation of CO₂ concentration that would be in equilibrium with carbamate:

$$F(10) = X(10) X(5) X(1) - \alpha K_1 K_5 X(7) = 0 \tag{A.31}$$

For calculation of CO₂ concentration that would be in equilibrium with HCO₃⁻:

$$F(11) = X(11) X(1) - \alpha K_1 X(2) = 0 \tag{A.32}$$

Ratio of carbamate flux to bicarbonate flux equals the ratio of rates of their formations:

$$F(12) = FLUXBIC \times RATCARB - RATBICA \times FLUXCAR = 0 \tag{A.33}$$

APPENDIX B

Derivation of the liquid film mass transfer coefficient correlation

Reference is made to the sketch of the cross section of the wetted wall column shown in figure B.1. The liquid flows in a film under the influence of gravity down a surface of a vertical tube.

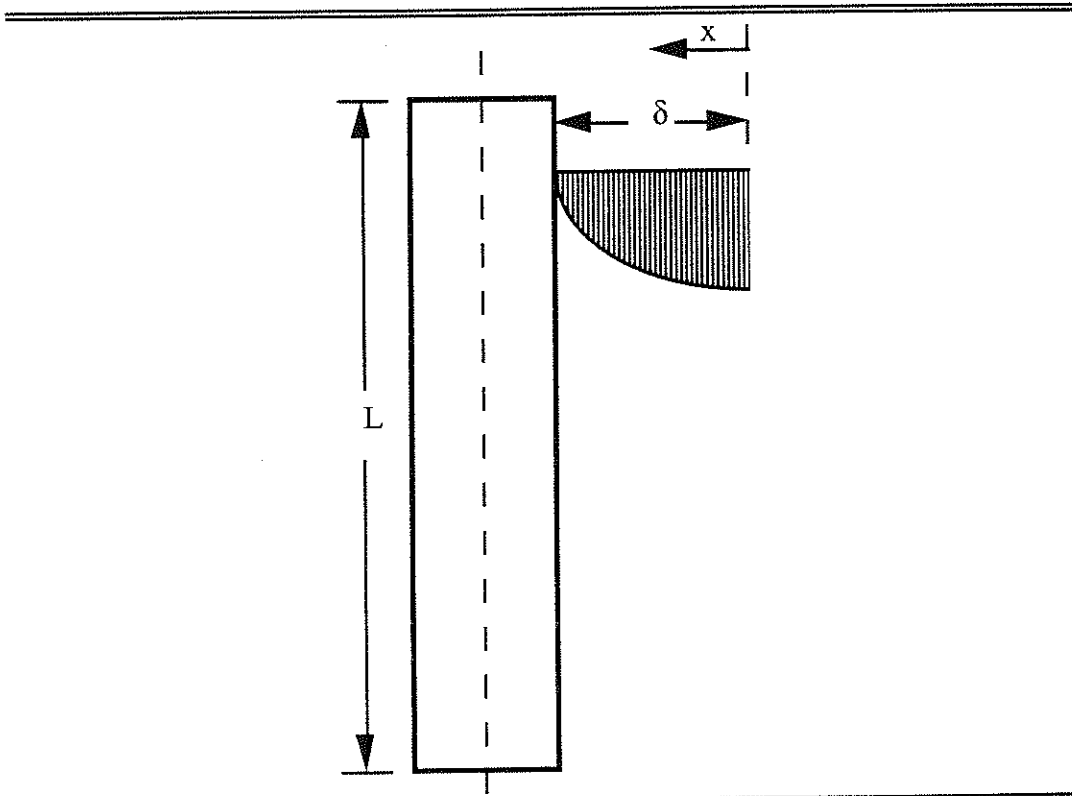


Figure B.1 Cross Section of the Wetted Wall Column Showing the Liquid Velocity Profile and Important Dimensions

When the film has attained its terminal velocity distribution, the velocity U at any depth x beneath the surface is given as (Bird et al., 1960):

$$U = U_{\max} \left(1 - \left(\frac{x}{\delta} \right)^2 \right) \quad (\text{B.1})$$

where

$$U_{\max} = \frac{3}{2} \left(\frac{\Gamma}{\rho} \right)^{\frac{2}{3}} \left(\frac{\rho g}{3\mu} \right)^{\frac{1}{3}} \quad (\text{B.2})$$

and Γ is mass flow rate per unit width and other symbols have usual meanings.

If the height of the wetted wall column is L , the exposure time, t_e , of any element of the surface to the gas is:

$$t_e = \frac{L}{U_{\max}} = \frac{2L}{3} \left(\frac{\rho}{\Gamma} \right)^{\frac{2}{3}} \left(\frac{3\mu}{\rho g} \right)^{\frac{1}{3}} \quad (\text{B.3})$$

Penetration theory gives the liquid side mass transfer coefficient as:

$$k_L = 2 \sqrt{\frac{D}{\pi t_e}} \quad (\text{B.4})$$

Substituting for t_e from (B.3) into (B.4) we obtain:

$$k_L = 2 \sqrt{\frac{D}{\pi}} \left(\frac{3}{2L} \right)^{\frac{1}{2}} \left(\frac{\Gamma}{\rho} \right)^{\frac{1}{3}} \left(\frac{\rho g}{3\mu} \right)^{\frac{1}{6}} \quad (\text{B.5})$$

$$k_L = \frac{2}{\sqrt{\pi}} \frac{\sqrt{3}}{\sqrt{2}} \left(\frac{1}{3} \right)^{\frac{1}{6}} D^{\frac{1}{2}} \left(\frac{1}{L} \right)^{\frac{1}{2}} \left(\frac{\Gamma}{\rho} \right)^{\frac{1}{3}} \left(\frac{\rho g}{3\mu} \right)^{\frac{1}{6}} \quad (\text{B.6})$$

or

$$k_L = 1.15 D^{\frac{1}{2}} \left(\frac{1}{L} \right)^{\frac{1}{2}} \left(\frac{\Gamma}{\rho} \right)^{\frac{1}{3}} \left(\frac{\rho g}{\mu} \right)^{\frac{1}{6}} \quad (\text{B.7})$$

Trying to put (B.7) in dimensionless form we proceed as follows:

$$k_L \left(\frac{L}{D} \right) = 1.15 \frac{L}{D} \frac{D^2}{L^{\frac{1}{2}}} \left(\frac{\Gamma}{\rho} \right)^{\frac{1}{3}} \left(\frac{\rho g}{\mu} \right)^{\frac{1}{6}} \quad (\text{B.8})$$

$$\frac{k_L L}{D} = 1.15 \frac{L^{\frac{1}{2}}}{D^{\frac{1}{2}}} \left(\frac{\Gamma}{\rho} \right)^{\frac{1}{3}} \left(\frac{\rho g}{\mu} \right)^{\frac{1}{6}} \quad (\text{B.9})$$

$$\frac{k_L L}{D} = 1.15 \left[\left(\frac{\mu}{\rho D} \right)^{\frac{1}{2}} \frac{L^{\frac{1}{2}} \rho^2}{\mu^2} \right] \left[\left(\frac{4\Gamma}{\mu} \right)^{\frac{1}{3}} \frac{1}{4^{\frac{1}{3}}} \frac{\mu^{\frac{1}{3}}}{\rho^{\frac{1}{3}}} \right] \left(\frac{\rho g}{\mu} \right)^{\frac{1}{6}} \quad (\text{B.10})$$

$$\frac{k_L L}{D} = \frac{1.15}{4^{\frac{1}{3}}} \left(\frac{\mu}{\rho D} \right)^{\frac{1}{2}} \left(\frac{4\Gamma}{\mu} \right)^{\frac{1}{3}} \frac{L^{\frac{1}{2}} \rho^2}{\mu^2} \frac{\mu^{\frac{1}{3}}}{\rho^{\frac{1}{3}}} \left(\frac{\rho g}{\mu} \right)^{\frac{1}{6}} \quad (\text{B.11})$$

$$\frac{k_L L}{D} = 0.724 \left(\frac{\mu}{\rho D} \right)^{\frac{1}{2}} \left(\frac{4\Gamma}{\mu} \right)^{\frac{1}{3}} \frac{L^{\frac{3}{6}} \rho^6}{\mu^6} \left(\frac{\rho g}{\mu} \right)^{\frac{1}{6}} \quad (\text{B.12})$$

$$\frac{k_L L}{D} = 0.724 \left(\frac{\mu}{\rho D} \right)^{\frac{1}{2}} \left(\frac{4\Gamma}{\mu} \right)^{\frac{1}{3}} \left(\frac{\rho^2 L^3 g}{\mu^2} \right)^{\frac{1}{6}} \quad (\text{B.13})$$

or

$$\text{Sh} = 0.724 \text{Sc}^{\frac{1}{2}} \text{Gr}^{\frac{1}{3}} \text{Ga}^{\frac{1}{6}} \quad (\text{B.14})$$

APPENDIX C

Physical Properties Correlations

C.1 VISCOSITY

Viscosity of the unloaded solution was calculated by the correlation developed by Glasscock et al. (1991) based upon the data of Al-Ghawas et al. (1988), Critchfield (1988) and Sada et al. (1978). To account for the effect of CO₂ loading on the viscosity of amine solutions, a correction proposed by Glasscock et al. (1991) is used.

C.1.1 Viscosity of the Unloaded Solution

Based upon the data of Al-Ghawas et al. (1988), Critchfield (1988) and Sada et al. (1978), Glasscock (1990) developed the following correlation:

$$w_{am} = w_{mdea} + 0.980 w_{dea} + 0.876 w_{mea} \quad (C.1)$$

$$B_1 = -19.52 - 23.40 w_{am} - 31.24 w_{am}^2 + 36.17 w_{am}^3 \quad (C.2)$$

$$B_2 = 3912 + 4894 w_{am} + 8477 w_{am}^2 - 8358 w_{am}^3 \quad (C.3)$$

$$B_3 = 0.02112 + 0.03339 w_{am} + 0.02780 w_{am}^2 - 0.04202 w_{am}^3 \quad (C.4)$$

$$\log_e \mu = B_1 + \frac{B_2}{T} + B_3 T \quad (C.5)$$

μ is in cP and T is the temperature in degrees Kelvin. w_{mdea} , w_{dea} and w_{mea} denote the weight fractions of MDEA, DEA, and MEA, respectively. The correlation is based upon the viscosity correlation for MDEA only by Al-Ghawas

et al., with the parameters in bold adjusted to fit the experimental data for all of the amines. The standard deviation for the 4 parameters are 0.980 ± 0.0274 , 0.876 ± 0.0449 , 4894 ± 199.5 , -0.04202 ± 0.00124 . The other parameters could not be adjusted with significance. This correlation is considered to be reasonable for 0 to 50 wt% total amine, and a temperature range of 290 to 320 K.

C.1.2 Viscosity of Loaded Solution

Toman (1989) determined the effect of CO₂ loading on the viscosity of 50 wt% MDEA at 298K. These data span the range of 0.001 to 0.76 moles of CO₂ per mole of amine, and Glasscock (1990) fit them by a second order equation:

$$\eta_{\text{MDEA}} = 1.000 + 0.8031 \text{ loading} + 0.35786 (\text{loading}^2) \quad (\text{C.6})$$

In order to estimate the viscosity of solutions other than 50 wt% MDEA, the corrected relative viscosity was estimated by Glasscock (1990) as follows:

$$\text{relative viscosity} = 1. + 2. (r-1) (w_{\text{am}}) \quad (\text{C.7})$$

For 50 wt% amine, this equation defaults to relative viscosity = r , whereas, for pure water (wt fraction amine = 0) this equation defaults to 1 for the relative viscosity, despite the loading. This correlation makes obvious physical sense and is used for all amine solutions. This relation is assumed to be correct at all temperatures.

C.2 DENSITY OF THE SOLUTION

The density correlation of Licht and Weiland (1989) was used for all amines. The correlation is of the following form:

$$\frac{1}{\rho} = u_w V_{w0} \exp\{b_w (T - T_0)\} + u_{A1} V_{A10} \exp\{b_{A1} (T - T_0)\} + u_{A2} V_{A20} \exp\{b_{A2} (T - T_0)\} + w_{CO2} V_{CO20} \exp\{b_{CO2} (T - T_0)\} \quad (C.8)$$

where:

T_0	=	308K
T	=	temperature in degrees K
u_w	=	weight fraction water
u_{A1}	=	weight fraction amine 1
u_{A2}	=	weight fraction amine 2 (if needed)
w_{CO2}	=	loaded basis weight fraction CO ₂
V_0	=	specific volume, shown in table C.1 below
b	=	bulk thermal expansivity

Table C.1 Some properties of the solution components

	Water	MDEA	DEA	MEA	CO ₂
specific volume (cm ³ /g)	1.01	0.918	0.894	0.964	0.0636
bulk expansivity (K ⁻¹)	0.000344	0.000528	0.000487	0.00568	0.0036

C.3 DIFFUSION COEFFICIENTS

The diffusion coefficient of CO₂ was estimated using N₂O analogy. First, diffusion coefficients of CO₂ and N₂O in water are calculated using the following equations regressed from literature data in Versteeg and Van Swaaij (1988c) (includes data from 30 different sources) and new data by Tamimi et al. (1994), who extends the temperature dependency to 95°C. These data are tabulated in Table C.2 and Table C.3, also, they are plotted on Figure C.1 and Figure C.2.

$$\ln(D_{CO2}) = -(12.69 \pm 0.13) - \frac{2199.24}{T} \quad (C.9)$$

$$\ln(D_{N2O}) = -(12.37 \pm 0.23) - \frac{2306}{T} \quad (C.10)$$

where T is in Kelvin and diffusion coefficient is in m^2/s .

Table C.2 Diffusivity of CO₂ in water used for correlation development

Temperature. [K]	$D_{\text{CO}_2} \times 10^9 [\text{m}^2\text{s}^{-1}]$	
	Versteeg and Van Swaaij (1988c)	Tamimi et al. (1994)
273.00	0.96	
279.50	1.15	
283.00	1.46	
288.00	1.60	
288.00	1.39	
289.00	1.57	
291.00	1.71	
291.50	1.65	
292.50	1.68	
293.00	1.64	
293.00	1.60	
293.00		1.77
293.16	1.76	
298.00	1.98	
298.00	1.87	
298.00	1.95	
298.00	2.05	
298.00	1.85	
298.00	2.00	
298.00		1.94
298.00	1.87	
298.00	1.90	
298.00	1.74	
298.16	1.94	
303.00	2.29	
303.00	2.15	
303.16		2.20
307.70	2.41	
308.00	2.18	
313.00	2.80	
313.16		2.93
318.20	3.03	
325.00	3.61	
327.90	3.68	
333.16		4.38
338.00	4.40	
338.00	4.30	
348.10	5.40	
353.16		6.58
368.16		8.20

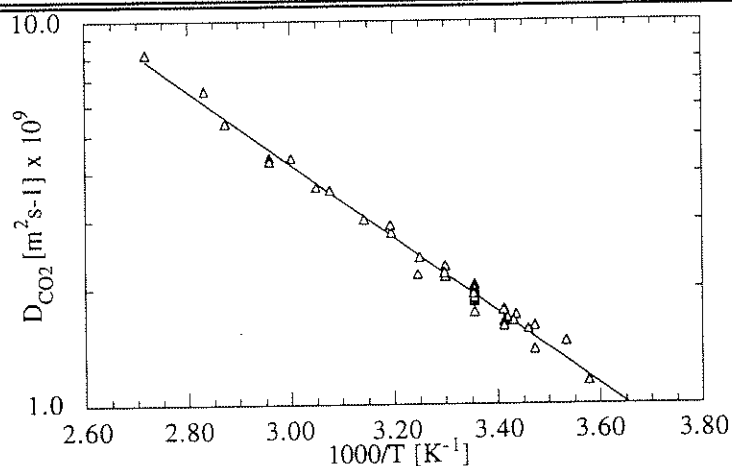


Figure C.1 Diffusivity of CO₂ in water as a Function of Temperature, Versteeg and van Swaaij (1988c), and Tamimi et al. (1994)

Table C.3 Diffusivity of N₂O in water used for correlation development

Temp. [K]	D _{CO₂} × 10 ⁹ m ² s ⁻¹	
	Versteeg and Van Swaaij (1988)	Tamimi et al. (1994)
288.00	1.39	
289.70	1.70	
291.10	1.47	
292.00	1.56	
292.90	1.48	
293.00	1.52	
293.00	1.92	
293.00	1.74	
293.00	1.45	
293.00	1.65	
293.16		1.84
297.90	2.09	
298.00	1.86	
298.00	1.69	
298.00	1.92	
298.00	1.78	
298.00	1.88	
298.00	1.80	
298.16		1.88
302.90	2.27	

Table C.3 Continued

Temp. [K]	$D_{CO_2} \times 10^9 \text{ m}^2\text{s}^{-1}$	
	Versteeg and Van Swaaij (1988)	Tamimi et al. (1994)
303.16		1.93
303.80	2.35	
308.00	2.03	
308.00	2.34	
312.90	2.35	
313.00	2.55	
313.00	2.58	
313.16		2.61
318.00	3.17	
322.70	2.85	
333.16		4.51
340.00	5.33	
343.00	5.43	
353.00	6.32	
353.16		6.50
368.16		7.30

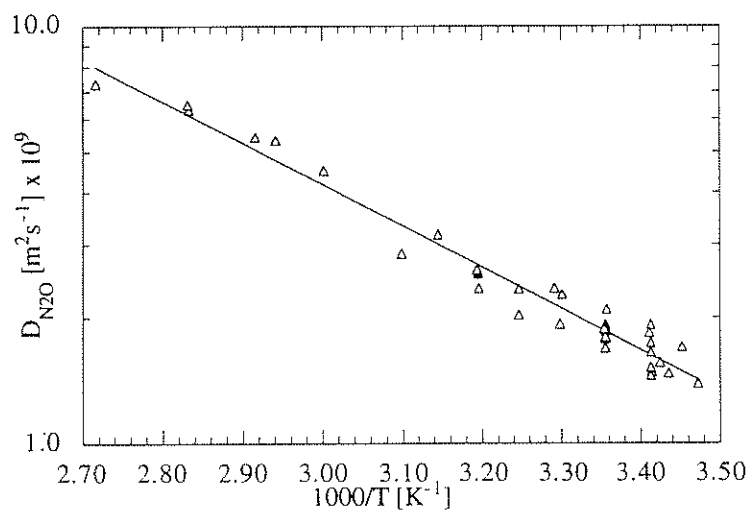


Figure 12. Diffusivity of N_2O in water as a function of temperature, Versteeg and van Swaaij (1988c), and Tamimi et al. 1994)

The diffusion coefficient for N_2O is then calculated according to the modified Stokes-Einstein relation:

$$(D_{N_2O} \mu^{0.6})_{\text{am soln}} = (D_{N_2O} \mu^{0.6})_{\text{water}} \quad (\text{C.11})$$

The diffusion coefficient of CO_2 in the amine solution is then calculated using the N_2O analogy:

$$\left(\frac{D_{N_2O}}{D_{CO_2}}\right)_{\text{am soln}} = \left(\frac{D_{N_2O}}{D_{CO_2}}\right)_{\text{water}} \quad (\text{C.12})$$

The amine diffusion coefficients in water for DEA and MDEA were calculated from the data of Versteeg and van Swaaij (1988) at 298K by Glasscock (1990). The resulting diffusion coefficients in water at 298K were $8.02 \times 10^{-10} \text{ m}^2/\text{s}$, and $8.08 \times 10^{-10} \text{ m}^2/\text{s}$, for MDEA and DEA respectively. The diffusion coefficients were corrected for viscosity and temperature using the modified Stokes-Einstein relationship:

$$D_{\text{am,soln}} = D_{\text{am,water}} \frac{T}{298} \left(\frac{\mu_{H_2O}}{\mu_{\text{soln}}}\right)^{0.6} \quad (\text{C.13})$$

The ratio of amine diffusion coefficient to that of CO_2 at 40°C was about 0.3. This ratio was assumed to be constant at all temperatures. Thus, diffusion coefficient for all other species, D_i , was obtained as:

$$D_i = 0.3 \cdot D_{CO_2} \quad (\text{C.14})$$

C.4 SOLUBILITY

To estimate the solubility of CO_2 in alkanolamine solutions the N_2O - CO_2 analogy is used:

$$\frac{H_{N_2O-H_2O}}{H_{CO_2-H_2O}} = \frac{H_{N_2O-\text{am}}}{H_{CO_2-\text{am}}} \quad (\text{C.15})$$

where H is the Henry's constant. The Henry's constant expressions for N_2O and CO_2 were developed by regressing data from Versteeg and van Swaaij (1988c); Duda and Vrentas (1968); Joosten and Danckwerts (1972) and Sandall et al. (1993).

$$H_{N_2O-H_2O} = 63612 \exp\left(\frac{-2189.8}{T}\right) \frac{m^3 \text{ bar}}{\text{kmol}} \quad (C.16)$$

$$H_{CO_2-H_2O} = 22633 \exp\left(\frac{-1971.2}{T}\right) \frac{m^3 \text{ bar}}{\text{kmol}} \quad (C.17)$$

Table C.4 Solubility of N_2O in water

Temperature [K]	H_{CO_2} m3bar/kmol			
	Versteeg and van Swaaij (1988c)	Duda and Vrentas (1968)	Joosten and Danckwerts (1972)	Sandall et al. (93)
291.2	33.445			
292	34.843			
292.9	33.333			
293	34.247			
298	41.322			
298.6	37.736			
302.9	49.505			
308	52.632			
312.9	59.172			
313	60.606			
318	69.930			
322.6	77.429			
322.9	77.074			
340	103.093			
353	128.205			
359.4	140.845			
298		39.063		
313		62.112		
298			41.494	
293				36.943
313				63.389
333				91.041
353				112.23

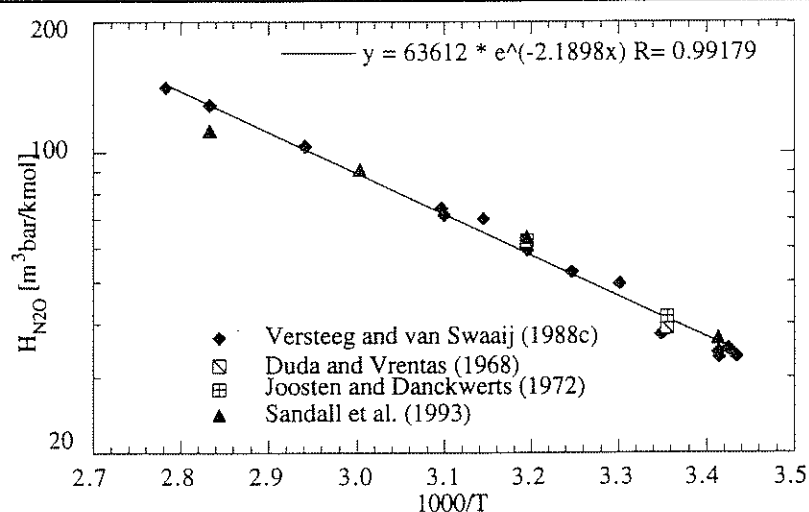


Figure C.3. Solubility of N_2O in Water as a Function of Temperature

Table C.5 Solubility of CO_2 in water

Temperature [K]	H_{CO_2} [$m^3 \text{ bar/kmol}$]	
	Versteeg and van Swaaij(1988)	Sandall et al. (1993)
291	24.691	
292	24.096	
292	25.707	
293	26.316	
298	29.674	
298	30.395	
303	35.714	
308	39.370	
311.4	40.984	
313	42.194	
313.4	42.017	
318	48.544	
323	51.546	
333	61.350	
343.5	71.429	
350.2	75.758	
355.2	83.333	
360.1	92.593	
293		27.439
313		45.7178
333		64.757
353		86

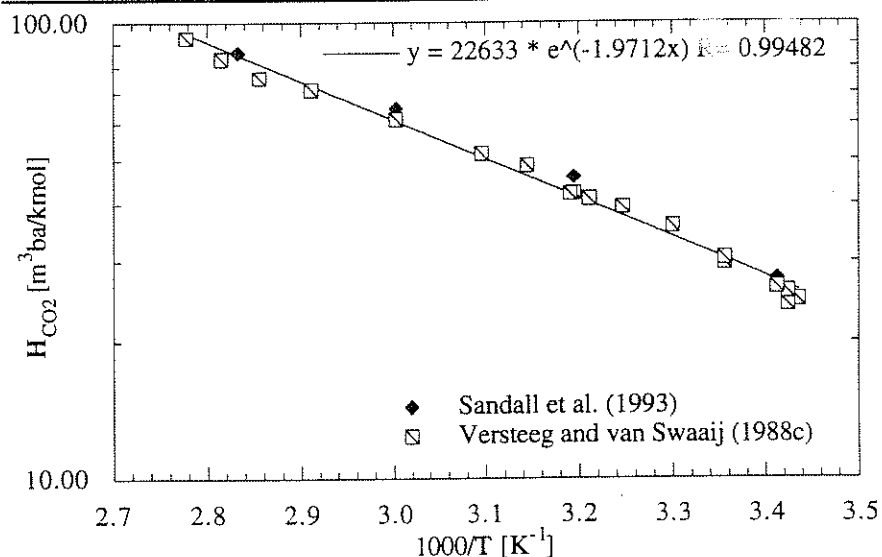


Figure C.4 Solubility of CO₂ in Water as a Function of Temperature

Solubility of N₂O in 50 wt% MDEA and 30 wt% DEA at different temperatures were estimated based on data by Sandal et al. (1993). The data at 30% DEA were used as though they were for 25 wt% DEA. For the mixed solutions a weighted average of the two was used.

$$H_{N_2O-MDEA} = 3263.1 \exp\left(\frac{-1211.9}{T}\right) \frac{\text{m}^3 \text{ bar}}{\text{kmol}} \quad (\text{C.18})$$

$$H_{N_2O-DEA} = 22217 \exp\left(\frac{-18248}{T}\right) \frac{\text{m}^3 \text{ bar}}{\text{kmol}} \quad (\text{C.19})$$

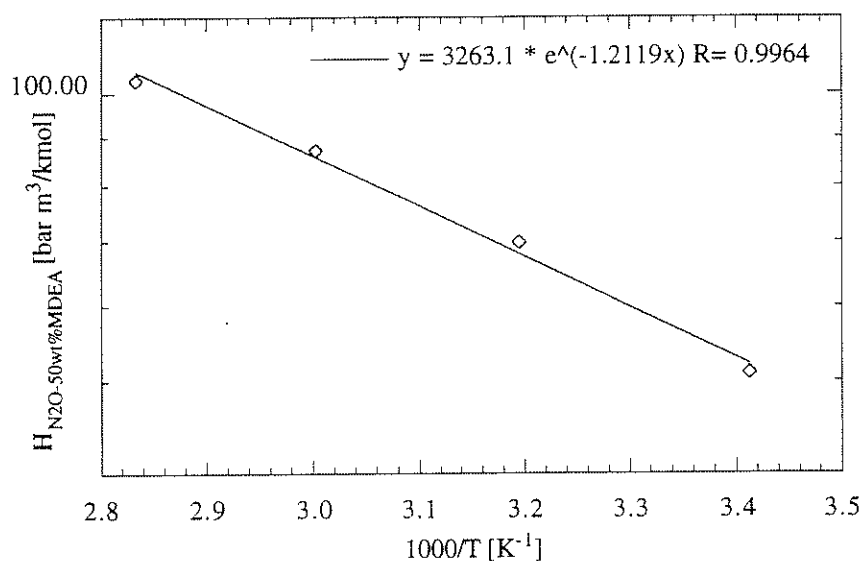


Figure C.5 Solubility of N_2O in 50 wt% MDEA as a Function of Temperature, Sandall et al., (1993)

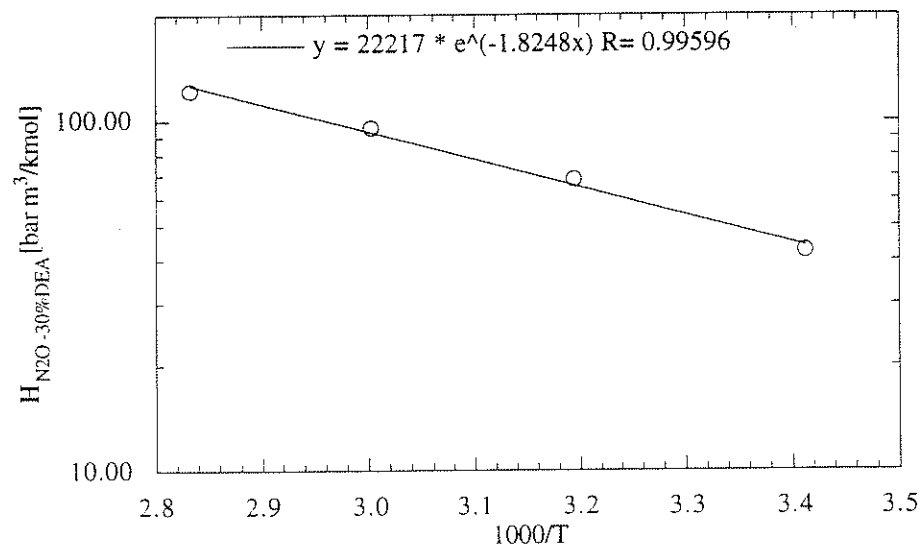


Figure C.6 Solubility of N_2O in 30 wt% DEA as a Function of Temperature, Sandall et al. (1993)

With all the other quantities in Equation C.15 estimated, the Henry constant of CO₂ in unloaded amine solution is calculated. To correct for the effect of loading on solubility, a correlation developed by Toman (1990) is used:

$$\text{Log} \frac{H^*_{\text{CO}_2\text{-am}}}{H_{\text{CO}_2\text{-am}}} = 0.09 \times \text{Total CO}_2 \text{ concentration} \quad (\text{C.20})$$

where total CO₂ concentration is in Molar units.

The value reported in the result section is the solubility, m_{CO_2} , which is the reciprocal of the corrected Henrys constant, $H^*_{\text{CO}_2\text{-am}}$.

$$m_{\text{CO}_2} = \frac{1}{H^*_{\text{CO}_2 \text{ am}}} \quad (\text{C.21})$$

Values of m_{CO_2} used for interfacial calculations are based on the bulk liquid phase loading. This simplification is justified because the difference in CO₂ loading between the bulk and the interface is typically less than 50%. Table C.6 presents the effects of CO₂ loading on the value of CO₂ solubility at three temperatures. At a constant temperature, doubling the CO₂ loading changes the solubility by a mere 10%. Also shown in Table C.6 is the case at the CO₂ loading of 0.6 mol/ mol amine. A factor of six increase in loading (from 0.1 to 0.6 mol CO₂/ mol amine) changes the solubility by only 30 to 40%.

Table C.6 **Effect of CO₂ loading on solubility**

T °C	CO ₂ loading [mol/ mol amine]	mCO ₂ 50 wt% (MDEA) [m ³ bar/kmol]	%-age change in mCO ₂	mCO ₂ 25 wt% DEA [m ³ bar/kmol]	%-age change in mCO ₂
40	0.1	0.0188		0.0194	
	0.2	0.0172	-8.6	0.0175	-9.5
	0.6	0.0132	-30.1	0.0118	-39.3
80	0.1	0.0131		0.0108	
	0.2	0.0120	-8.4	0.0098	
	0.6	0.0093	-29.6	0.0066	
120	0.1	0.0099		0.0068	
	0.2	0.0091	-8.3	0.0062	-9.2
	0.6	0.0070	-29.2	0.0042	-38.3

APPENDIX D

Experimental Data

D.1 MDEA Raw Data

Table D.1 Rate Data for MDEA. Initial Unloaded Solution is 50 wt%

MDEA at 40°C

Run Series #	Date	bulk loading $\frac{\text{mol CO}_2}{\text{mol amine}}$	P _{CO2} [bar]			Flux $\frac{\text{kmol}}{\text{m}^2\text{s}}$
			in	out	logmean	
70	01/03/95	0.019	0.459	0.173	0.293	6.75E-07
		0.033	0.855	0.383	0.588	1.21E-06
		0.048	1.322	0.691	0.973	1.81E-06
		0.103	2.254	1.120	1.621	4.04E-06
		0.147	2.953	1.644	2.235	5.78E-06
		0.329	3.496	2.171	2.781	7.20E-06
72	01/16/95	0.253	0.595	0.377	0.478	5.40E-07
		0.262	1.320	0.816	1.048	1.47E-06
		0.271	2.252	1.585	1.899	2.55E-06
		0.286	2.949	2.221	2.568	3.55E-06
		0.395	3.492	2.788	3.127	4.30E-06
74	01/20/95	0.136	0.596	0.275	0.415	7.82E-07
		0.164	1.321	0.655	0.950	1.90E-06
		0.184	2.254	1.181	1.660	3.86E-06
		0.240	2.952	1.801	2.329	5.22E-06
		0.271	3.495	2.416	2.923	6.13E-06
		0.403	4.723	4.723	4.723	7.70E-06

Table D.2 Rate Data for MDEA. Initial Unloaded Solution is 50 wt%

MDEA at 80°C						
Run Series #	Date	bulk loading mol CO ₂ mol amine	P _{CO2} [bar]			Flux kmol m ² s
			in	out	logmean	
71	01/10/95	0.242	1.039	1.473	1.243	-1.44E-06
		0.243	1.815	1.803	1.809	4.97E-08
		0.245	2.423	2.163	2.291	1.25E-06
		0.245	2.912	2.505	2.703	2.32E-06
73	01/17/95	0.309	0.564	1.643	1.009	-3.44E-06
		0.309	1.252	1.784	1.502	-1.93E-06
		0.288	2.134	2.319	2.226	-8.66E-07
		0.295	2.796	2.688	2.742	6.22E-07
		0.301	3.310	3.074	3.190	1.68E-06
75	01/22/95	0.308	2.424	2.525	2.474	-5.18E-07
		0.306	2.913	2.814	2.864	6.00E-07
		0.316	3.315	3.151	3.232	1.18E-06
		0.445	6.562	6.562	6.562	3.56E-06

Table D.3 Rate Data for MDEA. Initial Unloaded Solution is 50 wt%

MDEA at 120°C						
Run Series #	Date	bulk loading mol CO ₂ mol amine	P _{CO2} [bar]			Flux kmol m ² s
			in	out	logmean	
34	03/16/94	0.016	0.000	0.149	0.074	-4.32E-07
		0.026	0.806	0.696	0.749	4.10E-07
		0.033	1.420	1.064	1.234	1.62E-06
35	03/17/94	0.021	0.000	0.305	0.152	-9.09E-07
		0.021	0.431	0.372	0.401	1.92E-07
		0.128	0.806	0.602	0.699	7.44E-07
		0.033	1.420	1.030	1.215	1.76E-06
		0.047	1.903	1.508	1.698	2.21E-06
37	03/24/94	0.021	0.000	0.533	0.266	-1.66E-06
		0.023	0.431	0.568	0.496	-4.63E-07
		0.021	0.806	0.637	0.718	6.21E-07
		0.035	1.133	0.936	1.031	8.19E-07
		0.041	2.107	1.915	2.010	1.25E-06

Table D.3 Continued

Run Series #	Date	bulk loading $\frac{\text{mol CO}_2}{\text{mol amine}}$	P _{CO2} [bar]			Flux $\frac{\text{kmol}}{\text{m}^2\text{s}}$
			in	out	logmean	
76	01/25/95	0.036	0.450	0.612	0.527	-5.64E-07
		0.035	0.998	0.919	0.958	3.22E-07
		0.064	2.228	2.130	2.179	7.12E-07
		0.064	2.638	2.547	2.592	8.39E-07
77	01/26/95	0.156	5.280	5.280	5.280	3.65E-06
		0.100	0.827	1.160	0.984	-1.39E-06
		0.080	1.444	1.489	1.466	-2.34E-07
		0.100	2.483	2.268	2.374	1.74E-06

D.2 DEA RAW RATE MEASUREMENTS**Table D.4 Rate Data for DEA. Initial Unloaded DEA Solution is 25 wt%****DEA at 40°C**

Run Series #	Date	bulk loading $\frac{\text{mol CO}_2}{\text{mol amine}}$	P _{CO2} [bar]			Flux $\frac{\text{kmol}}{\text{m}^2\text{s}}$
			in	out	logmean	
61	10/29/94	0.040	0.036	0.015	0.024	4.04E-07
		0.037	0.053	0.014	0.029	7.64E-07
		0.046	0.069	0.017	0.037	1.03E-06
		0.075	0.084	0.023	0.047	1.27E-06
62	11/07/94	0.075	0.43	0.02	0.14	1.29E-06
		0.095	0.96	0.05	0.31	3.24E-06
		0.161	1.65	0.12	0.58	6.42E-06
	11/08/94	0.242	2.16	0.31	0.95	9.20E-06
		0.305	2.56	0.80	1.52	1.08E-05
65	11/30/94	0.2320	0.001	0.001	0.003	-1.29E-08
		0.2320	0.479	0.053	0.194	1.22E-06
		0.3065	1.075	0.094	0.403	3.14E-06
		0.3065	1.842	0.209	0.750	6.21E-06

Table D.5 Rate Data for DEA. Initial Unloaded DEA Solution is 25 wt%

DEA at 80°C						
Run Series #	Date	bulk loading $\frac{\text{mol CO}_2}{\text{mol amine}}$	PCO ₂ [bar]			Flux $\frac{\text{kmol}}{\text{m}^2\text{s}}$
			in	out	logmean	
63	11/09/94	0.294	0.55	0.38	0.46	4.34E-07
	11/10/94	0.297	1.24	0.64	0.91	1.79E-06
		0.296	2.12	0.99	1.48	4.18E-06
		0.316	2.79	1.49	2.07	5.92E-06
		0.340	3.30	2.08	2.65	6.95E-06
68	12/15/94	0.395	0.551	0.655	0.601	-2.80E-07
		0.400	1.238	0.877	1.047	1.12E-06
	12/16/94	0.426	2.121	1.116	1.565	3.78E-06
		0.470	2.783	1.709	2.203	5.10E-06
		0.496	3.298	2.308	2.774	5.91E-06

Table D.6 Rate Data for DEA. Initial Unloaded DEA Solution is 25 wt%

DEA at 120°C						
Run Series #	Date	bulk loading $\frac{\text{mol CO}_2}{\text{mol amine}}$	PCO ₂ [bar]			Flux $\frac{\text{kmol}}{\text{m}^2\text{s}}$
			in	out	logmean	
64	11/14/94	0.156	0.44	1.14	0.73	-2.70E-06
		0.149	0.98	1.21	1.10	-9.91E-07
		0.149	1.69	1.54	1.61	8.05E-07
		0.165	2.21	1.84	2.02	2.49E-06
		0.168	2.62	2.15	2.38	3.88E-06
67	12/05/94	0.226	0.438	0.863	0.627	-1.54E-06
		0.219	0.985	0.959	0.972	1.07E-07
		0.233	1.687	1.382	1.530	1.60E-06
		0.292	2.214	2.002	2.106	1.48E-06
		0.303	2.624	2.359	2.489	2.28E-06
69	12/20/94	0.251	0.439	1.058	0.704	-2.34E-06
		0.215	0.986	1.058	1.022	-3.05E-07
		0.229	1.689	1.375	1.527	1.64E-06
		0.249	2.216	1.762	1.980	2.97E-06
		0.291	2.626	2.239	2.427	3.22E-06

D.3 DEA/MDEA RAW RATE MEASUREMENTS

Table D.7 Rate Data for DEA/ MDEA. Initial Unloaded Solution is 5

wt% DEA/ 45 wt% MDEA at 40°C						
Run Series #	Date	bulk loading mol CO2 mol amine	PCO2 [bar]			Flux kmol m ² s
			in	out	logmean	
46	07/27/94	0.201	0.00	0.02	0.01	-1.11E-07
		0.198	0.23	0.05	0.12	5.00E-07
		0.200	0.55	0.20	0.35	1.04E-06
		0.225	1.06	0.37	0.66	2.31E-06
		0.271	1.56	0.79	1.13	3.01E-06
		0.306	2.51	1.60	2.03	5.22E-06
47	07/28/94	0.298	0.000	0.057	0.029	-1.52E-07
		0.294	0.231	0.125	0.173	2.93E-07
		0.290	0.463	0.225	0.330	6.96E-07
		0.301	1.239	0.601	0.882	2.29E-06
		0.338	2.088	1.304	1.665	3.82E-06
		0.374	2.698	2.013	2.339	4.50E-06
48	08/03/94	0.385	0.000	0.004	0.002	-3.12E-07
		0.377	0.231	0.060	0.127	1.28E-07
		0.384	0.463	0.173	0.295	4.02E-07
		0.384	1.064	0.473	0.729	1.40E-06
		0.431	1.837	1.192	1.491	2.91E-06
		0.497	2.415	1.805	2.095	3.56E-06
51	08/09/94	0.532	2.864	2.364	2.606	3.74E-06
		0.086	0.678	0.117	0.319	1.68E-06
		0.118	1.240	0.330	0.688	3.12E-06
		0.172	2.088	1.002	1.479	4.99E-06
		0.196	2.699	1.679	2.149	6.23E-06

Table D.8 Rate Data for DEA/ MDEA. Initial Unloaded Solution is 5

wt% DEA/ 45 wt% MDEA at 80°C						
Run Series #	Date	bulk loading $\frac{\text{mol CO}_2}{\text{mol amine}}$	PCO ₂ [bar]			Flux $\frac{\text{kmol}}{\text{m}^2\text{s}}$
			in	out	logmean	
43	07/19/94	0.039	0.000	0.040	0.020	-1.75E-07
		0.038	0.091	0.051	0.069	1.30E-07
		0.036	0.195	0.073	0.124	3.99E-07
		0.045	0.391	0.134	0.240	8.81E-07
		0.062	0.742	0.292	0.482	1.71E-06
		0.102	1.315	0.601	0.912	3.29E-06
		0.129	2.125	1.282	1.668	5.62E-06
45	07/23/94	0.178	0.000	0.667	0.333	-1.66E-06
		0.171	0.268	0.598	0.411	-8.41E-07
		0.170	0.787	0.763	0.775	6.71E-08
		0.176	1.438	0.996	1.204	1.43E-06
		0.183	2.133	1.292	1.677	3.22E-06
		0.199	2.804	1.705	2.209	5.15E-06

Table D.9 Rate Data for DEA/ MDEA. Initial Unloaded Solution is 5

wt% DEA/ 45 wt% MDEA at 120°C						
Run Series #	Date	bulk loading $\frac{\text{mol CO}_2}{\text{mol amine}}$	PCO ₂ [bar]			Flux $\frac{\text{kmol}}{\text{m}^2\text{s}}$
			in	out	logmean	
58	09/13/94	0.018	0.000	0.366	0.183	-1.08E-06
		0.027	0.443	0.466	0.454	-7.42E-08
		0.019	1.006	0.768	0.882	9.12E-07
		0.028	1.729	1.291	1.499	2.19E-06
59	09/13/94	0.010	0.219	0.254	0.127	-1.03E-07
		0.011	0.439	0.301	0.366	4.32E-07
		0.010	1.006	0.655	0.818	1.32E-06
		0.018	1.729	1.300	1.504	2.14E-06
		0.032	2.265	1.908	2.082	2.37E-06
60	09/16/94	0.009	0.439	0.540	0.270	-3.33E-07
		0.012	1.006	0.788	0.893	8.40E-07
		0.023	1.729	1.430	1.575	1.54E-06
		0.028	2.265	1.948	2.103	2.12E-06
		0.035	2.680	2.387	2.530	2.49E-06

Table D.10 Rate Data for DEA/ MDEA. Initial Unloaded Solution is 25

wt% DEA/ 25 wt% MDEA at 40°C						
Run Series #	Date	bulk loading $\frac{\text{mol CO}_2}{\text{mol amine}}$	P_{CO_2} [bar]		Flux $\frac{\text{kmol}}{\text{m}^2\text{s}}$	
			in	out	logmean	
78	01/28/95	0.080	0.595	0.032	0.193	1.33E-06
		0.040	1.320	0.113	0.491	3.21E-06
		0.083	2.252	0.174	0.811	6.49E-06
		0.136	2.949	0.263	1.111	9.71E-06
		0.190	3.492	0.356	1.374	1.29E-05
79	01/29/95	0.345	3.495	0.564	1.610	1.24E-05
		0.389	2.952	0.655	1.530	8.75E-06
		0.415	2.254	0.580	1.230	5.52E-06
		0.423	1.321	0.697	0.976	1.79E-06
		0.378	0.596	0.234	0.387	8.78E-07

Table D.11 Rate Data for DEA/ MDEA. Initial Unloaded Solution is 25

wt% DEA/ 25 wt% MDEA at 80°C						
Run Series #	Date	bulk loading $\frac{\text{mol CO}_2}{\text{mol amine}}$	P_{CO_2} [bar]		Flux $\frac{\text{kmol}}{\text{m}^2\text{s}}$	
			in	out	logmean	
81	01/31/95	0.487	3.495	2.923	1.042	-3.79E-06
		0.464	2.952	2.474	1.608	-2.95E-06
		0.456	2.254	1.831	2.253	-1.15E-06
		0.456	1.322	1.262	3.210	1.4155E-06
		0.485	5.902	5.902	5.902	5.40E-06
31	03/09/94	0.101	0.000	0.105	0.052	-2.51E-07
		0.103	0.516	0.129	0.279	1.00E-06
		0.107	1.168	0.159	0.5	2.92E-06
		0.122	1.702	0.264	0.772	4.65E-06
		0.143	2.007	0.330	0.929	5.81E-06
		0.164	2.405	0.492	1.206	7.36E-06

Table D.12 Rate Data for DEA/ MDEA. Initial Unloaded Solution is 25

wt% DEA/ 25 wt% MDEA at 120°C						
Run Series #	Date	bulk loading $\frac{\text{mol CO}_2}{\text{mol amine}}$	PCO ₂ [bar]			Flux $\frac{\text{kmol}}{\text{m}^2\text{s}}$
			in	out	logmean	
29	03/06/94	0.068	0.000	0.362	0.181	-1.17E-06
		0.053	0.405	0.323	0.363	2.82E-07
		0.071	0.917	0.468	0.668	1.77E-06
		0.086	1.576	0.864	1.184	3.54E-06
		0.106	1.888	1.303	1.578	3.49E-06
30	03/06/94	0.096	0.000	0.683	0.342	-2.34E-06
		0.097	0.405	0.762	0.565	-1.34E-06
		0.085	0.917	0.835	0.875	3.47E-07
		0.087	1.336	1.016	1.169	1.56E-06
		0.096	1.576	1.145	1.349	2.28E-06
		0.106	1.888	1.428	1.648	2.83E-06

APPENDIX E

Main Program

A listing of the main program as specifically applied to 25 wt% DEA/ 25 wt% MDEA data at 80°C.

```

PROGRAM OPTIMA
IMPLICIT DOUBLE PRECISION (A-H,O-Z)
EXTERNAL MODEL
DIMENSION OBS(40),PAR(3),BNDLW(3),BNDUP(3),CHMAX(3)
DIMENSION DSC(500),ISC(150),IOBS(10,1),IDET(3),DEL(3)
C LOAD THE VECTOR "OBS" THAT CONTAIN THE MEASURED FLUXES
OBS(1)=-3.79D-6
OBS(2)=-2.95D-6
OBS(3)=-1.15D-6
OBS(4)=1.4155D-6
OBS(5)=5.40d-6
OBS(6)=-2.51D-6
OBS(7)= 1.00D-6
OBS(8)=2.92D-6
OBS(9)=4.648D-6
OBS(10)=5.81D-6
OBS(11) = 7.36D-6
C INPUT DATA NEEDED FOR "GREG"
NOB=11
NPAR=3
C BOUNDS FOR THE PARAMETER

C BOUNDS FOR THE PARAMETER
BNDLW(1)=0.010D0
BNDLW(2)=0.010d0
BNDLW(3)=0.010D0
BNDUP(1)=5.0D0
BNDUP(2)=2.0D0
BNDUP(3)=2.0D0
CHMAX(1)=1.0d-1
CHMAX(2)=1.0d-1
CHMAX(3)= 1.0D-1
DEL(1)=1.0D-1
DEL(2)=1.0D-1
DEL(3)=1.0D-1
C
MISC=150
MDSC=500
C INITIAL GUESSES AND TOLERANCE OF PARAMETERS
PAR(1)=1.000D0
PAR(2)=1.00D0
PAR(3)=1.000D0
RPTOL=1.0D-1
RSTOL=1.0D-1
VPIV=1.D-1
APIV=1.D-1
C INITIALIZE "ISC" ARRAY
ISC(1)=1
ISC(2)=10
ISC(3)=1
ISC(4)=50

```

```
ISC(5)=2
ISC(6)=0
ISC(7)=1
ISC(8)=11
ISC(9)=1
EMOD=1.0D-2
c  IDET(1)=9
c  DO 5 I=1,NOB
C  DO 5 J=1,NOB
c  IOBS(I,1)=1
C 5 CONTINUE
C CALL "GREG"
  write(6,*)'hello'
  CALL GREG(NOB,OBS,NPAR,PAR,BNDLW,BNDUP,CHMAX,DEL,MDSC,
*          DSC,MISC,ISC,IOBS,IDET,EMOD,VPIV,APIV,RPTOL,
*          RSTOL,MODEL)
  write(6,*)'hello1'
  STOP
  END
```

APPENDIX F

Model Code and Input

A listing of the model program and associated subroutines is presented. Also included is the specific input data as specifically applied to 25 wt% DEA / 25 wt% MDEA case at 80°C .

```

SUBROUTINE MODEL(PAR,F,NOB,NPAR,IDER,DERIV,MINFO)
DOUBLE PRECISION X(15),FVEC(15),FJAC(15,15),WA1(15),
*   WA2(15),WA3(15),WA4(15),DIAG(15),QTF(15),R(120),
*   K1,K2,K3,K4,K5,TCO2,TDEA,TMDEA,XTOL,FACTOR,
*   CO2B,OHB,HCO3B,MDEAB,MDEAHB,DEAB,DEAHB,DEACOOB,
*   CO3B,PCO2,MCO2,KL,KMDEA,KMDEAOH,KMDEADE,KDEA,KDEAMDE,
*   DCO2,DOH,DHCO3,DMDEA,DMDEAH,DDEA,DDEAH,DDEACOO,DCO3,
*   PAR(2),F(5),DERIV(5,2)
COMMON /POINTER/INTER
COMMON /SOLFLAG/ISOL
COMMON /CONST/K1,K2,K3,K4,K5,TCO2,TDEA,TMDEA
COMMON /RATEC/KMDEA,KMDEAOH,KMDEADE,KDEA,KDEAMDE
COMMON /CO2P/PCO2,MCO2,KL,PCO2EQ
COMMON /DIFF/DCO2,DOH,DHCO3,DMDEA,DMDEAH,DDEA,DDEAH,DDEACOO,
*   DCO3
COMMON /BULK/CO2B,OHB,HCO3B,MDEAB,MDEAHB,DEAB,DEAHB,
*   DEACOOB,CO3B
EXTERNAL FCN
OPEN(12,FILE='252580.OUT',STATUS='UNKNOWN')
OPEN(11,FILE='252580.DAT',STATUS='UNKNOWN')
C SPECIFIC INPUT DATA
LDFJAC=15
LR=120
MAXFEV=400
MODE=1
NPRINT=0
C Some INPUT DATA
C
  KMDEAOH=0.0
  KMDEADE=0.0D0
  TDEA=2.3777D0
  TMDEA =2.0978D0
C
C "J" IS A POINTER FOR THE FLUX CALCULATION
  J=1
C FIRST POINT...
199 READ(11,*)GKMDEA
  READ(11,*)GKDEA
  READ(11,*)GKDEAMDE
  Kmdea = gkmdea
  kdea=gkdea
  KDEAMDE=PAR(1)*GKDEAMDE
  READ(11,*)ISOL
  READ(11,*)FACTOR
  READ(11,*)XTOL
  READ(11,*)NPOINT
  READ(11,*)X(1)
  READ(11,*)X(2)
  READ(11,*)X(3)
  READ(11,*)X(4)
  READ(11,*)X(5)

```

```

READ(11,*)X(6)
READ(11,*)X(7)
READ(11,*)X(8)
READ(11,*)X(9)
T=353.0
IF (J.EQ.1) THEN
PCO2=1.04193D0
TCO2=0.486838D0
CALL EQUICON(T,TCO2,ISOL,K1,K2,K3,K4,K5)
K1 = PAR(2) *K1
MCO2=0.01164795
KL=6.774D-05
END IF
C SECOND POINT...
IF (J.EQ.2) THEN
PCO2=1.60834D0
TCO2=0.463968D0
CALL EQUICON(T,TCO2,ISOL,K1,K2,K3,K4,K5)
K1 = PAR(2) *K1
MCO2=0.01245977D0
KL= 6.815D-05
END IF
C THIRD POINT...
IF (J.EQ.3) THEN
PCO2=2.253028D0
TCO2=0.456462D0
CALL EQUICON(T,TCO2,ISOL,K1,K2,K3,K4,K5)
K1 = PAR(2) *K1
KL= 6.828D-05
MCO2=0.0117308D0
END IF
C FOURTH POINT...
IF (J.EQ.4) THEN
PCO2=3.21016D0
TCO2=0.455528D0
CALL EQUICON(T,TCO2,ISOL,K1,K2,K3,K4,K5)
K1 = PAR(2)*K1
MCO2=0.011733D0
KL= 6.830D-05
END IF
C FIFTH POINT
IF (J.EQ.5) THEN
PCO2=5.9023D0
TCO2=0.484912D0
CALL EQUICON(T,TCO2,ISOL,K1,K2,K3,K4,K5)
K1 = PAR(2) *K1
MCO2=0.01165319D0
KL= 6.778D-05
END IF
C 6 TH POINT
IF (J.EQ.6) THEN

```

```

PCO2=0.052335d0
TCO2=0.10122D0
CALL EQUICON(T,TCO2,ISOL,K1,K2,K3,K4,K5)
K1 = PAR(3) *K1
MCO2=0.01275D0
KL= 7.505D-05
END IF
C 7 TH POINT
IF (J.EQ.7) THEN
PCO2=0.279455D0
TCO2=0.103211D0
CALL EQUICON(T,TCO2,ISOL,K1,K2,K3,K4,K5)
K1 = PAR(3) *K1
MCO2=0.01274D0
KL= 7.501D-05
END IF
C 8 TH POINT
IF (J.EQ.8) THEN
PCO2=5.05569D-1
TCO2=0.10746D0
CALL EQUICON(T,TCO2,ISOL,K1,K2,K3,K4,K5)
K1 = PAR(3) *K1
MCO2=0.01246D0
KL= 7.493D-05
END IF
C 9 TH POINT
IF (J.EQ.9) THEN
PCO2=7.7167D-1
TCO2=0.122028D0
CALL EQUICON(T,TCO2,ISOL,K1,K2,K3,K4,K5)
K1 = PAR(3) *K1
MCO2=0.01269
KL= 7.463D-05
END IF
C 10 TH POINT
IF (J.EQ.10) THEN
PCO2=9.28526D-1
TCO2=0.14268D0
CALL EQUICON(T,TCO2,ISOL,K1,K2,K3,K4,K5)
K1 = PAR(3) *K1
MCO2=0.01263D0
KL= 7.422D-05
END IF
C 11 TH POINT
IF (J.EQ.11) THEN
PCO2=1.20579D0
TCO2=0.16388D0
CALL EQUICON(T,TCO2,ISOL,K1,K2,K3,K4,K5)
K1 = PAR(3) *K1
MCO2=0.01256
KL= 7.380D-05

```



```

      END IF
C Loading in moles/lit
      TCO2=TCO2*(TMDEA+TDEA)
C
C CALL TO SUBROUTINES TO CALCULATE BULK, INTERFACE CONCENTRATION
C AND FLUX OF CO2
      N=9
C if INTER=1, then let's compute bulk concentrations...
      INTER=1
C CALL HYBRID #####
      CALL HYBRJ(FCN,N,X,FVEC,FJAC,LDFJAC,XTOL,MAXFEV,DIAG,MODE,
*              FACTOR,NPRINT,INFO,NFEV,NJEV,R,LR,QTF,WA1,WA2,
*              WA3,WA4)
C
C PRINT OUT RESULTS
C
      WRITE(12,*)INFO,NFEV,NJEV
      WRITE(12,*)'CO2',X(1)
      WRITE(12,*)'OH-',X(2)
      WRITE(12,*)'HCO3-',X(3)
      WRITE(12,*)'MDEA',X(4)
      WRITE(12,*)'MDEAH+',X(5)
      WRITE(12,*)'DEA',X(6)
      WRITE(12,*)'DEAH+',X(7)
      WRITE(12,*)'DEACOO-',X(8)
      WRITE(12,*)'CO3=',X(9)
C Store bulk concentrations in new variables
      CO2B=X(1)
      OHB=X(2)
      HCO3B=X(3)
      MDEAB=X(4)
      MDEAHB=X(5)
      DEAB=X(6)
      DEAHB=X(7)
      DEACOOB=X(8)
      CO3B=X(9)

C if INTER=0, then let's compute interface concentrations
      INTER=0
      N=12
C Initial guesses for interf. concent.
      READ(11,*)X(1)
      READ(11,*)X(2)
      READ(11,*)X(3)
      READ(11,*)X(4)
      READ(11,*)X(5)
      READ(11,*)X(6)
      READ(11,*)X(7)
      READ(11,*)X(8)
      READ(11,*)X(9)

```

```

      READ(11,*)X(10)
      READ(11,*)X(11)
      READ(11,*)X(12)
C READ DIFFUSIVITIES
      READ(11,*)DCO2
      READ(11,*)DOH
      READ(11,*)DHCO3
      READ(11,*)DMDEA
      READ(11,*)DMDEAH
      READ(11,*)DDEA
      READ(11,*)DDEAH
      READ(11,*)DDEACOO
      READ(11,*)DCO3
C   WRITE(6,*)DDEAH,DDEACOO,DCO3
      REWIND 11
      CALL HYBRJ(FCN,N,X,FVEC,FJAC,LDFJAC,XTOL,MAXFEV,DIAG,MODE,
*             FACTOR,NPRINT,INFO,NFEV,NJEV,R,LR,QTF,WA1,WA2,
*             WA3,WA4)
C
      WRITE(12,*)INFO,NFEV,NJEV
      WRITE(12,*)'CO2',X(13)
      WRITE(12,*)'OH-',X(1)
      WRITE(12,*)'HCO3-',X(2)
      WRITE(12,*)'MDEA',X(3)
      WRITE(12,*)'MDEAH+',X(4)
      WRITE(12,*)'DEA',X(5)
      WRITE(12,*)'DEAH+',X(6)
      WRITE(12,*)'DEACOO-',X(7)
      WRITE(12,*)'CO3=',X(8)
      WRITE(12,*)'DIFFFLUX=',X(9)
      WRITE(12,*)'CO2(carb.)=',X(10)
      WRITE(12,*)'CO2(HCO3)=',X(11)
      WRITE(12,*)'CO2(mixt.)=',X(12)
      WRITE(12,*)'E_CO2=',X(14)
C SAVE CALCULATED FLUX INTO "F(J)"
      F(J)=X(9)
C   write(6,*)F(J),J
      J=J+1
      IF (J.LE.NPOINT) GO TO 199
      RETURN
      END

C#####
      SUBROUTINE FCN(N,X,FVEC,FJAC,LDFJAC,IFLAG)
      COMMON /CONST/K1,K2,K3,K4,K5,TCO2,TDEA,TMDEA
      COMMON /RATEC/KMDEA,KMDEAOH,KMDEADE,KDEA,KDEAMDE
      COMMON /POINTER/INTER
      COMMON /SOLFLAG/SOL
      COMMON /CO2P/PCO2,MCO2,KL,PCO2EQ
      COMMON /DIFF/DCO2,DOH,DHCO3,DMDEA,DMDEAH,DDEA,DDEAH,DDEACOO,
*             DCO3

```

```

COMMON /BULK/CO2B,OHB,HCO3B,MDEAB,MDEAHB,DEAB,DEAHB,
*   DEACOOB,CO3B
INTEGER N,LDFJAC,IFLAG
DOUBLE PRECISION K1,K2,K3,K4,K5,X(15),FVEC(15),FJAC(15,15),
*   TCO2,TDEA,TMDEA,PCO2,MCO2,CO2I,K1BICAR,
*   CO2B,OHB,HCO3B,MDEAB,MDEAHB,DEAB,DEAHB,DEACOOB,CO3B,
*   KMDEA,KMDEAOH,KMDEADE,KDEA,KDEAMDE,K1CARB,PHI,K1B,EI,
*   ECO2,DCO2,DOH,DHCO3,DMDEA,DMDEAH,DDEA,DDEAH,DDEACOO,
*   DCO3,FCARB,RATCARB,RATBICA,FLUXCAR,FLUCBIC,KL

C -----
C   IF IFLAG = 1 CALCULATE THE FUNCTIONS AT X AND
C   RETURN THIS VECTOR IN FVEC. DO NOT ALTER FJAC.
C   IF IFLAG = 2 CALCULATE TH JACOBIAN AT X AND
C   RETURN THIS MATRIX IN FJAC. DO NOT ALTER FVEC.
C -----
C   IF (INTER.EQ.1) THEN
C Block for the bulk calculations
C   IF (IFLAG.EQ.1) THEN
C *****
C If 50%MDEA/50% water
C   IF (ISOL.EQ.1) THEN
C     X(6)=0.
C     X(7)=0.
C     X(8)=0.
C   END IF
C   IF (ISOL.EQ.4) THEN
C     X(4)=0.
C     X(5)=0.
C   END IF
C FUNCTIONS: F(I)=0
C   FVEC(1)=K1*X(3)-X(1)*X(2)
C   FVEC(2)=X(3)*X(2)-K2*X(9)
C   FVEC(3)=K3*X(4)-X(2)*X(5)
C   FVEC(4)=K4*X(6) -X(2)*X(7)
C   FVEC(5)=K5*X(8)-X(6)*X(3)
C   FVEC(6)=TCO2 - X(1)-X(3)-X(9)-X(8)
C   FVEC(7)=TMDEA - X(4) - X(5)
C   FVEC(8)=TDEA - X(6) - X(7) - X(8)
C   FVEC(9)=X(7) + X(5) - X(3) - 2.D0*X(9)-X(8) - X(2)
C   DO 299 I=1,9
C 299 WRITE(6,*) FVEC(I)
C   END IF
C   IF (IFLAG.EQ.2) THEN
C     DO 1 I=1,N
C       DO 1 J=1,N
C 1 FJAC(I,J)=0.0
C       FJAC(1,1)=-X(2)
C       FJAC(1,2)=-X(1)
C       FJAC(1,3)=K1
C       FJAC(2,2)= X(3)
C       FJAC(2,3)= X(2)

```

```

FJAC(2,9)= -K2
FJAC(3,2)= -X(5)
FJAC(3,4)= K3
FJAC(3,5)= -X(2)
FJAC(4,2)= -X(7)
FJAC(4,6)= K4
FJAC(4,7)= -X(2)
FJAC(5,3)= -X(6)
FJAC(5,6)= -X(3)
FJAC(5,8)=K5
FJAC(6,1)= -1.D0
FJAC(6,3)= -1.D0
FJAC(6,8)= -1.D0
FJAC(6,9)= -1.D0
FJAC(7,4)= -1.D0
FJAC(7,5)= -1.D0
FJAC(8,6)= -1.D0
FJAC(8,7)= -1.D0
FJAC(8,8)= -1.D0
FJAC(9,2)= -1.D0
FJAC(9,3)= -1.D0
FJAC(9,5)= 1.D0
FJAC(9,7)= 1.D0
FJAC(9,8)= -1.D0
FJAC(9,9)= -2.D0

```

```

C
  IF (ISOL.EQ.1) THEN
    FJAC(5,3)=0.
    FJAC(5,8)=0.
    FJAC(4,2)=0.
    FJAC(4,6)=0.
    FJAC(9,7)=0.
    FJAC(9,8)=0.
    FJAC(6,8)=0.
    DO 33 I=1,9
33  FJAC(8,I)=0.
    END IF

```

```

C
  IF (ISOL.EQ.4) THEN
    FJAC(9,5)=0.
    DO 34 I=1,9
    FJAC(7,I)=0.
    FJAC(3,I)=0.
34  CONTINUE
    END IF

```

```

C End of block for Jacobian calculation
  END IF

```

```

C End of block for bulk calculations
  END IF
  IF (INTER.EQ.1) GO TO 5
  IF (INTER.EQ.0) THEN

```

```

      IF (IFLAG.EQ.1) THEN
C *****
C Concentration of CO2 at the interface (C=P/H, H: HENRY'S CONSTANT)
      CO2I=PCO2*MCO2
      K1BICAR=KMDEA*X(3)+KMDEAOH*X(3)*X(1)+KMDEADE*X(3)*X(5)
      K1CARB=KDEA*X(5)+KDEAMDE*X(3)*X(5)
C   write(6,*)K1CARB,K1BICAR,CO2I
C   WRITE(6,*)X(3),X(5)
      FCARB=K1CARB/(K1CARB+K1BICAR)
      RATCARB=K1CARB*(CO2I-X(10))
      RATBICA=K1BICAR*(CO2I-X(11))
      FLUXCAR=KL*DSQRT(DDEACOO/DCO2)*(X(7)-DEACOOB)
      FLUXBIC=KL*(CO2I-CO2B+DSQRT(DHCO3/DCO2)*(X(2)-HCO3B)+
      *   DSQRT(DCO3/DCO2)*(X(8)-CO3B))
      PHI=(X(12)-CO2B)/(CO2I-CO2B)
C
      K1B=K1BICAR+K1CARB
      EI=DSQRT(1.D0 + (K1B*DCO2/(KL**2.)))
      ECO2=1.D0+(EI-1.D0)*(1.D0-PHI)
C AMINE FLUX EQUATIONS
C
      IF (ISOL.EQ.1) THEN
        X(5)=0.
        X(6)=0.
        X(7)=0.
        X(10)=0.
        RATCARB=0.
      END IF
      IF (ISOL.EQ.4) THEN
        X(3)=0.
        X(4)=0.
        K1BICAR=0.
        RATBICA=0.
      END IF
C
      FVEC(1)=DSQRT(DDEA)*(X(5)-DEAB)+DSQRT(DDEAH)*(X(6)-DEAHB)+
      *   DSQRT(DDEACOO)*(X(7)-DEACOOB)
      FVEC(2)=DSQRT(DMDEA)*(X(3)-MDEAB)+DSQRT(DMDEAH)*(X(4)-
      *   MDEAHB)
C CHARGE FLUX
      FVEC(3)=DSQRT(DMDEAH)*(X(4)-MDEAHB)+DSQRT(DDEAH)*(X(6)-DEAHB)-
      *   DSQRT(DOH)*(X(1)-OHB)-2.D0*DSQRT(DCO3)*(X(8)-CO3B)-
      *   DSQRT(DHCO3)*(X(2)-HCO3B)-DSQRT(DDEACOO)*(X(7)-
      *   DEACOOB)
C
      FVEC(4)=K3*X(3)-X(1)*X(4)
C
      FVEC(5)=K4*X(5)-X(1)*X(6)
C
      FVEC(6)=K2*X(8)-X(2)*X(1)
C

```

```

FVEC(7)=X(9)-KL*(CO2I-CO2B + DSQRT(DHCO3/DCO2)*(X(2)-HCO3B)+
*   DSQRT(DCO3/DCO2)*(X(8)-CO3B)+DSQRT(DDEACOO/DCO2)*
*   (X(7)-DEACOOB))
C
FVEC(8)=KL*ECO2*(CO2I-CO2B) - X(9)
C
FVEC(9)=X(12)-FCARB*X(10)-(1.D0-FCARB)*X(11)
C
FVEC(10)=X(10)*X(5)*X(1)-K1*K5*X(7)
C
FVEC(11)=X(11)*X(1)-K1*X(2)
C
FVEC(12)=FLUXBIC*RATCARB-RATBICA*FLUXCAR
END IF
IF (IFLAG.EQ.2) THEN
DO 2 I=1,N
DO 2 J=1,N
2 FJAC(I,J)=0.0
C JACOBIAN
FJAC(1,5)=DSQRT(DDEA)
FJAC(1,6)=DSQRT(DDEAH)
FJAC(1,7)=DSQRT(DDEACOO)
FJAC(2,3)=DSQRT(DMDEA)
FJAC(2,4)=DSQRT(DMDEAH)
FJAC(3,1)=-DSQRT(DOH)
FJAC(3,2)=-DSQRT(DHCO3)
FJAC(3,4)=DSQRT(DMDEAH)
FJAC(3,6)=DSQRT(DDEAH)
FJAC(3,7)=-DSQRT(DDEACOO)
FJAC(3,8)=-2.D0*DSQRT(DCO3)
FJAC(4,1)=-X(4)
FJAC(4,3)=K3
FJAC(4,4)=-X(1)
FJAC(5,1)=-X(6)
FJAC(5,5)=K4
FJAC(5,6)=-X(1)
FJAC(6,1)=-X(2)
FJAC(6,2)=-X(1)
FJAC(6,8)= K2
FJAC(7,2)=-KL*DSQRT(DHCO3/DCO2)
FJAC(7,7)=-KL*DSQRT(DDEACOO/DCO2)
FJAC(7,8)=-KL*DSQRT(DCO3/DCO2)
FJAC(7,9)= 1.D0
FJAC(8,1)=KL*(CO2I-CO2B)*(1-PHI)*0.5D0*1.0D0/DSQRT(1.0D0+
*   (K1B*DCO2)/KL**2.)*DCO2/KL**2*KMDEAOH*X(3)
FJAC(8,3)=KL*(CO2I-CO2B)*(1-PHI)*0.5D0*1.0D0/DSQRT(1.0D0+
*   (K1B*DCO2)/KL**2.)*DCO2/KL**2*(KMDEA+KMDEAOH*X(1)+
*   KDEAMDE*X(5))
FJAC(8,5)=KL*(CO2I-CO2B)*MCO2*(1-PHI)*0.5D0*1.0D0/DSQRT(1.0D0+
*   (K1B*DCO2)/KL**2.)*DCO2/KL**2*(KMDEADE*X(3)+KDEA+
*   KDEAMDE*X(3))

```

```

FJAC(8,12)=KL*(1-EI)
FJAC(8,9)=-1.D0
FJAC(9,1)=(X(10)-X(11))*K1CARB/(K1CARB+K1BICAR)**2.*KMDEAOH*X(3)
FJAC(9,3)=-(X(10)-X(11))*(KDEAMDE*X(5)/(K1CARB+K1BICAR)-
*      K1CARB/(K1CARB+K1BICAR)**2.*(KDEAMDE*X(5)+KMDEA+
*      KMDEAOH*X(1)+KMDEADE*X(5)))
FJAC(9,5)=-(X(10)-X(11))*((-K1CARB*(KDEA+KDEAMDE*X(3)+KMDEADE*
*      X(3))/(K1CARB+K1BICAR)**2.)+(KDEA+KDEAMDE*X(3))/
*      (K1CARB+K1BICAR))
FJAC(9,10)=-FCARB
FJAC(9,11)=-1.D0+FCARB
FJAC(9,12)=1.0D0
FJAC(10,1)=X(10)*X(5)
FJAC(10,5)=X(10)*X(1)
FJAC(10,7)=-K1*K5
FJAC(10,10)=X(5)*X(1)
FJAC(11,1)=X(11)
FJAC(11,11)=X(1)
FJAC(11,2)=-K1
FJAC(12,1)=-FLUXCAR*KMDEAOH*X(3)*(CO2I-X(11))
FJAC(12,2)=RATCARB*DSQRT(DHCO3/DCO2)*KL
FJAC(12,3)=FLUXBIC*(CO2I-X(10))*KDEAMDE*X(5)-FLUXCAR*
*      (CO2I-X(11))*(KMDEA+KMDEAOH*X(1)+KMDEADE*X(5))
FJAC(12,5)=FLUXBIC*(CO2I-X(10))*(KDEA+KDEAMDE*X(3))-
*      FLUXCAR*KMDEADE*X(3)*(CO2I-X(11))
FJAC(12,7)=-RATBICA * KL * DSQRT(DDEACOO/DCO2)
FJAC(12,8)=RATCARB * DSQRT(DCO3/DCO2)*KL
FJAC(12,10)=-FLUXBIC*K1CARB
FJAC(12,11)=FLUXCAR *K1BICAR
C
  IF (ISOL.EQ.1) THEN
    FJAC(3,7)=0.
    FJAC(3,6)=0.
    FJAC(7,7)=0.
  END IF
C
  END IF
C
C Begin block for interface calculations
C   DO 99 I=1,N
C   99 WRITE(6,*)X(I),FVEC(I)
C   WRITE(6,*)CO2B,OH,B, HCO3B,MDEAB,MDEAHB,DEAB,DEAHB,DEACOOB,CO3B
C   WRITE(6,*)DCO2,DOH,DHCO3,DMDEA,DMDEAH,DDEA,DDEAH,DDEACOO,
C   *      DCO3
C   X(13)=CO2I
C   X(14)=ECO2
C   END IF
C
  5 RETURN
  END
C*****

```

```

C
C Subroutine to estimate equilibrium constants
  SUBROUTINE EQUICON(T,TCO2,ISOL,K1,K2,K3,K4,K5)
    DOUBLE PRECISION K1,K2,K3,K4,K5,T,TCO2
C
  IF (ISOL.EQ.1) THEN
    WRITE(6,*)T,TCO2
    K1=DEXP(13.74000496 - 8497.83098/T - 0.68041*DLOG(T)+
    * 0.077308*TCO2+0.06916*(TCO2)**2.)
    K2=DEXP(-118.7991 + 1202.7238/T + 18.62966*DLOG(T)-
    * 8.04841*TCO2+7.44546*(TCO2)**2.)
    K3=DEXP(78.1316 -5356.06212/T - 12.8873*DLOG(T)+
    * 7.936311*TCO2 - 8.74536*(TCO2)**2.)
    WRITE(6,*) K1,K2,K3
  END IF
  IF (ISOL.EQ.2) THEN
    C11=7.11682643D0
    C21=-8199.08759D0
    C31=0.30945896
    C41=-0.10475731
    C51=0.23822403
    K1=DEXP(C11 + C21/T + C31*DLOG(T)+ C41*TCO2+C51*(TCO2)**2.)
    C12=-119.714561
    C22=1297.44507
    C32=18.7349526
    C42=-8.01542412
    C52=7.4065588
    K2=DEXP(C12 + C22/T + C32*DLOG(T)+C42*TCO2 + C52*(TCO2)**2.)
    C13=83.0765835
    C23=-5653.87789
    C33=-13.5758975
    C43=7.86143345
    C53=8.75845169
    K3=DEXP(C13 + C23/T + C33*DLOG(T)+ C43*TCO2+C53*(TCO2)**2.)
    C14=107.287214
    C24=-6096.3237
    C34=-17.4162001
    C44=7.20552199
    C54=8.00992394
    K4=DEXP(C14 +C24/T + C34*DLOG(T)+ C44*TCO2 + C54*(TCO2)**2.)
    C15=-76.1053454
    C25=1947.23603
    C35=12.0616197
    C45=0.35600102
    C55=0.5552832
    K5=DEXP(C15 + C25/T + C35*DLOG(T)+ C45*TCO2+C55*(TCO2)**2.)
  END IF
C The constants for 25% DEA/ 25% MDEA
  IF (ISOL.EQ.3) THEN
    C11=-2.73083676D0
    C21=-7856.90222D0

```



```

C31= 1.84316532
C41=-0.87471368
C51=1.00058634
K1=DEXP(C11 + C21/T + C31*DLOG(T)+ C41*TCO2+C51*(TCO2)**2.)
C12=-118.01557
C22=1283.32997
C32=18.4215101
C42=-7.69241583
C52=7.05227286
K2=DEXP(C12 + C22/T + C32*DLOG(T)+C42*TCO2 + C52*(TCO2)**2.)
C13=81.1895591
C23=-5436.03104
C33=-13.2650336
C43=5.83815753
C53=-7.17787878
K3=DEXP(C13 + C23/T + C33*DLOG(T)+ C43*TCO2+C53*(TCO2)**2.)
C14=89.2242364
C24=-4947.64214
C34=-14.7655909
C44=4.99442477
C54=-6.38546775
K4=DEXP(C14 +C24/T + C34*DLOG(T)+ C44*TCO2 + C54*(TCO2)**2.)
C15=-76.1960094
C25=1924.29684
C35=12.1186714
C45=-3.08593664
C55=2.73385925
K5=DEXP(C15 + C25/T + C35*DLOG(T)+ C45*TCO2+C55*(TCO2)**2.)
END IF

```

C The constants for 25% DEA

```

IF (ISOL.EQ.4) THEN
C11=-53.2256523D0
C21=-4468.44182D0
C31=8.81057365
C41=-0.43023758
C51=0.43917897
K1=DEXP(C11 + C21/T + C31*DLOG(T)+ C41*TCO2+C51*(TCO2)**2.)
C12=-96.590022
C22=87.9287931
C32=15.3730545
C42=-4.78477224
C52=4.31527632
K2=DEXP(C12 + C22/T + C32*DLOG(T)+C42*TCO2 + C52*(TCO2)**2.)
K3=0.
C14=170.609828
C24=-8775.9223
C34=-26.6337924
C44=3.78040147
C54=-4.33104387
K4=DEXP(C14 +C24/T + C34*DLOG(T)+ C44*TCO2 + C54*(TCO2)**2.)
C15=-58.4438558

```

```
C25=815.266261
C35=9.68782139
C45=-2.04733142
C55=1.42249805
K5=DEXP(C15 + C25/T + C35*DLOG(T)+ C45*TCO2+C55*(TCO2)**2.)
END IF
RETURN
END
```

APPENDIX G

Program Output

Result of parameter estimation runs is presented. These results are, in this specific order, for 50 wt% MDEA, 25 wt% DEA, 5 wt% DEA/45 wt% MDEA, and 25 wt% DEA/ 25 wt% MDEA. For each solution type the results are given for all three temperatures: 40, 80, and 120°C.

G.1 GREG RESULT FOR 50 WT % MDEA

G.1.1 Results at 40°C

```

***** G R E G *****
***** General Regression Software Package *****
***** for Nonlinear Parameter Estimation. *****
***** Version of August, 1990 *****
*****

***** Level = 10 *****
***** nonlinear least squares with *****
***** optional numerical derivatives. *****
*****

Start of problem no. 1 with 17 observations and 4 parameters

BNDUP(I)= 3.000000D+00 2.000000D+00 2.000000D+00 2.000000D+00
PAR(I) = 1.000000D+00 1.000000D+00 1.000000D+00 1.000000D+00
BNDLW(I)= 1.000000D-02 1.000000D+00 1.000000D-02 1.000000D-02

DEL(I) = -1.000000D-02 -1.000000D-02 -1.000000D-02 -1.000000D-02
CHMAX(I)= 1.000000D+01 0.000000D+00 0.000000D+00 0.000000D+00

APIV = 1.0000D-01 RSTOL = 1.0000D-01 ITMAX = 25 LISTS = 2
EMOD = 1.0000D-01 RPTOL = 1.0000D-03 IDIF = 0

All derivatives are obtained by finite differences

***** Iteration no. 1 no. of function calls 0 *****
PAR(I) = 1.000000D+00 1.000000D+00 1.000000D+00 1.000000D+00

***** Current sum of squares = 1.71858D-11 *****

***** Iteration no. 2 no. of function calls 6 *****
PAR(I) = 1.003047D+00 1.000000D+00 1.000000D+00 1.000000D+00

***** Current sum of squares = 1.66669D-11 *****

***** Iteration no. 3 no. of function calls 9 *****
PAR(I) = 7.955349D-01 1.000000D+00 1.000000D+00 1.000000D+00

***** Current sum of squares = 1.26314D-11 *****

***** Termination criteria satisfied *****

***** Final value of sum of squares = 1.26314D-11 *****

```

Standard error of weighted residuals = 8.88517D-07
 estimated with 17 residuals and 16 degrees of freedom

***** 2-sigma intervals PAR(I)+-DIF(I) for parameters in basis; *****
 **** last value and bounds for any parameters that are not in basis ****
 UPR(I) = 9.377524D-01 2.000000D+00 2.000000D+00 2.000000D+00
 PAR(I) = 7.955348D-01 1.000000D+00 1.000000D+00 1.000000D+00
 LWR(I) = 6.533172D-01 1.000000D+00 1.000000D-02 1.000000D-02
 DIF(I) = 1.422176D-01 1.000000D+30 1.000000D+30 1.000000D+30

Normalized test divisors for final basis selection.
 Values near 0.100000(=APIV) or less indicate indeterminate parameters.

1.000000 0.000000 0.000000 0.000000

The model parameter estimate consists of the particular vector par just given,
 plus an arbitrary linear combination of the null-space basis vectors which follow.
 Vector I is the derivative of this solution
 with respect to parameter I.

Vector 2:
 0.000 1.000 0.000 0.000
 Vector 3:
 0.000 0.000 1.000 0.000
 Vector 4:
 0.000 0.000 0.000 1.000

Normalized covariances of the posterior parameter distribution

1.00000
 0.00000 0.00000
 0.00000 0.00000 0.00000
 0.00000 0.00000 0.00000 0.00000

observed values	predicted values	residuals
6.74500D-07	1.30371D-06	-6.29213D-07
1.21100D-06	1.85199D-06	-6.40991D-07
1.80900D-06	2.96775D-06	-1.15875D-06
4.04100D-06	4.48308D-06	-4.42081D-07
5.78200D-06	5.67466D-06	1.07342D-07
7.20100D-06	4.92274D-06	2.27826D-06
5.40200D-07	8.85161D-07	-3.44961D-07
1.47300D-06	2.07828D-06	-6.05278D-07
2.55500D-06	3.79052D-06	-1.23552D-06
3.55300D-06	4.99239D-06	-1.43939D-06
4.29800D-06	4.75938D-06	-4.61379D-07
7.81900D-07	1.10115D-06	-3.19250D-07
1.90200D-06	2.32719D-06	-4.25189D-07
3.85500D-06	3.93640D-06	-8.14047D-08
5.21800D-06	4.97123D-06	2.46774D-07

6.12800D-06	5.86171D-06	2.66289E-07
7.70100D-06	7.09540D-06	6.05603E-07

MIN = -1.43939D-06 MAX = 2.27826D-06

End of problem no. 1 no. of function calls = 18
no. of iterations = 3

G.1.2 Results at 80°C

```
***** G R E G *****
***** General Regression Software Package *****
***** for Nonlinear Parameter Estimation. *****
***** Version of August, 1990 *****
*****
***** Level = 10 *****
***** nonlinear least squares with *****
***** optional numerical derivatives. *****
*****
```

Start of problem no. 1 with 13 observations and 4 parameters

BNDUP(I)= 2.500000D+00 2.500000D+00 2.500000D+00 2.500000D+00
PAR(I) = 1.000000D+00 1.000000D+00 1.000000D+00 1.000000D+00
BNDLW(I)= 1.000000D-01 1.000000D-01 1.000000D-01 1.000000D-01

```
DEL(I) = -1.000000D-03 -1.000000D-03 -1.000000D-03 -1.000000D-03
CHMAX(I)= 1.000000D-01 1.000000D-01 1.000000D-01 1.000000D-01
```

```
APIV = 1.0000D-01 RSTOL = 1.0000D-01 ITMAX = 25 LISTS = 2
EMOD = 1.0000D-08 RPTOL = 1.0000D-05 IDIF = 0
```

All derivatives are obtained by finite differences

```
***** Iteration no. 1 no. of function calls 0 *****
PAR(I) = 1.000000D+00 1.000000D+00 1.000000D+00 1.000000D+00
```

```
***** Current sum of squares = 4.95173D-11 *****
```

```
***** Iteration no. 2   no. of function calls 10 *****
PAR(I) = 9.000000D-01 1.100000D+00 1.100000D+00 1.100000D+00
```

```
***** Current sum of squares = 2.60671D-11 *****
```

```
***** Iteration no. 3  no. of function calls 19 *****
PAR(I) = 7.000000D-01 1.300000D+00 1.276079D+00 1.166051D+00
```

```
***** Current sum of squares = 9.85769D-12 *****
```

***** Iteration no. 4 no. of function calls 28 *****
 PAR(I) = 4.348740D-01 1.396222D+00 1.314710D+00 1.141097D+00

***** Current sum of squares = 6.62636D-12 *****

***** Iteration no. 5 no. of function calls 37 *****
 PAR(I) = 2.872214D-01 1.384775D+00 1.346304D+00 1.098262D+00

***** Current sum of squares = 6.19839D-12 *****

***** Iteration no. 6 no. of function calls 46 *****
 PAR(I) = 3.018752D-01 1.383175D+00 1.350792D+00 1.089399D+00

***** Current sum of squares = 6.16801D-12 *****

***** Termination criteria satisfied *****

***** Final value of sum of squares = 6.16800D-12 *****

Standard error of weighted residuals = 8.27849D-07
 estimated with 13 residuals and 9 degrees of freedom

***** 2-sigma intervals PAR(I)+-DIF(I) for parameters in basis; *****
 **** last value and bounds for any parameters that are not in basis ****
 UPR(I) = 6.005262D-01 1.689950D+00 1.572540D+00 1.285414D+00
 PAR(I) = 3.013775D-01 1.382968D+00 1.350912D+00 1.089493D+00
 LWR(I) = 2.228838D-03 1.075985D+00 1.129284D+00 8.935707D-01
 DIF(I) = 2.991487D-01 3.069824D-01 2.216279D-01 1.959219D-01

Normalized test divisors for final basis selection.
 Values near 0.100000(=APIV) or less indicate indeterminate parameters.

0.631367 0.944350 0.878108 0.721437

Normalized covariances of the posterior parameter distribution

1.00000
 0.23590 1.00000
 -0.34913 -0.08236 1.00000
 0.52779 0.12451 -0.18427 1.00000

observed values	predicted values	residuals
-1.44100D-06	-1.14026D-06	-3.00742D-07
4.96600D-08	1.16199D-07	-6.65387D-08
1.24600D-06	1.14893D-06	9.70713D-08
2.31700D-06	2.06866D-06	2.48341D-07
-3.44200D-06	-3.34563D-06	-9.63713D-08
-1.93400D-06	-2.33130D-06	3.97297D-07

-8.66300D-07	-2.13251D-07	-6.53049D-07
6.22400D-07	6.46509D-07	-2.41092D-08
1.67600D-06	1.34777D-06	3.28226D-07
-5.17700D-07	6.60332D-07	-1.17803D-06
6.00000D-07	1.51517D-06	-9.15173D-07
1.18200D-06	1.94669D-06	-7.64691D-07
3.56000D-06	1.98201D-06	1.57799D-06

MIN = -1.17803D-06 MAX = 1.57799D-06

End of problem no. 1 no. of function calls = 56
no. of iterations = 6

G.1.3 Results at 120°C

```

***** G R E G *****
***** General Regression Software Package *****
***** for Nonlinear Parameter Estimation. *****
***** Version of August, 1990 *****
*****

***** Level = 10 *****
***** nonlinear least squares with *****
***** optional numerical derivatives. *****
*****

```

Start of problem no. 1 with 19 observations and 6 parameters

```

BNDUP(I)= 3.500000D+00 3.500000D+00 3.500000D+00 3.500000D+00 3.500000D+00
3.500000D+00
PAR(I) = 1.000000D+00 1.000000D+00 1.000000D+00 1.000000D+00 1.000000D+00
1.000000D+00
BNDLW(I)= 1.200000D-01 1.000000D-01 1.000000D-01 1.000000D-01 1.000000D-01
1.000000D-01
DEL(I) = -1.000000D-02 -1.000000D-03 -1.000000D-03 -1.000000D-03 -1.000000D-03
-1.000000D-03
CHMAX(I)= 1.000000D-02 1.000000D-03 1.000000D-03 1.000000D-02 1.000000D-02
1.000000D-02

```

```

APIV = 1.0000D-02 RSTOL = 1.0000D-01 ITMAX = 25 LISTS = 2
EMOD = 1.0000D-08 RPTOL = 1.0000D-05 IDIF = 0

```

All derivatives are obtained by finite differences

```

***** Iteration no. 1 no. of function calls 0 *****
PAR(I) = 1.000000D+00 1.000000D+00 1.000000D+00 1.000000D+00 1.000000D+00
1.000000D+00

***** Current sum of squares = 1.61884D-10 *****

```


***** Iteration no. 2 no. of function calls 14 *****

PAR(I) = 9.900000D-01 1.001000D+00 1.001000D+00 1.010000D+00 1.010000D+00
9.900000D-01

***** Current sum of squares = 1.56349D-10 *****

***** Iteration no. 3 no. of function calls 27 *****

PAR(I) = 9.700000D-01 1.003000D+00 1.003000D+00 1.030000D+00 1.030000D+00
9.700000D-01

***** Current sum of squares = 1.45547D-10 *****

***** Iteration no. 4 no. of function calls 40 *****

PAR(I) = 9.300000D-01 1.007000D+00 1.007000D+00 1.070000D+00 1.070000D+00
9.300000D-01

***** Current sum of squares = 1.25034D-10 *****

***** Iteration no. 5 no. of function calls 53 *****

PAR(I) = 8.500000D-01 1.015000D+00 1.015000D+00 1.150000D+00 1.150000D+00
8.500000D-01

***** Current sum of squares = 8.85380D-11 *****

***** Iteration no. 6 no. of function calls 66 *****

PAR(I) = 6.900000D-01 1.031000D+00 1.031000D+00 1.310000D+00 1.295811D+00
6.900000D-01

***** Current sum of squares = 3.57417D-11 *****

***** Iteration no. 7 no. of function calls 79 *****

PAR(I) = 3.700000D-01 1.063000D+00 1.063000D+00 1.630000D+00 1.298017D+00
5.294006D-01

***** Current sum of squares = 8.91026D-12 *****

***** Iteration no. 8 no. of function calls 92 *****

PAR(I) = 1.200000D-01 1.106134D+00 1.019866D+00 2.061338D+00 1.273519D+00
5.049902D-01

The difference step of 0.173472D-17 in PAR(1) is very small.
therefore, the sensitivities for this parameter will be omitted.

***** Current sum of squares = 4.06239D-12 *****

***** Iteration no. 9 no. of function calls 103 *****

PAR(I) = 1.200000D-01 1.163151D+00 9.628488D-01 2.267923D+00 1.247603D+00
4.810057D-01

***** Current sum of squares = 3.59541D-12 *****

***** Iteration no. 10 no. of function calls 114 *****
 PAR(I) = 1.200000D-01 1.236852D+00 8.891475D-01 2.276949D+00 1.247724D+00
 4.811986D-01

***** Current sum of squares = 3.49906D-12 *****

***** Termination criteria satisfied *****

***** Final value of sum of squares = 3.49208D-12 *****

Standard error of weighted residuals = 4.99434D-07
 estimated with 19 residuals and 14 degrees of freedom

***** 2-sigma intervals PAR(I)+-DIF(I) for parameters in basis; *****
 **** last value and bounds for any parameters that are not in basis ****
 UPR(I) = 3.500000D+00 1.909509D+00 1.210516D+00 2.913636D+00 1.456307D+00
 5.361604D-01
 PAR(I) = 1.200000D-01 1.262869D+00 8.639430D-01 2.277107D+00 1.247726D+00
 4.811942D-01
 LWR(I) = 1.200000D-01 6.162290D-01 5.173700D-01 1.640578D+00 1.039144D+00
 4.262279D-01
 DIF(I) = 1.000000D+30 6.466400D-01 3.465730D-01 6.365288D-01 2.085815D-01
 5.496624D-02

Normalized test divisors for final basis selection.
 Values near 0.010000(=APIV) or less indicate indeterminate parameters.

0.000000 1.000000 1.000000 1.000000 1.000000 1.000000

The model parameter estimate consists of the particular vector par just given,
 plus an arbitrary linear combination of the null-space basis vectors which follow.
 Vector I is the derivative of this solution
 with respect to parameter I.

Vector 1:
 1.000 0.000 0.000 0.000 0.000 0.000

Normalized covariances of the posterior parameter distribution

0.00000
 0.00000 1.00000
 0.00000 0.00000 1.00000
 0.00000 0.00000 0.00000 1.00000
 0.00000 0.00000 0.00000 0.00000 1.00000
 0.00000 0.00000 0.00000 0.00000 0.00000 1.00000

observed values	predicted values	residuals
-4.32000D-07	-2.68497D-07	-1.63503D-07

4.10000D-07	7.32914D-07	-3.22914D-07
1.62000D-06	1.35454D-06	2.65464D-07
-9.09000D-07	-1.47978D-07	-7.61022D-07
1.92000D-07	5.02396D-07	-3.10396D-07
1.76000D-06	1.80084D-06	-4.08369D-08
2.21000D-06	1.91925D-06	2.90747D-07
-1.66000D-06	-6.10610D-07	-1.04939D-06
-4.63000D-07	-2.93321D-07	-1.69679D-07
6.21000D-07	4.76518D-07	1.44482D-07
1.25000D-06	8.66404D-07	3.83596D-07
-5.64000D-07	-6.12872D-07	4.88722D-08
3.22000D-07	4.70615D-07	-1.48615D-07
7.12000D-07	2.98181D-07	4.13819D-07
8.39000D-07	1.20073D-06	-3.61734D-07
3.65000D-06	3.75232D-06	-1.02324D-07
-1.39000D-06	-1.74691D-06	3.56906D-07
-2.34000D-07	5.42697D-07	-7.76697D-07
1.74000D-06	1.33604D-06	4.03965D-07

MIN = -1.04939D-06 MAX = 4.13819D-07

End of problem no. 1 no. of function calls = 126
no. of iterations = 10

G.2 GREG RESULT FOR 25WT% DEA

G.2.1 Results at 40°C

```
***** G R E G *****
***** General Regression Software Package *****
***** for Nonlinear Parameter Estimation. *****
***** Version of August, 1990 *****
*****
***** Level = 10 *****
***** nonlinear least squares with *****
***** optional numerical derivatives. *****
*****
```

Start of problem no. 1 with 13 observations and 4 parameters

BNDUP(I)= 2.000000D+30 2.000000D+30 2.000000D+30 2.000000D+30
PAR(I) = 1.000000D+00 1.000000D+00 1.000000D+00 1.000000D+00
BNDLW(I)= 1.000000D-31 -2.990000D+01 1.000000D-31 1.000000D-31

DEL(I) = 1.000000D-02 1.000000D-02 1.000000D-02 1.000000D-02
CHMAX(I)= 1.000000D+30 0.000000D+00 0.000000D+00 0.000000D+00

APIV = 1.0000D-01 RSTOL = 1.0000D-01 ITMAX = 50 LISTS = 2

EMOD = 1.0000D-08 RPTOL = 1.0000D-05 IDIF = 0

All derivatives are obtained by finite differences

***** Iteration no. 1 no. of function calls 0 *****

PAR(I) = 1.000000D+00 1.000000D+00 1.000000D+00 1.000000D+00

***** Current sum of squares = 6.33153D-12 *****

***** Iteration no. 2 no. of function calls 4 *****

PAR(I) = 1.227325D+00 1.000000D+00 1.000000D+00 1.000000D+00

***** Current sum of squares = 4.06700D-12 *****

***** Termination criteria satisfied *****

***** Final value of sum of squares = 4.05854D-12 *****

Standard error of weighted residuals = 5.81559D-07
estimated with 13 residuals and 12 degrees of freedom

***** 2-sigma intervals PAR(I)+-DIF(I) for parameters in basis; *****

**** last value and bounds for any parameters that are not in basis ****

UPR(I) = 1.440173D+00 2.000000D+30 2.000000D+30 2.000000D+30

PAR(I) = 1.240561D+00 1.000000D+00 1.000000D+00 1.000000D+00

LWR(I) = 1.040949D+00 -2.990000D+01 1.000000D-31 1.000000D-31

DIF(I) = 1.996118D-01 1.000000D+30 1.000000D+30 1.000000D+30

Normalized test divisors for final basis selection.

Values near 0.100000(=APIV) or less indicate indeterminate parameters.

1.000000 0.000000 0.000000 0.000000

The model parameter estimate consists of the particular vector par just given,
plus an arbitrary linear combination of the null-space basis vectors which follow.
Vector I is the derivative of this solution
with respect to parameter I.

Vector 2:

0.000 1.000 0.000 0.000

Vector 3:

0.000 0.000 1.000 0.000

Vector 4:

0.000 0.000 0.000 1.000

Normalized covariances of the posterior parameter distribution

1.00000

0.00000 0.00000

```

0.00000  0.00000  0.00000
0.00000  0.00000  0.00000  0.00000

```

observed values	predicted values	residuals
4.04000D-07	3.87216D-07	1.67844D-08
7.64000D-07	4.72799D-07	2.91201D-07
1.03000D-06	5.98160D-07	4.31840D-07
1.27000D-06	7.08129D-07	5.61871D-07
1.29000D-06	2.06128D-06	-7.71280D-07
3.24000D-06	4.33609D-06	-1.09609D-06
6.42000D-06	6.70969D-06	-2.89687D-07
9.20000D-06	8.58254D-06	6.17462D-07
1.08100D-05	1.07916D-05	1.84160D-08
-1.28900D-08	2.62610D-09	-1.55161D-08
1.22000D-06	1.83357D-06	-6.13566D-07
3.14000D-06	3.29641D-06	-1.56414D-07
6.21000D-06	5.31095D-06	8.99050D-07

```

MIN = -1.09609D-06  MAX = 8.99050D-07
=

```

```

End of problem no. 1 no. of function calls = 8
no. of iterations = 2

```

G.2.2 Results at 80°C

```

***** G R E G *****
***** General Regression Software Package *****
***** for Nonlinear Parameter Estimation. *****
***** Version of August, 1990 *****
*****

***** Level = 10 *****
***** nonlinear least squares with *****
***** optional numerical derivatives. *****
*****

```

Start of problem no. 1 with 10 observations and 3 parameters

```

BNDUP(I)= 1.000000D+02 1.000000D+02 5.000000D+01
PAR(I) = 1.000000D+00 1.000000D+00 1.000000D+00
BNDLW(I)= 1.000000D-02 1.000000D-02 1.000000D-03

```

```

DEL(I) = -1.000000D-03 -1.000000D-03 -1.000000D-03
CHMAX(I)= 1.000000D-01 1.000000D-01 1.000000D-01

```

```

APIV = 1.0000D-03 RSTOL = 1.0000D-01 ITMAX = 50 LISTS = 2
EMOD = 1.0000D-01 RPTOL = 1.0000D-05 IDIF = 0

```

All derivatives are obtained by finite differences

***** Iteration no. 1 no. of function calls 0 *****
PAR(I) = 1.000000D+00 1.000000D+00 1.000000D+00

***** Current sum of squares = 4.25646D-11 *****

***** Iteration no. 2 no. of function calls 8 *****
PAR(I) = 9.000000D-01 1.100000D+00 9.000000D-01

***** Current sum of squares = 3.01292D-11 *****

***** Iteration no. 3 no. of function calls 15 *****
PAR(I) = 7.000000D-01 1.300000D+00 7.000000D-01

***** Current sum of squares = 1.33084D-11 *****

***** Iteration no. 4 no. of function calls 22 *****
PAR(I) = 5.067384D-01 1.700000D+00 4.758604D-01

***** Current sum of squares = 5.54219D-12 *****

***** Iteration no. 5 no. of function calls 30 *****
PAR(I) = 5.187948D-01 1.743836D+00 4.828483D-01

***** Current sum of squares = 5.49201D-12 *****

***** Iteration no. 6 no. of function calls 38 *****
PAR(I) = 5.300550D-01 1.782377D+00 4.890106D-01

***** Current sum of squares = 5.45105D-12 *****

***** Iteration no. 7 no. of function calls 46 *****
PAR(I) = 5.403958D-01 1.816549D+00 4.945008D-01

***** Current sum of squares = 5.41788D-12 *****

***** Iteration no. 8 no. of function calls 53 *****
PAR(I) = 6.352147D-01 2.119901D+00 5.434572D-01

***** Current sum of squares = 5.28844D-12 *****

***** Termination criteria satisfied *****

***** Final value of sum of squares = 5.27800D-12 *****

Standard error of weighted residuals = 8.68332D-07
estimated with 10 residuals and 7 degrees of freedom

***** 2-sigma intervals PAR(I)+-DIF(I) for parameters in basis; *****
 **** last value and bounds for any parameters that are not in basis ****
 UPR(I) = 1.335350D+00 3.617044D+00 1.063074D+00
 PAR(I) = 6.558940D-01 2.126634D+00 5.521652D-01
 LWR(I) = -2.356244D-02 6.362243D-01 4.125608D-02
 DIF(I) = 6.794564D-01 1.490410D+00 5.109091D-01

Normalized test divisors for final basis selection.
 Values near 0.001000(=APIV) or less indicate indeterminate parameters.

0.109912 0.186981 0.210524

Normalized covariances of the posterior parameter distribution

1.00000
 0.90168 1.00000
 0.88852 0.80116 1.00000

observed values	predicted values	residuals
4.34000D-07	2.45950D-09	4.31540D-07
1.79500D-06	1.89442D-06	-9.94197D-08
4.18200D-06	4.32492D-06	-1.42924D-07
5.92300D-06	5.94554D-06	-2.25432D-08
6.95100D-06	7.02255D-06	-7.15469D-08
-2.79700D-07	1.05557D-06	-1.33527D-06
1.12200D-06	2.57254D-06	-1.45054D-06
3.78400D-06	3.76746D-06	1.65394D-08
5.10000D-06	4.44398D-06	6.56019D-07
5.90800D-06	5.04881D-06	8.59188D-07

MIN = -1.45054D-06 MAX = 8.59188D-07

End of problem no. 1 no. of function calls = 61
 no. of iterations = 8

G.2.3 Results at 120°C

***** G R E G *****
 ***** General Regression Software Package *****
 ***** for Nonlinear Parameter Estimation. *****
 ***** Version of August, 1990 *****

 ***** Level = 10 *****
 ***** nonlinear least squares with *****
 ***** optional numerical derivatives. *****

Start of problem no. 1 with 15 observations and 4 parameters

BNDUP(I)= 3.500000D+00 3.500000D+00 3.500000D+00 3.500000D+00
 PAR(I) = 1.000000D+00 1.000000D+00 1.000000D+00 1.000000D+00
 BNDLW(I)= 1.000000D-01 1.000000D-01 1.000000D-01 1.000000D-01

DEL(I) = -1.000000D-03 -1.000000D-03 -1.000000D-03 -1.000000D-03
 CHMAX(I)= 1.000000D-01 1.000000D-01 1.000000D-01 1.000000D-01

APIV = 1.0000D-03 RSTOL = 1.0000D-01 ITMAX = 50 LISTS = 2
 EMOD = 1.0000D-08 RPTOL = 1.0000D-05 IDIF = 0

All derivatives are obtained by finite differences

***** Iteration no. 1 no. of function calls 0 *****

PAR(I) = 1.000000D+00 1.000000D+00 1.000000D+00 1.000000D+00

***** Current sum of squares = 5.64034D-10 *****

***** Iteration no. 2 no. of function calls 10 *****

PAR(I) = 9.000000D-01 1.058568D+00 9.000000D-01 9.000000D-01

***** Current sum of squares = 4.18096D-10 *****

***** Iteration no. 3 no. of function calls 19 *****

PAR(I) = 7.000000D-01 1.055862D+00 7.000000D-01 7.000000D-01

***** Current sum of squares = 1.85008D-10 *****

***** Iteration no. 4 no. of function calls 28 *****

PAR(I) = 6.734665D-01 1.054093D+00 3.000000D-01 3.000000D-01

***** Current sum of squares = 6.15509D-12 *****

***** Iteration no. 5 no. of function calls 37 *****

PAR(I) = 1.041115D+00 1.069563D+00 3.414879D-01 3.558638D-01

***** Current sum of squares = 3.79990D-12 *****

***** Iteration no. 6 no. of function calls 46 *****

PAR(I) = 1.134185D+00 1.066674D+00 3.351240D-01 3.474679D-01

***** Current sum of squares = 3.56305D-12 *****

***** Termination criteria satisfied *****

***** Final value of sum of squares = 3.56294D-12 *****

Standard error of weighted residuals = 5.69125D-07
 estimated with 15 residuals and 11 degrees of freedom

***** 2-sigma intervals PAR(I)+-DIF(I) for parameters in basis; *****
 **** last value and bounds for any parameters that are not in basis ****
 UPR(I) = 1.716746D+00 1.174953D+00 3.681316D-01 3.838051D-01
 PAR(I) = 1.132954D+00 1.066645D+00 3.352766D-01 3.476751D-01
 LWR(I) = 5.491614D-01 9.583380D-01 3.024216D-01 3.115451D-01
 DIF(I) = 5.837924D-01 1.083073D-01 3.285502D-02 3.613000D-02

Normalized test divisors for final basis selection.
 Values near 0.001000(=APIV) or less indicate indeterminate parameters.

0.775408 0.989856 0.903471 0.852839

Normalized covariances of the posterior parameter distribution

1.00000
 0.10072 1.00000
 0.31069 0.03129 1.00000
 0.38362 0.03864 0.11919 1.00000

observed values	predicted values	residuals
-2.69530D-06	-2.83756D-06	1.42265D-07
-9.91430D-07	-7.10379D-07	-2.81051D-07
8.05200D-07	1.54505D-06	-7.39847D-07
2.49200D-06	2.36584D-06	1.26157D-07
3.87690D-06	3.16792D-06	7.08983D-07
-1.54240D-06	-1.57144D-06	2.90378D-08
1.06600D-07	3.09168D-07	-2.02568D-07
1.60100D-06	2.16716D-06	-5.66164D-07
1.47600D-06	1.27843D-06	1.97575D-07
2.28500D-06	1.98410D-06	3.00900D-07
-2.34000D-06	-2.41959D-06	7.95850D-08
-3.05000D-07	5.65760D-07	-8.70760D-07
1.64240D-06	2.19471D-06	-5.52310D-07
2.97000D-06	3.03487D-06	-6.48734D-08
3.22000D-06	2.30788D-06	9.12115D-07

MIN = -8.70760D-07 MAX = 9.12115D-07

End of problem no. 1 no. of function calls = 56
 no. of iterations = 6

G.3 GREG RESULT FOR 5 WT% DEA/ 45 WT% MDEA

G.3.1 Results at 40°C

```
***** G R E G *****
***** General Regression Software Package *****
***** for Nonlinear Parameter Estimation. *****
***** Version of August, 1990 *****
*****
***** Level = 10 *****
***** nonlinear least squares with *****
***** optional numerical derivatives. *****
*****
```

Start of problem no. 1 with 23 observations and 5 parameters

```
BNDUP(I)= 3.000000D+00 3.000000D+00 3.500000D+00 3.500000D+00 3.500000D+00
PAR(I) = 6.000000D-01 1.000000D+00 1.000000D+00 1.000000D+00 1.000000D+00
BNDLW(I)= 1.000000D-03 1.000000D-02 1.000000D-02 1.000000D-02 1.000000D-02
```

```
DEL(I) = -1.000000D-03 -1.000000D-03 -1.000000D-03 -1.000000D-03 -1.000000D-03
CHMAX(I)= 1.150000D-03 1.150000D-03 1.150000D-03 1.150000D-03 1.150000D-03
```

```
APIV = 1.0000D-01 RSTOL = 1.0000D-01 ITMAX = 25 LISTS = 2
EMOD = 1.0000D-02 RPTOL = 1.0000D-01 IDIF = 1
```

All derivatives are obtained by finite differences

```
***** Iteration no. 1 no. of function calls 0 *****
PAR = 6.000000D-01 1.000000D+00 1.000000D+00 1.000000D+00 1.000000D+00
```

```
***** Current sum of squares = 2.46494D-12 *****
```

```
***** Iteration no. 2 no. of function calls 7 *****
PAR(I) = 6.011500D-01 9.988500D-01 1.000837D+00 9.988500D-01 1.001150D+00
```

```
***** Current sum of squares = 2.45990D-12 *****
```

```
***** Iteration no. 3 no. of function calls 14 *****
PAR(I) = 6.011095D-01 9.988718D-01 1.000722D+00 9.986200D-01 1.001380D+00
```

```
***** Current sum of squares = 2.45909D-12 *****
```

```
***** Iteration no. 4 no. of function calls 22 *****
PAR(I) = 6.011173D-01 9.988488D-01 1.000716D+00 9.986085D-01 1.001392D+00
```

```
***** Current sum of squares = 2.45904D-12 *****
```

```
***** Iteration no. 5 no. of function calls 30 *****
```

PAR(I) = 6.011138D-01 9.988987D-01 1.000672D+00 9.985196D-01 1.001480D+00

***** Current sum of squares = 2.45873D-12 *****

***** Iteration no. 6 no. of function calls 38 *****

PAR(I) = 6.009149D-01 9.985749D-01 1.000631D+00 9.984386D-01 1.001561D+00

***** Current sum of squares = 2.45843D-12 *****

***** Iteration no. 7 no. of function calls 44 *****

PAR(I) = 6.008997D-01 9.979160D-01 1.000549D+00 9.982739D-01 1.001726D+00

***** Current sum of squares = 2.45760D-12 *****

***** Iteration no. 8 no. of function calls 52 *****

PAR(I) = 6.008337D-01 9.979081D-01 1.000524D+00 9.982230D-01 1.001777D+00

***** Current sum of squares = 2.45745D-12 *****

***** S cannot be reduced further for THE MODEL AND DERIVATIVES AS CALCULATED. *****

Summary of search:	grid points	factor RHO:=
HT	ST (ST-S0)/(PRED S1-S0)	
1.00000D+00	2.84630D-12	-3.26841D+02
1.00000D-01	2.46610D-12	-7.26561D+00
1.00000D-02	2.82534D-12	-3.09221D+02
1.00000D-03	2.84576D-12	-3.26384D+02
1.00000D-04	2.46621D-12	-7.36251D+00
1.00000D-05	2.46621D-12	-7.36260D+00
1.00000D-06	2.46621D-12	-7.36260D+00
1.00000D-07	2.46621D-12	-7.36260D+00
1.00000D-08	2.46621D-12	-7.36260D+00
1.00000D-09	2.46621D-12	-7.36260D+00
0.00000D+00	2.45745D-12	0.00000D+00

 ***** The following termination criteria are not satisfied: *****

CHMAX was active in the latest solution for the following parameters:

0 -2 -3 -4 5

***** Final value of sum of squares = 2.45745D-12 *****

Standard error of weighted residuals = 3.34219D-07
 estimated with 23 residuals and 22 degrees of freedom

***** 2-sigma intervals PAR(I)+-DIF(I) for parameters in basis; *****
 **** last value and bounds for any parameters that are not in basis ****

UPR(I) = 6.021822D-01 3.000000D+00 3.500000D+00 3.500000D+00 3.500000D+00
 PAR(I) = 6.008337D-01 9.979081D-01 1.000524D+00 9.982230D-01 1.001777D+00
 LWR(I) = 5.994852D-01 1.000000D-02 1.000000D-02 1.000000D-02 1.000000D-02
 DIF(I) = 1.348505D-03 1.000000D+30 1.000000D+30 1.000000D+30 1.000000D+30

Normalized test divisors for final basis selection.

Values near 0.100000(=APIV) or less indicate indeterminate parameters.

1.000000 0.000098 0.999999 1.000000 0.999996

Normalized covariances of the posterior parameter distribution

1.000000
 0.000000 0.000000
 0.000000 0.000000 0.000000
 0.000000 0.000000 0.000000 0.000000
 0.000000 0.000000 0.000000 0.000000 0.000000

observed values	predicted values	residuals
-1.11000D-07	-1.05477D-07	-5.52279D-09
5.00000D-07	3.36968D-07	1.63032D-07
1.04000D-06	1.21519D-06	-1.75192D-07
2.31000D-06	2.12264D-06	1.87355D-07
3.01000D-06	3.08306D-06	-7.30551D-08
5.22000D-06	4.75354D-06	4.66462D-07
-1.51000D-07	-1.68063D-07	1.70634D-08
2.93000D-07	2.91318D-07	1.68240D-09
6.96000D-07	7.76352D-07	-8.03521D-08
2.29000D-06	2.21094D-06	7.90581D-08
3.82000D-06	3.64353D-06	1.76470D-07
4.50000D-06	4.50880D-06	-8.80475D-09
-3.12000D-07	-5.62403D-08	-2.55760D-07
1.28000D-07	1.36509D-07	-8.50865D-09
4.02000D-07	5.256D-07	-1.47256D-07
1.40000D-06	1.18D-06	-1.61176D-07
2.91000D-06	2.59914D-06	5.10864D-07
3.56000D-06	2.63574D-06	9.24257D-07
3.74000D-06	2.85664D-06	8.83359D-07
1.67590D-06	1.72190D-06	-4.60047D-08
3.11510D-06	3.08997D-06	2.51301D-08
4.99000D-06	5.08201D-06	-9.20119D-08
6.23000D-06	6.50926D-06	-2.79257D-07

MIN = -2.79257D-07 MAX = 9.24257D-07

End of problem no. 1 no. of function calls = 68
 no. of iterations = 8

G.3.2 Results at 80°C

```
***** G R E G *****
***** General Regression Software Package *****
***** for Nonlinear Parameter Estimation. *****
***** Version of August, 1990 *****
*****
```

```
***** Level = 10 *****
***** nonlinear least squares with *****
***** optional numerical derivatives. *****
*****
```

Start of problem no. 1 with 13 observations and 3 parameters

```
BNDUP(I)= 3.500000D+00 3.500000D+00 3.500000D+00
PAR(I) = 1.000000D+00 1.000000D+00 1.000000D+00
BNDLW(I)= 1.000000D-02 1.000000D-01 1.000000D-01
```

```
DEL(I) = -1.000000D-02 -1.000000D-02 -1.000000D-02
CHMAX(I)= 1.000000D-01 1.000000D-01 1.000000D-01
```

```
APIV = 1.0000D-01 RSTOL = 1.0000D-01 ITMAX = 25 LISTS = 2
EMOD = 1.0000D-01 RPTOL = 1.0000D-01 IDIF = 1
```

All derivatives are obtained by finite differences

```
***** Iteration no. 1 no. of function calls 0 *****
PAR(I) = 1.000000D+00 1.000000D+00 1.000000D+00
```

```
***** Current sum of squares = 1.76858D-11 *****
```

```
***** Iteration no. 2 no. of function calls 6 *****
PAR(I) = 9.756303D-01 9.986232D-01 9.716485D-01
```

```
***** Current sum of squares = 1.57791D-11 *****
```

```
***** Termination criteria satisfied *****
```

```
***** Final value of sum of squares = 1.57751D-11 *****
```

Standard error of weighted residuals = 1.25599D-06
estimated with 13 residuals and 10 degrees of freedom

```
***** 2-sigma intervals PAR(I)+-DIF(I) for parameters in basis; *****
**** last value and bounds for any parameters that are not in basis ****
```

UPR(I) = 1.078604D+00 1.213929D+00 9.941405D-01
 PAR(I) = 9.753057D-01 9.985965D-01 9.716223D-01
 LWR(I) = 8.720074D-01 7.832636D-01 9.491042D-01
 DIF(I) = 1.032984D-01 2.153329D-01 2.251813D-02

Normalized test divisors for final basis selection.
 Values near 0.100000(=APIV) or less indicate indeterminate parameters.

0.996015 0.999992 0.996023

Normalized covariances of the posterior parameter distribution

1.00000
 0.00286 1.00000
 -0.06306 -0.00018 1.00000

observed values	predicted values	residuals
-1.75000D-07	-2.64102D-08	-1.48590D-07
1.30000D-07	1.60853D-07	-3.08532D-08
3.99000D-07	5.41176D-07	-1.42176D-07
8.81000D-07	1.07060D-06	-1.89596D-07
1.71100D-06	2.00144D-06	-2.90438D-07
3.29000D-06	2.89880D-06	3.91202D-07
5.62000D-06	9.25652D-06	-3.63652D-06
-1.66000D-06	-1.03855D-06	-6.21453D-07
-8.41000D-07	-1.31599D-07	-7.09401D-07
6.71000D-08	7.03375D-07	-6.36275D-07
1.43000D-06	2.00316D-06	-5.73157D-07
3.22000D-06	3.27951D-06	-5.95056D-08
5.15000D-06	4.37036D-06	7.79645D-07

MIN = -3.63652D-06 MAX = 7.79645D-07

End of problem no. 1 no. of function calls = 14
 no. of iterations = 2

G.3.3 Results at 120°C

```
***** G R E G *****
***** General Regression Software Package *****
***** for Nonlinear Parameter Estimation. *****
***** Version of August, 1990 *****
*****

***** Level = 10 *****
***** nonlinear least squares with *****
***** optional numerical derivatives. *****
```

Start of problem no. 1 with 14 observations and 4 parameters

BNDUP(I)= 3.500000D+00 3.500000D+00 3.500000D+00 3.500000D+00
 PAR(I) = 1.000000D+00 1.000000D+00 1.000000D+00 1.000000D+00
 BNDLW(I)= 1.000000D-03 1.000000D-01 1.000000D-01 1.000000D-01

DEL(I) = -1.000000D-02 -1.000000D-02 -1.000000D-02 -1.000000D-02
 CHMAX(I)= 1.000000D-01 5.000000D-01 5.000000D-01 5.000000D-01

APIV = 1.0000D-01 RSTOL = 1.0000D-01 ITMAX = 25 LISTS = 2
 EMOD = 1.0000D-02 RPTOL = 3.0000D-01 IDIF = 1

All derivatives are obtained by finite differences

***** Iteration no. 1 no. of function calls 0 *****

PAR(I) = 1.000000D+00 1.000000D+00 1.000000D+00 1.000000D+00

***** Current sum of squares = 3.29486D-11 *****

***** Iteration no. 2 no. of function calls 6 *****

PAR(I) = 1.100000D+00 1.500000D+00 1.500000D+00 1.500000D+00

***** Current sum of squares = 1.63479D-11 *****

***** Iteration no. 3 no. of function calls 11 *****

PAR(I) = 1.254166D+00 1.552521D+00 1.874108D+00 2.270829D+00

***** Current sum of squares = 8.21628D-12 *****

***** Iteration no. 4 no. of function calls 16 *****

PAR(I) = 1.466321D+00 1.884095D+00 1.857192D+00 2.309624D+00

***** Current sum of squares = 5.65363D-12 *****

***** Iteration no. 5 no. of function calls 24 *****

PAR(I) = 1.447000D+00 1.899242D+00 1.858095D+00 2.312123D+00

***** Current sum of squares = 5.34727D-12 *****

***** Termination criteria satisfied *****

***** Final value of sum of squares = 5.34725D-12 *****
 logout

Standard error of weighted residuals = 7.31249D-07
 estimated with 14 residuals and 10 degrees of freedom

***** 2-sigma intervals PAR(I)+-DIF(I) for parameters in basis; *****
 **** last value and bounds for any parameters that are not in basis ****
 UPR(I) = 1.503646D+00 2.144295D+00 2.835629D+00 3.298571D+00
 PAR(I) = 1.447001D+00 1.899242D+00 1.858095D+00 2.312129D+00
 LWR(I) = 1.390356D+00 1.654190D+00 8.805612D-01 1.325686D+00
 DIF(I) = 5.664498D-02 2.450526D-01 9.775339D-01 9.864425D-01

Normalized test divisors for final basis selection.
 Values near 0.100000(=APIV) or less indicate indeterminate parameters.

0.670000 0.670008 0.999994 0.999989

Normalized covariances of the posterior parameter distribution

1.00000
 0.57445 1.00000
 -0.00247 -0.00142 1.00000
 -0.00337 -0.00194 0.00001 1.00000

observed values	predicted values	residuals
-1.08000D-06	-8.81606D-08	-9.91839D-07
7.42000D-08	-4.18425D-07	4.92625D-07
9.12000D-07	1.44119D-06	-5.29186D-07
2.19000D-06	1.99278D-06	1.97219D-07
-1.03000D-07	2.29281D-08	-1.25928D-07
4.32000D-07	7.36861D-07	-3.04861D-07
1.32000D-06	7.11630D-07	6.08370D-07
2.14000D-06	1.63143D-06	5.08571D-07
2.37000D-06	2.83664D-06	-4.66637D-07
-3.33000D-07	1.57084D-07	-4.90084D-07
8.40000D-07	1.95691D-06	-1.11691D-06
1.54000D-06	7.61761D-07	7.78239D-07
2.12000D-06	2.87134D-06	-7.51343D-07
2.49000D-06	2.02446D-06	-4.34457D-07

MIN = -1.11691D-06 MAX = 7.78239D-07

End of problem no. 1 no. of function calls = 37
 no. of iterations = 5

G.4 GREG RESULT FOR 25 WT% DEA/ 25 WT% MDEA

G.4.1 Results at 40°C

***** G R E G *****
 ***** General Regression Software Package *****
 ***** for Nonlinear Parameter Estimation. *****
 ***** Version of August, 1990 *****


```

*****
***** Level = 10 *****
***** nonlinear least squares with *****
***** optional numerical derivatives. *****
*****

```

Start of problem no. 1 with 10 observations and 3 parameters

```

BNDUP(I)= 1.000000D+01 4.000000D+00 4.000000D+00
PAR(I) = 1.000000D+00 1.000000D+00 1.000000D+00
BNDLW(I)= 1.000000D-01 1.000000D-02 1.000000D-02

```

```

DEL(I) = 1.000000D-01 1.000000D-01 1.000000D-01
CHMAX(I)= 1.000000D+01 0.000000D+00 1.000000D+01

```

```

APIV = 1.0000D-01 RSTOL = 8.0000D-01 ITMAX = 50 LISTS = 2
EMOD = 3.7253D-09 RPTOL = 8.0000D-01 IDIF = 0

```

All derivatives are obtained by finite differences

```

***** Iteration no. 1 no. of function calls 0 *****
PAR(I) = 1.000000D+00 1.000000D+00 1.000000D+00

```

```

***** Current sum of squares = 6.30329D-11 *****

```

```

***** Termination criteria satisfied *****

```

```

***** Final value of sum of squares = 5.87835D-11 *****

```

Standard error of weighted residuals = 2.71071D-06
estimated with 10 residuals and 8 degrees of freedom

```

***** 2-sigma intervals PAR(I)+-DIF(I) for parameters in basis; *****
**** last value and bounds for any parameters that are not in basis ****
UPR(I) = 2.018070D+00 4.000000D+00 1.421123D+00
PAR(I) = 4.268449D-01 1.000000D+00 1.106665D+00
LWR(I) = -1.164380D+00 1.000000D-02 7.922064D-01
DIF(I) = 1.591225D+00 1.000000D+30 3.144583D-01

```

Normalized test divisors for final basis selection.
Values near 0.100000(=APIV) or less indicate indeterminate parameters.

```

0.984958 0.000000 0.984958

```

The model parameter estimate consists of the particular vector par just given,
plus an arbitrary linear combination of the null-space basis vectors which follow.
Vector I is the derivative of this solution
with respect to parameter I.

Vector 2:
0.000 1.000 0.000

Normalized covariances of the posterior parameter distribution

```
1.00000
0.00000 0.00000
0.12265 0.00000 1.00000
```

observed values	predicted values	residuals
1.33000D-06	2.34398D-06	-1.01398D-06
3.21000D-06	5.87031D-06	-2.66031D-06
6.49000D-06	8.56738D-06	-2.07738D-06
9.71000D-06	9.80038D-06	-9.03804D-08
1.29100D-05	1.01160D-05	2.79399D-06
1.24000D-05	7.33152D-06	5.06848D-06
8.75000D-06	6.06451D-06	2.68549D-06
5.52000D-06	4.58030D-06	9.39704D-07
1.79000D-06	3.78472D-06	-1.99472D-06
8.78000D-07	1.76390D-06	-8.85902D-07

MIN = -2.66031D-06 MAX = 5.06848D-06

End of problem no. 1 no. of function calls = 7
no. of iterations = 1

G.4.2 Results at 80°C

```
***** G R E G *****
***** General Regression Software Package *****
***** for Nonlinear Parameter Estimation. *****
***** Version of August, 1990 *****
*****
```

```
***** Level = 10 *****
***** nonlinear least squares with *****
***** optional numerical derivatives. *****
*****
```

Start of problem no. 1 with 11 observations and 3 parameters

```
BNDUP(I)= 5.000000D+00 2.000000D+00 2.000000D+00
PAR(I) = 1.000000D+00 1.000000D+00 1.000000D+00
BNDLW(I)= 1.000000D-02 1.000000D-02 1.000000D-02
```

DEL(I) = 1.000000D-01 1.000000D-01 1.000000D-01
 CHMAX(I)= 1.000000D-01 1.000000D-01 1.000000D-01

APIV = 1.0000D-01 RSTOL = 1.0000D-01 ITMAX = 50 LISTS = 2
 EMOD = 1.0000D-02 RPTOL = 1.0000D-01 IDIF = 0

All derivatives are obtained by finite differences

***** Iteration no. 1 no. of function calls 0 *****
 PAR(I) = 1.000000D+00 1.000000D+00 1.000000D+00

***** Current sum of squares = 6.36301D-11 *****

***** Iteration no. 2 no. of function calls 8 *****
 PAR(I) = 1.100000D+00 9.219740D-01 9.000000D-01

***** Current sum of squares = 2.29270D-11 *****

***** Iteration no. 3 no. of function calls 15 *****
 PAR(I) = 1.105530D+00 8.219740D-01 9.547570D-01

***** Current sum of squares = 1.17750D-11 *****

***** Iteration no. 4 no. of function calls 22 *****
 PAR(I) = 1.126873D+00 7.392293D-01 9.264027D-01

***** Current sum of squares = 1.09884D-11 *****

***** Termination criteria satisfied *****

***** Final value of sum of squares = 1.06682D-11 *****

Standard error of weighted residuals = 1.15478D-06
 estimated with 11 residuals and 8 degrees of freedom

***** 2-sigma intervals PAR(I)+-DIF(I) for parameters in basis; *****

**** last value and bounds for any parameters that are not in basis ****

UPR(I) = 1.149266D+00 9.250306D-01 1.703538D+00
 PAR(I) = 1.120677D+00 7.536811D-01 9.204193D-01
 LWR(I) = 1.092087D+00 5.823317D-01 1.373008D-01
 DIF(I) = 2.858973D-02 1.713495D-01 7.831185D-01

Normalized test divisors for final basis selection.

Values near 0.100000(=APIV) or less indicate indeterminate parameters.

0.762274 0.765960 0.993726

Normalized covariances of the posterior parameter distribution

```

1.00000
-0.48378  1.00000
-0.07921  0.03832  1.00000

```

observed values	predicted values	residuals
-3.79000D-06	-5.11957D-06	1.32957D-06
-2.95000D-06	-2.12376D-06	-8.26242D-07
-1.15000D-06	-3.52191D-07	-7.97809D-07
1.41550D-06	1.91693D-06	-5.01433D-07
5.40000D-06	4.98573D-06	4.14273D-07
-2.51000D-06	-1.41754D-07	-2.36825D-06
1.00000D-06	1.61725D-06	-6.17252D-07
2.92000D-06	3.15801D-06	-2.38005D-07
4.64800D-06	4.80369D-06	-1.55687D-07
5.81000D-06	5.34295D-06	4.67048D-07
7.36000D-06	6.42748D-06	9.32517D-07

MIN = -2.36825D-06 MAX = 1.32957D-06

End of problem no. 1 no. of function calls = 30
no. of iterations = 4

G.4.3 Results at 120°C

```

***** G R E G *****
***** General Regression Software Package *****
***** for Nonlinear Parameter Estimation. *****
***** Version of August, 1990 *****
*****

```

```

***** Level = 10 *****
***** nonlinear least squares with *****
***** optional numerical derivatives. *****
*****

```

Start of problem no. 1 with 11 observations and 3 parameters

```

BNDUP(I)= 1.000000D+01 4.000000D+00 4.000000D+00
PAR(I) = 1.000000D+00 1.000000D+00 1.000000D+00
BNDLW(I)= 5.000000D-01 1.000000D-01 1.000000D-01

```

```

DEL(I) = 1.000000D-01 1.000000D-01 1.000000D-01
CHMAX(I)= 2.000000D-01 2.000000D-01 2.000000D-01

```

```

APIV = 1.0000D-01 RSTOL = 1.0000D-01 ITMAX = 50 LISTS = 2
EMOD = 1.0000D-02 RPTOL = 1.0000D-02 IDIF = 0

```

All derivatives are obtained by finite differences

```

***** Iteration no. 1 no. of function calls 0 *****
PAR(I) = 1.000000D+00 1.000000D+00 1.000000D+00

***** Current sum of squares = 5.44865D-11 *****

***** Iteration no. 2 no. of function calls 8 *****
PAR(I) = 8.000000D-01 8.000000D-01 8.000000D-01

***** Current sum of squares = 4.35714D-11 *****

***** Iteration no. 3 no. of function calls 15 *****
PAR(I) = 1.200000D+00 5.521365D-01 4.000000D-01

***** Current sum of squares = 3.81613D-11 *****

***** Iteration no. 4 no. of function calls 23 *****
PAR(I) = 1.217320D+00 4.433951D-01 3.952803D-01

***** Current sum of squares = 2.26939D-11 *****

***** Iteration no. 5 no. of function calls 31 *****
PAR(I) = 1.096057D+00 3.879232D-01 3.975792D-01

***** Current sum of squares = 1.97228D-11 *****

***** Iteration no. 6 no. of function calls 38 *****
PAR(I) = 1.036780D+00 3.897991D-01 3.890874D-01

***** Current sum of squares = 1.56790D-11 *****

***** Iteration no. 7 no. of function calls 47 *****
PAR(I) = 1.042327D+00 3.898445D-01 3.939557D-01

***** Current sum of squares = 1.51969D-11 *****

***** Iteration no. 8 no. of function calls 57 *****
PAR(I) = 1.042382D+00 3.898560D-01 3.940028D-01

***** Current sum of squares = 1.51923D-11 *****

***** Iteration no. 9 no. of function calls 66 *****
PAR(I) = 1.042748D+00 3.899154D-01 3.940475D-01

***** Current sum of squares = 1.51883D-11 *****

***** Iteration no. 10 no. of function calls 74 *****
PAR(I) = 1.050036D+00 3.900659D-01 3.943835D-01

***** Current sum of squares = 1.51692D-11 *****

```

***** Iteration no. 11 no. of function calls 82 *****

PAR(I) = 1.053681D+00 3.901111D-01 3.945515D-01

***** Current sum of squares = 1.51598D-11 *****

***** Iteration no. 12 no. of function calls 90 *****

PAR(I) = 1.055503D+00 3.912530D-01 3.946356D-01

***** Current sum of squares = 1.51482D-11 *****

***** Iteration no. 13 no. of function calls 99 *****

PAR(I) = 1.055682D+00 3.913011D-01 3.946436D-01

***** Current sum of squares = 1.51474D-11 *****

***** Iteration no. 14 no. of function calls 107 *****

PAR(I) = 1.056575D+00 3.914396D-01 3.946841D-01

***** Current sum of squares = 1.51445D-11 *****

***** Iteration no. 15 no. of function calls 116 *****

PAR(I) = 1.056620D+00 3.914438D-01 3.946861D-01

***** Current sum of squares = 1.51443D-11 *****

***** Termination criteria satisfied *****

***** Final value of sum of squares = 1.51434D-11 *****

Standard error of weighted residuals = 1.29715D-06
estimated with 11 residuals and 9 degrees of freedom

***** 2-sigma intervals PAR(I)+-DIF(I) for parameters in basis; *****

**** last value and bounds for any parameters that are not in basis ****

UPR(I) = 1.062886D+00 3.925043D-01 4.000000D+00

PAR(I) = 1.056549D+00 3.915742D-01 3.946861D-01

LWR(I) = 1.050211D+00 3.906441D-01 1.000000D-01

DIF(I) = 6.337450D-03 9.300979D-04 1.000000D+30

Normalized test divisors for final basis selection.

Values near 0.100000(=APIV) or less indicate indeterminate parameters.

1.000000 1.000000 0.000002

The model parameter estimate consists of the particular vector par just given,
plus an arbitrary linear combination of the null-space basis vectors which follow.
Vector I is the derivative of this solution
with respect to parameter I.

Vector 3:
 1.000 0.000 1.000

Normalized covariances of the posterior parameter distribution

```

1.00000
0.00063 1.00000
0.00000 0.00000 0.00000

```

observed values	predicted values	residuals
-1.17000D-06	-1.22261D-06	5.26053D-08
2.82000D-07	1.12614D-07	1.69386D-07
1.77000D-06	-3.14023D-07	2.08402D-06
3.54000D-06	3.39955D-06	1.40449D-07
3.49000D-06	3.85260D-06	-3.62598D-07
-2.34000D-06	-3.23817D-07	-2.01618D-06
-1.34000D-06	-1.16160D-07	-1.22384D-06
3.47000D-07	3.20107D-07	2.68934D-08
1.55500D-06	3.04338D-06	-1.48838D-06
2.28000D-06	3.41940D-06	-1.13940D-06
2.83000D-06	4.07122D-06	-1.24122D-06

MIN = -2.01618D-06 MAX = 2.08402D-06

End of problem no. 1 no. of function calls = 124
 no. of iterations = 15

APPENDIX H

Detailed Program Output

A detailed results showing the concentrations of all species at both the bulk and the interface, along with the model calculated fluxes and enhancement factors are presented. These results are specific to the 25 wt% DEA/ 25 WT% MDEA case at 80°C .

RESULTS FOR POINT NUMBER 1

BULK PHASE

CO2 3.7726855964076528E-02
OH- 1.3368255938615402E-05
HCO3- 1.158295120843441
MDEA 0.8749523959403662
MDEAH+ 1.222847604059634
DEA 0.4765961305752891
DEAH+ 0.9860741701170352
DEACOO- 0.9150296993076756
CO3= 6.7791792884806900E-02

INTERFACE

CO2 1.2136348543500000E-02
OH- 1.5953444166207400E-05
HCO3- 1.167131020497127
MDEA 0.9662212397122565
MDEAH+ 1.131578760287715
DEA 0.5766845730637564
DEAH+ 0.9998105136857071
DEACOO- 0.8012049132504322
CO3= 8.1518693390788986E-02
DIFFFLUX= -5.1195694337889395E-06
CO2(carb.)= 2.2876601171611952E-02
CO2(HCO3)= 3.1854536777320073E-02
CO2(mixt.)= 2.3806963314304835E-02
E_CO2= 2.953312120670808

RESULTS FOR POINT NUMBER 2

BULK PHASE

CO2 3.0240397872609653E-02
OH- 1.5369826560646477E-05
HCO3- 1.069329725789363
MDEA 0.9351197756457297
MDEAH+ 1.162680224354270
DEA 0.5171978080622921
DEAH+ 0.9539328402284612
DEACOO- 0.9065693517092467
CO3= 7.0349308628780418E-02

INTERFACE

CO2 2.0039546481800000E-02
OH- 1.6528110368052738E-05
HCO3- 1.072493578889362
MDEA 0.9729082964608624
MDEAH+ 1.124891703539134
DEA 0.5591149013233093
DEAH+ 0.9589764764309690
DEACOO- 0.8596086222457249
CO3= 7.5874725362323727E-02
DIFFFLUX= -2.1237579824090590E-06
CO2(carb.)= 2.4665424951731714E-02
CO2(HCO3)= 2.8204364871927012E-02

CO2(mixt.)= 2.5044202039552006E-02
E_CO2= 3.054940410849867

RESULTS FOR POINT NUMBER 3

BULK PHASE

CO2 2.8134617191873575E-02
OH- 1.6075417342311903E-05
HCO3- 1.040900519712858
MDEA 0.9554332845558363
MDEAH+ 1.142366715444164
DEA 0.5314290321234264
DEAH+ 0.9433902153047940
DEACOO- 0.9028807525717797
CO3= 7.0979791523488888E-02

INTERFACE

CO2 2.6429820862400000E-02
OH- 1.6269448234253242E-05
HCO3- 1.041426679867455
MDEA 0.9616788183972555
MDEAH+ 1.136121181602745
DEA 0.5383189060698353
DEAH+ 0.9442242634201661
DEACOO- 0.8951568305099986
CO3= 7.1872832598611490E-02
DIFFFLUX= -3.5219057162314509E-07
CO2(carb.)= 2.7208513869413877E-02
CO2(HCO3)= 2.7813133269205027E-02
CO2(mixt.)= 2.7274932601038780E-02
E_CO2= 3.025601392254957

RESULTS FOR POINT NUMBER 4

BULK PHASE

CO2 2.7883502723174532E-02
OH- 1.6164935859915119E-05
HCO3- 1.037391320996866
MDEA 0.9579790419710208
MDEAH+ 1.139820958028979
DEA 0.5332319915363342
DEAH+ 0.9420779759236305
DEACOO- 0.9023900325400353
CO3= 7.1050707739924283E-02

INTERFACE

CO2 3.7664807280000000E-02
OH- 1.5147580509811450E-05
HCO3- 1.034207077895164
MDEA 0.9242509430244079
MDEAH+ 1.173549056975622
DEA 0.4970092599358883
DEAH+ 0.9370566567657213
DEACOO- 0.9436340832988626
CO3= 6.6374702483534333E-02

DIFFFLUX= 1.9169328105604415E-06
 CO2(carb.)= 3.3384055321148031E-02
 CO2(HCO3)= 2.9664903542636491E-02
 CO2(mixt.)= 3.2957025486691033E-02
 E_CO2= 2.869388845163955

RESULTS FOR POINT NUMBER 5

BULK PHASE

CO2 3.7028120356652113E-02
 OH- 1.3528380815188255E-05
 HCO3- 1.150675829614610
 MDEA 0.8799123139278924
 MDEAH+ 1.217887686072108
 DEA 0.4798589160192064
 DEAH+ 0.9833638149843712
 DEACOO- 0.9144772689964223
 CO3= 6.8042437032315769E-02

INTERFACE

CO2 6.8780623337000000E-02
 OH- 1.1456500144805943E-05
 HCO3- 1.138663089395455
 MDEA 0.7963065498980442
 MDEAH+ 1.301493450101956
 DEA 0.3988037778707127
 DEAH+ 0.9650587960826803
 DEACOO- 1.013837426046607
 CO3= 5.7020137121214640E-02
 DIFFFLUX= 4.9857267550008709E-06
 CO2(carb.)= 5.8327750971998251E-02
 CO2(HCO3)= 4.3268094929248093E-02
 CO2(mixt.)= 5.6431401333761209E-02
 E_CO2= 2.073751320289258

RESULTS FOR POINT NUMBER 6

BULK PHASE

CO2 8.9216420578232939E-04
 OH- 1.0674488806422818E-04
 HCO3- 0.1603757442657969
 MDEA 1.917868321616892
 MDEAH+ 0.1799316783831083
 DEA 1.813664786172406
 DEAH+ 0.2913931379961286
 DEACOO- 0.2726420758314658
 CO3= 1.9100125696954968E-02

INTERFACE

CO2 6.6727124999999999E-04
 OH- 1.0760468899509746E-04
 HCO3- 0.1604245623158936
 MDEA 1.919183627596087
 MDEAH+ 0.1786163724039128
 DEA 1.818473135566668

DEAH+ 0.2898311623819447
 DEACOO- 0.2693957020513864
 CO3= 1.9259832864790327E-02
 DIFFFLUX= -1.4175377502366454E-07
 CO2(carb.)= 8.7218497114604640E-04
 CO2(HCO3)= 8.8530488969328682E-04
 CO2(mixt.)= 8.7291006460145732E-04
 E_CO2= 8.398622949376799

RESULTS FOR POINT NUMBER 7
 BULK PHASE

CO2 9.2352129970311924E-04
 OH- 1.0506727627415373E-04
 HCO3- 0.1636216132464926
 MDEA 1.913789753504959
 MDEAH+ 0.1840102464950411
 DEA 1.803232174064666
 DEAH+ 0.2965127667986745
 DEACOO- 0.2779550591366598
 CO3= 1.9420636817144486E-02

INTERFACE

CO2 3.5602567000000001E-03
 OH- 9.6213629731495786E-05
 HCO3- 0.1629178712730762
 MDEA 1.898465958933906
 MDEAH+ 0.1993340410660577
 DEA 1.748761317387180
 DEAH+ 0.3140170017651569
 DEACOO- 0.3149216808477536
 CO3= 1.7707638540338380E-02
 DIFFFLUX= 1.6172519675160512E-06
 CO2(carb.)= 1.1782313232769720E-03
 CO2(HCO3)= 1.0044667748975536E-03
 CO2(mixt.)= 1.1683120683568547E-03
 E_CO2= 8.176961872093249

RESULTS FOR POINT NUMBER 8
 BULK PHASE

CO2 9.9205639743450222E-04
 OH- 1.0167400355012616E-04
 HCO3- 0.1705680594190627
 MDEA 1.905009634950993
 MDEAH+ 0.1927903650490069
 DEA 1.781066403259388
 DEAH+ 0.3073713093845207
 DEACOO- 0.2892622873560908
 CO3= 2.0114826827411961E-02

INTERFACE

CO2 6.2993897400000000E-03
 OH- 8.6295504260605966E-05
 HCO3- 0.1689651969612025

MDEA 1.874313112760738
MDEAH+ 0.2234868872388842
DEA 1.675659385544806
DEAH+ 0.3407145757492227
DEACOO- 0.3613260387059494
CO3= 1.6911965907987245E-02
DIFFFLUX= 3.1580052077182055E-06
CO2(carb.)= 1.5518864033430327E-03
CO2(HCO3)= 1.1578643080711432E-03
CO2(mixt.)= 1.5286804532987517E-03
E_CO2= 7.941101438708550

RESULTS FOR POINT NUMBER 9

BULK PHASE

CO2 1.2440861458754620E-03
OH- 9.1640847865445008E-05
HCO3- 0.1946132196548523
MDEA 1.874122603650756
MDEAH+ 0.2236773963492439
DEA 1.706114519447982
DEAH+ 0.3439059874067464
DEACOO- 0.3276794931452719
CO3= 2.2599515054000290E-02

INTERFACE

CO2 9.7924923000000000E-03
OH- 7.3078019593487241E-05
HCO3- 0.1918635498514576
MDEA 1.824702077842588
MDEAH+ 0.2730979221585222
DEA 1.548984328062269
DEAH+ 0.3915443044566375
DEACOO- 0.4371713674892347
CO3= 1.7767115630058796E-02
DIFFFLUX= 4.8036872124994888E-06
CO2(carb.)= 2.2925371659979941E-03
CO2(HCO3)= 1.5380587360043227E-03
CO2(mixt.)= 2.2454298851449189E-03
E_CO2= 7.529673260889008

RESULTS FOR POINT NUMBER 10

BULK PHASE

CO2 1.6493153148006728E-03
OH- 8.0478450421194353E-05
HCO3- 0.2294488372919073
MDEA 1.828276506679544
MDEAH+ 0.2695234933204561
DEA 1.602761802791543
DEAH+ 0.3938628641608302
DEACOO- 0.3810753330476263
CO3= 2.6390854345665780E-02

INTERFACE

CO2 1.1727283380000000E-02
OH- 6.3992899815393494E-05
HCO3- 0.2263570971149912
MDEA 1.769702559516690
MDEAH+ 0.3280974404885907
DEA 1.432196867519210
DEAH+ 0.4426154665631665
DEACOO- 0.5028876659630761
CO3= 2.0702075546243615E-02
DIFFFLUX= 5.3429524976466280E-06
CO2(carb.)= 3.0632180841877259E-03
CO2(HCO3)= 2.0462550365482069E-03
CO2(mixt.)= 2.9960908598138266E-03
E_CO2= 7.143110774743850

RESULTS FOR POINT NUMBER 11
BULK PHASE

CO2 2.1308809643387277E-03
OH- 7.1448879624502944E-05
HCO3- 0.2663707520955131
MDEA 1.778757711018789
MDEAH+ 0.3190422889812113
DEA 1.500413474125777
DEAH+ 0.4429268627366990
DEACOO- 0.4343596631375237
CO3= 3.0583643802624513E-02

INTERFACE

CO2 1.5144722400000000E-02
OH- 5.5370025143084917E-05
HCO3- 0.2625082010209662
MDEA 1.703523945682250
MDEAH+ 0.3942760543050181
DEA 1.301300977114926
DEAH+ 0.4957006894633137
DEACOO- 0.5806983334398952
CO3= 2.3357419642259597E-02
DIFFFLUX= 6.4274825783174499E-06
CO2(carb.)= 4.2385194813422396E-03
CO2(HCO3)= 2.7097937144915587E-03
CO2(mixt.)= 4.1306180438980671E-03
E_CO2= 6.692356005358959

APPENDIX I

Limitations on Experimental Conditions

$$Ha = \sqrt{\frac{k_2 [\text{amine}] D_{CO_2}}{k_{LCO_2}^o{}^2}} > 1 \quad (I.1)$$

or

$$\sqrt{k_2 [\text{amine}] D_{CO_2}} > k_{LCO_2}^o \quad (I.2)$$

$$k_{Lp} \Delta[CO_2]_T > \sqrt{k_{LCO_2}^o{}^2 + k_2 [\text{am}] D_{CO_2}} \Delta[CO_2] \quad (I.3)$$

$$k_L^o \sqrt{\frac{D_i}{D_{CO_2}}} \Delta[CO_2]_T > \sqrt{k_{LCO_2}^o{}^2 + k_2 [\text{am}] D_{CO_2}} \Delta[CO_2] \quad (I.4)$$

$$k_L^o{}^2 \frac{D_i}{D_{CO_2}} \Delta[CO_2]_T^2 > (k_{LCO_2}^o{}^2 + k_2 [\text{am}] D_{CO_2}) \Delta[CO_2]^2 \quad (I.5)$$

$$k_{LCO_2}^o{}^2 \frac{D_i}{D_{CO_2}} \frac{\Delta[CO_2]_T^2}{\Delta[CO_2]^2} - k_{LCO_2}^o{}^2 > k_2 [\text{am}] D_{CO_2} \quad (I.6)$$

$$k_{LCO_2}^o{}^2 \left\{ \frac{D_i}{D_{CO_2}} \frac{\Delta[CO_2]_T^2}{\Delta[CO_2]^2} - 1 \right\} > k_2 [\text{am}] D_{CO_2} \quad (I.7)$$

$$k_{\text{LCO}_2}^o > \frac{k_2[\text{am}] D_{\text{CO}_2}}{\frac{D_i}{D_{\text{CO}_2}} \frac{\Delta[\text{CO}_2]^2_{\text{T}}}{\Delta[\text{CO}_2]^2} - 1} \quad (\text{I.8})$$

$$k_{\text{LCO}_2}^o > \sqrt{\frac{k_2[\text{am}] D_{\text{CO}_2}}{\left(\frac{D_i}{D_{\text{CO}_2}} \frac{\Delta[\text{CO}_2]^2_{\text{T}}}{\Delta[\text{CO}_2]^2} - 1\right)}} \quad (\text{I.9})$$

or

$$\sqrt{k_2[\text{amine}] D_{\text{CO}_2}} k_{\text{LCO}_2}^o > \sqrt{\frac{k_2[\text{am}] D_{\text{CO}_2}}{\frac{D_i}{D_{\text{CO}_2}} \frac{\Delta[\text{CO}_2]^2_{\text{T}}}{\Delta[\text{CO}_2]^2} - 1}} \quad (\text{I.10})$$

Equations I.2 and I.10 may be combined to end up with Equation I.11:

$$1 > \frac{k_{\text{LCO}_2}^o}{\sqrt{k_2[\text{am}] D_{\text{CO}_2}}} > \frac{1}{\sqrt{\frac{D_p}{D_{\text{CO}_2}} \frac{\Delta[\text{CO}_2]^2_{\text{T}}}{\Delta[\text{CO}_2]^2} - 1}} \quad (\text{I.11})$$

or

$$1 < \frac{\sqrt{k_2[\text{am}] D_{\text{CO}_2}}}{k_{\text{LCO}_2}^o} < \sqrt{\frac{D_i}{D_{\text{CO}_2}} \frac{\Delta[\text{CO}_2]^2_{\text{T}}}{\Delta[\text{CO}_2]^2} - 1} \quad (\text{I.12})$$

The condition specified by Equation I.12 is tested to some of the the conditions used for MDEA at 40°C and 120°C.

I.1 CASE 1

MDEA at 40°C and high loading point:

$$k_2 = 7.96 \text{ m}^3/\text{kmol} \cdot \text{s}$$

$$\text{loading} = 0.403 \text{ mol/mol}; P_{\text{CO}_2} = 4.723 \text{ bar}$$

$$[\text{CO}_2]_{\text{b}} = 3.081 \times 10^{-3} \text{ M}$$

$$[\text{CO}_2]_i = 6.7683 \times 10^{-2} \text{ M}$$

$$[\text{CO}_2]_{\text{T}}^* = L_i \cdot 4.19 = 0.824 \times 4.19 = 3.452 \text{ M}$$

$$[\text{CO}_2]_{\text{T,b}} = L_b \cdot 4.19 = 0.403 \cdot 4.19 = 1.688 \text{ M}$$

$$\frac{\Delta[\text{CO}_2]_{\text{T}}}{\Delta[\text{CO}_2]} = \frac{3.452 - 1.6885}{6.768 \times 10^{-2} - 3.081 \times 10^{-3}} = 27.299$$

$$\sqrt{\frac{D_i}{D_{\text{CO}_2}} \cdot \frac{\Delta[\text{CO}_2]_{\text{T}}^2}{\Delta[\text{CO}_2]^2} - 1} = \sqrt{0.3 \cdot 27.29^2 - 1} = 14.92$$

$$\text{Ha} = \sqrt{\frac{7.96 \times 1.926 \cdot D_{\text{CO}_2}}{3.8 \times 10^{-5}}} = 2.82$$

$$1 < 2.821 < 14.918$$

I.2 CASE 2

For a lower loading at 0.019 mol/mol

$$P_{\text{CO}_2} = 0.293 \text{ bar}$$

$$[\text{CO}_2]_i = 5.922 \times 10^{-3} \text{ M}$$

$$[\text{CO}_2]_{\text{b}} = 1.7303 \times 10^{-5} \text{ M}$$

$$[\text{CO}_2]_{\text{Tb}}^* = 1.6969 \text{ M}$$

$$[\text{CO}_2]_{\text{Tib}} = 0.0796 \text{ M}$$

$$\frac{\Delta[\text{CO}_2]_{\text{T}}^*}{\Delta[\text{CO}_2]^2} = \frac{1.6969 - 0.07961}{5.922 \times 10^{-3} - 1.7303 \times 10^{-5}} = 273.9$$

$$\sqrt{\frac{D_i}{D_{\text{CO}_2}} \cdot \frac{\Delta[\text{CO}_2]_{\text{T}}^2}{\Delta[\text{CO}_2]^2} - 1} = \sqrt{0.3 \cdot (273.9)^2 - 1} = 150.01$$

$$\text{Ha} = \sqrt{\frac{7.96 \cdot 4.04 \cdot 7.5 \times 10^{-10}}{4.21 \times 10^{-5}}} = 3.688$$

$$1 < 3.688 < 150.01$$

Calculations at other conditions are given in Chapter 4

APPENDIX J

Overall Gas Phase Mass Transfer Coefficient

Table J.1 Overall Mass Transfer Coefficient

Solution	T [°C]	loading $\frac{\text{mol CO}_2}{\text{mol amine}}$	P _{CO2} [bar]	P _{CO2} * [bar]	K _G x 10 ⁶ $[\frac{\text{kmol}}{\text{bar m}^2 \text{s}}]$
50 wt% MDEA	40	0.019	0.293	0.001	4.46
		0.033	0.588	0.002	3.16
		0.048	0.973	0.005	3.07
		0.103	1.621	0.018	2.80
		0.147	2.235	0.031	2.57
		0.329	2.781	0.126	1.85
		0.253	0.478	0.074	2.20
		0.262	1.048	0.079	2.15
		0.271	1.899	0.085	2.09
		0.286	2.568	0.094	2.02
		0.395	3.127	0.202	1.63
		0.136	0.415	0.027	2.84
		0.164	0.950	0.036	2.55
		0.184	1.660	0.044	2.44
		0.240	2.329	0.068	2.20
		0.271	2.923	0.084	2.07
		0.403	4.723	0.215	1.57
	80	0.242	1.243	1.747	2.26
		0.243	1.809	1.757	2.25
		0.245	2.291	1.779	2.24
		0.245	2.703	1.779	2.24
		0.309	1.009	2.664	2.02
		0.309	1.502	2.654	2.02
		0.288	2.226	2.328	2.08
		0.295	2.742	2.427	2.06
		0.301	3.190	2.526	2.03
		0.308	2.474	2.151	2.04

Table J.1 Continued

Solution	T [°C]	loading $\frac{\text{mol CO}_2}{\text{mol amine}}$	P _{CO2} [bar]	P _{CO2} * [bar]	K _G x 10 ⁶ $\left[\frac{\text{kmol}}{\text{bar m}^2 \text{s}}\right]$
		0.306	2.864	2.123	2.05
		0.316	3.232	2.263	2.01
		0.445	6.562	5.293	1.56
	120	0.016	0.074	0.179	2.58
		0.026	0.749	0.451	2.45
		0.033	1.234	0.667	2.39
		0.021	0.152	0.210	2.58
		0.021	0.401	0.205	2.57
		0.033	1.215	0.483	2.46
		0.047	1.698	0.887	2.37
		0.021	0.266	0.521	2.39
		0.023	0.496	0.620	2.36
		0.021	0.718	0.518	2.38
		0.041	2.010	1.612	2.17
		0.036	0.527	0.784	2.38
		0.035	0.958	0.760	2.38
		0.064	2.179	2.043	2.19
		0.064	2.592	2.043	2.19
		0.156	5.280	3.435	2.03
		0.100	0.984	1.762	2.25
		0.080	1.466	1.232	2.32
		0.100	2.374	1.776	2.23
25 wt% DEA	40	0.040	0.024	0.0001	16.31
		0.037	0.029	0.0001	16.45
		0.046	0.037	0.0001	15.07
		0.075	0.047	0.0002	15.14
		0.075	0.139	0.0002	14.90
		0.095	0.313	0.0004	13.87

Table J.1 **Continued**

Solution	T [°C]	loading $\frac{\text{mol CO}_2}{\text{mol amine}}$	P _{CO2} [bar]	P _{CO2} * [bar]	K _G × 10 ⁶ $\left[\frac{\text{kmol}}{\text{bar m}^2 \text{s}}\right]$
		0.161	0.583	0.0012	11.53
		0.242	0.954	0.0032	9.02
		0.305	1.516	0.0065	7.15
		0.232	0.003	0.0029	10.75
		0.262	0.194	0.0040	9.67
		0.307	0.403	0.0066	8.32
		0.342	0.750	0.0099	7.17
	80	0.294	0.463	0.457	4.46
		0.297	0.907	0.469	4.35
		0.296	1.484	0.468	4.25
		0.316	2.070	0.566	3.95
		0.340	2.646	0.710	3.62
		0.395	0.601	0.313	3.71
		0.400	1.047	0.331	3.60
		0.426	1.565	0.424	3.30
		0.470	2.203	0.651	2.87
		0.496	2.774	0.844	2.62
	120	0.156	0.734	1.384	4.37
		0.149	1.095	1.257	4.40
		0.149	1.612	1.254	4.32
		0.165	2.022	1.449	4.13
		0.168	2.377	1.584	3.99
		0.226	0.627	0.969	4.59
		0.219	0.972	0.905	4.62
		0.233	1.530	1.037	4.40
		0.292	2.106	1.764	3.74
		0.303	2.489	1.938	3.60
		0.251	0.704	1.269	4.28
		0.215	1.022	0.900	4.64
		0.229	1.527	1.030	4.42
		0.249	1.980	1.249	4.15
		0.291	2.427	1.804	3.70

Table J.1 **Continued**

Solution	T [°C]	loading $\frac{\text{mol CO}_2}{\text{mol amine}}$	PCO ₂ [bar]	PCO ₂ * [bar]	K _G x 10 ⁶ $\left[\frac{\text{kmol}}{\text{bar m}^2 \text{s}}\right]$
5 wt% DEA/45 wt% MDEA	40	0.201	0.011	0.0365	4.19
		0.198	0.117	0.0354	4.13
		0.200	0.347	0.0361	3.91
		0.225	0.659	0.0451	3.46
		0.271	1.132	0.0661	2.89
		0.306	2.026	0.0866	2.45
		0.298	0.029	0.0817	3.16
		0.294	0.173	0.0794	3.12
		0.290	0.330	0.0770	3.07
		0.301	0.882	0.0839	2.77
		0.338	1.665	0.1118	2.35
		0.374	2.339	0.1484	2.06
		0.385	0.058	0.1611	0.55
		0.377	0.207	0.1519	2.47
		0.384	0.391	0.1601	2.38
		0.384	0.850	0.1601	2.26
		0.431	1.491	0.2348	1.91
		0.497	2.095	0.4135	1.57
		0.532	2.606	0.5695	1.40
		0.086	0.319	0.0079	5.53
		0.118	0.688	0.0141	4.59
		0.172	1.479	0.0276	3.50
		0.196	2.149	0.0350	3.08
	80	0.039	0.020	0.047	1.00
		0.038	0.070	0.044	6.32
		0.036	0.126	0.040	6.31
		0.045	0.244	0.061	5.87
		0.062	0.489	0.107	5.24
		0.102	0.925	0.250	4.29
		0.129	1.692	0.374	7.02
		0.178	0.331	0.614	3.67
		0.171	0.408	0.575	0.79
		0.170	0.768	0.572	3.59

Table J.1 **Continued**

Solution	T [°C]	loading $\frac{\text{mol CO}_2}{\text{mol amine}}$	P _{CO2} [bar]	P _{CO2} * [bar]	K _G x 10 ⁶ $\left[\frac{\text{kmol}}{\text{bar m}^2 \text{s}}\right]$
	120	0.176	1.190	0.603	3.41
		0.183	1.660	0.648	3.23
		0.199	2.190	0.742	3.02
		0.018	0.183	0.223	0.92
		0.027	0.454	0.480	0.81
		0.019	0.882	0.250	2.77
		0.028	1.500	0.497	2.47
		0.010	0.127	0.080	1.02
		0.011	0.366	0.097	3.30
		0.010	0.818	0.074	3.16
		0.018	1.504	0.393	2.33
		0.032	2.082	1.079	2.09
		0.009	0.270	0.112	0.94
		0.012	0.893	0.170	2.65
		0.023	1.575	0.559	2.27
		0.028	2.103	0.812	2.16
		0.035	2.531	1.170	2.07
25 wt% DEA/ 25 wt% MDEA	40	0.080	0.193	0.0010	12.21
		0.040	0.491	0.0003	11.97
		0.083	0.811	0.0011	10.58
		0.136	1.111	0.0028	8.84
		0.190	1.374	0.0057	7.39
		0.345	1.610	0.0371	4.66
		0.389	1.530	0.0618	4.13
		0.415	1.230	0.0840	4.00
		0.423	0.976	0.0874	4.26
		0.378	0.387	0.0545	5.30
	80	0.487	1.042	3.239	2.33
		0.464	1.608	2.427	2.59
		0.456	2.253	2.398	2.42
		0.456	3.210	2.377	2.30
		0.485	5.902	3.178	1.83
		0.101	0.052	0.070	8.04

Table J.1 **Continued**

Solution	— [°C]	loading $\frac{\text{mol CO}_2}{\text{mol amine}}$	P _{CO2} [bar]	P _{CO2} * [bar]	K _G x 10 ⁶ $[\frac{\text{kmol}}{\text{bar m}^2 \text{s}}]$
		0.103	0.279	0.072	7.81
		0.107	0.506	0.080	7.41
		0.122	0.772	0.098	7.13
		0.143	0.929	0.131	6.70
		0.164	1.206	0.170	6.20
	120	0.068	0.181	0.371	6.42
		0.053	0.363	0.246	0.97
		0.071	0.668	0.994	0.96
		0.086	1.184	0.554	5.39
		0.106	1.578	0.791	4.90
		0.096	0.342	0.675	0.97
		0.097	0.565	0.685	0.97
		0.085	0.875	0.548	0.98
		0.087	1.169	0.587	5.24
		0.096	1.349	0.681	5.12
		0.106	1.648	0.807	4.84

APPENDIX K

SRP Annual Report

Carbon dioxide Desorption/ Absorption with Aqueous Mixtures of Methyldiethanolamine and Diethanolamine at 40 to 120°C

K.1 INTRODUCTION

There were three main objectives of this work. The first was to design and construct a mass transfer apparatus for measurements of carbon dioxide absorption and desorption with alkanolamine solutions. The second, to perform the experiments with concentrated solutions at higher temperatures typical of the stripper. The third, to model the absorption/ desorption process and use the model in estimation of kinetic parameters.

A laboratory wetted wall column was used as a mass transfer apparatus to collect high temperature data on CO₂ absorption/ desorption into concentrated MDEA, DEA and mixtures of MDEA and DEA solutions. These data can be used as is for industrial calculations because the mass transfer characteristics of the laboratory wetted wall column falls in the range of the industrial equipment. Thus, this work reports the overall mass transfer coefficients under widely varying conditions.

The rate expression used to describe the reactions of MDEA and CO₂ is given in Equation K.1

$$\text{Rate} = ([\text{CO}_2] - [\text{CO}_2]_e)[\text{MDEA}]_i k_{\text{MDEA}} \quad (\text{K.1})$$

The variable $[\text{CO}_2]_e$ refers to the CO_2 concentration that would be in chemical equilibrium with HCO_3^- and other species in solution. The effective second order rate constant k_{MDEA} was regressed from the absorption and desorption data for 50 wt% MDEA. In analyzing the pure DEA data the following rate expression was used. An effective rate constant, k_{DEA} , was regressed from the 25 wt% DEA data.

$$\text{rate} = ([\text{CO}_2] - [\text{CO}_2]_e) [\text{DEA}] k_{\text{DEA}} \quad (\text{K.2})$$

where $[\text{CO}_2]_e$ is the concentration of CO_2 that would be in chemical equilibrium with carbamate, protonated amine and free amine.

CO_2 reactions with mixed amines involves all the above reactions specific to MDEA and DEA systems. The rate expression used for mixed amines was:

$$\begin{aligned} \text{rate} = & ([\text{CO}_2] - [\text{CO}_2]_e) [\text{MDEA}]_i k_{\text{MDEA}} + \\ & ([\text{CO}_2] - [\text{CO}_2]_e) [\text{DEA}]_i \{k_{\text{DEA}} + k_{\text{DEA MDEA}} [\text{MDEA}]_i\} \end{aligned} \quad (\text{K.3})$$

The cross apparent rate constant $k_{\text{MDEA DEA}}$ was regressed from the mixed amine data. Table K.1 presents the apparent rate constants regressed for the four solutions, while the equilibrium CO_2 partial pressure results are entered in Table K.2.

K.2 OVERALL GAS PHASE MASS TRANSFER COEFFICIENT

The two film theory of gas/ liquid mass transfer coefficient usually represents flux by using mass transfer coefficients and driving forces defined in one of several ways. The overall gas film mass transfer coefficient, K_G , uses the

bulk gas partial pressure, P_{CO_2} , and the equilibrium partial pressure over the bulk solution, $P^*_{CO_2}$:

$$K_G = \frac{\text{Flux}}{P_{CO_2} - P^*_{CO_2}} \quad (K.4)$$

Equation K.4 was used to calculate overall gas phase mass transfer coefficient from model calculated flux for each data point. The data points included are those with absolute flux greater than $0.45 \times 10^{-6} \text{ kmol/m}^2\text{s}$. This minimizes the uncertainties in the accuracy of the measured fluxes which the model matches in estimating parameters, and thus gives good values of overall mass transfer coefficients. The curves included in the plots are for the purposes of making the reading easier only. The overall gas phase mass transfer coefficient is found to be directly affected by temperature, solution type, and CO_2 loading.

K.2.1 Temperature Effect

On Figure K.1, K_G values for 50 wt% MDEA solution are plotted as a function of CO_2 loading. The general trend is for the K_G to decrease with an increase in CO_2 loading. The values at 40°C varied from $4.46 \text{ kmol}/(\text{m}^2 \text{ s bar})$ at a CO_2 loading of $0.019 \text{ mol/mol MDEA}$ to a lowest value of about $1.6 \text{ kmol}/(\text{m}^2\text{s bar})$ at a loading of $0.4 \text{ mol } CO_2/\text{mol MDEA}$. The values of K_G at 80°C ranged from 2.3 to $1.6 \text{ kmol}/(\text{m}^2\text{s bar})$ for the respective CO_2 loading range of 0.24 to $0.45 \text{ mol } CO_2/\text{mol MDEA}$. In the range of CO_2 loading covered by 80°C data, the K_G values at 40°C are indistinguishable from those at 80°C . Data at 120°C covers a range of CO_2 loading from 0.016 to 0.156 mol for which the range of K_G values was 2.6 to 2.0 . In this range K_G at 120°C are significantly lower than those at 40°C .

The K_G results for 25 wt% DEA solution are presented in Figure K.2. At 40°C the K_G decreased from 16.5 to 7.1 kmol/(m²s bar) for corresponding CO₂ loading increase from 0.04 to 0.34 mol/ mol DEA. While, at 80°C the range of K_G was from 4.5 to 2.6 kmol/(m²s bars) for an increase in CO₂ loading from 0.39 to 0.5 mol/ mol DEA. There was only a slight decrease of K_G value at 120°C. Its value decreased from 4.4 to 3.7 kmol/(m²s bar) for a CO₂ loading increase from 0.15 to 0.29 mol/ mol DEA. Generally the K_G value at high temperatures 80 and 120°C were significantly lower than at 40°C for the same loading conditions.

For 5 wt% DEA/45 wt% MDEA the 40°C data with a CO₂ loading range from 0.09 to 0.53 mol/ mol amine, had the K_G value spanning from 5.5 down to 1.4 kmol/ (m²s bar). The range of loading for 80°C is small but goes to lower end than data at 40°C. It ranged from 0.04 to 0.2 mol/ mol amine, while the K_G values ranged from 6.3 down to 3.0 kmol/ (m²s bar). In the range of data where CO₂ loading overlap for 40°C and 80°C, the K_G for 40°C is just slightly higher than at 80°C. The K_G values at 120°C were the lowest and they fell from about 3.2 kmol/ (m²s bar) at a CO₂ loading of 0.01 mol/ mol amine down to 2.0 kmol/ (m²s bar) at a loading of 0.03 mol/ mol amine. These results are presented on Figure K.3.

The results for K_G for 25 wt% DEA/ 25 wt% MDEA are plotted in Figure K.4. For this system at all loading levels the K_G values decrease with temperature increase. The values at 40°C decreased from 12.2 kmol/ (m²s bar) at a CO₂ loading of 0.08 mol/ mol CO₂ down to 4.0 kmol/ (m²s bar) at a CO₂ loading of 0.42 mol/ mol amine. The range at 80°C was from 8.0 to 1.8 kmol/

($\text{m}^2\text{s bar}$) corresponding to CO_2 loading of 0.10 to 0.49 mol/ mol amine. The K_G values at 120°C ranged from 6.4 to 4.8 $\text{kmol/ (m}^2\text{s bar)}$ for a CO_2 loading range of 0.07 to 0.11 mol/ mol CO_2 .

K.2.2 Solution Type Effect

The effect of adding DEA to a solution of MDEA is to increase the overall gas phase mass transfer coefficient at all levels of CO_2 loading and at all three temperatures. The effect of addition of DEA is remarkable at 40°C and decreases with increase in temperature.

K.2.2.1 *Solution Type Effect at 40°C*

Figure K.5 shows the results at 40°C for all four solution types. For all solutions K_G value decreased with increasing loading. 25 wt% DEA had the highest K_G followed by 25 wt% DEA/ 25 wt% MDEA, and then 5 wt% MDEA/45 wt% DEA, with MDEA having the lowest value. At CO_2 loadings higher than 0.3 mol/mol amine 50 wt% MDEA and 5 wt% DEA/45 wt% DEA have almost the same values of K_G . This may be because all the DEA has been depleted by the reaction and only MDEA remains in the mixture.

Overall mass transfer coefficient, K_G , values for all four solution types at 80°C are plotted on Figure K.6. Same trends as those described in the previous section for 40°C are observed. 25 wt% DEA providing the highest value and 50 wt% MDEA giving the lowest.

Figure K.7 presents results for all four solutions at 120°C for the range of CO_2 loading where data overlap for 50 wt% MDEA and 5 wt% DEA/45 wt%

MDEA the value of K_G are the same. 25 wt% DEA/25 wt% MDEA and 25 wt% DEA seem to have the same values, although data available here do not overlap.

K.3 CONCLUSIONS

A wetted wall column as a laboratory mass transfer device was designed and fabricated. It was then used in measurement of both absorption into and desorption of CO_2 from mixtures of methyldiethanolamine and diethanolamine. A wide range of conditions in terms of CO_2 partial pressure, CO_2 loading and temperature were studied. The data are made available in the form of overall mass transfer coefficients which may be used in equipment design. These coefficients are given as a function of solution type, CO_2 loading, and temperature.

Overall mass transfer coefficient, K_G , decreased with the increase in temperature. This effect was more significant for the change in temperature from 40° to 80°C than between 80°C and 120°C. At a constant temperature and for a specific amine solution, K_G decreased with increase in CO_2 loading. Addition of DEA in a basic solution of MDEA increased the K_G values at all conditions. Thus K_G values decreased in the following order at all conditions: 25 wt% DEA, 25 wt% DEA/ 25 wt% MDEA, 5 wt% DEA/ 45 wt% MDEA, and 50 wt% MDEA.

A mass transfer model based on the film theory that coupled the chemical reaction and equilibrium has been developed. The model was used with a parameter estimation package (GREG). Apparent reaction rate constants and equilibrium correction factors were estimated. CO_2 equilibrium correction factor α was evaluated simultaneously with the apparent rate constants. This parameter

allowed for extraction of equilibrium CO₂ partial pressure from the rate measurement data.

Equilibrium data were determined on average within a confidence interval of 16%. CO₂ flux predictions were good. At 80°C and to a larger extent at 120°C the statistical determination of the apparent rate constants were not good.

Table K.1 Apparent Rate Constants

	40°C	80°C	120°C
kMDEA [m ³ /kmol-s]	8.0 ± 1.4	6 ± 6	2.4 ± •
kDEA [m ³ /kmol-s]	186 ± 30	66 ± 68	68 ± 33
kDEAMDEA (5/45) [m ⁶ /kmol ² -s]	60.0 ± 0.1	49 ± 5	14.5 ± 0.6
kDEAMDEA (25/25) [m ⁶ /kmol ² -s]	43 ± 160	22.4 ± 0.6	21.1 ± 0.1

Table K.2 Equilibrium Pressure Over Amine Solutions

Solution	Temperature °C	loading	PCO ₂ [*] , bar
50 wt% MDEA	80	0.243	1.78
		0.288	2.36
		0.308	2.17
	120	0.016	0.18
		0.021	0.204
		0.023	0.67
		0.035	0.77
25 wt% DEA	80	0.08	1.14
		0.294	0.47
	80	0.395	0.32
	120	0.149	1.27
	120	0.219	0.87
	120	0.215	0.87
5 wt% DEA/ 45 wt% MDEA	80	0.038	0.044
	80	0.171	0.57
	120	0.027	0.64
	120	0.010	0.11
	120	0.010	0.11
25 wt% DEA/ 25 wt% MDEA	40	0.378	0.054
	80	0.456	2.88
	80	0.101	0.057
	120	0.053	0.24

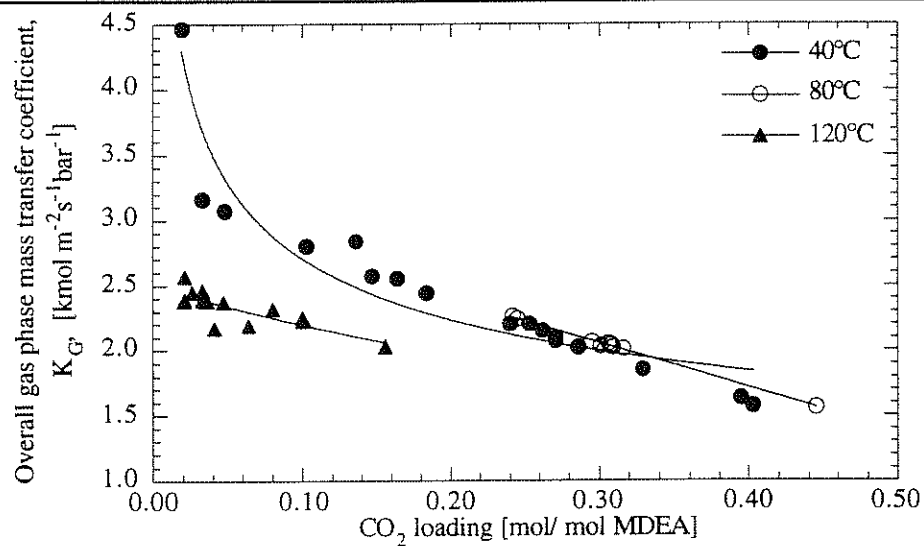


Figure K.1 K_G for 50 wt% MDEA at Different Temperatures

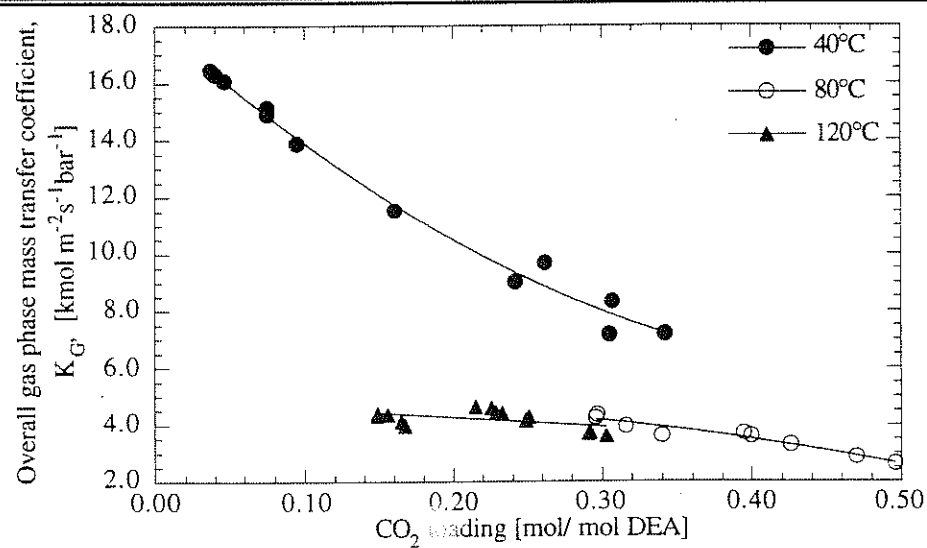


Figure K.2 K_G for 25 wt% DEA at Different Temperatures

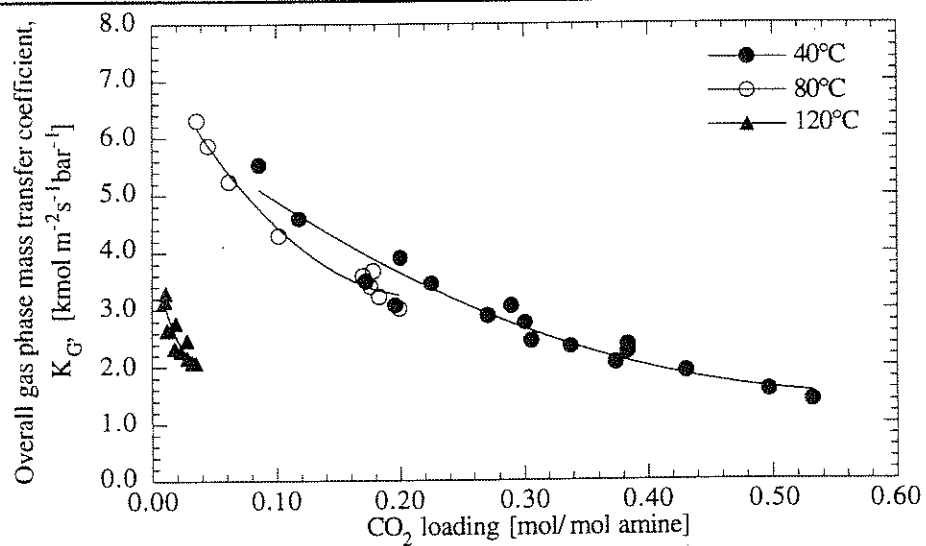


Figure K.3 K_G for 5 wt% DEA/ 45 wt% MDEA at Different Temperatures

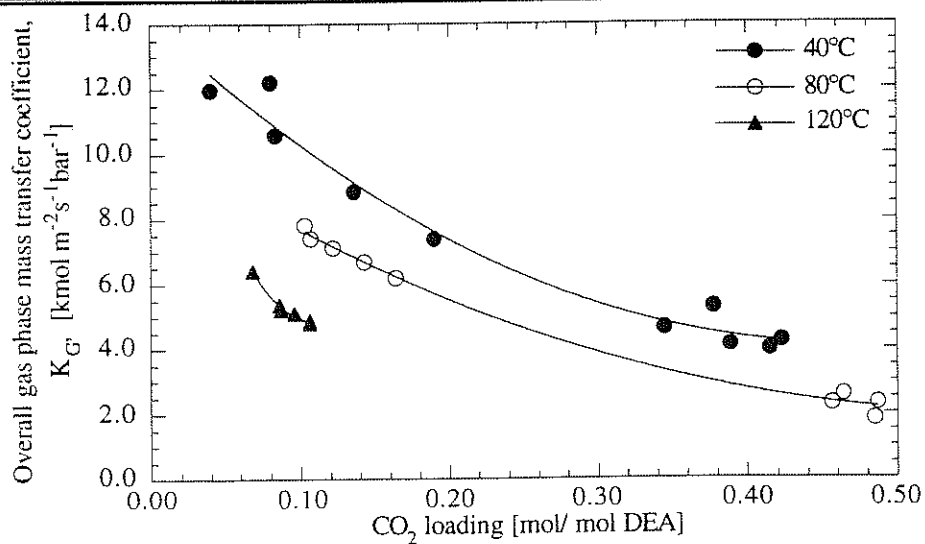


Figure K.4 K_G for 25 wt% DEA/ 25 wt% MDEA at Different Temperatures

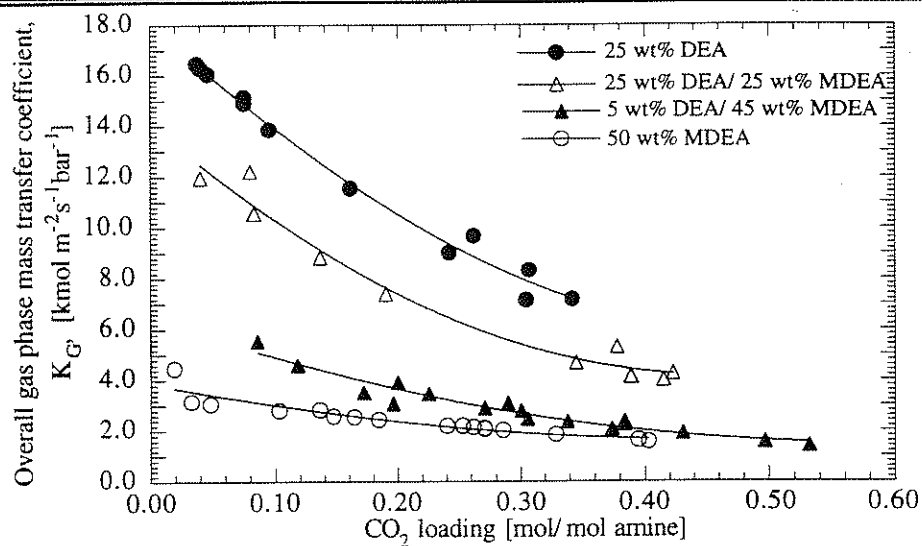


Figure K.5 K_G at 40°C for the Four Solutions

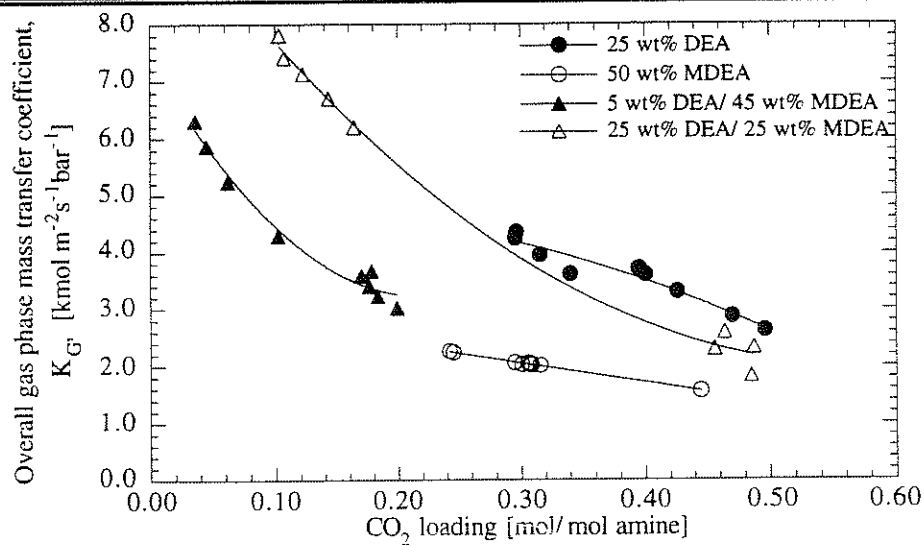


Figure K.6 K_G at 80°C for the Four Solutions

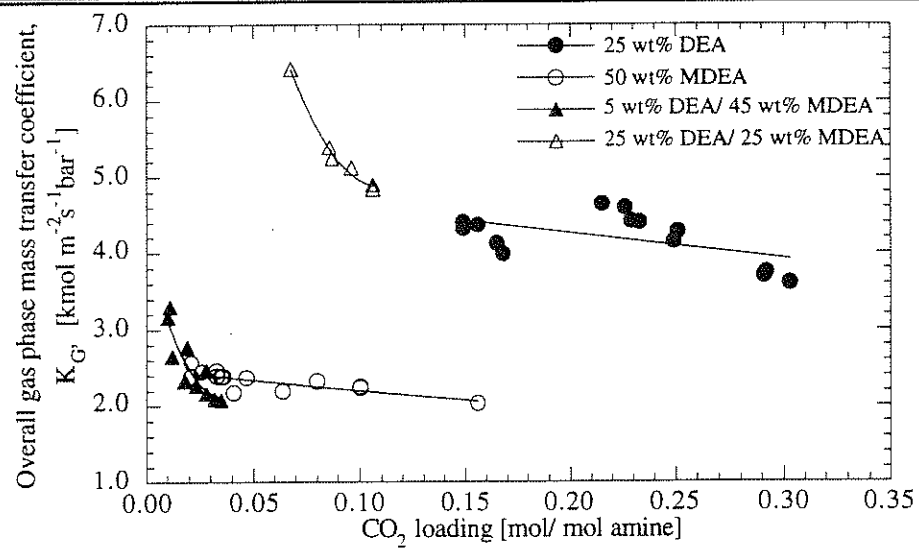


Figure K.7 K_G at 120°C for the Four Solutions

NOTATION

a	interfacial area, m^2/m^3
a_i	coefficient in equilibrium expressions on table 3.1
$[\text{Amine}]_T$	total initial amine concentration, kmol/m^3
b_i	basic species in amine solution
C	concentration, kmol/m^3
CO_2^*	Carbon dioxide concentration that would be in equilibrium with the local concentrations of carbamate, protonated DEA and other species in solution.
CO_2^*	Carbon dioxide concentration that would be in equilibrium with the local concentrations of bicarbonate, protonated MDEA and other species in solution.
ΔC_i	difference between interfacial and bulk concentrations of species i
C_i	interfacial concentration
C_{gin}	concentration of CO_2 in inlet gas stream
C_{gout}	concentration of CO_2 in outlet gas stream
D	diffusion coefficient, m^2/s
D_i	diffusion coefficient for all other species i , where i is not CO_2
E_a	activation energy, kcal/gmol
E_{actual}	enhancement factor, ratio of absorption rate with and without reaction calculated from actual experimental data
E_{CO_2}	enhancement factor, ratio of absorption rate with and without reaction
E_i	enhancement factor, calculated using interfacial concentrations

E_{ins}	instantaneous enhancement factor
EG	ethylene glycol
G	gas flow rate, m^3/s
g	gravitational acceleration, m/s^2
Ga	Galileo number, $Ga = \frac{gl^3}{\nu^2}$
H_{CO_2}	Henry's constant, $m^3bar/kmol$ for CO_2
k	rate constant
k_{bi}	Second order forward rate constant in equation (2.6) $m^3/kmol-s$
k_{-bi}	Second order reverse rate constant in equation (2.6) $m^3/kmol-s$
KCARB	equilibrium constant of reaction (3.8)
KCO ₂	equilibrium constant of reaction (3.4)
KDEA	equilibrium constant of reaction (3.7)
k_{DEA}	apparent second order rate constant, $m^3/kmol-s$
K_G	overall gas phase mass transfer coefficient, $kmol/m^2/bar/s$
k_G	gas film mass transfer coefficient, $kmol/m^2/bar/s$
KHCO ₃	equilibrium constant of reaction (3.5)
K_i	equilibrium constant
k_L^0	physical mass transfer coefficient, m/s
KMDEA	equilibrium constant of reaction (3.6)
k_{MDEA}	apparent second order rate constant, $m^3/kmol-s$
k_1	pseudo first order rate constant, $1/s$

k_{-1}	reverse rate constant in equation (2.5)
k_2	second order rate constant, $\text{m}^3/\text{kmol}\cdot\text{s}$
$k_{T\text{ref}}$	apparent second order rate constant at reference temperature, $\text{m}^3/\text{kmol}\cdot\text{s}$
L_{CO_2}	carbon dioxide loading, $\text{gmol CO}_2/\text{gmol amine}$
l	length of wetted wall column, m
m_{CO_2}	solubility parameter of CO_2 in unloaded amine solution, $\text{kmol}/\text{m}^3\text{ bar}$
M	molarity
N	flux, $\text{kmols}/\text{m}^2\text{s}$
N_A	Flux of A, $\text{kmols}/\text{m}^2\text{s}$
P	pressure, bar
P^*	equilibrium pressure, bar
$P^*_{\text{CO}_2i}$	CO_2 equilibrium pressure at interface, bar
$P^*_{\text{CO}_2b}$	CO_2 equilibrium pressure at bulk phase, bar
q	volumetric flow rate per unit perimeter, m^2/s
R	mass transfer rate
r	net production rate of species, kmol/s
Γ_{MDEA}	relative factor for effect of loading on viscosity for 50 wt% MDEA defined by Equation B.6
Re	Reynolds number, $\frac{4q}{v}$
Sc	Schmidt number, $\frac{v}{D_{\text{CO}_2}}$

Sh	Sherwood number, $\frac{k_{LCO_2}^o l}{D_{CO_2}}$
Soln	solution
t	time
T	temperature, K
T _i	inlet temperature
T _o	outlet temperature
T _{ref}	reference temperature
U	velocity,
V _L	volume of solution
w _{am}	weight fraction of amine in solution
w _{MDEA}	weight fraction of MDEA in solution
w _{DEA}	weight fraction of DEA in solution
Z	film thickness

Greek Letters

α	correction factor to K _{CO2}
δ	film thickness, m
Φ	dimensionless driving force defined by Equation A.17
γ	coefficient in equation 4.10
Γ	mass flow rate per unit width, kg/m/s
μ	absolute viscosity, cP

ν kinematic viscosity, m^2/s

ρ density, kg/m^3

Subscripts

am amine

b bulk phase

calc calculated

e equilibrium

i interface, inlet, chemical species

ins instantaneous

max maximum

meas measured

o outlet

Superscripts

® registration mark

TM trade mark

BIBLIOGRAPHY

- Al-Ghawas, H. A., Ruiz-Ibanez, G. and Sandall, O.C., 1989 Absorption of carbonyl sulfide in aqueous methyldiethanolamine, *Chem. Engng. Sci.*, **44**(3), 631.
- Alvarez-Fuster, C., Midoux, N., Laurent, A., and Charpentier, J. C., 1980, Chemical Kinetics of the Reaction of Carbon Dioxide with Amines in Pseudo m-nth Order Conditions in Aqueous and Organic Solutions, *Chem. Engng. Sci.*, **35**, 1717.
- Astarita, G., Savage, D. W. and, Bisio A., 1983, *Gas Treating with Chemical Solvents*, John Wiley and Sons, New York .
- Astarita, G., 1967, *Mass Transfer with Chemical Reaction*, Elsevier Publishing Company, New York.
- Austgen, D. M., 1989, *A Model of Vapor-Liquid Equilibria for Acid Gas-Alkanolamine-Water Systems*, Ph.D. dissertation, The University of Texas at Austin.
- Barth, D., Tondre, C., Lappai, G., and Delpuech, J.-J., 1981, Kinetic Study of Carbon dioxide Reaction with Tertiary Amines in Aqueous Solution. *J. Phys. Chem.* **85**, 3660-3667.
- Barth, D., Tondre, C. and Delpuech, J.-J., 1983, Stopped-Flow Determination of Carbon dioxide - Diethanolamine Reaction Mechanism: Kinetics of Carbamate Formation. *Int. J. Chem. Kinetics* **15**, 1147-1160.
- Barth, D., Tondre, C. and Delpuech, J.-J., 1984, Kinetics and mechanisms of the reactions of carbon dioxide with alkanolamines: a discussion concerning the cases of MDEA and DEA. *Chem Engng. Sci.* **39**, 1753-1757.
- Barth, D., C. Tondre, and Delpuech, J.-J., 1986, Stopped-Flow Investigations of the Reaction Kinetics of Carbon Dioxide with Some Primary and Secondary Alkanolamines in Aqueous Solutions, *Int. J. Chem. Kinetics*, **18**, 445.
- Bird, B. R., Stewart, W. E., and Lightfoot, E. N., 1960, *Transport Phenomena*, John Wiley and Sons, New York.
- Blanc, C. and Demarais, G., 1984, The Reaction rate of CO₂ with Diethanolamine, *Int. Chem. Engng.* **24**, 43-51.

- Blauwhoff, P. M. M. , Versteeg, G. F. and Van Swaaij, W.P.M., 1984, A study on the Reaction Between CO₂ and Alkanolamines in Aqueous Solutions, *Chem. Engng. Sci.* **39**, 207-225.
- Blauwhoff, P. M. M., and Van Swaaij W.P.M., 1985, Simultaneous Mass Transfer of H₂S and CO₂ with Complex Chemical Reactions in an Aqueous Diisopropanolamine Solution, *Chem. Engng. Process*, **19**, 67.
- Box G. E. P. and Draper N. R., 1965, Bayesian Estimation of Common Parameters from Several Responses, *Biometrika*, **52**, 355.
- Box G. E. P. and Draper N. R., 1972, Estimation and Design Criteria for Multi-response Non -Linear Models with Non-homogeneous Variance, *Applied Statistics*, **21**, 13-24.
- Campbell, S. W., and Weiland, R. H., 1989, Modeling CO₂ removal by amine blends, Presented at the AIChE Spring National Meeting, Houston, TX.
- Caplow, M., 1968, Kinetics of Carbamate Formation and Breakdown. *J. Am. Chem. Soc.* **90**, 6795-6803.
- Caracotsios, M., *Model Parametric Sensitivity Analysis and Nonlinear Parameter Estimation. Theory and Applications*, Ph.D. Dissertation, The University of Wisconsin, Madison, 1986.
- Chakravarti, S., 1992, *Absorption of Carbon dioxide in Aqueous Blends of Diethanolamine and Methyldiethanolamine*, M.S. Thesis, The University of Texas at Austin.
- Coldrey, P. W and Harris, I. J., 1976, Kinetics of the Liquid Phase Reaction Between Carbon Dioxide and Diethanolamine, *Canadian Journal of Chemical Engineering*, **54**, 566.
- Cordi, E. M. and Bullin, J. A., 1992, Kinetics of Carbon dioxide and Methyldiethanolamine with Phosphoric Acid, *AIChE J.*, **38**(3), 455.
- Critchfield, J. E., 1988, *CO₂ Absorption/ Desorption in Methyldiethanolamine Solutions Promoted with Monoethanolamine and Diethanolamine: Mass Transfer and Reaction Kinetics*, Ph.D.. dissertation, The University of Texas at Austin .
- Critchfield, J. E. and Rochelle, G. T., 1987, CO₂ Absorption into Aqueous MDEA and MDEA/ MEA Solutions. Paper 43e, AIChE National Meeting, Houston TX.

- Danckwerts, P. V., 1951, Absorption by Simultaneous Diffusion and Chemical Reaction into Particles of Various Shapes and into Falling Drops, *Trans. Faraday Soc.*, **47**, 1014.
- Danckwerts, P. V., 1970, *Gas-Liquid Reactions*, McGraw-Hill, New York.
- Danckwerts, P. V., 1979, The Reaction of CO₂ with Ethanolamines, *Chem. Engng. Sci.* **34**, 443-446.
- Donaldson, T. L. and Nguyen, Y.N., 1980, Carbon dioxide reaction kinetics and transport in aqueous amine membranes. *Ind. Engng. Chem. Fundam.* **19**, 260-266.
- Duda, J. L., and Vrentas, J. S., 1968, Laminar liquid jet diffusion studies, *AIChE J.*, **14** (2), 286.
- Garbow, B. S., Hillstrom, K. E., and More, J. J., June 1983, Argonne National Laboratory, MINPACK Project.
- Glasscock, D. A., 1990, *Modeling and Experimental Study of Carbon dioxide Absorption into Aqueous Alkanolamines*, Ph.D. Dissertation, The University of Texas at Austin, Austin, TX.
- Glasscock, D. A., Critchfield, J. E. and Rochelle, G. T., 1991, CO₂ Absorption/Desorption in mixtures of Methyldiethanolamine of Diethanolamine, *Chem. Engng. Sci.*, **46**(11), 2829.
- Haimour, N., Bidarian, A. and Sandall, O.C., 1987, Kinetics of the Reaction Between Carbon dioxide and Methyldiethanolamine, *Chem. Engng. Sci.*, **42**(6), 1393.
- Haimour, N., and Sandall, O. C., 1984, Absorption of Carbon Dioxide into Aqueous Methyldiethanolamine, *Chem. Engng. Sci.*, **39**(12), 1791.
- Hayduk, W., and Malik, V. K., 1971, Density, Viscosity, and Carbon Dioxide Solubility and Diffusivity in Aqueous Ethylene Glycol Solutions, *J. Chem. Engng. Data*, **16**(2), 143.
- Higbie, R., 1935, The Rate of Absorption of a Pure Gas into a Still Liquid During Short Periods of Exposure, *Trans. Am. Inst. Chem. Engng.*, **31**, 365.
- Hikita, H., Asai, S., Ishikawa, H. and Honda, M., 1977, The Kinetics of Reactions of Carbon dioxide with Monoethanolamine, Diethanolamine and Triethanolamine by a Rapid Mixing Method. *Chem. Engng. J.* **13**, 7-12.

- Jensen, A., Jensen, M. B., and Faurholt, C., 1954, Studies on Carbamates X. The Carbamates of Di-n-Propylamine and Di-iso-Propylamine, *Acta Chemica Scandinavica*, **8**, 1129.
- Johnson, S. L., and Morrison, D. L. 1972, Kinetics and Mechanism of Decarboxylation of N-Arylcarbamates. Evidence for Kinetically Important Zwitterionic Carbamic Acid Species of Short Lifetime, *J. Am. Chem. Soc.*, **94**(4), 1323.
- Joosten, G. E., and Danckwerts, P. V., 1972, Solubility and diffusivity of nitrous oxide in equimolar potassium carbonate-potassium bicarbonate solutions at 25°C and 1 atm. *J. Chem. Engng. Data*, **17** (4), 452.
- Jorgensen, E., 1956, Reactions Between Carbon dioxide and Amino alcohols III: Diethanolamine. *Acta Chemica Scandinavica* **10**, 747-755.
- Jorgensen, E., and C. Faurholt, 1954, Reactions Between Carbon Dioxide and Amino Alcohols II. Triethanolamine, *Acta Chemica Scandinavica*, **8**, 1141.
- Jou, F. Y., Mather, A. E. and Otto, F. D., 1982, Solubility of H₂S and CO₂ in aqueous methyldiethanolamine solutions, *Ind. Engng. Chem. Process Des. Dev.*, **21**, 539.
- Katti, S. S., and Wolcott, R.A., 1987, Fundamental aspects of gas treating with formulated amine mixtures, Presented at AIChE National Meeting, Minneapolis, MN.
- Kohl, A. L., and Riesenfeld, F. C., 1985, *Gas Purification*, 4th ed., Gulf Publishing Co., Houston.
- Laddha, S.S., and Danckwerts, P. V., 1981, Reaction of CO₂ with ethanolamines: Kinetics from Gas Absorption, *Chem. Engng. Sci.*, **36**, 479.
- Laddha, S.S., and P. V. Danckwerts, 1982, The Absorption of CO₂ by Amine-Potash Solutions, *Chem. Engng. Sci.*, **37**(5), 665.
- Leder, F., 1971, The Absorption of CO₂ into Chemically Reactive Solutions at High Temperatures, *Chem. Engng. Sci.*, **26**, 1381.
- Licht, S. E., and Weiland, R. H., 1989, Density and physical solubility of CO₂ in partially loaded solutions of MEA, DEA and MDEA, Presented at AIChE 1989 Spring National Meeting, Paper No. 57f, Houston, TX.
- Littel, R. J., Versteeg, G. F., Van Swaaij, W.P.M., 1992, Kinetics of CO₂ with Primary and Secondary Amine in Aqueous Solutions—I. Zwitterion

- Deprotonation Kinetics for DEA and DIPA in Aqueous Blends of Alkanolamines, *Chem. Engng. Sci.*, **47**, 2027.
- Littel, R. J., Van Swaaij, W.P.M., and Versteeg, G.F., 1990, Kinetics of Carbon dioxide with Tertiary Amines in Aqueous Solution, *AIChE J.*, **36**(11), 1633.
- Nunge, R. J. and Gill, W. N., 1963, Gas-Liquid Kinetics: The Absorption of Carbon dioxide in Diethanolamine. *AIChEJ.* **9**, 469-474.
- Polasek, J.C., Donnelly, S. T., and Bullin, J. A., 1990, The use of MDEA and mixtures of amines for bulk CO₂ removal, Presented at the AIChE National Spring Meeting, Orlando, FL.
- Rangwala, H.A., Tomcej, R.A., Xu, S., Mather, A. E. and Otto, F. D., 1989, Absorption of carbon dioxide in amine solutions, Paper 56b, AIChE Spring National Meeting, Houston, TX.
- Rangwala, H.A., Morrell, B. R., Mather, A. E. and Otto, F. D., 1992, Absorption of carbon dioxide in Aqueous Tertiary amine /MEA Solutions, *Canadian Journal of Chemical Engineering* **70**, 482.
- Sada, E., H. Kumazawa, and M. A. Butt, 1976, Gas Absorption with Consecutive Chemical Reaction: Absorption of Carbon Dioxide into Aqueous Amine Solutions, *Can. J. Chem. Engng.*, **54**, 421.
- Sada, E., Kumazawa, H. and Butt, M. A., 1978, Solubility and diffusivity of gases in aqueous solutions of amines, *J. Chem. Engng. Data*, **23**, 161-163.
- Sandall, O.C., Rinker, E. B., and Ashour S., 1993, Acid Gas Treating by Aqueous Alkanolamines, Annual Report to The Gas Research Institute.
- Sandall, O.C., Rinker, E. B., and Ashour S., 1994, Acid Gas Treating by Aqueous Alkanolamines, Annual Report to The Gas Research Institute.
- Sartori, G., and Savage, D. W., 1983, Sterically Hindered Amines for CO₂ Removal from Gases, *Ind. Engng. Chem. Fundam.*, **22**, 239.
- Savage, D. W., and Kim, C. J., 1985, Chemical Kinetics of Carbon dioxide Reactions with Diethanolamine and Diisopropanolamine in Aqueous Solutions, *AIChEJ.* **31**, 296-301.
- Seader, J. D, 1989, The Rate-based Approach for Modeling Staged Separations, *Chem. Engng. Prog.*, **85**(10), 41.
- Sherwood, T. K., Pigford, R. L., and Wilke, C. R., 1975, *Mass Transfer*, McGraw-Hill, New York.

- Stewart W. E., 1987, Multi-response parameter Estimation with a New and Non Informative Prior, *Biometrika*, **74**, 557.
- Stewart W. E., Caracotsios, M. and Sorenson, J. P., 1992, Parameter Estimation from Multi-Response Data, *AIChE J.*, **38**, 641-650.
- Tamimi, A., Rinker, E. B., and Sandall, O.C., 1994, Diffusion Coefficients for Hydrogen Sulfide, Carbon Dioxide, and Nitrous Oxide in water over the Temperature Range 293-368K, *J. Chem. Engng. Data*, **39**, 330-332.
- Toman, J. J., 1990, Ph.D. dissertation draft, The University of Texas at Austin, Austin, TX.
- Toman, J. J., and Rochelle, G. T., 1989, Carbon dioxide Absorption Rates and Physical Solubility in 50% Aqueous Methyldiethanolamine Partially Neutralized with Sulfuric Acid, Presented at the AIChE Spring National Meeting, Paper No. 56c, Houston, TX.
- Tomcej, R. A., Lal, D., Rangwala, H. A., and Otto, F. D., Nov. 1986, Absorption of Carbon Dioxide into Aqueous Solutions of Methyldiethanolamine," Presented at the AIChE Annual Meeting, Miami Beach, Florida.
- Tomcej, R. A., and F. D. Otto, 1989, Absorption of CO₂ and N₂O into Aqueous Solutions of Methyldiethanolamine, *AIChE J.*, **35**(5), 861.
- Van Krevelen, D. W., and Hoftijzer, P. J., 1948, Kinetics of Simultaneous Absorption and Chemical Reaction, *Chem. Engng. Prog.*, **44**(7), 529.
- Versteeg, G. F. and van Swaaij, W. P. M., 1988a, On the kinetics between CO₂ and alkanolamines both in aqueous and non-aqueous solutions-I. Primary and secondary amines, *Chem. Engng. Sci.* **43**, 573-585.
- Versteeg, G. F. and Van Swaaij, W. P. M., 1988b, On the Kinetics Between CO₂ and Alkanolamines both in Aqueous and Non-aqueous Solutions-II. Tertiary amines, *Chem. Engng. Sci.* **43**, 587-591.
- Versteeg, G.F., and W.P.M. van Swaaij, 1988c, Solubility and Diffusivity of a Gases (CO₂, N₂O) in Aqueous Alkanolamines Solutions, *J. Chem. Engng. Data*, **33**, 29.
- Versteeg, G.F. and Oyevaar, M. H., 1989, The Reaction Between CO₂ and Diethanolamine at 298 K. *Chem. Engng. Sci.* **44**, 1264-1268.
- Vivian, J. E., and Peaceman, D. W., 1956, Liquid-Side Resistance in Gas Absorption, *AIChE J.*, **2**(4), 437.

- Yu, Wei-Chung, Astarita, G., and Savage, D. W., 1985, Kinetics of Carbon dioxide Absorption in Solution of Methyldiethanolamine, *Chem. Engng. Sci.*, **40**, 1585.

Vita

Msafiri Mmasa Mshewa was born in Makanya, Kilimanjaro, Tanzania on April 13, 1962, the son of Ludia Hadija Zuberi and Mmasa Mshewa Mmbaga. After graduating with a bachelor of science degree in Process Engineering from the University of Dar es Salaam in April 1988, he was employed by the University of Dar es Salaam as a Tutorial Assistant. He entered graduate school at the University of Texas at Austin in Fall 1989. In August 1991 he earned a Master of Science degree in Chemical Engineering under the supervision of Dr. James R. Fair.

Permanent address: P.O. Box 35131

Dar es Salaam, Tanzania

This dissertation was typed by the author